THE INFLUENCE OF RICE BRAN OIL BLENDED AND INTAKE AIR TEMPERATURE ON COMBUSTION BEHAVIOURS AND KNOCKING OF SINGLE CYLINDER FOUR STROKE DIRECT INJECTION COMPRESSION IGNITION ENGINE

NORHAFANA BINTI MOHAMED

DOCTOR OF PHILOSOPHY

UNIVERSITI MALAYSIA PAHANG
AL-SULTAN ABDULLAH

UNIVERSITI MALAYSIA PAHANG AL-SULTAN ABDULLAH

DECLARATION OF THESIS AND COPYRIGHT

Author's Full Name	:	NORHAFANA BINTI MOHAMED
Date of Birth	:	14 JANUARY 1989
Title	:	THE INFLUENCE OF RICE BRAN OIL BLENDED AND INTAKE AIR TEMPERATURE ON COMBUSTION BEHAVIOURS AND KNOCKING OF SINGLE CYLINDER FOUR STROKE DIRECT INJECTION COMPRESSION IGNITION ENGINE
Academic Session	:	SEMESTER II 2023/2024

I declare that this thesis is classified as:

☐	CONFIDENTIAL	(Contains confidential information under the Official Secret Act 1997)*
☐	RESTRICTED	(Contains restricted information as specified by the organization where research was done)*
☒	OPEN ACCESS	I agree that my thesis to be published as online open access (Full Text)

I acknowledge that Universiti Malaysia Pahang Al-Sultan Abdullah reserves the following rights:

1. The Thesis is the Property of Universiti Malaysia Pahang Al-Sultan Abdullah
2. The Library of Universiti Malaysia Pahang Al-Sultan Abdullah has the right to make copies of the thesis for the purpose of research only.
3. The Library has the right to make copies of the thesis for academic exchange.

Certified by:

(Student's Signature)	(Supervisor's Signature)
	Assoc. Prof. Ts. Dr. Muhamad Bin Mat Noor
New IC/Passport Number Date: 5 July 2024	Name of Supervisor Date: 5 July 2024

UMPSA
UNIVERSITI MALAYSIA PAHANG
AL-SULTAN ABDULLAH

UNIVERSITI MALAYSIA PAHANG AL-SULTAN ABDULLAH

SUPERVISOR'S DECLARATION

I hereby declare that I have checked this thesis and in my opinion, this thesis is adequate in terms of scope and quality for the award of the degree of Doctor of Philosophy.

(Supervisor's Signature)

Full Name : Ts. Dr. Muhamad Bin Mat Noor

Position : Associate Professor

Date : 5 July 2024

UMPSA
اونيۏرسيتي مليسيا ڤهڠ السلطان عبدالله
UNIVERSITI MALAYSIA PAHANG
AL-SULTAN ABDULLAH

اونيۏرسيتي مليسيا ڤهڠ السلطان عبدالله
UNIVERSITI MALAYSIA PAHANG
AL-SULTAN ABDULLAH

STUDENT'S DECLARATION

I hereby declare that the work in this thesis is based on my original work except for quotations and citations which have been duly acknowledged. I also declare that it has not been previously or concurrently submitted for any other degree at Universiti Malaysia Pahang Al-Sultan Abdullah or any other institutions.

____

(Student's Signature)

Full Name : Norhafana Binti Mohamed

ID Number : PMA17002

Date : 5 July 2024

اونيۏرسيتي مليسيا ڤهڠ السلطان عبدالله
UNIVERSITI MALAYSIA PAHANG
AL-SULTAN ABDULLAH

THE INFLUENCE OF RICE BRAN OIL BLENDED AND INTAKE AIR TEMPERATURE ON COMBUSTION BEHAVIOURS AND KNOCKING OF SINGLE CYLINDER FOUR STROKE DIRECT INJECTION COMPRESSION IGNITION ENGINE

NORHAFANA BINTI MOHAMED

Thesis submitted in fulfillment of the requirements

for the award of the degree of

Doctor of Philosophy

UMPSA
UNIVERSITI MALAYSIA PAHANG
AL-SULTAN ABDULLAH

Faculty of Mechanical and Automotive Engineering Technology

UNIVERSITI MALAYSIA PAHANG AL-SULTAN ABDULLAH

JULY 2024

ACKNOWLEDGEMENTS

First and foremost, a special thank you to my main supervisor, Associate Professor Ts Dr Muhamad bin Haji Mat Noor, for his strategic advice, guidance, constructive criticism, and technical assistance. To my field supervisor, Associate Professor Dr Abdul Aziz bin Hairuddin, for his generosity, grounding advice and help with the experimental part of the study. I truly appreciate their help and support throughout my studies, which has helped me broaden my knowledge and develop new skills.

I would also like to thank the technical staff for their help in developing my experimental setup and fabricating the experimental apparatus. I have not forgotten Che Ku Ihsan, who helped provide technical support and helped provide the required resources.

A big thank you to my parents (Mohamed and Puziah) and siblings for their endless support throughout my studies. Also, I thank my extended family members for their direct or indirect support. Their support in this manner is much appreciated.

Finally, I express my most significant appreciation to the Ministry of Education Malaysia and Universiti Malaysia Pahang Al-Sultan Abdullah, which supported my studies. Without them, I would not have been able to achieve my goal.

UMPSA
اونيۏرسيتي مليسيا ڤهڠ السلطان عبدالله
UNIVERSITI MALAYSIA PAHANG
AL-SULTAN ABDULLAH

ABSTRAK

Penggunaan tenaga semakin meningkat setiap hari khususnya sektor pengangkutan sama ada di udara, darat atau laut.Kebanyakan tenaga yang digunakan dalam sektor pengangkutan diekstrak daripada proses pembakaran dalam enjin.Pembakaran dalaman enjin yang lengkap penting untuk memaksimumkan prestasi enjin, kecekapan bahan api, dan meminimumkan pelepasan gas ekzos.Sifat bahan api adalah salah satu faktor untuk memastikan campuran bahan api-udara terbakar sepenuhnya semasa proses pembakaran.Apabila berlakunya pembakaran yang tidak lengkap, beberapa molekul bahan api gagal terbakar sepenuhnya, menyebabkan pelepasan bahan daripada pelbagai bahan pencemar dalam gas ekzos.Karbon dioksida terhasil daripada pembakaran bahan api fosil, adalah penting yang menyumbang kepada perubahan iklim.Keseriusan bagi mewujudkan sumber tenaga cecair bahan api alternatif telah diketengahkan oleh krisis berkembar pengurangan bahan api fosil dan kemerosotan alam sekitar beberapa dekad kebelakangan ini.Akibatnya, terdapat keperluan kritikal untuk mengenal pasti sumber tenaga alternatif yang boleh diperbaharui, bersih dan kos efektif.Oleh itu, kajian menyeluruh mengenai pengaruh minyak dedak padi dan suhu udara masuk adalah penting untuk memahami sepenuhnya proses pembakaran enjin pencucuhan mampatan suntikan langsung.Kajian ini bermula dengan mengkaji sifat fizikokimia minyak dedak beras dalam jumlah peratusan yang berbeza.Kajian ini diteruskan dengan analisis kesan minyak dedak padi dan suhu udara masuk pada prestasi enjin, tingkah laku pembakaran dan intensiti ketukan pada satu silinder empat lejang enjin pencucuhan mampatan suntikan langsung.Kajian ini fokus kepada sifat minyak dedak padi termasuk ketumpatan, kelikatan kinematik, nilai tenaga dan nombor cetane mengikut Persatuan Ujian dan Bahan Amerika.Kemudian, penyiasatan kesan bahan api dan suhu udara masuk penting untuk kajian enjin pencucuhan mampatan yang menggunakan minyak dedak padi.Analisis ini merangkumi ciri-ciri prestasi enjin (kuasa brek,penggunaan bahan api khusus brek,kecekapan haba brek,karbon monoksida,karbon dioksida,hidrokarbon dan oksida nitrogen),tingkah laku pembakaran (suhu gas ekzos,tekanan dalam silinder,kadar pelepasan haba dan kadar kenaikan tekanan) dan akhirnya, intensiti ketukan.Eksperimen ini menggunakan KIPOR 170FS, satu silinder empat lejang, penyejuk udara, enjin pencucuhan mampatan suntikan langsung.Terdapat lima jenis bahan api yang terlibat iaitu RBO00,RBO25,RBO50,RBO75,RBO100 dengan keadaan operasi yang berbeza (kelajuan enjin, beban enjin, suhu udara masuk).Hasil eksperimen menunjukkan bahawa enjin yang beroperasi dengan minyak dedak padi dan suhu udara masuk 45°C menghasilkan kecekapan haba brek yang lebih tinggi dan penggunaan bahan api khusus brek yang lebih tinggi (tetapi masih dalam julat optimum 200-400 gkW/h) kerana kandungan tenaga minyak dedak beras yang rendah berbanding diesel tulen.Oksida pelepasan nitrogen sedikit lebih tinggi, tetapi karbon monoksida dan hidrokarbon yang lebih rendah dihasilkan.Tekanan dalam silinder dan kadar pelepasan haba sedikit lebih tinggi daripada diesel tulen kerana nombor cetane yang tinggi dan kandungan oksigen kemudian memberi kesan proses pracampuran yang cepat dan kelewatan pencucuhan pengurangan untuk pembakaran mutlak.Akhir sekali, intensiti ketukan yang diperhatikan ditentukan berada di bawah julat yang ditetapkan apabila nisbah kesetaraan dalam julat 0.1 hingga 0.55.Penemuan eksperimen sejajar dengan kajian literatur.Ringkasnya, minyak dedak padi telah dikenal pasti sebagai pilihan yang menjanjikan sebagai bahan api alternatif kerana ketersediaan sumbernya yang luas dan kualiti prestasi yang baik, dan kerja masa depan disyorkan untuk meningkatkan dinamik pembakaran enjin pencucuhan mampatan.

ABSTRACT

Energy is increasingly used around the globe daily for transportation purposes whether in air, land or sea. Most of the energy used in the transportation sector is extracted from the combustion processes in engines. Achieving complete combustion in an engine is essential for maximizing engine performance, fuel efficiency, and minimizing exhaust gas emissions. The properties of fuel in one of the several factors contribute to ensuring that the fuel-air mixture burns completely during the combustion process. When combustion is incomplete, some fuel molecules fail to burn completely, leading to the emission of various pollutants in the exhaust gases. Carbon dioxide, which is emitted mostly from the combustion of fossil fuels, is the most important gas that contributes to climate change. The urgency of creating alternative liquid-fuel energy sources has been highlighted by the twin crises of fossil fuel depletion and environmental degradation that have emerged in recent decades. As a result, there is a critical need to identify a renewable, clean, dependable, and cost-effective alternative energy source. Therefore, a thorough study of the influence of rice bran oil blended and intake air temperature is vital to fully understand the combustion process of direct injection compression ignition engine. The study starts with the examination of the physicochemical properties of rice bran oil blended in different percentages volume basis. Then, the study continues with the analysis of the effect of rice bran oil and intake air temperature on engine performance, combustion behaviors and knocking intensity of single-cylinder four-stroke direct injection compression ignition engine. The study focuses on the rice bran oil properties including density, kinematic viscosity, calorific value and cetane number according to American Society for Testing and Materials. Then, the investigation of the effect of fuel and intake air temperature is vital for the study of compression ignition engine operating with rice bran oil. The analysis includes the engine performance characteristics (brake power, brake specific fuel consumption, brake thermal efficiency, carbon monoxide, carbon dioxide, hydrocarbon and oxide of nitrogen), combustion behaviors (exhaust gas temperature, in-cylinder pressure, rate of heat release and rate of pressure rise) and lastly, knocking intensity. The experiment was performed using a KIPOR 170 FS single-cylinder, four-stroke, air-cooled, compression ignition engine. There are five fuel types involved in this study which are RBO00, RBO25, RBO50, RBO75, RBO100 with different operating conditions (engine speed, engine load, intake air temperature). The experimental results show that in general, the engine operating with rice bran oil and 45 °C intake air temperature produces higher brake thermal efficiency and higher brake specific fuel consumption (but still in optimal range 200 – 400 gkW/h) due to low energy content of rice bran oil as compared to pure diesel. The oxide of nitrogen emissions is slightly higher, but lower carbon monoxide and hydrocarbon are produced. The in-cylinder pressure and rate of heat release are slightly higher than pure diesel due to high cetane number and oxygen content then led to rapid premixing process and a reduce ignition delay for absolute combustion. Lastly, the observed knocking intensity was determined to be below the established threshold when the equivalency ratio was systematically varied within the range of 0.1 to 0.55. The experimental findings align with the literature review. In a nutshell, rice bran oil has been identified as a promising candidate as an alternative fuel due to its extensive resource availability and good performance qualities, and future work is recommended to improve the dynamics of compression ignition engine combustion.

UNIVERSITI MALAYSIA PAHANG
AL-SULTAN ABDULLAH

TABLE OF CONTENT

UMPSA
اونيۏرسيتي مليسيا ڤهڠ السلطان عبدالله
UNIVERSITI MALAYSIA PAHANG
AL-SULTAN ABDULLAH

UMPSA
اونيۏرسيتي مليسيا ڤهڠ السلطان عبدالله
UNIVERSITI MALAYSIA PAHANG
AL-SULTAN ABDULLAH

UMPSA
اونيۏرسيتي مليسيا ڤهڠ السلطان عبدالله
UNIVERSITI MALAYSIA PAHANG
AL-SULTAN ABDULLAH

UMPSA
اونيۏرسيتي مليسيا ڤهڠ السلطان عبدالله
UNIVERSITI MALAYSIA PAHANG
AL-SULTAN ABDULLAH

اونيۏرسيتي مليسيا ڤهڠ السلطان عبدالله
UNIVERSITI MALAYSIA PAHANG
AL-SULTAN ABDULLAH

LIST OF TABLES

اونيۏرسيتي مليسيا ڤهڠ السلطان عبدالله
UNIVERSITI MALAYSIA PAHANG
AL-SULTAN ABDULLAH

LIST OF FIGURES

UMPSA
UNIVERSITI MALAYSIA PAHANG
AL-SULTAN ABDULLAH

UMPSA
اونيۏرسيتي مليسيا ڤهڠ السلطان عبدالله
UNIVERSITI MALAYSIA PAHANG
AL-SULTAN ABDULLAH

UMPSA
اونيۏرسيتي مليسيا ڤهڠ السلطان عبدالله
UNIVERSITI MALAYSIA PAHANG
AL-SULTAN ABDULLAH

LIST OF SYMBOLS

$\alpha_{m,n}$	Corresponding wave number
c_s	Speed of Sound
$f_{m,n}$	Resonant frequency
h	Heat transfer coefficient
m_f	Mass of fuel
m_a	Mass of air
$\dot{m}_f$	Mass flow rate of fuel
$\dot{m}_a$	Mass flow rate of air
P_{max}	Maximum pressure
$\mathrm{RoPR}_{\mathrm{max}}$	The maximum rate of pressure rise
$R_{mixture}$	Gas constant mixture
t	Time
θ_{max}	Crank angle at which maximum pressure occurs
ϕ	Equivalent ratio
$\left(\frac{F}{A}\right)_{act}$	Actual fuel-air ratio
$\left(\frac{F}{A}\right)_{stoich}$	Stoichiometric fuel-air ratio
$\left(\frac{A}{F}\right)_{act}$	Actual air-fuel ratio
$\left(\frac{A}{F}\right)_{stoich}$	Stoichiometric air-fuel ratio

UMPSA
اونيۏرسيتي مليسيا ڤهڠ السلطان عبدالله
UNIVERSITI MALAYSIA PAHANG
AL-SULTAN ABDULLAH

LIST OF ABBREVIATIONS

ASTM	American Society for Testing and Materials
ATDC	After Top Dead Centre
BDC	Bottom Dead Centre
BMEP	Brake Mean Effective Pressure
BP	Brake Power
BSFC	Brake Specific Fuel Consumption
BTDC	Before Top Dead Centre
BTE	Brake Thermal Efficiency
CAD	Crank Angle Degree
CI	Compression Ignition
CN	Cetane Number
CO	Carbon Monoxide
CO_2	Carbon Dioxide
DI	Direct Injection
EGR	Exhaust Gas Recirculation
EGT	Exhaust Gas Temperature
EOI	End of Injection
HC	Hydrocarbon
IMEP	Indicated Mean Effective Pressure
IP	In-cylinder Pressure
KI	Knocking Intensity
KV	Kinematic Viscosity
LHV	Low Heating Value
NO_X	Oxide of Nitrogen
NO_2	Nitrogen Dioxide
PM	Particulate Matter
RoHR	Rate of Heat Release
RoPR	Rate of Pressure Rise
rpm	Revolution per minutes
SI	Spark Ignition
SOC	Start of Combustion

UMPSA
اونيۏرسيتي مليسيا ڤهڠ السلطان عبدالله
UNIVERSITI MALAYSIA PAHANG
AL-SULTAN ABDULLAH

SOI	Start of Injection
TDC	Top Dead Centre

اونيۏرسيتي مليسيا ڤهڠ السلطان عبدالله
UNIVERSITI MALAYSIA PAHANG
AL-SULTAN ABDULLAH

LIST OF APPENDICES

UMPSA
اونيۏرسيتي مليسيا ڤهڠ السلطان عبدالله
UNIVERSITI MALAYSIA PAHANG
AL-SULTAN ABDULLAH

CHAPTER 1

INTRODUCTION

1.1 Background

There has been a double digit increase in global energy consumption over the last three decades. Fossil fuels dominate the global energy mix, accounting for more than 80% of the world's total energy supplies (Chong et al., 2021). An increase in the use of energy sources is projected due to current life demands and rapid economic development. This causes fossil fuel stocks to rapidly deplete and undesired pollutants to be released into the atmosphere. Oil is the fossil resource that is most at risk of depletion, as its supply is steadily diminishing.

The sources of this fuel are only found in a few parts of the planet, and they are nearing their maximum production capacity. In 2022 years (Figure 1.1), global oil output is likely to reach its highest, which is estimated at 511 Exajoule (EJ). The fossil fuel supply decreased in 2030, 2035 and 2050, which estimated 362 EJ, 237 EJ and 88 EJ, respectively. The rate at which the demand for fossil fuels is decreasing is significant enough to negate the necessity of initiating new long-term upstream oil and gas conventional projects, as well as constructing new coal mines or extending existing ones (Birol, 2023).

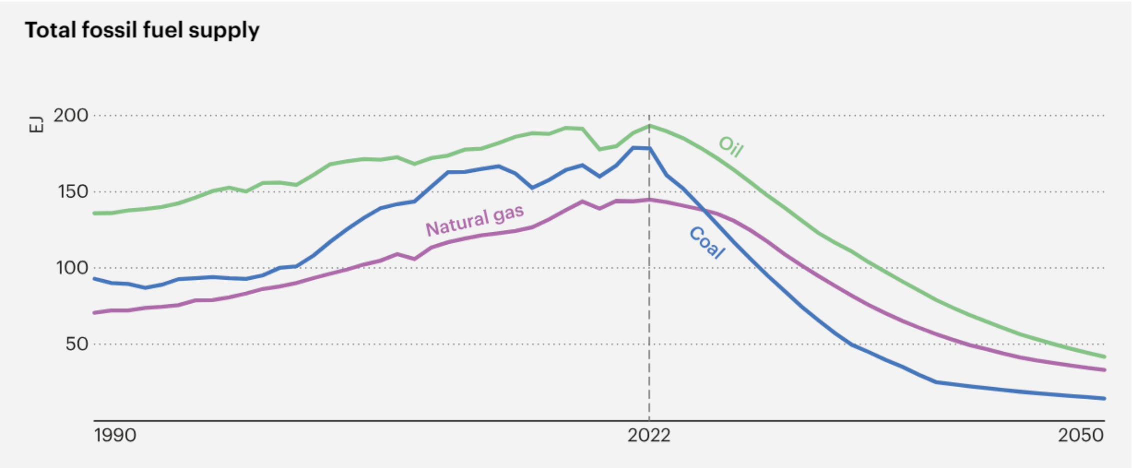

Figure 1.1 The overal proportion of fossil fuels available for extraction and consumption.

Source: Birol (2023)

Based on Figure 1.2, the aggregate demand for fossil fuels experiences a decline of around 26%, equivalent to a reduction of 140 EJ, by the year 2030. The urgency of creating alternative liquid-fuel energy sources has been highlighted by the twin crises of fossil fuel depletion and environmental degradation that have emerged in recent decades. As a result, there is a critical need to identify a renewable, clean, dependable, and cost-effective alternative energy source. Many experiments have been carried out in the search for a viable alternative to petroleum fuels. The depletion of fossil fuels has prompted a hunt for a substitute for this limited resource (Atabani et al., 2012; A. Singh et al., 2022).

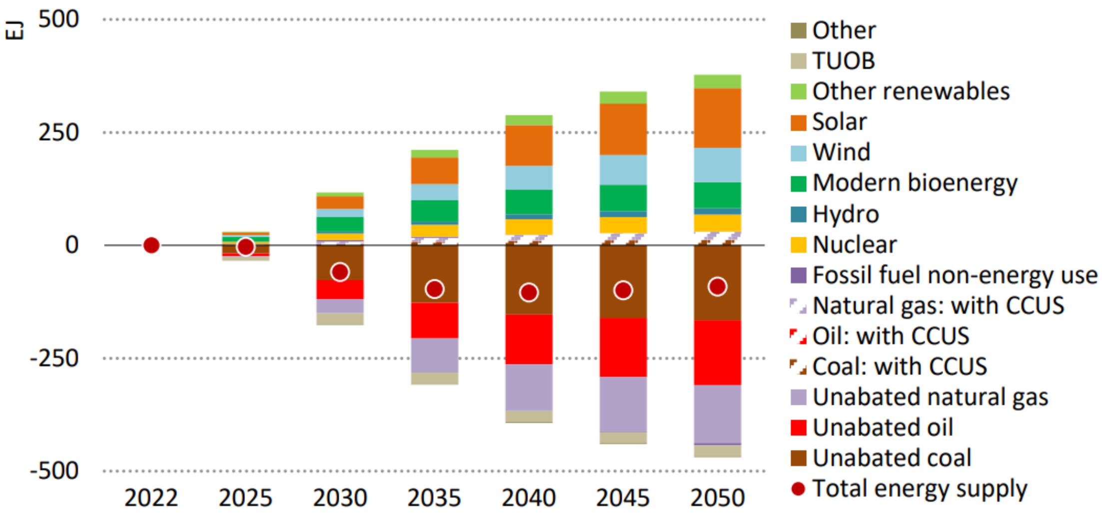

Figure 1.2 Changes in total energy supply by source in the NZE scenario, 2022-2050

Source: Birol (2023)

The transportation sector is the major element that is responsible for the depletion of the earth's resources (Altarazi et al., 2022). The petroleum product from fossil fuels is the source of the most air pollution and is the primary cause of global warming (Chakraborty & Mukhopadhyay, 2019). The world's top goal is to develop a solution for fossil fuels and an alternative fuel that will work with existing engines, particularly diesel engines, which are heavily employed in the transportation sector. As the engine was designed to run on mineral-derived diesel fuel, it is necessary for the alternative fuels to be able to meet the same requirements including it physicochemical properties (Awad et al., 2017). Many renewable resources were suggested, but many of them had a problem with the current engine, necessitating a change at a significant expense. Fuels produced from bio-origin have been discovered to have the potential to be a unique renewable alternative that can be combined with diesel fuel with little or no modification to present engines.

There is a strong probability that many of the biofuels available throughout the world are produced domestically. Furthermore, this alternative fuel saves a great deal of greenhouse gas emissions especially the carbon dioxide (CO_2) emissions (Figure 1.3) (R. Singh et al., 2022). The major criteria for using biofuels would be to locate one with a low cost of production (D. Xu et al., 2021). Excess rice bran was freely accessible in most Asian countries with paddy fields and was used to make rice bran oil. RBO has a high free fatty acid (FFA) content when compared to other processed grains, and active lipase is present, hence the oil is not suited for direct food ingestion (Zaidel et al., 2019). Rice bran oil has potential as a biofuel because it is widely available in rice-producing regions.

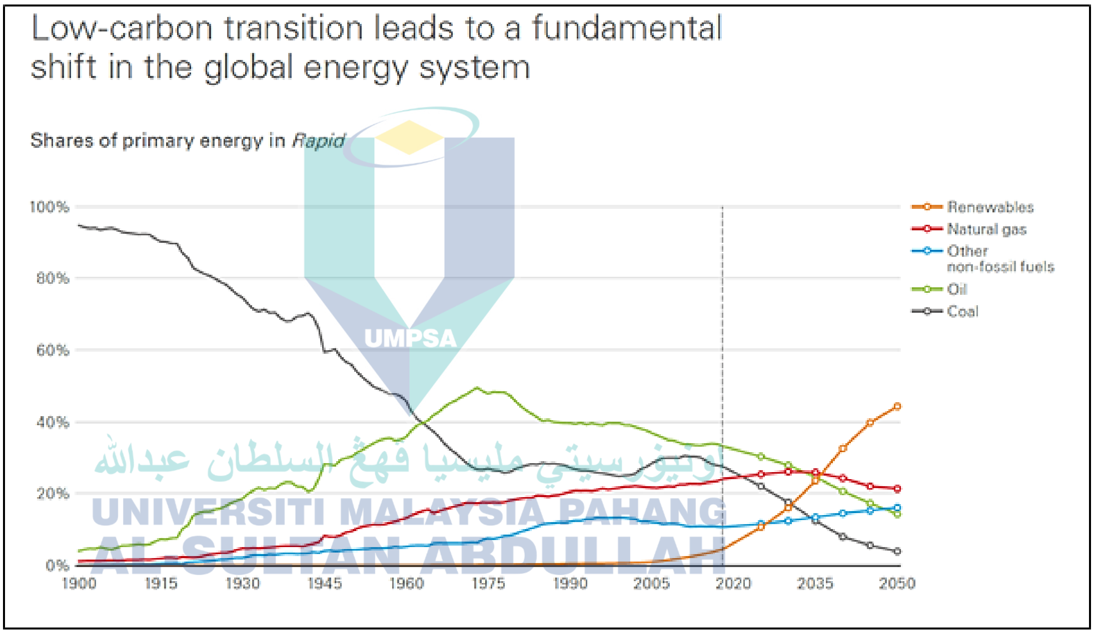

Figure 1.3 Low-carbon transition leads to a fundamental shift in the global energy system

Source: Mobin Siddique et al. (2021)

1.2 Alternative Fuels for Compression Ignition (CI) Engines

Compression Ignition (CI); also known as diesel engine and gasoline engine are the two most common liquid hydrocarbon fuels used in the transportation industry worldwide. It has been decades since efforts have been made to discover alternative fuels, despite changing objectives (Gülüm, 2022). Reduced exhaust emissions were a major factor in the development of alternative fuels in North America and Europe in the 1990s. In order to mitigate climate change emissions, lessen reliance on petroleum imports, improve energy security, and ultimately address the depletion of crude oil resource, which are limited and non-renewable; current developments are justified by a decreased reliance of the transportation sector on fossil fuels, particularly on oil (Guo & Song, 2019).

The goals that drive the development of alternative fuels are not necessarily compatible. For instance, the usage of methanol generated from coal as a vehicle fuel in China is an example of how alternative fuels can boost energy security while emitting more greenhouse gases than the diesel fuel. The same factors that have traditionally influenced the market for fossil fuels have also spurred the development of alternative fuels: commercial interests and industry urging (Yesilyurt, 2020). A few alternative fuels have made progress in the fuel markets, even though a suitable, technically feasible, and economically viable alternative to diesel and gasoline has not yet been fully discovered. These include biodiesel, natural gas, or ethanol (made from corn in North America or sugar cane in Brazil) (Verma et al., 2021). Many further alternative fuels fall into the category of experimental or niche market fuels. Future developments, for example, can be anticipated in the field of synthetic electro fuels. (Abdullah et al., 2019).

اونيۏرسيتي مليسيا ڤهڠ السلطان عبدالله
UNIVERSITI MALAYSIA PAHANG
AL-SULTAN ABDULLAH

An alternative fuel must meet the criteria to present a viable replacement option for petroleum fuels which are resource base and energy density, energy return on investment and renewable character and low carbon emissions. An alternative fuel's compatibility with engines, whether the normal diesel or gasoline engine or a modified engine design, must be guaranteed, including any short- and long-term consequences, before it can be widely adopted for use in existing powertrains (Kothiyal et al., 2022). It is necessary to create and establish standard specifications for each of the pertinent fuel attributes. Several factors need to be covered by the standard standards and protected, such as engine performance, impact on emissions, regulated and unregulated, impact on engine materials, including metals, plastics, rubber, impact on handling, operability, safety, toxicity, the need for any fuel additives, impact of fuel impurities on additives and availability of standardized test method (Raju et al., 2020).

1.3 Problem Statement

Recently, internal combustion engine research focused on improving fuel efficiency, developing alternative fuels owing to energy depletion, and reducing emissions in order to solve environmental concerns (Nema et al., 2022). All countries in the world have policies aiming to reduce the use of diesel fuel in automobiles as well as reduction emission standards by introducing policies such as the real driving emissions standards (Dharmaraja et al., 2019). The compression ignition engine has a much higher thermal efficiency than the spark-ignition engine, however combustion begins with a non-uniform distribution of the air-fuel mixture in the combustion chamber as fuel is injected directly into the combustion chamber at the end of compression (Pulkrabek, 2004). Therefore, particulate matter (PM) is generated where the fuel is locally enriched in the combustion chamber, and a large amount of oxide of nitrogen (NO_X) is generated in the high-temperature flame area (Rahman et al., 2019). Therefore, automobile and engine part manufacturers are attempting to improve combustion through various methods and employ after-treatment devices to comply with the stricter emissions regulations. Initially, Euro-5 fuels included diesel particulate filters (DPFs) as an after-treatment device to reduce restricted particulates, and Euro-6 now requires additional nitrogen oxide reduction devices (Jayaraman et al., 2022). The most common types of nitrogen oxide reduction equipment are Selective Catalytic Reduction (SCR), Lean NO_X-Trap (LNT), and SCR coated DPF (SDPF), so that it is necessary to apply two or more nitrogen oxide reduction devices simultaneously to meet the standard. According to the emission standard, the use of an after-treatment device on a vehicle may have a negative impact on fuel economy and can increase the cost of manufacturing the vehicle (Kannan & Vijayakumar, 2022). Therefore, it is necessary to reduce or simplify unused after-treatment devices, and to conduct studies on combustion techniques which focusing on the intake air temperature parameter and alternative fuels that can inhibit the production of emissions from combustion process and improving combustion performance. This research purpose is to analyse the effects of rice bran oil and intake air temperature on engine performance characteristics, combustion behaviours and knocking intensity of single-cylinder four-stroke direct injection compression ignition engine.

اونيۏرسيتي مليسيا ڤهڠ السلطان عبدالله
UNIVERSITI MALAYSIA PAHANG
AL-SULTAN ABDULLAH

1.4 Research Objectives

The overall aim of this research is to conduct experimental study investigating the effect of rice bran oil blended and intake air temperature on the engine performance characteristics, combustion behaviours and knocking intensity of single cylinder four stroke direct injection compression ignition engine. The main objective of this study is summarized as follows:

i. To examine the physicochemical properties of rice bran oil blended with pure diesel fuel in different percentages volume basis.
ii. To analyse the effect of rice bran oil blended and intake air temperature on engine performance characteristics and combustion behaviours of single cylinder four stroke direct injection compression ignition engine.
iii. To evaluate the influence of rice bran oil blended and intake air temperature on knocking intensity of single cylinder four stroke direct injection compression ignition engine.

1.5 Scope of the Study

This thesis described to introduce rice bran oil blended with pure diesel as a fuel for the unmodified compression ignition engine. Several points are listed here to interpret the scope of the study as follows:

UMPSA
UNIVERSITI MALAYSIA PAHANG
AL-SULTAN ABDULLAH

i. The fuel compositions utilized in this study consist of five distinct blends: 100% pure diesel (RBO00), a mixture of 25% RBO and 75% pure diesel (RBO25), a mixture of 50% RBO and 50% pure diesel (RBO50), a blend of 75% RBO and 25% pure diesel (RBO75), and 100% RBO (RBO100).
ii. Experimental study was conducted to examine the physicochemical properties of rice bran oil (RBO) blended according to the American Society for Testing and Materials (ASTM).
iii. The physicochemical properties tests conducted following the ASTM standard to measure density (ASTMD1298), kinematic viscosity (ASTMD445-01), calorific value (ASTMD4809) and cetane number (ASTMD4737).

iv. The experiment was performed using KIPOR 170 FS single-cylinder, four-stroke, air-cooled, direct injection compression ignition engine. There are three different types of experiments were conducted in this study. The first experiment involved different engine speeds from 1500 rpm to 3500 rpm with intervals of 500 rpm. The second experiment examined the different level of intake air temperature which are at 30 °C, 45 °C and 65 °C at 2500 rpm, from 0 until 720 crank angle degree. The third experiment involved at different equivalent ratio from 0.1 until 0.7 at the engine speed of 1500 rpm.

v. The analysis includes the effect of RBO blended and intake air temperature on the engine performance characteristics which are brake power (BP), brake specific fuel consumption (BSFC), brake thermal efficiency (BTE), carbon monoxide (CO), carbon dioxide (CO_2), hydrocarbon (HC) and oxide of nitrogen (NO_X). Then, the study continues with the analysis of the influence of RBO and intake air temperature on the combustion behaviours including exhaust gas temperature (EGT), in-cylinder pressure (IP), rate of heat release (RoHR) and rate of pressure rise (RoPR) and lasty, knocking intensity (KI).

1.6 Organizational of the Thesis

This thesis consists of five chapters, including the introduction. The background of the study, the alternative fuels considered, rationale of the study and the scope of the study are briefly introduced in this chapter.

UMPSA
اونيۏرسيتي مليسيا ڤهڠ السلطان عبدالله
UNIVERSITI MALAYSIA PAHANG
AL-SULTAN ABDULLAH

Chapter 2 reviews the RBO as an alternative fuel, its production as well as RBO fuel properties. Then, fundamental of CI engine and combustion process covered in the chapter. The literature review includes an overview of engine performance and exhaust emission characteristics, as well as combustion behaviours on the CI engine. Then, the knocking phenomenon and knocking detection method in CI engine were discussed in this chapter.

Chapter 3 presents the experimental setup for engine test bed and fuel measurement explained in this chapter. The physicochemical property test equipment is explained in addition to the fuel preparation and property testing method and standard. Furthermore, it includes an experimental instrumentations and facilities, which are utilized to conduct the engine testing and data collecting. The test procedure and operating condition were included, and the last part of this chapter provides an experimental accuracy and error.

Chapter 4 is dedicated to illustrating the experimental results and discussing the physicochemical property of RBO blended. The influence of RBO and intake air temperature on the engine performance, combustion behaviours and knocking intensity were evaluated based on the experimental data.

Chapter 5 covers the conclusions and limitations of the presented work. This chapter also includes the recommendations for future work is recommended to improve the dynamics of CI engine combustion and this experimental test.

UMPSA
اونيۏرسيتي مليسيا ڤهڠ السلطان عبدالله
UNIVERSITI MALAYSIA PAHANG
AL-SULTAN ABDULLAH

CHAPTER 2

LITERATURE REVIEW

2.1 Introduction

The literature review presented and addressed the topics of Rice Bran Oil (RBO) production and standardisation, as well as the qualities of biofuel. This chapter encompasses the examination, specifically in employing alternative fuels Then, it also discussed on the biofuel properties including density, kinematic viscosity, calorific value, cetane number, cloud and pour point and flash point. This chapter plays a pivotal role in examining combustion of CI engines, including the conceptual framework, operational mechanisms, the air-fuel mixture classification. The ignition delay, mixing controlled combustion and intake air temperature also examined in this chapter. In addition, the previous studies on the effect of biodiesel and biofuel on the engine performance, exhaust emission characteristics and combustion behaviours of CI engine also were discussed. The comparative analysis of alternate fuel and pure diesel carries significant importance. Moreover, these studies addressed the occurrence of knocking in CI engines, as well as the various components that contribute to this phenomenon. Furthermore, a comprehensive examination of knocking was examined including types of knocking, factor led to knocking in CI engine and knocking detection methods. Knocking analysis and method reducing it were also included in this chapter.

2.2 Rice Bran Oil (RBO) as Alternative Fuel for Compression Ignition (CI) Engine

There is an increasing price of crude oil, depletion of crude oil reserves, and global concern about protecting the environment (Mobarak et al., 2014; Ye et al., 2018). The usage of biofuel would eventually reduce environmental levels of CO_2 because more plants would be grown, which would use atmospheric CO_2 for photosynthesis. RBO was produced from rice husks after the separation process with rice. RBO contains 13.5 % of oil when derived from its source (Hoang et al., 2021). There has been a duplication of global energy consumption over the past three decades. Over 80% of the world's total energy supply comes from fossil fuels, leading them the key component of the world's energy (Chong et al., 2021). It is expected that energy sources will be utilized more extensively in the future because of modern life demands and rapid economic development. Consequently, fossil fuels are rapidly depleted, and unwanted emissions are produced. There is a growing concern that oil will run out soon, as its availability is rapidly declining. Sources of this fuel are restricted to certain regions of the world, and their production levels are near their maximum.

A peak in global oil production is expected in the next few years. Based on data provided by the World Trade Organization, the fuel market accounted for a significant proportion of approximately 15.8% of the overall trade of merchandise and primary products (R. Singh et al., 2022). Most of these emissions can be attributed to the utilization of diesel fuel, which plays a crucial role in operating transportation systems and heavy-duty engines. Moreover, the contemporary world is confronted with significant global warming and environmental contamination issues. The primary gas responsible for the greenhouse effect is CO_2, predominantly released from the combustion of fossil fuels. The escalating levels of CO_2 emissions in the present context have rendered the objective of mitigating the global warming phenomena progressively more arduous and financially burdensome as time elapses. Moreover, the contemporary world is confronted with significant global warming and environmental contamination issues.

Many experiments have been done in the search for an alternative to petroleum fuels. The extinction of fossil fuel drives the search for a surrogate for this depleting resource (Ramachandran et al., 2023). The transportation sector is the primary element contributing to the depletion of prime factors. The combustion of fossil fuels, particularly petroleum products, is a significant contributor to air pollution and is also recognized as a primary driver of global warming on a worldwide scale (Srivastava et al., 2023).

UMPSA
UNIVERSITI MALAYSIA PAHANG
AL-SULTAN ABDULLAH

The global imperative to seek a substitute for fossil fuels and identify an alternative fuel compatible with current engine technologies, particularly diesel engines, is paramount. Diesel engines have gained widespread usage in the transportation sector, necessitating urgent exploration for a viable surrogate fuel. The engine was specifically designed to utilize diesel fuel obtained from minerals petroleum. Therefore, any surrogate replacements must possess comparable qualities. Numerous alternative fuel options have been proposed; however, the majority encounter compatibility issues with existing engines, necessitating costly modifications. Bio-derived fuels have been identified as a promising sustainable option that can be blended with diesel fuel without significantly modifying existing engines (Gülüm, 2022).

Although biofuels are generally straightforward, they are often confused with biodiesel by the public. Biodiesel, a variant of biofuel, is derived from oils sourced from plants and serves as a viable alternative to conventional diesel or gasoline when utilized in engines. In 1937, during the period of expansion in the automotive industry, Chavanne introduced the concept of biodiesel. Biodiesel, an alternative to conventional gasoline or diesel engine, is a type of oil derived from plant sources. The blend ratios or percentages of biodiesel and conventional diesel may vary depending on the engine's requirements. The term "biofuel" encompasses various fuels derived from organic matter and living organisms. Biofuels predominantly derive from organic waste sources, encompassing plant and animal materials. Consequently, several types of biodiesels might be classified as biofuels. The basic materials undergo various processes (Kumar & Goga, 2023).

Liquid biofuel is the sole form of biofuel available. Biofuel, being solely available in liquid state, is primarily employed for the purpose of heating structures and propelling engines, namely locomotive ones. Conversely, biofuel can be found in all states of matter. Biofuel is commonly used in its gaseous form for culinary purposes, with methane derived from biogas as a notable illustration. Liquid biofuels are commonly utilized for transportation purposes. It encompasses a range of substances, including ethanol, alcohol, and several types of biodiesels. Solid biofuels are limited, but those that are available are primarily used to cook, derived from plant residues such as corn cobs.

Briquettes represent a widely recognized kind of solid biofuel that is extensively employed in commercial applications. Briquettes refer to compacted remnants of plant matter that are utilized for heating and cooking. These briquettes are typically composed of materials such as sawdust, coal dust, or other forms of combustible biomass. Other examples of solid biofuels that can be considered are peat, wood pellets, wood ash, and animal waste (Torres-Mayanga et al., 2019). Most biofuels on the global continent are primarily sourced from native resources. This fuel possesses an additional benefit in the form of substantial CO_2 reduction, resulting from decreased fuel emissions. The fuel qualities exhibit variations based on the diverse sources of feedstock origin, as outlined by the ASTM standards. It is customary to blend them with diesel fuel in varying proportions in order to utilize these biofuels in diesel engines (Dharmaraja et al., 2019).

The suitable percentage for an effective blending ratio depends on the feedstock fuel property (Hoang et al., 2021). Evaluating the blended fuel properties is crucial for a suitable blending proportion. The main attribute of using biofuels would be to find one with low production cost (D. Xu et al., 2021). RBO is derived from surplus rice bran, readily accessible in many Asian countries with paddy fields. According to the Food and Agriculture Organization (FAO), the global output of rice reached a total of 513 million tons. Within rice milling and polishing, an additional byproduct is generated in the form of a brown layer between the rice kernels and the outer rice husks.

UNIVERSITI MALAYSIA PAHANG
AL-SULTAN ABDULLAH

In some Asian nations, including Vietnam, China, Bangladesh, and India, the surplus bran is utilized as animal feed or incinerated as a solid fuel (Hasan, 2014). Around 16-32 wt% of the oil content in rice bran varies by the degree of polishing process and rice type (Mazaheri et al., 2018). The free fatty acid (FFA) content of RBO is relatively elevated compared to other processed cereals. Additionally, the presence of active lipase in the oil renders it unsuitable for direct consumption as a food product. The oil obtained from rice bran holds significant potential as a biofuel due to its abundant availability in nations that cultivate rice.

2.3 Introduction to Rice Bran Oil (RBO)

Rice bran is a byproduct of milling paddy rice to make refined rice. It includes the seed coat, pericarp, aleurone layer, nucellar layer embryo, and outer segment of the stiff endosperm and accounts for 12 to 20 % of the weight of the entire kernel (Wancura et al., 2023). Oryza sativa pericarp and seeds are found in rice bran, which contains about 10% paddy seeds.

It is the most nutrient-dense component of rice and a good source of proteins with high nutritional value and a high starch content. The term "rice bran" refers to a fine, smooth particle that includes seeds and the pericarp, seed coat, aleurone, germ, and endosperm (Zullaikah, 2005). The cuticle between the paddy husk and the rice grain, or rice bran, is a part of raw rice source of edible and essential oils in the future (Ijaz et al., 2021).

Three million tons of RBO (approximately) are produced annually, of which two million tons are unfit for human consumption. It has been discovered that RBO is the most nutrient-dense oil due to its distinctive combination of naturally occurring substance, including antioxidants and FFA (Zullaikah, 2005).

The RBO is extracted from the germ and inner husk (bran), and it is very difficult to refine due to its high FFA content, insoluble in acetone, and dark colour (Fan et al., 2022). Only a tiny portion (less than 10%) of the total production of RBO is converted into edible oil due to the rapid hydrolysis reaction that follows the milling process and results in the presence of active lipase in the bran (Zullaikah, 2005). Production of rice bran could be increased as RBO could be significant.

UMPSA
اونيۏرسيتي مليسيا ڤهڠ السلطان عبدالله
UNIVERSITI MALAYSIA PAHANG
AL-SULTAN ABDULLAH

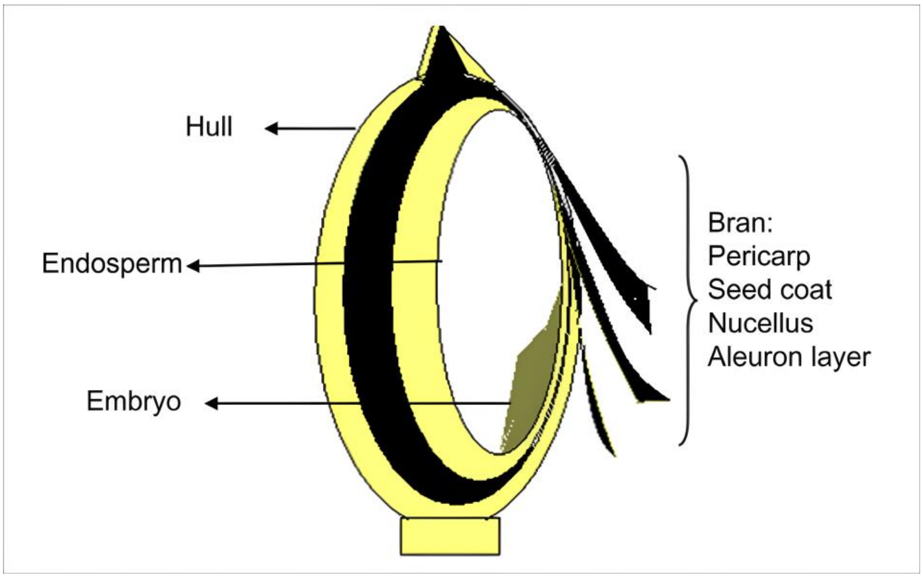

Figure 2.1 Structure of rice bran oil
Source: Zullaikah (2005)

2.4 Rice Bran Oil (RBO) Production and Standardization

There is an abundance of FFA, waxes, unsaponifiable components (4.3%), and polar lipids in RBO. However, the extraction procedure is complicated. Studies have been done on a variety of extraction techniques, such as cold pressing, Soxhlet extraction, supercritical CO_2 extraction (SC-CO_2) and microwave extraction (Sahini & Mutegoa, 2023).

UMPSA UNIVERSITI MALAYSIA PAHANG AL-SULTAN ABDULLAH

2.4.1 Conventional Method

Conventional methods of extracting RBO primarily involve solvents and cold-pressing depicted in Figure 2.2.

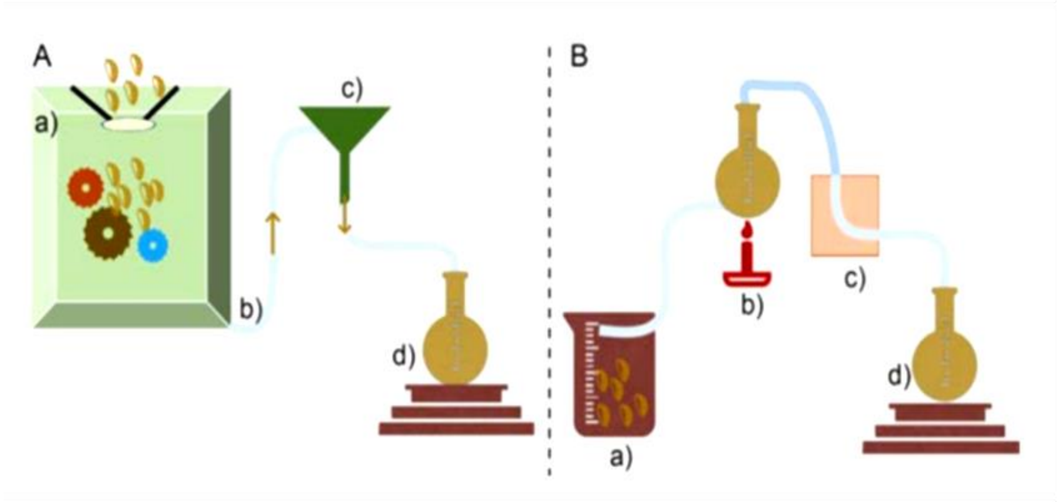

Figure 2.2 Conventional methods for rice bran oil extraction.
Source: D. Xu et al. (2021)

2.4.1.1 Solvent Extraction Method

Solvents are frequently used to increase the oil content of pre-pressed oil cakes or to reduce the oil content of seeds (Figure 2.2-A). Hexane of commercial grade is the solvent of preference around the globe for financial reasons. It is a suitable oil solvent in terms of solubility and simplicity of recovery. Hexane is the cause of numerous difficulties, however. In addition to causing major environmental issues (air pollution) and other health risks due to its toxicity, it creates RBO with poor colour quality. Alternative solvents have been sought after for a long time, with alcohols, halogenated hydrocarbons, hydrocarbons, carbon dioxide (supercritical fluid extraction), and even water among the most popular solvents (D. Xu et al., 2021). Several short-chain alcohols, such as ethanol and isopropanol, have also been suggested as substitute solvents because of their high safety. The use of d-limonene, a by-product of the citrus industry, is also a viable alternative to hexane-based solvents for the production of high-quality crude edible oils (He & Liu, 2019). However, the issue of high energy expenditure mainly caused by limonene's high boiling point and slightly high latent heat makes it problematic for use as a solvent for the extraction of edible oils.

The cost of limonene-based oil extraction could be reduced due to energy-efficient solvent recovery techniques like membrane separations. The extraction of RBO at varied solvent hydration levels (0%, 6%, or 12%) was attempted. They utilized a rice bran to solvent ratio (3:1) at various temperatures (50 °C to 80 °C for one hour. The highest -oryzanol yield was produced using ethanol with 6% of water, regardless of temperature, whereas the highest RBO extraction yield (160 g/kg) was obtained using ethanol and isopropanol at 80 °C. In a different investigation, after 4 hours of extraction using a Soxhlet apparatus, the exact yield of RBO (170.9 g/kg) was obtained by using isopropanol and hexane, which is higher than the yield of ethanol. Additionally, RBO extracted with ethanol showed greater-oryzanol content (2.609 mg/kg) than with hexane (2.229 mg/kg) or isopropanol (2.094 mg/kg) (Mathias et al., 2024).

2.4.1.2 Cold Pressing Method

The mechanical pressing technique, also known as cold pressing, does not include the use of organic solvents or heat treatment (Figure 2.2-B). Due to its cost-effectiveness and reduced labour requirements compared to solvent extraction, this technology presents a feasible alternative to conventional approaches for oil extraction. Another advantage of cold pressing is its simplicity, efficacy, and safety. Moreover, cold-pressed plant oils have enhanced nutritional attributes and are devoid of chemical by-products, generating considerable interest in their utilization (Charoonratana, 2020). Although mechanical presses are preferred because of their advantages, they have a severe drawback that leaves 8% to 14% of the available oil in the cake. The cold pressing method uses a mechanical screw press accompanied by mild heating and subsequent filtration in order to achieve purified RBO. Implementing low-temperature pre-treatment on rice bran prior to cold pressing has the potential to yield refined rice bran oil (RBO) of superior quality (Dharmaraja et al., 2019). Combining brief cooking durations and cold pressing yields enhanced productivity and efficiency. The combination of mechanical pressing with ultrasonication, heating, and pre-treatment enhances the quality and extraction rate of RBO (He & Liu, 2019). Due to this combination, the structure, fissures, or cavities of the rice bran fractions undergo modifications, leading to enhanced efficiency in mass transfer and oil extraction (Sebayang et al., 2023).

UMPSA
اونيۏرسيتي مليسيا ڤهڠ السلطان عبدالله
UNIVERSITI MALAYSIA PAHANG
AL-SULTAN ABDULLAH

2.4.2 Non-Conventional Method

The implementation of standardized, advanced extraction techniques that are environmentally sustainable is of utmost importance in the processing of chemicals and biochemicals. In recent decades, scholars have directed their attention to the development of extraction processes that are both ecologically friendly and sustainable while also enhancing their efficiency. Non-conventional approaches, such as supercritical fluid extraction (SFE), ultrasound-assisted extraction (UAE), microwave-assisted extraction (MAE), and enzyme-assisted aqueous extraction (EAAE), have been adopted as alternatives to classic solvent-based and mechanical extraction methods (Figure 2.3).

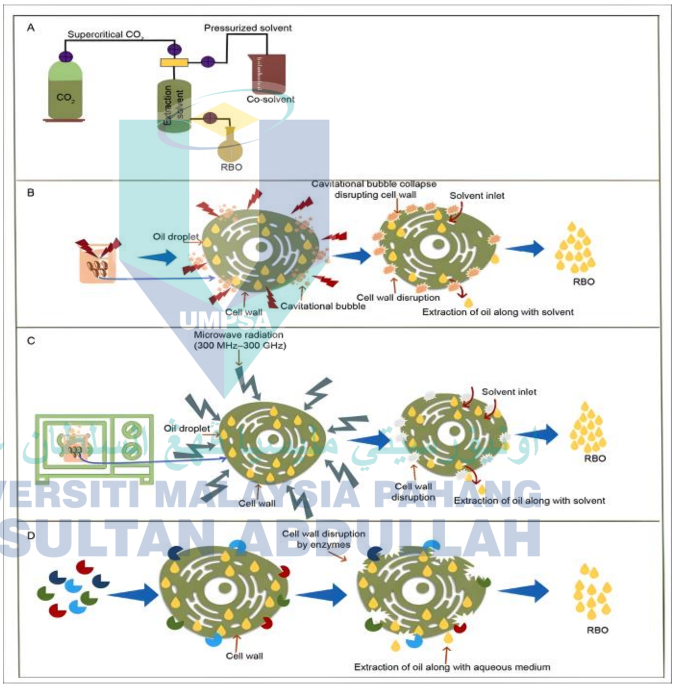

UMPSA
UNIVERSITI MALAYSIA PAHANG
AL-SULTAN ABDULLAH

Figure 2.3 Non-conventional methods for rice bran oil extraction
Source: D. Xu et al. (2021)

2.4.2.1 Supercritical CO_2 Extraction (SC-CO_2)

Free Supercritical fluid extraction (SFE) presents several notable benefits, including the elimination of solvent contamination risks, along with strategies to mitigate some limitations associated with traditional extraction methods. Supercritical fluid extraction (SFE) has superior efficiency and speed compared to organic solvent extraction. This can be attributed to its enhanced capacity to penetrate matrices and favourable transport properties. In recent years, there has been a notable surge in attention directed towards SC-CO_2 extraction, as evidenced by Figure 2.3-A. The term "supercritical fluid extraction" pertains to a technique that employs carbon dioxide (CO_2) above its critical temperature and pressure as a solvent. This approach is particularly advantageous for extracting chemicals that exhibit sensitivity to changes in temperature (Mathias et al., 2024). Polar compounds are combined with CO_2 to boost the solubility and extraction rate to increase the extraction efficiency (Charoonratana, 2020). The kinetics of the RBO extraction may be improved by using SC-CO_2 and ultrasound. The extraction of RBO is conducted by supercritical carbon dioxide (SC-CO_2) at an extraction efficiency ranging from 7.00% to 9.60%. The presence of oryzanol precursors, namely campesterol, ß-sitosterol, stigmasterol, and 4-methylene cycloartenol, was identified in RBO using the SC-CO_2 + ultrasound extraction method. The assertion was made that this combination has the potential to serve as a method for extracting specific functional molecules. In 2018, Soares et al. conducted a study investigating the impact of varying ratios of co-solvents, namely SC-CO2 and ethanol (Soares et al., 2018). Oil yields are generally high (25.48%) at 40 °C and 200 bar pressure without residual solvent in RBO.

2.4.2.2 Subcritical CO_2 Fluid Extraction (SFE)

UMPSA
اونيۏرسيتي مليسيا ڤهڠ السلطان عبدالله
UNIVERSITI MALAYSIA PAHANG
AL-SULTAN ABDULLAH

A fresh approach has recently emerged to address the limitations associated with the solubility of CO_2 under high pressure in supercritical conditions. The subcritical CO_2 soxhlet technique is an innovative approach that utilizes the advantages of both Soxhlet extraction and CO_2 extraction to create RBO (Kumar Karedla et al., 2024). Both subcritical and supercritical CO_2 extraction methods for RBO are conducted at temperatures lower than 31.1 °C and CO_2 pressures of 72.9 bar, following the same fundamental concept. The process of boiling and subsequent precipitation continuously replenishes CO_2 in this procedure. The extraction procedures for RBO yield 13.0%-14.5% and 22.0% using subcritical CO_2 and hexane, respectively (He & Liu, 2019). When comparing hexane-extracted oil to oil obtained through the subcritical CO_2 method, it is seen that the latter exhibits approximately ten times higher concentrations of oryzanol and tool compounds, as well as lower levels of FFA and peroxide values.

2.4.2.3 Subcritical Water Extraction (SWE)

When compared to alternative technologies, SWE offers a viable, cost-effective, and environmentally sound solution due to its utilization of the distinct characteristics exhibited by supercritical water under elevated temperatures and pressures (ranging from 100 °C to 374 °C, with pressures exceeding 5 MPa) (Moreira et al., 2023). The fundamental basis of the SWE theory is derived from the molecular composition and thermodynamic properties of water. Subcritical water (SW) refers to water that is maintained at a pressure of 22.1 MPa and a temperature lower than 374 °C (Saikia & Dutta, 2022). The process is called SWE when SW is utilized for functional component extraction. Its vapour pressure, mass transfer, and diffusion all increase with temperature while its surface tension and viscosity decrease (Sahini & Mutegoa, 2023).

The dielectric constant (ε) of water is modified by SWE through the induction of favourable alterations in pressure and temperature. The temperature and pressure conditions cause water to undergo a decrease in temperature from its initial value of 80 to a final value of 25. This phenomenon facilitates the alteration of water's behaviour to resemble that of organic solvents, simplifying the extraction process of desirable bioactive compounds with varying degrees of polarity. Temperature is the primary and crucial determinant in Solid Waste Extraction (SWE) since it is employed to control the rate of analyte extraction.

UMPSA
اونيۏرسيتي مليسيا ڤهڠ السلطان عبدالله
UNIVERSITI MALAYSIA PAHANG
AL-SULTAN ABDULLAH

Moreover, when the temperature parameters of other extracting solvents are elevated, subcritical water may exhibit heightened reactivity and corrosiveness compared to ambient water, rendering it unsuitable for the extraction of heat-sensitive oil components (A. Pal & Das, 2022). The energy emanating from solar wind has the potential to disturb the interactions between solutes and their surrounding surroundings, hence reducing the activation energy necessary for desorption. The utilization of solid waste encapsulation (SWE) has been recognized as an environmentally advantageous approach for the stabilization of residual biomass oil (RBO) and the deactivation of lipase due to its green nature, simplicity, and non-flammable properties.

The quantity obtained through the process of hexane extraction exhibits similarity to the maximum yield of rice bran oil (RBO), which is 249 mg/g, accounting for approximately 94% of the total oil content in rice bran (P. Pal, 2017). SWE, however, has reported excellent outcomes for the extraction of other oils, such as sunflower, soybean, cottonseed, or jojoba oil (Nguyen et al., 2019), as well as some functional compounds, such as polyphenols, essential oils, carotenoids, flavonoids, and flavour and fragrance compounds (P. Pal, 2017). RBO extraction, however, still needs to be widely used for SWE.

2.4.2.4 Ultrasound-Assisted Extraction (UAE) Method

The United Arab Emirates (UAE) has recently experienced a significant increase in its utilization. When ultrasound propagates through a medium in the form of a pressure wave, it induces an increase in the velocity of molecular motion (Figure 2.3-B). Ultrasonication-induced cavitation leads to an increased permeability of plant tissues. Additional support for the mechanical effects of ultrasound can be observed through the occurrence of microfractures and the subsequent breakdown of cell walls, facilitating the subsequent release of their contents. (Charoonratana, 2020). The United Arab Emirates (UAE) provides several advantages in extraction. These advantages encompass a high extraction yield, ensuring a significant number of desired compounds are obtained. Additionally, the UAE offers high repeatability, ensuring consistent results across multiple extraction processes. Another benefit is the minimal use of solvents, reducing the amount of chemicals required for extraction.

UMPSA
اونيۏرسيتي مليسيا ڤهڠ السلطان عبدالله
UNIVERSITI MALAYSIA PAHANG
AL-SULTAN ABDULLAH

Moreover, the UAE boasts quick extraction times, enabling efficient processing. Furthermore, the operating costs associated with extraction in the UAE are relatively low, making it a cost-effective option. The environmental impact of extraction in the UAE is also minimal, contributing to sustainable practices. Lastly, the UAE's extraction methods can be easily adapted for industrial-scale applications, facilitating their implementation in large-scale operations. UAE is mainly used for drying, extracting, and emulsifying food products. According to Martinez-Padilla et al., sonication (2 MHz) assisted extraction of RBO produces FFA and peroxide values below the industrial standard level, as well as an increase in phenolic compounds. Researchers used the response surface method to optimize the UAE parameters to maximize the RBO yield (Mathias et al., 2024). Compared to oil extracted using hexane, oil extracted by the UAE contained less FFA and components contributing to colour. When compared to raw rice bran, both extraction processes yield a larger percentage of oil from parboiled rice bran.

2.4.2.5 Microwave-Assisted Extraction (MAE) Method

Compared to conventional fat and oil extraction methods, microwave-assisted extraction (MAE) demonstrates a higher level of environmental friendliness, as depicted in Figure 2.3-C. This approach's recent surge in popularity can be attributed to its advantages, including decreased extraction time, energy consumption, and solvent usage, as well as its potential as an alternative to the conventional solvent extraction method. The susceptibility of lipids to radiation is attributed to their low specific heat, which enhances their solubility in the extractant (Nguyen et al., 2019). When isopropanol is combined with microwave-assisted extraction (MAE) under specific parameters, such as an extraction length of 30 minutes and operating settings of 82 °C, 2.1 bar, and 95 W, it results in a more significant recovery of RBO (Rapid Biochemical Oxygen Demand) compared to the use of hexane. According to Nguyen, the RBO that was extracted using isopropanol and under identical experimental conditions exhibited a γ-oryzanol content of 2.256 mg/kg (Nguyen et al., 2019). The process of refining crude vegetable oil involves additional steps to produce vegetable oil suitable for consumption. This can be achieved by either chemical means, such as using an excess of sodium hydroxide to remove FFA, or by physical methods, which involve removing FFA and deodorizing the oil using a water degumming phase. Moreover, due to the prevalence of extraction being carried out under atmospheric circumstances, microwave-assisted extraction (MAE) exhibits little danger and needs substantial safety challenges. Furthermore, the Mean Absolute Error (MAE) exhibits certain limitations and constraints. As previously mentioned, it is generally advisable to refrain from using non-polar solvents due to their limited capacity for absorbing microwave energy.

UMPSA
اونيۏرسيتي مليسيا ڤهڠ السلطان عبدالله
UNIVERSITI MALAYSIA PAHANG
AL-SULTAN ABDULLAH

2.4.2.6 Enzyme-Assisted Aqueous Extraction (EAAE) Method

The utilization of the environmentally conscious technology known as EAAE facilitates the efficient release of oil during aqueous extraction processes while simultaneously reducing the reliance on organic solvents (Figure 2.3-D). The proposed approach involves the utilization of enzymes to degrade the cell walls of oil-containing materials, facilitating the extraction of oil and other constituents using milder processing conditions (He & Liu, 2019). The EAAE manufacturing process yields a higher quality product, obviating the necessity for supplementary refinement techniques. Moreover, this process consumes less energy and solvent than conventional solvent extraction methods. The three primary kinds of enzymes employed in the extraction of rice bran oil (RBO) are cellulase, pectinase, and protease. The extraction of RBO has been facilitated using amylase. However, this method only results in a 5% improvement in oil recovery. The exclusive utilization of enzymatic processing does not result in substantial yields. Significant oil yields were seen when rice bran underwent processing with cellulase and pectinase enzymes, followed by extraction using n-hexane. Protease, α-amylase, and cellulase enzymes are employed to enhance the yield, resulting in a recovery of 76%–78% of the RBO typically produced using conventional extraction methods (He & Liu, 2019).

2.5 Biofuel Fuel Properties

اونيۏرسيتي مليسيا ڤهڠ السلطان عبدالله
UNIVERSITI MALAYSIA PAHANG
AL-SULTAN ABDULLAH

Fuel properties play a crucial role in determining engine performance due to their direct impact on combustion behaviours and exhaust emission characteristics and overall engine operation. There are several fuel properties of biofuel described in this section which include the density, kinematic viscosity, density, calorific value, cetane number, cloud and pour point, and a flash point. Table 2.1 shows the physicochemical properties of different biofuel blends and with various additives.

Table 2.1 Physicochemical properties of various biofuel

Properties / Fuel	Density	Kinematic Viscosity	Calorific Value (MJ/kg)	Cetane Number	Flash Point (°C)	Cloud Point (°C)	Pour Point (°C)	References
			Rice bran + cerium oxide/zirconium oxide (CeO_2/ZrO_2)					(Jayaraman et al., 2023)
D100	820	2.72	45	48	56			
RB100	868	5.03	39.454	57	165			
RB30	846	3.47	42.886	49	78			
RBO30 + 50CeO_2	851	3.54	43.987	51	62			
RB30 + 50ZrO_2	850	3.52	43.732	50	65			
RBO30 + 25CeO_2 + 25ZrO_2	849	3.51	44.198	53	60			
			Rice bran + Graphene oxide					
D100	840	2.8	46	46	56			(El-Seesy & Hassan, 2019)
B100	880	5.6	35	42	170			
B5D95GO30	865	3.8	36.23	38	160			
B15D85GO	871	3.8	36.76	38	158			

UMPSA
اونيۏرسيتي مليسيا ڤهڠ السلطان عبدالله
UNIVERSITI MALAYSIA PAHANG
AL-SULTAN ABDULLAH

Table 2.1: Continued

Properties Fuel	Density	Kinematic Viscosity	Calorific Value (MJ/kg)	Cetane Number	Flash Point (°C)	Cloud Point (°C)	Pour Point (°C)	References
Eucalyptus + zirconium oxide								(Sajeevan & Sajith, 2016)
Diesel	820	2.47	45.5	51	65			
Eu20	835	2.376	44.854	45	54			
Eu20 + ZrO2	841.5	2.51	44.982	50.1	62.8			
Eu40 + ZrO2	847.3	2.58	45.093	51.6	63.4			
Eucalyptus + n-butanol								
Diesel	830	2.5	45.6	48	58			
B100	875	2.2	44.1	55	100			
B20	868	2.4	43.6	50	76			
B20 + 5Bu	856	2.7	42.9	48	72			
B20 + 10Bu	848	2.9	42.4	47	69			
B20 + 15Bu	840	2.2	42.1	46	65			

اونيۏرسيتي مليسيا ڤهڠ السلطان عبدالله
UNIVERSITI MALAYSIA PAHANG
AL-SULTAN ABDULLAH

Table 2.1: Continued

Properties **Fuel**	**Density**	**Kinematic Viscosity**	**Calorific Value (MJ/kg)**	**Cetane Number**	**Flash Point (°C)**	**Cloud Point (°C)**	**Pour Point (°C)**	**References**
Algae + CuO_2								(Kale & Patle, 2022)
B20	830	4.73	43.54	58	176	-1	-4	
B20 + 25	831	5.1875	44.51	54.75	176.5	-4	-4	
B20 + 50	831.7	5.6449	45.48	51.5	177	-4	-4	
B20 + 75	831.8	5.6671	45.501	51.75	177.5	-4	-4	
B20 + 100	831.9	5.6894	45.519	52	178	-4	-4	

UMPSA
اونيۏرسيتي مليسيا ڤهڠ السلطان عبدالله
UNIVERSITI MALAYSIA PAHANG
AL-SULTAN ABDULLAH

2.5.1 Density

Density can be defined as substance's mass per unit volume. Most of the studies use the method of ASTMD 1298 for density measurement (Mathew et al., 2021). The primary determinant of fuel density is its effect on engine performance. In general, biofuel produced from vegetables oils and fats and contained triglycerides which are esters of fatty acids. The complex molecules in biofuel contribute to its higher density than pure diesel. There is evidence that a higher density of biofuel may have an adverse effect on the fuel injector system and the spray pattern during combustion based on researchers. The density of fuel exerts influence on both the air-fuel ratio and the energy content within the combustion chamber, manifesting a tangible effect on the combustion process in diesel engines. Moreover, it should be noted that a fuel with a lower density necessitates a lengthier injection duration to inject an equivalent mass of fuel.

2.5.2 Kinematics Viscosity

Kinematic viscosity (KV) can be defined as the quantification of a liquid's resistance to flow, which arises from the internal friction between different components of the fluid in relation to its molecular composition and temperature (D. Xu et al., 2021). Since a precise amount of fuel must be injected, this crucial feature has an impact on how fuel injection behaves. High KV can be ascribed to larger droplet sizes, decreased vaporization efficiency, a narrower injection spray angle, and increased in-cylinder fuel spray penetration (P. Pal, 2017). This phenomenon may lead to a decline in combustion efficiency, increased in pollutant emissions, and a higher of oil dilution. Biofuel which is specific to RBO generally exhibits a KV that is approximately two to three times higher than that of pure diesel. If the fuel's KV is excessively high, the injection pump will be unable to supply enough amount of gasoline to fill the pumping chamber, leading to a reduction in engine power (D. Xu et al., 2021). Conversely, if the KV is excessively low, there is a possibility of fuel leakage occurring via the seals of the fuel injection system. Moreover, many challenges arising from elevated viscosity become more conspicuous in circumstances involving the initiation of engines under cold conditions and in environments with reduced ambient temperatures.

UMPSA
UNIVERSITI MALAYSIA PAHANG
AL-SULTAN ABDULLAH

2.5.3 Calorific Value

It can be defined as the energy content inherent in fuels, representing the amount of heat a substance produced after complete combustion. It is worth noting that a fuel with low density possesses a higher energy content per unit mass than a high-density fuel. In cases where multiple fuels with different energy contents are used without adjusting the fuel injection accordingly, the same engine will produce varying power outputs. Specifically, rice bran oil exhibits lower mass energy values than pure diesel due to its elevated oxygen concentration (H. Li et al., 2022). RBO must be fed at a higher rate of fuel flow to achieve equivalent power output when compared to diesel fuel.

2.5.4 Cetane Number

Cetane number is a critical parameter in the diesel fuel industry, indicating the fuel's ignition quality and performance in compression ignition engines. It is a measure of the fuel's ability to ignite spontaneously when injected into the combustion chamber, with a higher cetane number implying a shorter ignition delay and leading to smoother engine operation and reduced emissions. The reduction in ignition delays due to increased cetane numbers leads to a decrease in the amount of fuel injected during the premix burn phase and an increase during the diffusion burn phase. Consequently, this leads to a reduction in cylinder pressure rise and potentially decreases cylinder temperatures (Uyumaz et al., 2020). The ignition timing is advanced simultaneously with the increase in combustion pressures and temperatures due to the shorter ignition delay resulting from the use of a fuel with a higher cetane rating.

2.5.5 Cloud and Pour Point

The phenomenon wherein waxes, or minute crystals begin to precipitate in fuel due to a decrease in temperature is sometimes referred to as the cloud point. At this temperature, the fuel undergoes a transition from a liquid state to a solid state, resulting in a reduction in its flowability. This solidification process can occur partially or entirely (Devarajan et al., 2022). In contrast, the pour point is the lowest temperature at which fuel flows. The cloud and pour points of all biodiesel fuels are significantly

UMPSA
UNIVERSITI MALAYSIA PAHANG
AL-SULTAN ABDULLAH

higher than those of diesel fuel. Obstruction of the flow line has the potential to give rise to significant complications, impeding the effective utilization of biofuel, particularly in regions characterized by low temperatures. Low-temperature performance is crucial for biofuel users (R. Singh et al., 2022). It is imperative to implement precautionary measures similar to those that are employed with conventional diesel fuel in order to ensure the satisfactory performance of biofuel and its mixes at low temperatures. In cold temperatures, inadequate performance can be observed through two primary manifestations: filter blockage caused by wax formation and engine starvation resulting from reduced fuel flow. The current fuel regulations in the United States and Europe do not specifically outline the cold flow characteristics for either conventional diesel or biofuel. Additionally, there is no universally agreed-upon method for assessing the performance of both fuels at low temperatures (Puricelli et al., 2021). Biofuel derived from feedstocks characterized by a high concentration of saturated fatty acids, such as palm oil, has suboptimal cold flow characteristics. Fuels derived from feedstocks characterized by high unsaturation in their fatty acid structures, such as rapeseed and safflower oil, have enhanced performance.

2.5.6 Flash Point

The flash point exhibits an inverse relationship with fuel volatility. The purpose of implementing biofuel standards for flash points is to safeguard against potential contamination caused by the presence of mostly highly volatile pollutants, particularly the excess methanol residue remaining after the product stripping processes. The presence of even minimal amounts of residual methanol in biodiesel result in a significant reduction in its flash point. The flash point of various biofuel types is often significantly higher than of diesel fuel, with an increase ranging from 25% to 90%.

2.6 Compression Ignition (CI) Engine

Since the original diesel-powered engine began in 1898, these engines have been extensively utilized as a predominant method of propulsion across many types of transportation, industrial applications, and energy generation. The primary distinction between a CI engine and a SI engine fuelled by gasoline is essentially attributed to the method by which fuel combustion is initiated (Pierce et al., 2019). The ignition process in a gasoline engine is initiated by a spark generated by the spark plug, whereas in a CI engine, the ignition is initiated through spontaneous compression ignition. The compression process of a diesel engine induces a rise in both temperature and pressure, creating an optimal setting for the subsequent operations of fuel injection, atomization, evaporation, and combustion. CI engines are widely recognized for their reduced emissions of CO and HC, as well as their enhanced fuel efficiency (Sharkey, 1997). A diesel engine's air compression ratio typically ranges from 12 to 24 (Heywood, 1988).

Increased compression ratios promote enhanced fuel combustion efficiency due to the elongated effective expansion stroke. In addition, it is worth noting that diesel engines often operate under lean conditions, characterized by air-fuel ratios as high as 65:1, unless they function at their maximum power output (Heywood, 1988). Diesel engines exhibit high thermal efficiency due to their ability to modulate engine speed and output by adjusting fuel injection quantities instead of restricting intake air (Stone, 1999).

CI engines are widely employed in numerous trucks, as well as almost all railroad engines, maritime vessels, and power sources for various industrial purposes, owing to their notable advantages, such as reduced fuel consumption and fewer CO and HC emissions. CI engines are frequently employed in the transportation sector owing to their fundamental arrangement design, enhanced reliability, greater power output achieved with less fuel usage, and higher thermal efficiency.

In addition, CI engines are commonly employed throughout various applications, wherein engines operating at speeds of up to 1200 rpm are utilized for transportation purposes. These engines are equipped with pumps and small electrical generators. Medium-speed engines operating at speeds ranging from 300 to 1200 rpm are commonly employed in various applications such as large-scale electrical generators, ships, and sizable compressors and pumps. Internal combustion engines can be classified in several ways as summarized in Appendix E.

2.6.1 Evolution of Compression Ignition (CI) Engine

The historical development of the compression ignition engine has exhibited a clear correlation with the economic conditions and the progress made in fuel technology. The concept of compression ignition was initially introduced by Schmidt in 1861. However, Rudolph Diesel made the most notable progress in this area by inventing the pressure-ignited heat engine in 1897 (Heywood, 1988). Introducing peanut oil into the cylinder via a high-pressure air burst resulted in its spontaneous ignition under elevated pressure and temperature conditions. The initial diesel engines had significant dimensions and weight due to the requisite inclusion of a costly high-pressure air pump and a robust container to accommodate the forceful air blast. The utilization of diesel engines was limited to stationary applications exclusively before the year 1920, primarily due to the constraints imposed by the dimensions of the fuel injection pump. In 1920, they brought a significant milestone in the advancement of diesel engines, attributed to introducing a groundbreaking injection pump design. This design facilitated the precise fuel metering upon entry into the engine, eliminating the need for pressurized air (Stone, 1999). This development expanded the utilization of CI engines and facilitated the creation of diminutive and efficient diesel engines.

اونيۏرسيتي مليسيا ڤهڠ السلطان عبدالله
UNIVERSITI MALAYSIA PAHANG
AL-SULTAN ABDULLAH

In contrast, the initial diesel engines were fully mechanical, encompassing components such as the fuel pump and injectors. The fuel system's working pressure did not adequately deliver a uniform, well-defined fuel spray pattern (Pierce et al., 2019). The evolution of CI engines was notably influenced by variations in fuel resources as well. Modifications to diesel fuel injection systems were implemented in the early 1920s to enable the substitution of biomass-derived fuel with fossil remnants of reduced viscosity (Stone, 1999). The feasibility of this outcome was facilitated by the concurrent growth and consolidation of the petroleum industry, which provided a conducive environment for the advancement of diesel engine technology. The production of diesel-powered vehicles by Mercedes Benz commenced in the mid-1930s, while the advent of direct-injection diesel truck engines occurred in 1964. By 1974, the production of diesel-powered automobiles had exceeded one million units. In addition to enhanced fuel efficiency, the engine's substantial torque and extended lifespan were unequivocal benefits.

2.6.2 Types of Compression Ignition (CI) Engine

CI engines can be classified into two basic types: two-stroke engines and four-stroke engines. There are two piston strokes for every one power stroke in a four-stroke engine. The strokes are identified as the intake, compression, expansion, and exhaust strokes as illustrated in Figure 2.4. In modern times, most four-stroke engines employ the utilization of turbocharging and intercooling techniques to enhance power output relative to the engine's weight. Furthermore, these engines are equipped with state-of-the-art electronic controls that can modify the timing of fuel injection and other engine parameters to mitigate emissions (Lilly, 1984).

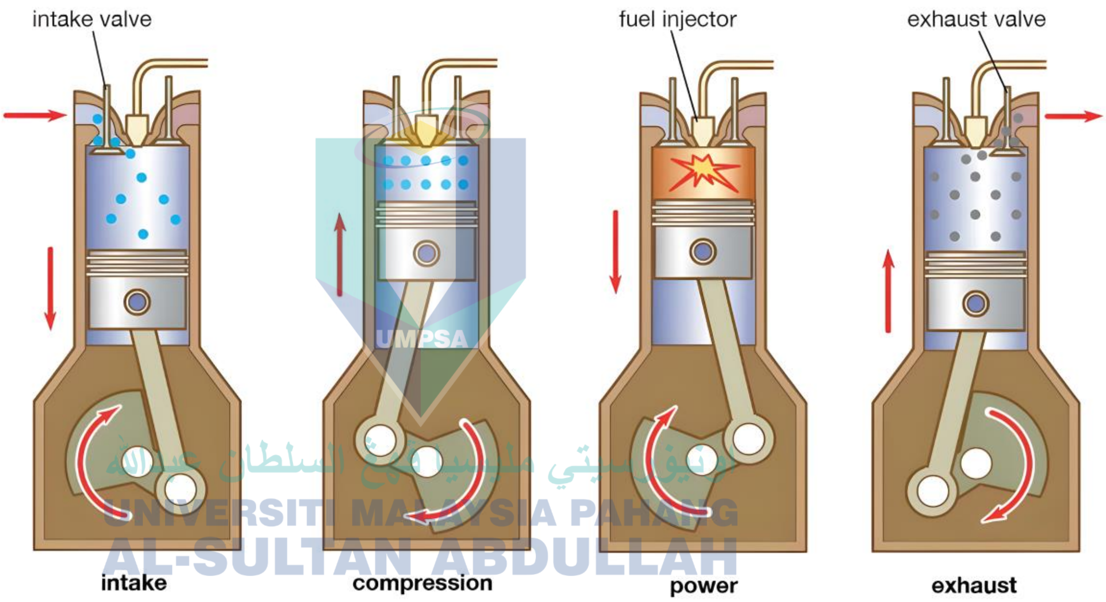

Figure 2.4 Four stroke compression ignition engine cycles
Source: Lilly (1984)

Two-stroke engines effectively combine the induction and exhaust strokes, performing the intake and exhaust processes concurrently at the commencement of the compression stroke and the end of the combustion stroke. Consequently, a higher power level is generated with each piston stroke. As a two-stroke engine exhibits a greater number of power strokes per unit of time than a four-stroke engine, it is reasonable to conclude that the former will have greater power.

Two notable limitations are associated with the two-stroke engine: the direct transfer of the fuel-air mixture into the exhaust system and the blending of the fresh fuel-air mixture with the remnants of the exhaust gases. During the simultaneous opening of the intake and exhaust valves, a certain amount of air is introduced into the cylinder to remove the exhaust gases effectively. The utilization of two-stroke engines reduces exhaust temperature compared to four-stroke engines, hence influencing the performance of the turbocharger (Heywood, 1988). In the scavenging phase of the two-stroke cycles, oil droplets may be expelled, leading to a notable increase in lubrication oil losses through the exhaust system. This phenomenon is also associated with excessive emissions of particulate matter and hydrocarbon compounds.

2.6.3 Modern Compression Ignition (CI) Engines

The evolution of the compression ignition engine is influenced by several significant aspects, namely cost, the availability of adequate fuel, and adherence to pollution restrictions. Contemporary advancements in diesel engine technology have resulted in the development of diesel engines that exhibit seamless operation, enhanced fuel efficiency, reliability, and notable acceleration capabilities. The maximum power output of a diesel engine is contingent upon the optimal combustion of fuel within the cylinder. The microprocessor in the electronic control injector calculates the optimal injection timing and fuel quantity based on the driver's request, engine speed, air inlet temperature, and engine coolant temperature. The electronic injector exhibits a notable fuel pressure capability of up to 1000 bar; nevertheless, due to its elevated cost, widespread adoption of this technology has been limited. The common rail injection system, which emerged in the early 1990s, represents a significant technological in fuel injection systems.

The operation of common rail diesel fuel injectors differs from that of mechanical fuel injectors, which rely on the position and speed of the camshaft to drive the plungers. Common rail fuel injection systems are designed to deliver gasoline to an individual injector that is electronically controlled. A central accumulator rail stores the fuel at high pressure prior to injection. This suggests that the gasoline pump has the capability to pressurize the fuel rail without any fuel being discharged, reaching

UMPSA
اونيۏرسيتي مليسيا ڤهڠ السلطان عبدالله
UNIVERSITI MALAYSIA PAHANG
AL-SULTAN ABDULLAH

pressures as high as 250 kpsi (Teoh et al., 2019). The enhancement of fuel efficiency, reduction in exhaust emissions, and mitigation of engine noise are attributed to the more exact management of atomized fuel quantities.

2.7 Combustion in Compression Ignition (CI) Engines

Compression ignition (CI) engines have a complex combustion mechanism. The behaviours of the combustion process in an engine cylinder have been studied extensively. In a CI engine, combustion began after only a few crank angle degrees of injection initiation. In an engine cylinder, a chemical reaction occurs that produces a diffusion flame at the fuel-air interface. As a quick burning spreads in the combustion chamber, the heat release begins and increases, then reduces as the available oxygen is consumed (Heywood, 1988). There are two main steps to the combustion process. Mixing controlled combustion and premixed combustion. The liquid fuel delivered to the engine is compressed into a finely atomized form, evaporated, and injected into the combustion chamber's hot and highly compressed air. When the local temperature approaches or exceeds the auto-ignition temperature, combustion begins. The ignition delay is the time gap between the start of injection (SOI) and the start of combustion (SOC). In a diesel engine, this characteristic has a significant impact on the quality of combustion (Pulkrabek, 2014).

UMPSA
اونيۏرسيتي مليسيا ڤهڠ السلطان عبدالله
UNIVERSITI MALAYSIA PAHANG
AL-SULTAN ABDULLAH

The premixed combustion phase is formed from the initial combustion of the fuel vapor-air mixture. The mixing-controlled combustion phase is the final stage of the combustion process. The double peak shape of the heat release rate emerges in diesel combustion because of two-phase combustion occurring throughout the combustion stroke. The premixed combustion produces the first peak. The heat release curve is relatively independent of engine load in the premixed combustion phase since early mixing is independent of engine injection length. The mixing regulated combustion phase produced the second peak of the heat release curve. The mixing-controlled heat release's magnitude and duration are proportional to the injection time. Typically, the heat release curve is produced using cylinder pressure data ranging from -20 ° BTDC to 40 ° ATDC (Heywood, 1988).

Cylinder pressure is one of the most important characteristics to measure to acquire a thorough understanding of the combustion process in the engine cylinder (Heywood, 1988). The assumptions used to calculate the heat release rate include quasi-static (temperature and pressure), uniform gases in the cylinder, no dissociation of the chemical compounds present after combustion, the cylinder engine being a closed system, and the specific heat of the gaseous mixture being calculated as a function of temperature. The contour of the heat release rate, which indicates various combustion behaviours, varies depending on the engine type, speed, and load (Dabi & Saha, 2022). As illustrated in Figure 2.5, two distinct categories of diesel engine combustion systems exist: direct injection (DI) engines and indirect injection (IDI) engines.

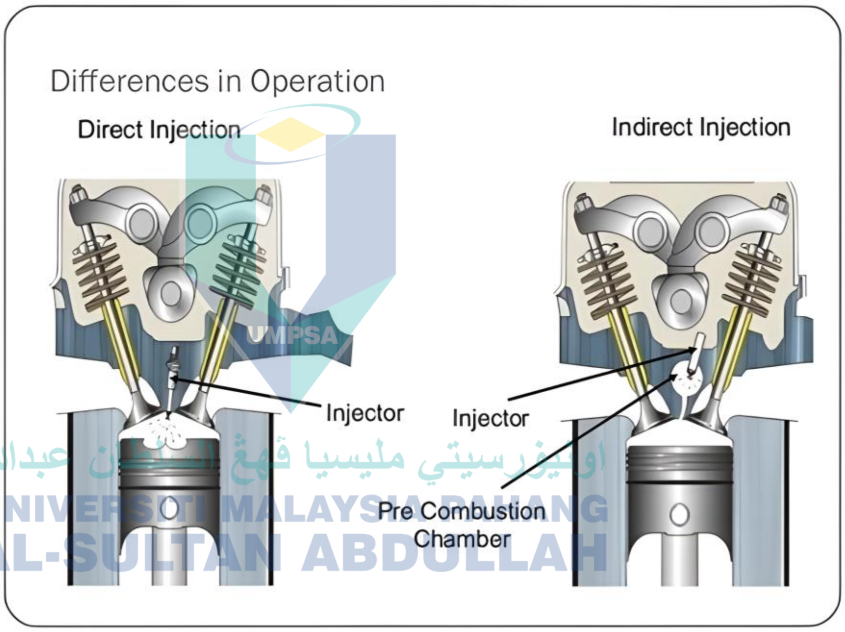

UMPSA
UNIVERSITI MALAYSIA PAHANG
AL-SULTAN ABDULLAH

Figure 2.5 Direct injection and indirect injection combustion systems in compression ignition engines

Source: Heywood (1988)

In comparison to internal combustion engines (IDI), which incorporate a partitioned combustion chamber and introduce fuel at a lower injection pressure into the pre-chamber where the combustion process initiates, direct injection (DI) engines have a solitary open combustion chamber where fuel is directly injected. The rise in pressure resulting from the process of combustion induces the fuel to be pushed back into the primary chamber. Subsequently, the air present in the primary chamber becomes entrained and blends with the jet emanating from the nozzle. The implementation of a partitioned combustion chamber facilitates the enhancement of combustion velocity and the maintenance of optimal fuel-air blending. IDI combustion systems exclusively utilize small engines. The production and discharge of diesel emissions are impacted by various factors related to the engine and fuel components, which can be understood by acquiring a basic understanding of the combustion process in CI engines.

The fuel injection system initiates the introduction of low-volatility diesel fuel into the cylinder at a significantly high pressure during the final stage of the compression stroke (Heywood, 1988; Stone, 1999). The cold liquid fuel undergoes atomization to generate minuscule fuel droplets, which then evaporate and blend with the surrounding air under elevated temperature and pressure conditions. Autoignition occurs due to this phenomenon; however, the commencement of combustion is temporally postponed by a few degrees of crank angle. The ignition delay refers to the temporal interval, measured in crank angle or time, that transpires from the initiation of fuel injection to the commencement of combustion. The phenomenon known as diesel knock arises from the rapid and premature combustion resulting from the initial rapid increase in pressure. A notable proportion of the introduced diesel will undergo spontaneous ignition in the presence of an extended ignition delay, leading to the characteristic knocking sound during the initial stages of combustion. During the delay period, there is a reduction in the quantity of the mixture, and the delay duration is decreased to mitigate the occurrence of diesel knock.

UNIVERSITI MALAYSIA PAHANG AL-SULTAN ABDULLAH

The combustion process will occur spontaneously when specific regions of the adjacent vapor-air combination attain or exceed the autoignition temperature (Heywood, 1988; Stone, 1999). The stage of combustion referred to as "premixed burn" is the appropriate terminology in this context. The period under consideration exhibits the highest heat release rate, accompanied by elevated temperatures and pressures. The increased temperature and enhanced mixing result in a higher production of NOx and a reduced emission of soot particles. This phenomenon occurs when the combustion process progresses to a stage when the initial mixture of fuel and air, which was ignited during the ignition delay, is fully consumed. At this point, the rate at which the remaining fuel and air are combined becomes the primary limiting factor for the burning rate. The phase is referred to as certain properties that characterize mixing-controlled, or diffusion burn. There is a subsequent peak in the heat release as the phase progresses. During the piston stroke, the expanding working volume causes the temperature of the gases in the cylinder to decrease. The oxidation of soot and combustion products with excess fuel can release a portion of the fuel's energy, although at a reduced rate. The term "late oxidation" pertains to a certain temporal period.

2.7.1 Combustion Phase of Compression Ignition (CI) Engines

An investigation of the rate of heat release (RoHR) can prove to be a valuable tool in understanding and describing combustion when implementing CI engine. The calculation or derivation of this parameter is based on the analysis of in-cylinder pressure data (Heywood, 1988). Specifically, it involves the utilization of the pressure signal obtained from an in-cylinder pressure sensor. The parameter in question denotes the speed at which the system undergoes the conversion of chemical energy derived from the fuel. It can be seen as the rate of the underlying reaction from a chemical perspective. In a four-stroke CI engine, the critical temporal interval during which the response occurs is a concise duration encompassing the TDC position, occurring between the compression and expansion strokes (as depicted in Figure 2.4). This is the moment when the fuel is fed into the cylinder. Figure 2.6 illustrates the RoHR during the operation of a conventional direct injection compression ignition (DI CI) engine utilizing diesel fuel.

UMPSA
اونيۏرسيتي مليسيا ڤهڠ السلطان عبدالله
UNIVERSITI MALAYSIA PAHANG
AL-SULTAN ABDULLAH

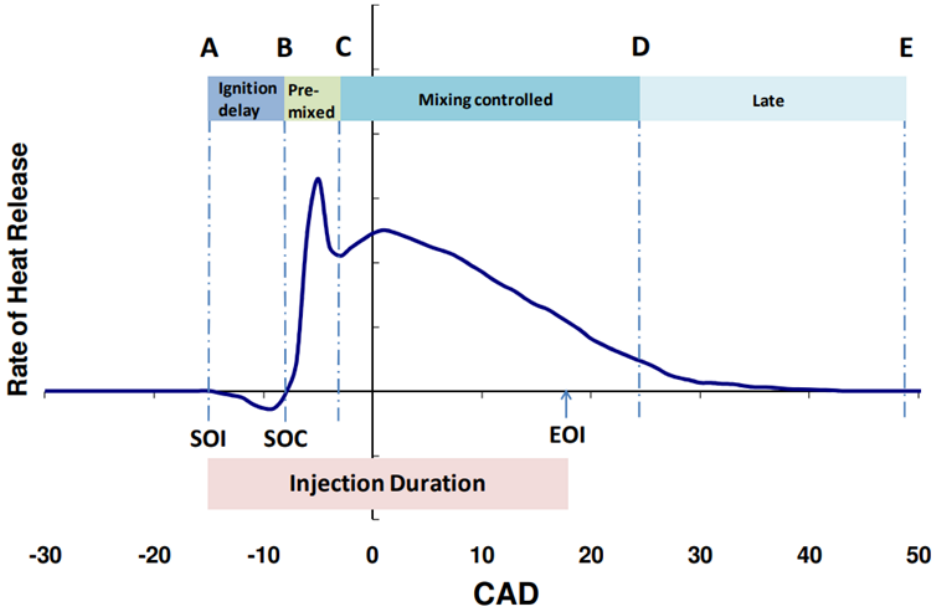

Figure 2.6 The phase of combustion for a direct injection compression ignition engine

Source: Heywood (1988)

A-B Ignition delay- The duration between initiation of fuel injection and concluding at the commencement of combustion, commonly referred to as the SOC. The observed phenomenon can be identified as a phase characterized by the vaporization of fuel, as indicated by the initial minor negative RoHR depicted in Figure 2.6. The commencement of the SOC (or reaction/burn) is characterized by the occurrence of the initial positive RoHR (Heywood, 1988).

UMPSA
UNIVERSITI MALAYSIA PAHANG
AL-SULTAN ABDULLAH

B-C Premixed combustion phase: During the ignition delay phase, fuel that has been combined with air, forming a premixed fuel-air mixture, undergoes fast combustion. This phenomenon occurs because of the sufficient duration for the fuel and air to thoroughly blend, leading to the attainment of the mixture's flammability threshold and subsequent combustion within a limited number of crank angle degrees (CAD). Simultaneously, the injection of fuel occurs within this thermally intense combustion blend, so facilitating the liberation of heat. The sharp, distinctive peak is attributed to the premixed phase (Heywood, 1988).

The mixing-controlled combustion phase is responsible for most of the combustion in CI engines. The ignition delay results in the entire pre-mixed mixture being consumed within a short period of time. Currently, the regulation of the heat release rate is solely dependent on the speed at which the mixture becomes accessible for combustion. The rate in question is primarily governed by the process of fuel vapor-air mixing, which is subject to the influence of numerous parameters (Heywood, 1988).

D-E Late combustion phase: The combustion phase persists throughout the expansion stroke. The heat generated during this period could be attributed to the presence of unburned fuel or incomplete combustion products, such as CO, which are now able to release further heat. This phenomenon could be attributed to the promotion of mixing within the expanding cylinder. It is essential to consider that the heat release will be diminished during this interval since the cylinder temperatures are decreasing because of the expansion of the stroke. Even though NOx formation is given priority because of their harmful effects and the challenges associated with reducing them, the model presented here provides a concise analysis of the combined formation of soot and NOx.

2.7.2 Thermochemistry

The primary source of energy for internal combustion engines is derived from the combustion process involving hydrocarbon fuel and air. This chemical reaction converts the chemical energy into internal energy within the gases present in the engine (Pulkrabek, 2014). There is a vast array of hydrocarbon fuel constituents, numbering in the thousands, primarily composed of hydrogen and carbon, with the potential inclusion of oxygen (in the form of alcohols), nitrogen, sulfur, and other elements. The most effective amount of chemical energy that can be released (in the form of heat) from the fuel occurs during its reaction (combustion) with an exact stoichiometric proportion of oxygen. Stoichiometric oxygen, also known as theoretical oxygen, refers to the precise amount of oxygen required to completely convert all carbon present in the fuel to CO_2 and all hydrogen to H_2O, without any excess oxygen remaining (Pulkrabek, 2014). The overall complete combustion equation using the following Eq. (2.1):

$$C_aH_b + \left(a + \frac{b}{4}\right)(O_2 + 3.773N_2) \rightarrow aCO_2 + \frac{b}{2}H_2O + 3.773\left(a + \frac{b}{4}\right)N_2 \qquad 2.1$$

2.7.3 Air-Fuel Mixture Classification

The air-fuel mixture refers to the ratio at which air and fuel, often petrol, are combined to facilitate the optimal functioning of an engine. In the suction process of a petrol engine, the air-fuel mixture is drawn in, after which combustion occurs by the ignition of sparks. Engines may exhibit varying performance characteristics under different conditions during their operational cycle. The engine may operate under varying conditions, including slow, high, and medium speeds, with the speed being influenced by the composition of the air and fuel combination. The composition of the air-fuel mixture is contingent upon the operational velocities at which the engine is intended to operate (Cengel & Boles, 2006). The categorization of engine speeds will be distinguished into low, average, and high speeds, hence influencing the classification of air-fuel mixtures, which are discussed below.

2.7.3.1 Stoichiometric Mixture

A stoichiometric mixture (also known as a chemically correct mixture) refers to an air-fuel mixture when the quantity of air present is sufficient to oxidise the fuel fully during the combustion process. The term "complete combustion" refers to the process by which all hydrocarbons present in a fuel are fully transformed into CO_2 and water (Cengel & Boles, 2006).

2.7.3.2 Rich Mixture

This rich mixture is characterized by a lower air content than the stoichiometric mixture. More air supply is needed to ensure the achievement of complete fuel combustion. The composition of this mixture exhibits an abundance of fuel (Heywood, 1988).

2.7.3.3 Lean Mixture

This mixture refers to the air-fuel combination with excess of air compared to the stoichiometric ratio. The combination exhibits a great deal of air. The lean mixture demonstrates greater efficiency in comparison to a stoichiometric mixture. There are several benefits associated with the utilization of lean mixture in engines. These advantages encompass reduced heat loss, decreased occurrence of engine knocking, minimized throttling loss, and the ability to attain greater compression ratios (Heywood, 1988).

Eq. (2.15) defines the stoichiometric (or chemically correct or theoretical) proportion of fuel and air in which there is just enough oxygen for conversion of all the fuel into completely oxidized products. The stoichiometric air-fuel (A/F) or fuel-air (F/A) ratios depend on fuel composition. For actual combustion in an engine, the equivalence ratio (ϕ) is a measure of the fuel-air mixture relative to stoichiometric conditions. It is defined as:

$$\phi = \frac{\left(\frac{F}{A}\right)_{act}}{\left(\frac{F}{A}\right)_{stoich}} = \frac{\left(\frac{A}{F}\right)_{stoich}}{\left(\frac{A}{F}\right)_{act}} \qquad 2.2$$

UMPSA
اونيۏرسيتي مليسيا ڤهڠ السلطان عبدالله
UNIVERSITI MALAYSIA PAHANG
AL-SULTAN ABDULLAH

where $\left(\frac{F}{A}\right)_{act}$ is actual fuel-air ratio

$\left(\frac{F}{A}\right)_{stoich}$ is stoichiometric fuel-air ratio

$\left(\frac{A}{F}\right)_{act}$ is actual air-fuel ratio

$\left(\frac{A}{F}\right)_{stoich}$ is stoichiometric air-fuel ratio

There are two methods (Eq. 2.3 and 2.4) to identify the ratio of air-fuel or fuel-air, which are by using an equation consisting of a mass of air-fuel or fuel-air or by using an equation consisting of the mass flow rate of air-fuel or fuel-air.

$$\frac{F}{A} = \frac{m_f}{m_a} = \frac{\dot{m}_f}{\dot{m}_a} \quad 2.3$$

$$\frac{A}{F} = \frac{m_a}{m_f} = \frac{\dot{m}_a}{\dot{m}_f} \quad 2.4$$

where m_f is the mass of fuel

m_a is the mass of air

$\dot{m}_f$ is the mass flow rate of fuel

$\dot{m}_a$ is the mass flow rate of air

Table 2.2 below is the summary of the relation equivalent ratio with the types of air-fuel mixtures (Heywood, 1988). When the value of the equivalent ratio is less than 1, the mixture is considered lean; while the equivalent ratio is more than 1, the mixture is described as rich. The stoichiometric mixture can be obtained and measured when the equivalent ratio is 1.

Table 2.2 Relation equivalent ratio with the types of air-fuel mixtures

Equivalent Ratio (ϕ)	**Types of Mixture**
$\phi < 1$	Lean mixture (oxygen in exhaust)
$\phi > 1$	Rich mixture (CO and fuel in exhaust)
$\phi = 1$	Stoichiometric mixture (maximum energy released from fuel)

UMPSA
UNIVERSITI MALAYSIA PAHANG AL-SULTAN ABDULLAH

2.7.4 Ignition Delay

Ignition delay is the period during which some fuel has been admitted but has not yet been ignited. An injection curve is counted from the moment the injection begins until the point at which it separates from a pure air compression curve. There are two general types of ignition delay: physical delay and chemical delay. The physical delay is the time elapsed between the beginning of injection and the achievement of chemical reaction conditions. The fuel is atomized, vaporized, mixed with air, and raised in temperature during the physical delay period. The chemical delay is another type of ignition delay. Pre-flame reactions begin slowly during this time period and then accelerate until local inflammation or ignition occurs. At high temperatures, chemical reaction is quicker and physical delay is longer than chemical delay.

There are several factors affecting ignition delay period. i) Fuel: Lower self-ignition temperature means a lower delay period. Higher CN means a lower delay period and smooth engine operation. ii) Intake Temperature: Increase in intake temperature would result in increase in compressed air temperature which would reduce the delay period. iii) Compression ratio: Increase in compression ratio reduces delay period as it raises both temperature and density. iv) Type of combustion chamber: A pre-combustion chamber gives shorter delay compared to an open type of combustion chamber. v) Injection advance: Delay period increases with increase in injection advance angle. (with increase in injection angle, pressure and temperature are lower when injection begins). If the Ignition delay period is long, a large amount of fuel will be injected and accumulated in the chamber. The auto-ignition of this large amount of fuel may cause high RoPR and high maximum pressure which may cause knocking in CI engines. A long delay period not only increases the amount of fuel injected by the moment of ignition, but also improves the homogeneity of the fuel- air mixture and its chemical preparedness for explosion type of self-ignition similar to detonation in SI engines (Pulkrabek, 2004).

2.7.5 Mixing Controlled Combustion

The compression ignition combustion process in different types of CI engines is interpreted how the diesel diffusion flame forms, following ignition and start of the premixed-burned phase, spreads rapidly and envelops the spray. Depending on the spray configuration, the visible flame may then fill almost the entire combustion chamber. the diffusion flame and spray geometries are closely related.

Mixing processes are also critical during the ignition delay period: while the duration of the delay period is not influenced in a major way by the rates of spray processes which together control "mixing", the amount of fuel mixed with air to within combustible limits during the delay (which affects the RoPR once ignition has occurred) is obviously directly related to mixing rates. However, while it is well accepted that CI combustion is normally controlled by the fuel-air mixing rate, the mechanism by which the diffusion flame forms, spread rapidly and then stabilizes are not well understood. The difficulties are twofold. First, the spray geometries in real CI combustion systems are extremely complex. Second, the phenomenon of the development of the unsteady turbulent diffusion flame (Heywood, 1988).

UMPSA
اونيۏرسيتي مليسيا ڤهڠ السلطان عبدالله
UNIVERSITI MALAYSIA PAHANG
AL-SULTAN ABDULLAH

2.7.6 Intake Air Temperature

It is important to note that the ignition delay is a crucial parameter which characterizes the initiation of combustion and, consequently, its development in diesel engines. It is primarily determined by chemical factors related to the fuel structure and its properties as well as physical factors related to the engine operating conditions. Table 2.3 presented the several studies have been conducted regarding the effect of intake air temperature on the performance of CI engines. Further, the effect of the charge intake air temperature has been extremely important in recent developments of HCCI engines worldwide. Air properties such as density, which is related to intake air temperature, play a significant role in determining mass flow rate. When the intake air temperature of the charge is reduced, the volumetric efficiency is increased.

Table 2.3 Effects of increase intake air temperature studied in a CI engine

Engine Type	Engine Performance Characteristics	Exhaust Emission Characteristics	Combustion Behaviours	References
Single cylinder 4-stroke, 661 cc		HC ↓ CO ↓	IP ↑ ID ↓	(Z. Xu et al., 2018)
Single cylinder 4-stroke water cooled HCCI, 661 cc	BTE ↑	NOx ↑ HC ↓ CO ↓		(Veza et al., 2022)
Single-cylinder naturally aspirated water-cooled 4-stroke, 473 cc		NOx ↓ Soot ↑	IP ↑ ID ↓	(Yilmaz & Gumus, 2018)
6-cylinder turbo-charge CRDI, 2993 cc	BSFC ↓	PM ↓ HC ↓	ID ↓	(Sajjad et al., 2023)

اونيۏرسيتي مليسيا ڤهڠ السلطان عبدالله
UNIVERSITI MALAYSIA PAHANG
AL-SULTAN ABDULLAH

Nonetheless, an increase in intake air temperature may also improve fuel vaporization within engine cylinders. This is especially important for compression ignition engines that run on biofuels and biodiesels. There has been considerable research conducted to explain the effect of fuel vaporization for biofuels and biodiesels. Both biofuels and biodiesels are composed of mono alkyl esters of vegetable oils and animal fats. As a result of the difference in chemical structure between the fuels, there is a distinct effect on the chemical reaction pathways during ignition and combustion. It was observed that an increase in intake air temperature resulted in a reduction in the mass of the in-cylinder trap (thermal throttling effect). Thus, when intake air temperature increases, oxygen and heat capacity of the air charge are significantly reduced.

(Zhou et al., 2018) investigated the effect of charge intake air temperature on compression ignition engines. The author has carried out a series of experiments with an inline-4 CI engine. An EGR system, a common-rail injection system, and a Variable Geometry Turbocharger (VGT) were all included in this engine. This experiment involved operating the engine with pure diesel fuel at a constant engine speed, EGR ratio, and boost pressure at the intake. During the test, the charge intake temperature was varied from 20 °C to 38 °C. He concluded that increasing the intake air temperature at constant boost pressure results in a slight decrease in RoHR. The fuel jet has been suggested to entrain less air at constant boost pressure due to a reduced in-cylinder gas density, which causes less oxygen-fuel mixing and a lower RoHR.

The study conducted by Veza on influence of intake air charge temperature on the performance and emissions of a compression ignition engine. A variable intake air temperature was used, but the coolant temperature was controlled to isolate the temperature of the cylinder wall. It was concluded from the report that an increase in intake air temperature leads to an increase in NOx emissions (Veza et al., 2022). It is believed that biofuel and biodiesel are more likely to form fuel rich zones at low load conditions than other fuels, because of its higher viscosity and higher fuel distillation curves. Furthermore, biofuel and biodiesel are less likely to atomize and vaporize than pure diesel fuel due to their higher density, kinematic viscosity, and distillation temperature. The argument supported by the researcher; Sajad on a SI natural gas engine suggested that even a small change in air intake temperature significantly changed the engine's performance and emissions (Sajjad et al., 2023). As part of the study, he evaluated the engine performance and emissions of the engine with three different air intake temperatures (10°C, 26.7°C, 54.4°C).

2.8 Engine Performance from Compression Ignition (CI) Engine

CI engines have gained popularity in the power production and transportation sectors owing to their comparatively low fuel consumption rates. CI engines are widely recognized as significant contributors to environmental pollution, primarily due to the substantial generation of emissions during the combustion process.

Biodiesel and biofuel are considered a viable solution for reducing emissions from CI engines (Jayaraman et al., 2023). This section provides an analysis and evaluation of different alternative fuels and additives that are commonly utilized. The present section explores alternative fuels and additives that are combined with traditional fuels such as diesel or petrol.

Table 2.4 show the engine performance characteristics, exhaust emission characteristics and combustion behaviours of different fuel blends. The details explanation was discussed in the next sub section. Figure 2.7 present a visual representation of the disparities seen the manufacturer-provided data pertaining to the output power, torque as well as BSFC. The engine performance limit to the 3500 rpm (highest) and the performance of engine dropped after exceeding 3500 rpm.

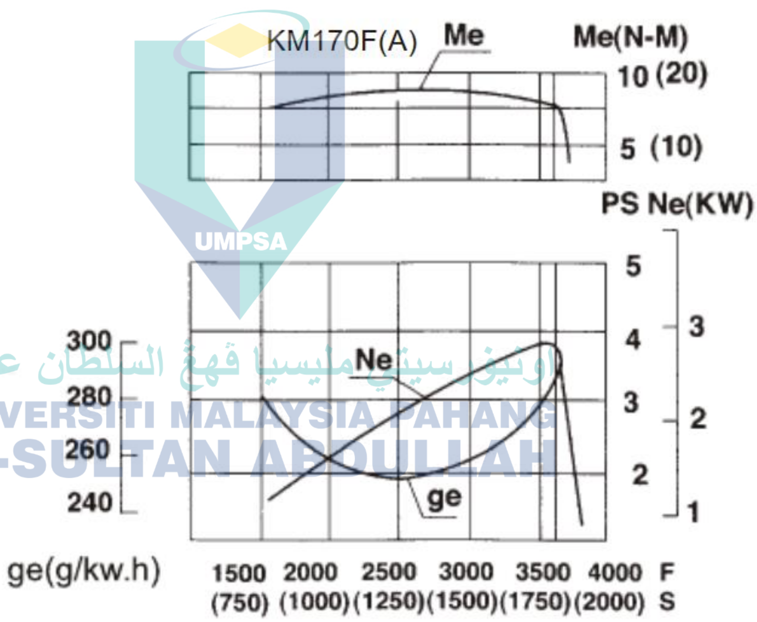

UMPSA
UNIVERSITI MALAYSIA PAHANG
AL-SULTAN ABDULLAH

Figure 2.7 A KIPOR 170FS diesel engine performance curve

Source: Stone (1999)

Table 2.4 Engine performance characteristics, exhaust emission characteristics and combustion behaviours of different fuel blends

Engine Specifications	**Fuel and Its Blends**		**Operating Parameters**	**Engine Performance Characteristics**			**Exhaust Emissions Characteristics**			**Combustion Behaviours**		**References**
	Fuel	**Additives**		**BP**	**BTE**	**BSFC**	**HC**	**CO**	**NOx**	**CP_{Max}**	**RoHR**	
			1st Generation biodiesel									
1-C, 4-S, CR-18, 3.5kw @1500 rpm	Palm + Hydrogen D, D + 7lpm, D + 10lpm, P20, P20 + 7lpm,P20 + 10lpm		@90% load for P20 + 10lpm H2		↑	↓	↓	↓	↑	↑	↑	(Jeyaseelan et al., 2021)
CR-18.5:1, 7.5 kW@1500–2400rpm, FIP 240–500 bar	Palm B30GNP40DMC10,B30GNP80DMC10,B30GNP120DMC10	Graphene nano-particles, Dimethyl carbonate	@1900RPM for B30GNP40DMC10		↑	↓	↓	↓	↑			(Hirner et al., 2019)
4-C,4-S, CI engine CR-22.5:1;Rated power 89 kW at 3200 rpm	Soyabean + H2 B20, B100, B20 + A, H + B20 + A, B100, B100+ A, B100 + H + A	Nanoparticles (Alumina) Al_2O_3	@2400 rpm for H + B20 + A	↑	↑	↓	↓	↓	↑			(Das et al., 2022)

UMPSA
UNIVERSITI MALAYSIA PAHANG AL-SULTAN ABDULLAH

Table 2.4: Continued

Engine Specifications	Fuel and Its Blends		Operating Parameters	Engine Performance Characteristics			Exhaust Emissions Characteristics			Combustion Behaviours		References
	Fuel	**Additives**		**BP**	**BTE**	**BSFC**	**HC**	**CO**	**NOx**	**CP_{Max}**	**RoHR**	
			2nd Generation biodiesel									
1-C, CR-17.5:1, 7.5 KW at 1500 to 3000 rpm	Cottonseed + octanol + MWCNTB20(O5, O10,O20),B40(O, O10, O20), B60(O5, O10,O20),B100 (O5, O10, O20)		@75% Load for B40 + O15		↓	↑	↓	↓	↑			(R. Li & Wang, 2018)
	B20(O5, O10, O20) + MWCNTB40 (O5, O10, O20) + MWCNTB60 (O5, O10, O20) + MWCNTB100 (O5, O10, O20) + MWCNT		@100% Load for B20 + O15 + MWCNT		↓	↑	↓	↓	↑			

UMPSA
اونيۏرسيتي مليسيا ڤهڠ السلطان عبدالله
UNIVERSITI MALAYSIA PAHANG
AL-SULTAN ABDULLAH

Table 2.4: Continued

Engine Specifications	Fuel and Its Blends		Operating Parameters	Engine Performance Characteristics			Exhaust Emissions Characteristics			Combustion Behaviours		References
	Fuel	Additives		BP	BTE	BSFC	HC	CO	NOx	CP_{Max}	RoHR	
CR-17.5:1; Rated power-5.2KW @1500	Waste cooking oil biodiesel + H2 + CeO2 B20H0.5C40, B20H1.0C40, B20H1.5C40, B20H0.5C80, B20H1.0C80, B20H1.5C80		B20 H1.5C80		↑	↓	↓	↓	↓			(Jayaraman et al., 2022)
4-S,1-C, CR-17.5:1 Rated Power 5.2 kW @ 1500 rpm	Neem biodiesel + n-Decanol NB20; NB20DI10; NB20DI30; NB	n-Decanol			↓	↑	↓	↓	↑	↑	↑	(Sakthivadivel et al., 2022)

UMPSA
اونيۏرسيتي مليسيا ڤهڠ السلطان عبدالله
UNIVERSITI MALAYSIA PAHANG
AL-SULTAN ABDULLAH

Table 2.4: Continued

Engine Specifications	Fuel and Its Blends		Operating Parameters	Engine Performance Characteristics			Exhaust Emissions Characteristics			Combustion Behaviours		References
	Fuel	**Additives**		**BP**	**BTE**	**BSFC**	**HC**	**CO**	**NOx**	**CP_{Max}**	**RoHR**	
2-C,4-S; CR-18:1; Rated Power 3.5kW@1500 rpm; FIT-23CA bTDC; FIP-240 bar	Karanja + Rice bran oil KB20 + H2; KB10 + H2; RB10 + H2: RB20 + H2: D:D + H2		Speed-700 to 1500 RPM for KB20		↑	↓	↓	↓	↑	↑	↑	(Krishana et al., 2022)
1-C,4-S, CI engine CR-17.5:1; Rated power 4.5 kW @ 1500 rpm	Karanja and roselle oil D, KB10, KB20, KB100, LA10, LA20, LA100		At full load for KB20		↓	↑	↓	↓	↑	↑	↑	(Lee et al., 2017)

UMPSA
اونيۏرسيتي مليسيا ڤهڠ السلطان عبدالله
UNIVERSITI MALAYSIA PAHANG
AL-SULTAN ABDULLAH

Table 2.4: Continued

Engine Specifications	Fuel and Its Blends		Operating Parameters	Engine Performance Characteristics			Exhaust Emissions Characteristics			Combustion Behaviours		References
	Fuel	Additives		BP	BTE	BSFC	HC	CO	NOx	CP_{Max}	RoHR	
1-C,4-S, CI engine CR-18:1; Rated power 5.2 kW @ 1500 rpm	Eucalyptus + n-butanol B20, B100, B20-5Bu, B20-10Bu, and B20-15Bu	n-butanol	At full load for B20 + 15bu		↓	↑	↓	↓	↓	↑	↑	(Kumar & Goga, 2023)
1-C,4-S, CI engine CR-17.5:1; Rated power 3.7 kW @ 1500 rpm	Rice bran B5D95GO30 and B15D85GO30	Graphene oxide + nanoparticles	IT@23 deg for B15D85GO30		↑	↓	↓	↓	↑	↑	↑	(Hoang et al., 2021)

UMPSA
اونيۏرسيتي مليسيا قهڠ السلطان عبدالله
UNIVERSITI MALAYSIA PAHANG
AL-SULTAN ABDULLAH

Table 2.4: Continued

Engine Specifications	Fuel and Its Blends		Operating Parameters	Engine Performance Characteristics			Exhaust Emissions Characteristics			Combustion Behaviours		References
	Fuel	Additives		BP	BTE	BSFC	HC	CO	NOx	CP_{Max}	RoHR	
3rd Generation biodiesel												
1-C,4-S, CI engine, CR-17.5:1, Speed1500rpm@ 5.2 kW	Algae ES20D80 + GO20 + 3lpm, ES20D80 + GO40+ 3lpmES20D80 + GO60 + 3lpm, ES20D80 + GO80 + 3lpm	Graphene oxide			↓	↑	↓	↓	↓			(Jayaraman et al., 2023)
CR-17.5:1; Rated power- 3.2KW @1500	Spirullina biodiesel + H2 + TiO2/CeO2 D, B30, B30T, B30C, B30TH, B30CH				↓	↑	↓	↓	↑	↑	↑	(Yao et al., 2019)

UMPSA
اونيۏرسيتي مليسيا ڤهڠ السلطان عبدالله
UNIVERSITI MALAYSIA PAHANG
AL-SULTAN ABDULLAH

2.8.1 Engine Brake Power (BP)

Engine power is used to represent experimental data to illustrate engine performance with different fuels. There is a direct relationship between engine torque and engine speed that governs brake power. The dynamometer controller directly records the engine output as engine brake torque. The engine brake power is calculated using the output torque using the formula Eq. (2.5) (Heywood, 1988):

$$P = \frac{2\pi NT}{60000} \qquad 2.5$$

where P is the engine brake power (kW)

T is the engine brake torque (N.m)

N is the engine speed (rpm)

The power output of a CI engine fuelled with biodiesel is influenced by the chemical mechanism of the engine arrangement and the qualities inherent in the biodiesel. This power output can vary, either being low or high, depending on these factors. The study has investigated and experimented to evaluate the performance of soybean biodiesel on a single-cylinder, four-stroke diesel engine operating at maximum load (Nema et al., 2022).

UMPSA
اونيۏرسيتي مليسيا ڤهڠ السلطان عبدالله
UNIVERSITI MALAYSIA PAHANG
AL-SULTAN ABDULLAH

It has been observed that the power output is nearly equivalent to that of ordinary diesel fuel. An analysis has been conducted on the impact of two widely used feedstocks, namely coconut oil and palm oil, on the performance and emission levels of a 10 kW, horizontal, single-cylinder direct injection diesel engine (Muhammed Niyas & Shaija, 2022). According to their assertions, the utilization of PB15CB15 (a blend consisting of 15% palm oil biodiesel and 15% coconut oil) has been shown to enhance brake torque and power output. Similarly, the implementation of PB30 (a blend comprising 30% palm oil biodiesel) has been seen to enhance brake thermal efficiency. In their study, Atabani examines the comparison between two types of biodiesel, Millettia pinnata (MP) and Croton megalocarpus (CM), in relation to neat diesel fuel (Atabani et al., 2014). The study evaluated the performance and emission characteristics of fuel blends, including 20% biodiesel and diesel fuel. The experiments were conducted using a single-cylinder diesel engine under varying load and speed conditions. The implementation of MP20 and CM20 resulted in a decrease in braking power by 3.70% and 0.53%, respectively. Additionally, the brake thermal efficiency saw a reduction of 3.36% and 1.41% due to the application of MP20 and CM20, respectively. The power output may decrease due to the insufficient energy content of biodiesel to generate thermal energy in the engine. However, it is worth noting that biodiesel exhibits enhanced emission characteristics when compared to conventional diesel fuel.

A study conducts a preliminary heating of the rapeseed biodiesel prior to its utilization in the compression ignition (CI) engine. The findings indicate that the increase in power for the blends is comparatively smaller than that of diesel fuel. This can be attributed to the decrease in viscosity of the mix due to preheating, which leads to increased leakages in the pump and injector. Consequently, this results in lower power outputs (Bhattacharyya et al., 2021). An investigation was carried out on a CI engine to evaluate the emission and performance characteristics when utilizing a blend of N-butanol and rice bran biodiesel. In this experiment, the engine's performance and emissions were evaluated by testing the effects of n-butanol, rice bran biodiesel, and diesel blends. A finding was made indicating that the production of biodiesel could be achieved using a singular alkaline transesterification process. Subsequently, this biodiesel was combined with diesel fuel to generate blends known as B10, B20, and B10 nb10/nb20. A 3.73 kW single-cylinder diesel engine was used to examine the performance of these mixtures compared with pure diesel. Recent studies have revealed that the utilization of a blend consisting of butanol and rice bran biodiesel in a diesel engine can be achieved without necessitating any modifications (D. Xu et al., 2021)

2.8.2 Brake Specific Fuel Consumption (BSFC)

Engine fuel consumption as a function of engine output power is referred to as BSFC. It is the ratio of an engine's fuel consumption to its rate of producing power while utilizing a particular fuel. The fuel flow meter calculates the mass flow rate of fuel that the engine uses per unit of time. The engine brake power is used to calculate the BSFC, which is expressed as Eq. (2.6) (Heywood, 1988):

$$BSFC = \frac{\dot{m}_f}{BP} \qquad 2.6$$

where *BSFC* is brake specific fuel consumption (g/kW.hr)

$\dot{m}_f$ is the fuel mass flow rate (g/hr)

BP is the engine brake power (kW)

The BSFC is intricately linked to both the efficiency and emission output of an engine, as it is derived from the division of fuel consumption by the power generated by the engine. Variations in the chemical characteristics of the oil content will result in variations in the engine's performance capabilities. The BSFC exhibits lower values when the engine is fuelled with diesel fuel in comparison to biodiesel. The higher BSFC seen in the biodiesel samples can be attributed to their lower heating value. This decrease in heating value necessitates an increase in fuel consumption by the engine in order to achieve a certain power output. A study published by Kumar (Kumar & Goga, 2023) determined the BSFC of diesel, NB20, NB20DI10, NB20DI20, and NB20DI30 (n-butanol and Neem biodiesel), respectively, to be 0.25, 0.32, 0.29, 0.28, and 0.26. Diesel had the lowest BSFC. NB20DI30 fuel with manifold injection also demonstrated the lowest BSFC due to its improved homogeneity which allowed for faster combustion. In contrast, BTE was found to be higher for diesel than for other blends which is 1.29% lower for a blend with 30% n-decanol.

A study conducted by (Yao et al., 2019) showed that the BTE for a blend with TiO_2 and hydrogen in microalgae biodiesel was 4.84% lower than diesel. A similar blend of fuel consumed the same amount of fuel as diesel. High BSFC was primarily due to a low CV and a high KV. It has been shown in previous studies that adding hydrogen and nanoparticles to the fuel can increase its CV and CN. A further benefit of the nanoparticles is that they enhance the catalytic activity of the combustion process. As a result, the BSFC is reduced.

UMPSA
اونيۏرسيتي مليسيا ڤهڠ السلطان عبدالله
UNIVERSITI MALAYSIA PAHANG
AL-SULTAN ABDULLAH

In the study conducted by Rakopoulos et al., a combination of 10% and 20% volumes of different vegetable oil biodiesels, including cottonseed oil, soybean oil, sunflower oil, rapeseed oil methyl ester, palm oil methyl ester, corn oil, and olive kernel oil, was examined. The researchers observed that there was no significant alteration in fuel consumption when comparing the biodiesel and vegetable oil blends from various sources to that of pure diesel fuel. However, it was noted that higher specific fuel consumption was observed at high loads, while the minimum specific fuel consumption was observed at the 10% blends for medium loads (Rajak & Verma, 2019).

The findings indicate by (Awad et al., 2017) that there was a 15% fuel consumption seen at low load conditions. In comparison, a 10% fuel consumption was recorded during heavy load conditions, ranking as the first and second highest results, respectively. The incorporation of diethyl ether into diesel fuel blends at concentrations of up to 10% does not necessitate any alterations to the architecture of the diesel engine. The combustion phase persists throughout the expansion stroke. The heat generated during this time period could perhaps be attributed to the presence of unburned fuel or incomplete combustion products, such as CO.

2.8.3 Brake Thermal Efficiency (BTE)

One of the critical features of the engine that specifies how well it performs with various test fuels is brake thermal efficiency. The relationship between engine output and heat input determines it. Many parameters relating to distinct test fuels with varying qualities have an impact. As shown in Eq. (2.7), the brake thermal efficiency is calculated (Heywood, 1988):

$$BTE = \frac{BP}{\dot{m}_f \times Q_f} \times 100 \tag{2.7}$$

where *BTE* is the engine brake thermal efficiency

$\dot{m}_f$ is the fuel mass flow rate (g/hr)

BP is the engine brake power (kW)

Q_f is the heating value of the test fuel (MJ/kg)

The Brake Thermal Efficiency (BTE) is contingent upon the brake power. The study unveiled the extent to which the engine's response is influenced by the diesel fuel to the engine. A study conducted by (Surya Kanth, 2021); a number of fuel blends were tested, including D + 7H2, D + 10H2, P20, P20 + 7H2, and P20 + 10H2, for different load conditions. According to his findings, the BTE increases by 19.5% at 90% loading for D + 7H2 but decreases at 10 lpm concentration because of reduced oxygen availability and poor combustion. The BTE of P20 + 10H2 is lower than that of D100 due to the faster burning velocity of hydrogen, which results in quicker combustion of accumulated fuel.

Study examined that that when 75% load was applied, the maximum BTE for waste cooking oil biodiesel (B20) was reached, followed by a slight reduction when 100% load was applied (Jayaraman et al., 2022). A blend of H_2O_2 emulsified with CeO_2 nanoparticles performs better BTE than a neat blend of B20 fuel that contains no CeO_2. H_2O_2 concentrations that exceeded 40 ppm resulted in a 0.713% and 0.65% improvement in BTE, respectively, as a result of increasing H_2O_2 concentrations. A 75% of BSFC was observed at the minimum load, whereas a BSFC of 90% was observed when the fuel is neat (B20). As the concentration of H2O2 in the engine was increased from 0.5% to 1.5% at 75% load, the BSFC of the engine was reduced by 2.07% and 1.88%, respectively. A significant contribution to the improvement of the BTE and BSFC values has been made by the thermal conductivity of CeO2 nanoparticles.

A CI engine was used by Nanthagopahl to determine the performance of biodiesel derived from Calophyllum inophyllum and oxygenated additives such as ethylene and ethanol. A series of tests on direct injection (DI) diesel engines have been conducted under the same operating conditions. The addition of diethyl ether (DEE) or ethanol to biodiesel increases BTE by up to 6.2% and 3.7%, respectively. In general, there is a higher positive value for net heat output and in-cylinder pressure with fuels mixed with DEE than with other fuel blends, by 0.4 – 2.7% and 1.1 – 5.2%, respectively, when compared to fuel mixes without DEE. In addition, DEE is more

UMPSA
اونيۏرسيتي مليسيا ڤهڠ السلطان عبدالله
UNIVERSITI MALAYSIA PAHANG
AL-SULTAN ABDULLAH

volatile and has a higher cetane number, which makes it more impactful and thus increasing the NO_X emissions. The lower CN and higher latent heat of vaporization of ethanol give it a lower cylinder pressure of around 0.4–2.6%, which results in the release of more unburned HC and CO (Nanthagopal et al., 2019). According to (Ramachandran et al., 2023), tabacco seeds biodiesel blends (B20) containing graphite nanoparticles and 3lpm hydrogen supply increased BTHE by 28.4%, 29.1%, 29.8%, and 30.8%, respectively, when using B20D80 + GO20, B20D80 + G40, and B20D80 + G60, compared to 30.53% for B20D80.

2.9 Exhaust Emissions from Compression Ignition (CI) Engine

Energy plays a pivotal role in driving the progress and advancement of any nation. Meeting the energy demands is a crucial factor in achieving diverse home and industrial necessities. Transportation is a critical industrial requirement that necessitates a substantial quantity of energy. Considering the significance of transportation in the advancement of a nation, the significance of energy sources is further amplified. The predominant utilization of conventional fuels as energy sources has resulted in various forms of pollution (Stone, 1999). Extensive research efforts have been dedicated to mitigating pollution by exploring various strategies, leading to the identification of numerous alternative fuels and gasoline additives. This section provides a comprehensive analysis of different alternative fuels and additives utilized in CI engines, focusing on their impact on exhaust emissions.

UMPSA
اونيۏرسيتي مليسيا ڤهڠ السلطان عبدالله
UNIVERSITI MALAYSIA PAHANG
AL-SULTAN ABDULLAH

2.9.1 Carbon Monoxide (CO)

CO is a resultant of incomplete combustion and can be described as fuel that has undergone partial combustion. Hence, in the absence of sufficient oxygen, the process of combustion results in incomplete oxidation of carbon atoms, preventing their complete conversion into CO_2. A reduction in CO emissions has been observed while utilizing biodiesel in comparison to conventional diesel fuel. The emission of CO is closely associated with HC emissions, as the exact underlying mechanism produces both. The study observed a decrease in CO emissions while utilizing plain rapeseed oil blends B5 and B100 fuels compared to diesel fuel. Specifically, the CO emissions were found to be 9% and 32% lower, respectively. Additionally, the smoke opacity was reduced by up to half a percent. The researchers conducted a study wherein they employed the trans-esterification method, utilizing methanol and potassium hydroxide (KOH) as a catalyst, to create biodiesel from papaya and watermelon. The researchers formulated a mixture consisting of papaya seed oil biodiesel and watermelon seed oil biodiesel in a 1:1 ratio. This blend was developed for various biodiesel-diesel fuel ratios, namely B0, B20, B30, B40, and B100. The experiment focused on evaluating the performance and emission characteristics of a single-cylinder, four-stroke diesel engine. The performance of different blends and types of biodiesels influenced the experimental outcomes. The brake thermal efficiency of B20 is significantly elevated and comparable to that of the reference fuel, namely diesel fuel. Moreover, the reduction in emissions of CO, HC, and smoke is 27%, 23%, and 8% accordingly when using a B20 blend compared to conventional diesel fuel (Ali et al., 2020).

A study conducted by (Jayaraman et al., 2023) has demonstrated an improvement in the formation of HC due to the use of different biodiesel blends. MCV-B20 showed the greatest improvement in HC emissions, with a reduction of 51.1%. This was followed by MCV-B10 with a reduction of 44.3%, and WB20 with a reduction of 42.7%. The average formation of HC in ES-B10, ES-B20, and WB10 was respectively 28.2%, 38.2%, and 36.6% lower than that in pure diesel. It was found that microalgae biodiesel emits significantly less HC than other feedstocks due to its high oxygen content and long-chain fatty acid structure. As a result, MCVB20 produced the lowest average amount of CO generation, which was 47.4% lower than B0. It was found that when compared to diesel, ES-B10, ES-B20, WB10, WB20, and MCV-B10 had an average CO formation reduction of 22.1%, 30.9%, 29.9%, 38.0%, and 41.7%, respectively.

اونيۏرسيتي مليسيا ڤهڠ السلطان عبدالله
UNIVERSITI MALAYSIA PAHANG
AL-SULTAN ABDULLAH

2.9.2 Carbon Dioxide (CO_2)

Carbon monoxide (CO) is a resultant of incomplete combustion and can be described as fuel that has undergone partial combustion. Hence, in the absence of sufficient oxygen, the process of combustion results in incomplete oxidation of carbon atoms, preventing their complete conversion into CO_2. A reduction in CO emissions has been observed while utilizing biodiesel in comparison to conventional diesel fuel. The emission of CO is closely associated with HC emissions, as both are produced by the same underlying mechanism. The study observed a decrease in CO emissions while utilizing plain rapeseed oil blends B5 and B100 fuels compared to diesel fuel. Specifically, the CO emissions were found to be 9% and 32% lower, respectively. Additionally, the smoke opacity was reduced by up to half a percent.

Niyas et al. demonstrated that the utilization of palm cooking oil biodiesel resulted in a reduction of CO and HC emissions in the exhaust gases, in comparison to the emissions produced by traditional diesel fuel (Muhammed Niyas & Shaija, 2022). They conducted experiments on a single-cylinder engine to investigate the effects of different loads and engine speeds on the combustion of canola oil-diesel fuel blend. In the context of biodiesel, it is observed that emissions are comparatively lower in comparison to neat diesel throughout the whole spectrum of testing. Hence, it leads them to the conclusion that the emission of CO was reduced for all blends across all levels of engine (rpm). Additionally, the emission of HC dropped within the low to medium range of rpm but exhibited a tiny rise at high engine speeds.

2.9.3 Hydrocarbon (HC)

Typically, hydrocarbons are generated through the reaction of fuel with oxygen during the process of combustion, resulting in the formation of water vapour (H_2O) and CO_2. An experiment performed by (Hoang AT, 2019) has measured the amount of HC emitted when different fuel blends are used in an engine. A mixture of biodiesel blends (JCB50, CPB50, and CIB50) emitted HC at levels of 30.73 ppm, 30.86 ppm, and 31.96 ppm, respectively, while diesel fuel emitted 27.56 ppm at 1900 rpm. Conversely, when 10 % biodiesel was used, HC generation was significantly reduced compared to D100. The formation of HC for JCB10, CPB10, and CIB10 was noted to be 18.66 ppm, 19.03 ppm, and 19.08 ppm at 1900 rpm, respectively. Lastly, biodiesel blends emit more NOx than diesel. The study by (Trivedi et al., 2019) examined diesel fuel and chlorella vulgaris biodiesel blends and concluded that the formation of HC and CO was highest at 100% load for diesel fuel and all biodiesel blends, except for B50 and B60, which produced 105 and 104 ppm HC respectively, approximately 17 ppm lower than diesel fuel's emissions of 122 ppm HC at 1500 rpm and 0.13 and 0.12% CO emissions,

UMPSA
اونيۏرسيتي مليسيا ڤهڠ السلطان عبدالله
UNIVERSITI MALAYSIA PAHANG
AL-SULTAN ABDULLAH

respectively. The NOx emissions from the blends were nearly the same as those from diesel fuel. Furthermore, a study conducted by Nayak et al. (2017) revealed a considerable reduction in CO, HC, and NO_X emissions when compared to diesel fuel. The purpose of the experiment was to examine the possibilities of utilizing Neem blends in diesel fuel, specifically B10, B20, and B30, on a single-cylinder, four-stroke diesel engine operating at a constant speed of 1500 rpm with a compression ratio of 18. The utilization of Neem biodiesel B10 resulted in a notable increase in braking thermal efficiency while concurrently exhibiting a reduction of 23% in CO emissions, 8.5% in HC emissions, and 22% in NOx emissions as compared to conventional diesel fuel. The authors additionally assert that B10 represents the most favourable blend for commercialization, as it exhibits lower emissions compared to alternative blends (Nayak & Mishra, 2017).

2.9.4 Oxide of Nitrogen (NO_X)

The emission of NO_X is shown to be elevated in CI engines when fuelled with biodiesel and biofuel. The application of these fuels in CI engines has been observed to typically decrease the release of HC, CO and PM. A study by (Nema et al., 2022) evaluated the implementation of blended hydrogen and cerium oxide with waste cooking oil biodiesel (B20), decreased at high loads and low emissions were observed with 1.5% H2O2 at 75% load. As a result, HC formation was reduced by 41 to 48% on average. An average reduction of 56–60% was achieved in CO through 1.5% H_2O_2 emulsification over B20. In contrast to B20, H_2O_2 concentrations of 0.5%, 1%, and 0.5% resulted in 0.6%, 16.1%, and 22.7% decreases in NOx, respectively.

However, certain researchers have stated that the utilization of biodiesel has been found to contribute to the enhancement of NO_X emissions during production. The production of NO_X occurs as a result of the combustion process, wherein nitrogen and oxygen present inside the biodiesel react with each other. The quantity of emissions produced is contingent upon the power and efficiency of the engine. In their study, Niyas et al. conducted experiments to investigate the impact of coconut oil on engine performance. Specifically, they sought to improve the engine volume by operating a 10 kW, horizontal, single-cylinder direct injection diesel engine at full load and variable speed conditions. The data shown illustrates the decrease in NO_X emissions observed in

UMPSA
UNIVERSITI MALAYSIA PAHANG
AL-SULTAN ABDULLAH

biodiesel blends PB30, CB30, and PB15CB15 in comparison to conventional diesel fuel (Muhammed Niyas & Shaija, 2022).

Veza investigated on a biogas-diesel engine. The impact of compression ratio (CR), EGR, and EGR temperature on the performance and emissions of CI engines has been extensively investigated. During the initial phase, the engine underwent rigorous testing with compression ratios (CRs) of 16.5, 17.5, 18.5, and 19.5. The study demonstrated that increased compression ratios (CRs) had a favourable impact on both engine emissions and horsepower. The study investigated the effects of exhaust gas recirculation (EGR) on a diesel engine operating at a compression ratio (CR) of 19.5. The achievement of reduced NO_X emissions was attained with the implementation of increased Exhaust Gas Recirculation (EGR) percentages, namely at 10% and 15%. On the other hand, a marginal reduction in engine efficiency was seen with an increase in exhaust gas recirculation (EGR) levels under conditions of high engine load (Veza et al., 2022).

2.10 Combustion Analysis from Compression Ignition (CI) Engine

The utilization of diesel-fuelled in CI engines is prevalent in both power generation and transportation sectors owing to its notable advantage of comparatively low fuel consumption (Ali et al., 2022). This section provides an analysis and evaluation of different alternative fuels and additives that are commonly utilized based on Table 2.4. The present section examines alternative fuels and additives that are combined with traditional fuels such as diesel or petrol. This section focuses on the examination of three distinct categories of alternative fuels, specifically biodiesel, alcohols, and ethers. The investigation centres on their impact on various engine parameters, including EGT, IP, RoHR and RoPR.

2.10.1 Exhaust Gas Temperature

Researchers conducted a study that improved the physical and chemical properties of the fuel used in diesel engines by mixing heptane and Jatropha oil with diesel fuel. An evaluation of the influence of heptane content was conducted by comparing engine findings (comparing combustion characteristics and performance of

Jatropha oil and diesel fuel). According to research, Jatropha oil has lower combustion properties and performance when compared to diesel fuel when its heptane content is approximately 10% higher. The best combination (J70G20H10) was a mixture consisting of 10% heptane, 20% diesel, and 70% Jatropha oil. There was no difference in overall efficiency or exhaust gas temperatures between any of the fuels evaluated. Use of J70G20H10 may lead to improvements in exhaust emissions (Dharma et al., 2017).

2.10.2 Cylinder Pressure

The primary objective of exhibiting the in-cylinder pressure pattern is to ascertain the extent of output work performed during a single complete cycle of engine combustion. The determination of high or low pressure in the cylinder pattern is contingent upon the conditions of the parameters and the fuels utilized. Prior to fuelling the engine, it is necessary to conduct an assessment of the chemical properties of the fuel in order to prevent the occurrence of excessively high and unpredictable pressures. The determination of potential engine damage or failure caused by fuels, excluding diesel fuel, can be facilitated by understanding the constraints of pressure and the maximum rate of pressure change. The in-cylinder pressure exhibits variations across different fuel types (Nema et al., 2022).

UMPSA
اونيۏرسيتي مليسيا ڤهڠ السلطان عبدالله
UNIVERSITI MALAYSIA PAHANG
AL-SULTAN ABDULLAH

Experiment on the combustion characteristics of diesel engines using pure diesel as well as biodiesel made from Calophyllum inophyllum were analysed. BHT 500 ppm combined with CIME resulted in the lowest peak pressure in the cylinder. Researchers have found that adding ZrO2 nanoparticles in concentrations of 50 or 100 parts per million to Eu20 fuel increases cylinder pressure by reducing the cetane number, which delays combustion, and by adding ZrO2 nanoparticles, rapid evaporation is achieved as well as improved air–fuel mixing is achieved, thereby accelerating combustion and increasing cylinder pressure. The higher CV and better auto-ignition properties of pure diesel contributed to higher in-cylinder pressure. In contrast, the addition of higher alcohols to the fuel blends, such as hexanol and decanol, produced an interesting variation in the profile of in-cylinder pressures. There was an increase in in-cylinder pressure due to excessive oxygen content in ternary blends with 30% and 40% hexanol, whereas decanol displayed a lower oxygen content and higher in-cylinder pressure due to better atomization properties. A decanol 40% blend had the highest in-cylinder pressure among the fuel blends that were tested at 100% load, other than pure diesel (Ashok et al., 2019).

A comparative study has been done to assess the differences between two types of biodiesels, namely Millettia pinnata (MP) and Croton mega-locarpus (CM), in comparison to neat diesel fuel. The authors assert that the utilization of MP5CM15, a fuel mixture consisting of 80% diesel, offers significant advantages over standard diesel fuel in terms of enhancing combustion behaviours. This is attributed to its ability to generate higher in-cylinder pressure, a more significant RoHR, as well as shorter ignition delay and combustion duration. The engine performance of biodiesel and vegetable oil blends from different sources exhibited comparable characteristics to neat diesel fuel, with similar BTE. However, during high load conditions, these blends demonstrated higher specific fuel consumption. Notably, the 10/90 blends showcased the lowest specific fuel consumption at medium load conditions (Atabani et al., 2014).

2.10.3 Rate of Heat Release (RoHR)

The combustion for the utilized engine is examined using the rate of heat release. The amount of heat that would have needed to be added to the contents of the cylinder to create the observed pressure fluctuations is calculated using heat release analysis. The following Eq. (2.8) is utilized in accordance with the first law of thermodynamics (Heywood, 1988):

$$\frac{dQ_{net}}{d\theta} = \frac{\gamma}{\gamma - 1} p \frac{dV}{d\theta} + \frac{1}{\gamma - 1} V \frac{dp}{d\theta} \qquad 2.8$$

where γ is the ratio of specific heats

Q_{net} is the net heat release rate (J/deg)

UMPSA
UNIVERSITI MALAYSIA PAHANG
AL-SULTAN ABDULLAH

p is the cylinder pressure (Pa)

V is the cylinder volume (m^3)

The gross heat release can be determined by considering in the effect of heat transfer to the cylinder walls using Eq. (2.9) (Heywood, 1988) below:

$$\frac{dQ_{ht}}{d\theta} = h(T_{gas} - T_{wall})\frac{dp}{d\theta} \tag{2.9}$$

where h is the heat transfer coefficient (W/m^2K)

T_{gas} is the mean cylinder gas temperature (K)

T_{wall} is the mean cylinder wall temperature (K)

A is the instantaneous heat transfer surface area of the combustion chamber (m^2)

The experiment was performed experiment and the effects of utilizing multiple biodiesel sources on a 6-kW air-cooled single-cylinder four-stroke diesel engine were investigated. The engine was fuelled with neat Jatropha, Karanja, and Polanga biodiesel, as well as their respective mixes at 20% and 50% with conventional diesel fuel. The study examined the combustion characteristics of three distinct types of biodiesel fuels in comparison to conventional diesel fuel. Three types of biodiesel exhibit variations in in-cylinder pressure. The utilization of neat Polanga biodiesel leads to the attainment of the highest peak cylinder pressure. In contrast, the utilization of neat Jatropha biodiesel results in a shorter duration of diesel consumption.

A study found compared the performance, combustion and emission of animal and vegetable origin biodiesel. Each fuel that was examined was compared to diesel, which served as the reference fuel. The experiment examined the performance of fuel blends consisting of 75% swine lard methyl esters (SLME), turkey lard methyl esters (TLME), and rapeseed methyl esters (RME) in combination with mineral diesel fuel. During periods of high and medium engine load, both soybean oil methyl ester (SLME)

UMPSA
اونيۏرسيتي مليسيا ڤهڠ السلطان عبدالله
UNIVERSITI MALAYSIA PAHANG
AL-SULTAN ABDULLAH

and tallow methyl ester (TLME) exhibited elevated levels of in-cylinder pressure, with SLME seeing a 16% increase and TLME showing an 18% increase. In contrast, rapeseed oil methyl ester (RME) shown comparable in-cylinder pressure to that of standard diesel fuel. Additionally, they notice higher RoHR and combustion temperature for biodiesel derived from animal sources. The engine combustion varies across different biodiesel sources, resulting in distinct outcomes. Given that the maximum pressure did not exceed the established threshold, it can be concluded that the act of fuelling the engine was deemed safe (Hellier et al., 2019).

According to (Asokan et al., 2019), The maximum RoHR for diesel fuel is greater than that of blended juliflora biodiesel fuel and followed by B40 fuel. Biodiesel blended with Juliflora has a lower peak RoHR as a result of its shorter ignition delay and longer combustion duration. In contrast, it should be noted that the maximum RoHR of pure diesel is slightly higher than that of biodiesel and its blends at high engine loads. Thus, an important tool for evaluating fuel efficiency is the RoHR curve. Sakthi et al. examined the impact of using Diethyl ether as an oxygenated addition in a mixture of diesel and biodiesel on engine efficiency, combustion characteristics, and emissions. The diesel-biodiesel blend (D60FME40) was produced by combining biodiesel with diesel fuel at a volume ratio of 40%. In the premixed phase of the diesel-biodiesel blend, the in-cylinder gas pressure and the rate of heat release exhibited lower values initially. However, these parameters increased upon the inclusion of Diethyl Ethane (Sakthivadivel et al., 2022).

اونيۏرسيتي مليسيا ڤهڠ السلطان عبدالله
UNIVERSITI MALAYSIA PAHANG
AL-SULTAN ABDULLAH

2.10.4 Rate of Pressure Rise (RoPR)

The rate of pressure rise in a CI engine can be calculated using the following Eq. (2.10) (Heywood, 1988) :

$$RoPR\ (\frac{d\theta}{dP}) = \frac{\theta_{max}}{P_{max}} \qquad 2.10$$

where P_{max} is the maximum pressure (bar)

θ_{max} is crank angle at which maximum pressure occurs (degree)

This formula is used to calculate the rate of pressure rise in a compression ignition engine based on cylinder pressure data. The maximum pressure can be obtained from the cylinder pressure diagram. The crank angle at which maximum pressure occurs can be determined by finding the point of maximum slope on the pressure diagram (Heywood, 1988). Cao did a study on engine combustion and emissions. The study investigated three different injection methodologies, namely single injection, divided injection time, and varying the number of injector nozzle holes. When the injection duration of diesel fuel at the baseline is raised from 17 to 70 CAD ATDC, there is an observed increase in the maximum pressure value from 46 to 84.2 bars. Additionally, there is a significant reduction in unburned HC (98%) and CO emissions (99%). However, it is worth noting that there is a substantial increase in NO_X emissions by 339%. In the context of split injection, it is advised to employ pilot diesel fuel injection timings of 80 CAD ATDC for the initial pulse and 60 CAD ATDC for the succeeding pulses. Consequently, the implementation of the measures, as mentioned earlier, has led to a reduction of 98% in UHC emissions and a reduction of 99.99% in CO emissions (Cao DN, 2020).

2.11 Knocking Phenomenon

اونيۏرسيتي مليسيا ڤهڠ السلطان عبدالله
UNIVERSITI MALAYSIA PAHANG
AL-SULTAN ABDULLAH

CI engines have gained significant recognition due to their exceptional endurance and impressive power output, rendering them a widely favoured option for heavy-duty vehicles and machines. Nevertheless, a prevalent concern encountered by diesel engines is the occurrence of knocking, a phenomenon that can result in detrimental consequences and a decline in overall operational efficiency. The occurrence of knocking in a CI engine can be attributed to a multitude of variables, including but not limited to improper fuel injection timing and substandard fuel quality. Fortunately, there exist numerous measures that may be undertaken to mitigate the occurrence of knocking in a diesel engine and maintain its optimal performance (Heywood, 1988). The phenomenon of knocking in a diesel engine refers to the sound expression that arises when the combustion of fuel within the engine's cylinders undergoes spontaneous or premature detonation.

This phenomenon is alternatively referred to as "diesel knock" or "engine knock". The auditory phenomenon seen is a result of the combustion process within the cylinder, characterized by the rapid and unregulated burning of the fuel-air mixture. This combustion generates a shock wave that manifests as a distinctive knocking sound. The phenomenon of knocking may manifest in a diesel engine when there is inadequate burning of fuel, resulting in incomplete combustion. The occurrence of this phenomenon can be attributed to various variables, including but not limited to inaccurate fuel injection timing, substandard fuel composition, or insufficient air intake to the engine. Knocking may also manifest itself in cases when the compression ratio within the engine exceeds optimal levels or when an excessive accumulation of carbon is present within the combustion chamber. If not adequately addressed, the act of knocking can result in significant harm to the engine, such as the occurrence of fractured pistons, impaired bearings, and potentially even engine seizure. Hence, it is imperative to promptly identify and rectify the underlying factors contributing to the occurrence of knocking in a diesel engine in order to mitigate any potential development of harm (Stone, 1999).

2.11.1 Types of Knocking

There exist two distinct categories of diesel engine banging, namely mechanical knock and combustion knock. If left unattended, both forms of diesel knock can cause significant damage to the engine. Hence, it is crucial to ascertain the precise nature of the knocking phenomenon and its underlying factors in order to apply a suitable remedy effectively.

UMPSA
اونيۏرسيتي مليسيا ڤهڠ السلطان عبدالله
UNIVERSITI MALAYSIA PAHANG
AL-SULTAN ABDULLAH

2.11.1.1 Mechanical Knocking

Mechanical knock, commonly referred to as "hard knock," arises from the collision between metallic constituents within the engine, such as the piston or connecting rod (Heywood, 1988). The auditory manifestation of this impact is commonly perceived as a distinct metallic resonance, which can be attributed to the presence of deteriorated engine bearings, loosely fitted piston pins, or impaired pistons.

2.11.1.2 Combustion Knocking

Combustion knock, alternatively referred to as "soft knock," arises from the inadequate combustion of gasoline within the engine. The auditory manifestation of this particular knock is commonly perceived as a muted pounding resonance, which can be attributed to various issues, including inaccurate fuel injection timing, substandard fuel composition, or inadequate air intake to the internal combustion engine (Heywood, 1988).

2.11.2 Factors Lead to Knocking in Compression Ignition (CI) Engine

The primary factor contributing to diesel knock is the inadequate combustion of fuel within the engine. The production of a discernible knocking sound occurs when the fuel-air mixture within the cylinders of an engine undergoes premature or spontaneous ignition, resulting in the generation of a shock wave (Heywood, 1988). Next section will discuss the several factors causes the knocking in CI engines.

2.11.2.1 Incorrect Fuel Injection Timing

The term "incorrect fuel injection timing" pertains to the circumstance in which the fuel is injected into the combustion chamber of the engine at an inaccurate moment within the engine's combustion cycle. The precise timing of fuel injection plays a crucial role in ensuring the optimal functioning of a diesel engine since it governs the specific moments and quantities of fuel that are introduced into the combustion chamber. If fuel injection occurs prematurely, before the piston's arrival at the TDC, there is a possibility of premature ignition within the combustion cycle, resulting in the occurrence of knocking.

On the contrary, if the fuel injection occurs belatedly, after the initiation of the piston's downward motion within the cylinder, there is a possibility of incomplete ignition, leading to suboptimal combustion and a consequent decrease in the overall efficiency of the engine. CI engines employ intricate fuel injection systems to achieve accurate fuel injection timing that incorporate high-pressure pumps, injectors, and electronic controllers to regulate the timing and quantity of fuel injection meticulously.

Implementing routine maintenance procedures, such as adhering to the manufacturer's recommendations for cleaning or replacing fuel injectors and optimizing injection timing, can effectively mitigate the occurrence of knocking resulting from inaccurate fuel injection timing (Heywood, 1988).

2.11.2.2 Poor Fuel Quality

The term "poor fuel quality" pertains to diesel fuel that is characterized by the presence of pollutants, contaminants, or a low cetane rating. These factors have the potential to negatively impact the performance of an engine and elevate the probability of experiencing knocking. Diesel fuel commonly harbours impurities such as water, dirt, and various particle matter. Additionally, contaminants that may be present encompass bacteria, fungi, or other microorganisms capable of proliferating within the fuel tank and obstructing fuel filters. Diesel fuel of inferior quality may exhibit a diminished cetane rating, indicating a reduced propensity for ignition. Insufficient cetane rating of the fuel might result in incomplete combustion and the occurrence of knocking (Stone, 1999).

It is imperative to procure diesel fuel exclusively from trustworthy suppliers who strictly adhere to established industry benchmarks for fuel quality and to mitigate the risk of substandard fuel quality. Ensuring the appropriate storage and handling of diesel fuel is crucial to mitigate the risk of contamination. This entails maintaining the cleanliness and dryness of the fuel tank, as well as implementing regular drainage of the water separator.

Furthermore, the utilization of fuel additives, such as fuel stabilizers or cetane boosters, can effectively enhance the overall quality of diesel fuel while concurrently mitigating the occurrence of knocking. Implementing a routine maintenance practice of periodically replacing fuel filters and seeking the expertise of a certified mechanic to conduct thorough inspections of the fuel system can effectively promote optimal functioning of the fuel system and mitigate the occurrence of engine knocking attributed to substandard fuel quality (Heywood, 1988).

UMPSA
UNIVERSITI MALAYSIA PAHANG
AL-SULTAN ABDULLAH

2.11.2.3 Inadequate Air Supply

Insufficient air delivery to the engine can be a contributing factor to incomplete combustion and a heightened propensity for knock occurrence in a diesel engine. The efficient operation of diesel engines necessitates a meticulous equilibrium between fuel and air, whereby a compromised or obstructed air supply might result in a low fuel mixture, thus inducing knocking. Several factors can contribute to insufficient air supply in diesel engines, such as a congested air filter, a faulty turbocharger, or a compromised or restricted air intake system. The presence of a blocked air filter has the potential to impede the intake of air into the engine, whilst a defective turbocharger may fail to generate sufficient air pressure for the engine, resulting in incomplete combustion. The air filter must be consistently examined and replaced according to the manufacturer's recommendations to prevent knocking in CI engine due to insufficient air supply. It is imperative to verify the appropriate functioning of both the air intake system and turbocharger while also ensuring their freedom from any damage or obstruction. The implementation of routine maintenance practices, such as the regular cleaning or replacement of the air filter, as well as the periodic inspection of the air intake system by a certified technician, can effectively mitigate the occurrence of knocking resulting from insufficient air supply (Heywood, 1988).

UMPSA
اونيۏرسيتي مليسيا ڤهڠ السلطان عبدالله
UNIVERSITI MALAYSIA PAHANG
AL-SULTAN ABDULLAH

2.11.2.4 High Engine Load

An elevated engine load, such as the act of towing a substantial load or navigating a steep incline, has the potential to be a contributing factor to the occurrence of knocking in a CI engine. During periods of elevated demand, the engine is compelled to provide increased power, resulting in potential overheating and premature ignition of the gasoline. The occurrence of early ignition can lead to the phenomenon of knocking and result in a decrease in engine efficiency. It is vital to minimize engine load wherever possible to mitigate the occurrence of knocking during periods of high load. The objective can be accomplished through the implementation of many strategies, such as diminishing the weight of the load being towed, employing a lower gear ratio to alleviate the burden on the engine, or adopting a slower driving pace. It may be advantageous, if feasible, to refrain from ascending steep inclines since such actions can augment the engine's workload and heighten the probability of experiencing knocking. Engaging in routine maintenance activities, such as the regular cleaning or replacement of the air filter and fuel injectors, can effectively enhance engine performance and mitigate the occurrence of knocking during periods of heightened load. Furthermore, it is imperative to utilize diesel fuel of superior quality that possesses a high cetane rating, as this attribute might facilitate a more thorough combustion process and diminish the probability of engine knocking (Pulkrabek, 2004).

2.11.2.5 Excessive Carbon Buildup

The presence of an excessive amount of carbon deposits within a CI engine has the potential to contribute to the occurrence of knocking and a subsequent decrease in engine performance. The phenomenon of carbon buildup arises from the incomplete combustion of fuel, resulting in the accumulation of carbon deposits, including soot, within the combustion chamber, cylinder walls, and pistons of an engine. The presence of an excessive amount of carbon buildup within the engine might impede its optimal functioning by diminishing the quantity of air and fuel accessible within the combustion chamber. Consequently, this can result in incomplete combustion and the occurrence of knocking.

The accumulation of carbon can also lead to accelerated wear of engine components, resulting in a decrease in both engine efficiency and performance. In order to mitigate the accumulation of carbon deposits in a diesel engine, it is imperative to utilize diesel fuel of superior quality and adhere to a routine maintenance schedule, which includes the cleaning or replacement of the air filter, fuel injectors, and EGR valve in accordance with the manufacturer's guidelines. Frequent oil and oil filter replacements have the potential to mitigate carbon accumulation within the engine by eliminating impurities present in the oil.

Furthermore, the utilization of fuel additives, such as fuel system cleaners, can effectively eliminate carbon deposits and mitigate their accumulation within the engine. Periodically subjecting the engine to high speeds or high load situations can also facilitate the combustion of excessive carbon buildup and mitigate the occurrence of knocking. The implementation of routine maintenance practices, such as the periodic

UMPSA
اونيۏرسيتي مليسيا ڤهڠ السلطان عبدالله
UNIVERSITI MALAYSIA PAHANG
AL-SULTAN ABDULLAH

cleansing of fuel injectors and the timely replacement of air filters, can serve as a preventive measure against the occurrence of knocking (Stone, 1999).

2.11.3 Knocking Detection Methods

Numerous techniques for detecting knocking exist, which can be categorized into two groups: direct and indirect methods. The previous approach relies on the direct monitoring and analysis of internal cylinder characteristics, which may be susceptible to knock-induced influences. Alternative approaches rely on indirect measurement techniques, such as sound pressure or cylinder block vibration. Knock detection can be performed based on several types of methods, for instance, in-cylinder pressure analysis, cylinder block vibration analysis, ion current analysis, light radiation and acoustic emissions analysis, heat transfer analysis and temperature analysis. Here are some major application methods to review.

2.11.3.1 Methods based on In-Cylinder Pressure Analysis

This method is used to analyse inside cylinder pressure signals to study the inside combustion processes, which are influenced by knock directly. It is often used as a reference for the calibration of detection strategies based on some sensors. The typical high-frequency knock signature is related to the combustion chamber resonant frequencies, which are excited by the rapid rise in pressure. This method requires pressure signal processing. The expected resonant knock frequencies can first be estimated by using the analytical solution of the wave equation as shown in Eq. (2.11). The resonant frequency of the m, n vibration mode can be written as:

$$f_{m,n} = \frac{\alpha_{m,n} c_s}{\pi B} \qquad 2.11$$

where $\alpha_{m,n}$ is the corresponding wave number (determined using Bessel's equations), m and n denote the numbers of radial and circumferential pressure nodes, respectively; cs is the speed of sound inside the combustion chamber (estimated to be about 1000 m/s), B represents the cylinder bore. The definition of knock intensity usually uses the maximum amplitude of the filtered cylinder pressure, so the cylinder

UMPSA
اونيۏرسيتي مليسيا ڤهڠ السلطان عبدالله
UNIVERSITI MALAYSIA PAHANG
AL-SULTAN ABDULLAH

pressure is band-pass filtered with a software filter. The lower cut-off frequency is 4 kHz, and the higher cut-off frequency is well above the frequency of the in-cylinder oscillations. The pressure wave amplitude can be used to define knock indexes: the drawback of such indexes is that they are based on observations referring to a narrow spatial domain. So, the methods based on in-cylinder pressure analysis have some major drawbacks: i) the sensors are very expensive.

Besides, if the sensors are installed inside the cylinder chamber, they will make direct contact with hot and high-pressure mixtures, so their lifetime expectancy and accuracy will be reduced. ii) During non-knocking combustion conditions, the sensor measured the value at the sensor location can be representative of the whole combustion chamber pressure value; as knock occurs, huge non-homogeneities take place, preventing the extension of the local data to the global domain. When knock occurs, it will generate a pressure wave, but it evolves throughout a non-homogeneous medium, interacting with the complex chamber boundary. So, the measured pressure wave amplitude has a local meaning; it cannot be considered as the maximum value of the whole combustion chamber pressure wave. iii) If one set for each cylinder, which not only increases cost but also requires the use of various hardware and software. Therefore, the method based on in-cylinder pressure analysis is extensively used in experimental research.

اونيۏرسيتي مليسيا ڤهڠ السلطان عبدالله
UNIVERSITI MALAYSIA PAHANG
AL-SULTAN ABDULLAH

2.11.3.2 Methods based on Engine Block Vibration

This methodology aims to ascertain the presence of knock in an engine by quantifying the level of vibration. The occurrence of knock generates significant pressure waves, specifically those above approximately 2 bars in amplitude (peak to peak), within the combustion chamber.

Pressure waves could propagate sound within the range of frequencies that the human ear can detect. Additionally, these pressure waves can induce vibrations in the engine block, resulting in the production of an audible signal commonly known as a knock. The oscillation frequencies are significantly influenced by the dimensions and geometry of the chamber, as well as the formation of resonant modes and the local speed of sound.

These factors, in turn, exhibit variations across different engine operating conditions during the combustion process. Nonintrusive vibration sensors possess numerous advantages, such as exceptional durability and cost-effectiveness. Hence, the emergence of nonintrusive pressure sensors has led to the prominence of knock detection techniques that rely on block vibration analysis, making them very suitable for the mass production of automotive engines (Takeda et al., 2016).

2.11.3.3 Methods based on Exhaust Gas Temperature (EGT)

The detection of engine knock can be achieved through the monitoring of exhaust gas temperature. A significant association has been established between engine knock and exhaust gas temperature. Under conditions of knocking combustion, it was observed that the temperature of the exhaust gas was decreased. The efficacy of this knock detection methodology can be attributed to several factors. Firstly, the technique is immune to engine noise, ensuring the purity and accuracy of knock-detection. Secondly, the method is characterized by its speed and convenience, allowing for efficient knock detection. Lastly, the technique is versatile and can be employed across various engine types (Dharmaraja et al., 2019).

2.11.3.4 Methods based on Intermediate Radicals and Species Analysis

UMPSA
اونيۏرسيتي مليسيا ڤهڠ السلطان عبدالله
UNIVERSITI MALAYSIA PAHANG
AL-SULTAN ABDULLAH

In contemporary times, the analysis of chemical reactions resulting from end-gas autoignition can be facilitated through the utilization of chemical luminescence emissions. Spectroscopic and chemiluminescence techniques are employed to discern the presence of methylidyne (CH), hydrocarbon (HCO), formaldehyde (HCHO), and hydroxide (OH) radicals, which serve as indicators for distinct combustion stages. For example, formaldehyde (HCHO) accumulates in the unburned fuel mixture before the flame front. The presence of elevated HCHO levels can serve as an indicator for identifying hot patches. Additionally, the presence of CH and OH radicals can be utilized as markers for assessing typical combustion reactions and the burned zone, respectively. Consequently, knock detection can be achieved by studying intermediate radicals and species.

2.11.3.5 Methods based on In-Cylinder Pressure Analysis

The knock phenomenon is widely recognised to increase heat transfer within the combustion chamber. The study revealed that KI beyond 0.2 MPa significantly impact heat flow. Furthermore, knock intensities surpassing 0.6 MPa can result in a peak heat flux up to 2.5 times greater than that observed during non-knocking combustion. In general, it can be observed that knocking combustion results in significantly elevated wall heat fluxes compared to conventional combustion. The study reveals that knock can increase temperature variations (Heywood, 1988). This approach would enhance the identification of knock events by utilising heat transfer studies.

2.11.4 Knocking Analysis from Compression Ignition (CI) Engine

There are a variety of approaches available for the detection of knock either using direct or indirect methods. The preceding methodology is dependent on the direct observation and examination of internal cylinder characteristics, which could potentially be affected by knock-induced factors. Other methodologies involve employing indirect inspections, such as evaluating sound pressure or analysing the vibration of the cylinder block. Methods for detecting knock include, but are not limited to, measuring pressure inside the cylinder, measuring vibrations in the cylinder block, measuring ion currents, measuring light and sound emissions, measuring heat transfer, and measuring temperatures.

UMPSA
UNIVERSITI MALAYSIA PAHANG
AL-SULTAN ABDULLAH

The method of direct measurement was used in this study. The purpose of this methodology is to examine the signals of inner cylinder pressure to directly investigate the burning processes impacted by the occurrence of knock. It's often used as a benchmark for calibrating detection systems with specific sensors. The impulsive increase in pressure within the combustion chamber causes the resonance frequencies to vibrate, producing the distinctive high-frequency knock signal. Figure 2.8 and Figure 2.9 display the pressure profiles commonly observed throughout a knocking and non-knocking cycle.

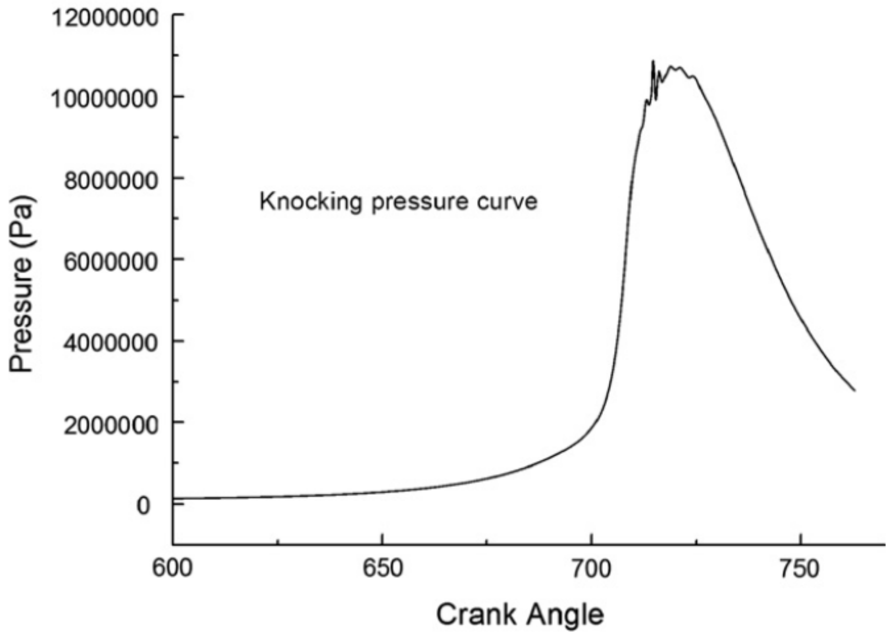

Figure 2.8 Typical knocking cycles
Source: Heywood (1988)

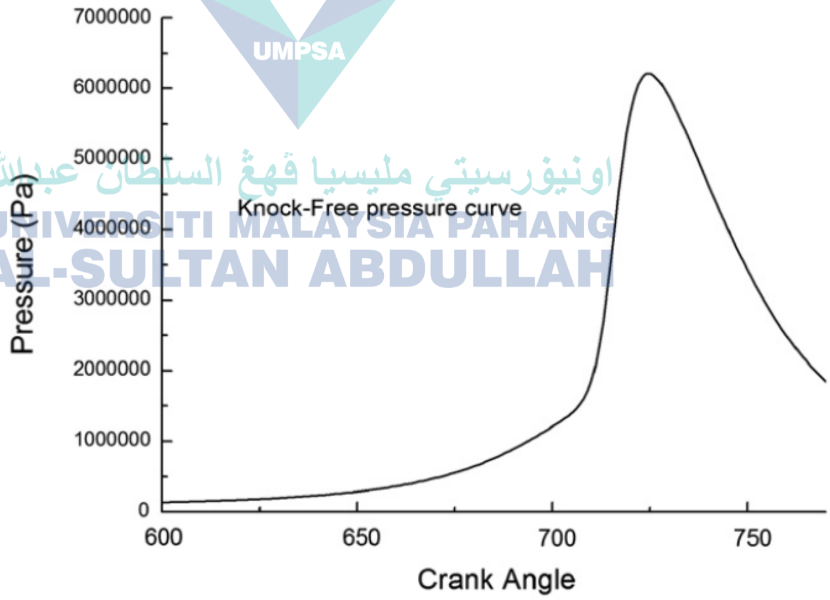

UMPSA
اونيۏرسيتي مليسيا ڤهڠ السلطان عبدالله
UNIVERSITI MALAYSIA PAHANG
AL-SULTAN ABDULLAH

Figure 2.9 Typical non-knocking cycles
Source: Heywood (1988)

It is possible to make an estimate of the stoichiometric air–fuel ratio for RBO fuel by using the stoichiometric combustion equation, which is shown in Eq. (2.12) (Pulkrabek, 2014).

$$C_{30}H_{45}N_9O_5 + \left(30 + \frac{45}{4}\right)(O_2 + 3.773N_2) \rightarrow 30CO_2 + \frac{45}{2}H_2O + 3.773\left(30 + \frac{45}{4}\right)N_2 + O_2 \qquad 2.12$$

The determination of the equivalency ratio holds great importance in CI engines exploiting RBO as a fuel, as it becomes a key factor in assessing the influence on combustion parameters. This part is devoted to the investigation and evaluation of the results about the impact of the equivalency ratio on the method of combustion. There are two primary methods that impose restrictions on the CI combustion fuelled by RBO.

The lean air-fuel ratio limit refers to the condition when the mixture of RBO and air has a low equivalency ratio. In this scenario, the consumption of RBO fuel is reduced, resulting in a lower combustion temperature. Consequently, the incomplete oxidation of the charge occurs, leading to elevated levels of CO and HC emissions, as well as a decrease in engine output.

UMPSA
اونيۏرسيتي مليسيا ڤهڠ السلطان عبدالله
UNIVERSITI MALAYSIA PAHANG
AL-SULTAN ABDULLAH

The rich air-fuel ratio limit refers to the condition in which a higher amount of RBO blends fuel is consumed in a rich RBO-air mixture. This results in increased combustion pressure and temperature, accompanied by an excessively high heat release rate. However, this rapid increase in pressure can lead to knocking combustion, which is undesirable as it can cause significant damage to the engine. Additionally, this type of combustion also contributes to the formation of high levels of NOx emissions.

The knocking intensity (KI) was determined by using Eq. (2.13) (Anilkumar Shere, 2022):

$$KI = \frac{1}{2}\sqrt{\gamma RT_{max}}\frac{1}{\gamma p_{max}}\ (0.05RoPR_{max})^2 \qquad 2.13$$

where γ is the specific heat ratio of air

R is the gas constant of air (J/kgK)

T_{max} is the maximum temperature in in-cylinder pressure (K)

$RoPR_{max}$ is the maximum rate of pressure rise (bar)

The in-cylinder temperature (T) was determined by using Eq. (2.14):

$$T = \frac{pV}{m_{RBO-air\ charge} R_{mixture}} \tag{2.14}$$

where p is the pressure (Pa)

V is the instantaneous volume of cylinder (m^3)

$m_{RBO-air\ charge}$ is flow rate of RBO (g/s)

$R_{mixture}$ is the gas constant of mixture (J/kgK)

Alternative fuels are being utilized in diesel engines worldwide to comply with strict pollution regulations and mitigate the costs associated with fossil fuels. Nevertheless, it is worth noting that most alternative fuels exhibit low cetane values, resulting in an elevated ignition delay and subsequent knocking in CI engines. Hence, it is crucial to identify the occurrence of knocking in diesel engines, particularly when alternative fuels power them (Devarajan et al., 2022). Alcohols are widely used as fuels in both SI and CI engines, owing to their notable capacity to mitigate pollutants effectively (Kothiyal et al., 2022). However, owing to their relatively low cetane number, they exhibit a higher vulnerability to knocking than diesel fuel.

The phenomenon of diesel engine knocking can be described as the propagation of noise resulting from a rapid increase in pressure within the combustion chamber (Heywood, 1988). Severe knocking can potentially result in detrimental effects on both the piston and connecting rod, as indicated by previous research (Teoh et al., 2019). In order to achieve knock-free combustion in a CI engine, it is necessary for the rate of pressure rise to be at or below 2-3 bar/CAD. According to the literature, it has been established that the upper limit for the rate of pressure rise that a standard diesel engine can endure is 10 bar/CAD. In their study, a 6% ethanol mix with diesel fuel referred to as E6D94 to investigate on the engine's vibration and noise levels. A noteworthy reduction in vibration or noise of the diesel engine was seen when operating with the (E6D94) fuel blend. In a study conducted by Patel et al. and Ahmed et al., it was observed that the incorporation of biodiesel and hydrogen gas resulted in a reduction in both noise and vibration acceleration (Çalık, 2018).

The present study conducted by Pradeep Kumar Vishnoi aimed to examine the impact of combustion knock in CI engines fuelled with mixtures of methanol, diesel, and n-pentanol. The test samples consisted of various fuel blends, namely diesel, MnP5 (90% diesel, 5% n-pentanol, 5% methanol), MnP10 (80% diesel, 10% n-pentanol, 10% methanol), MnP15 (70% diesel, 15% n-pentanol, 15% methanol), MnP20 (60% diesel, 20% n-pentanol, 20% methanol), and MnP25 (50% diesel, 25% n-pentanol, 25% methanol). The cylinder pressure data was utilised for the assessment of KI (Pradeep Kumar Vishnoi, 2022). The combustion knock in CI engines is quantified by utilising KI. The term "combustion knock" refers to the magnitude of the sudden increase in pressure experienced during the combustion process. The occurrence of an abrupt rise in pressure can be ascertained by evaluating the third derivative of pressure throughout the period in which knock may transpire. A substantial negative value of the third derivative indicates the presence of an abrupt rise in pressure. The determination of a certain value can be achieved through the calculation of the third derivative of the equation provided by Checkel and Dale in Eq. (2.15) (M.D. Checkel, 1986):

$$dP\,(\theta) = \frac{86(P_{i-4} - P_{i+4}) + 142(P_{i+3} - P_{i-3}) + 193(P_{i+2} - P_{i-2}) + 126(P_{i+1} - P_{i-1})}{1118 d\theta} \qquad 2.15$$

The degree of engine knock exhibits a positive correlation with engine load because of elevated in-cylinder pressure experienced during higher load conditions. The research findings indicate that the KI of MnP5 is consistently higher than that of diesels across all loading circumstances. This can be attributed to MnP5's higher peak pressure in comparison to diesel. The KI value for MnP5 was determined to be greater than that of diesel by 5.63%, 13.31%, 13.45%, and 14.59% at 25%, 50%, 75%, and 100%

UMPSA
UNIVERSITI MALAYSIA PAHANG
AL-SULTAN ABDULLAH

concentrations, respectively. In the case of MnP10, it was observed that its value was 10.86% lower than diesel at a load of 25%. However, at load levels of 50.75% and 100%, it was determined that the value of MnP10 was higher than diesel by 7%, 26.77%, and 21.91% respectively. The KI value for MnP15 was observed to be 28.19% lower than that of diesel at a loading condition of 25% and 2.53% lower at a loading level of 50% (Pradeep Kumar Vishnoi, 2022).

Conversely, under loading circumstances of 75% and 100%, the KI value for MnP15 was discovered to be 29.26% and 39.77% greater than diesel, respectively. The KI value for MnP20 was observed to be lower than that of diesel by 40.62%, 34.68%, and 0.68% under load conditions of 25%, 50%, and 75%, respectively. However, at a load condition of 100%, the KI value for MnP20 was discovered to be greater than that of diesel by 24.35%. The KI value of MnP25 was seen to be significantly lower than that of diesel at various load conditions, with reductions of 93.36%, 91.48%, 83.86%, and 80.61% at 25%, 50%, 75%, and 100% load, respectively (Raju et al., 2020).

The present analysis determined that all ternary blends' KI improve on that of diesel under greater loading conditions. The existing literature reveals a need for more studies pertaining to the investigation of knock or vibration in diesel engines utilising various alternative fuels. Hence, the current investigation aims to analyse the knock intensity under various loading conditions in CI engines utilising diesel-methanol-n-pentanol blends. This analysis will be facilitated by the utilisation of cylinder pressure data acquired from a pressure transducer.

UMPSA
اونيۏرسيتي مليسيا ڤهڠ السلطان عبدالله
UNIVERSITI MALAYSIA PAHANG
AL-SULTAN ABDULLAH

2.11.5 Methods Reducing Knocking in Compression Ignition (CI) Engine

Various techniques have been devised to regulate the occurrence of knocking in CI engines. Modifying the fuel injection timing has the potential to mitigate the occurrence of knocking in a diesel engine. If the ignition timing is excessively advanced, it might result in premature fuel ignition, leading to the occurrence of knocking. By slightly delaying the injection timing, it is possible to enhance the combustion process, leading to a more thorough fuel burn and thereby decreasing the probability of engine knocking (Safarov et al., 2018).

The utilization of diesel fuel of superior quality, characterized by a high cetane rating, has the potential to mitigate the occurrence of knocking in a diesel engine. Fuel with a high cetane rating exhibits enhanced ignition characteristics and improved combustion efficiency, hence mitigating the occurrence of knocking. The optimization of air supply to the engine is of utmost importance in mitigating the occurrence of knocking in a diesel engine. Incomplete combustion and banging can occur when the air supply is restricted due to a blocked air filter or a malfunctioning turbocharger (Rajan et al., 2020).

Subsequently, the utilization of gasoline additives will be explored. Fuel additives, such as cetane boosters, have the potential to enhance fuel quality and mitigate knocking occurrences in diesel engines. These additives have the potential to enhance the cetane rating of the fuel and optimize combustion efficiency. One of the approaches to mitigate knocking in CI engines is through the use of regular maintenance. The implementation of routine maintenance procedures, such as the cleansing of fuel injectors and the replacement of air filters, has the potential to mitigate the accumulation of carbon deposits within the combustion chamber. This, in turn, serves as a preventive measure against the occurrence of knocking.

Decreasing Engine Load: Mitigating the engine load, for instance, by diminishing the weight of the cargo being hauled or by engaging a lower gear ratio, can effectively alleviate the occurrence of banging in a diesel engine when subjected to high load circumstances. By employing these techniques, it is feasible to mitigate or eradicate the occurrence of knocking in a diesel engine, hence enhancing its operational efficiency and lifespan.

UMPSA
اونيۏرسيتي مليسيا ڤهڠ السلطان عبدالله
UNIVERSITI MALAYSIA PAHANG
AL-SULTAN ABDULLAH

2.12 Research Gap

There are number of studies explored the effect of rice bran oil on engine performance characteristics, emission exhaust characteristics and combustion behaviours of CI engine. Table 2.5 presented the summary of researchers studied the implementation of rice bran oil without and with different kind of additives. They often investigated at the effect of rice bran oil, but they have not always sufficiently explored the exhaust emissions characteristics on carbon dioxide.

Then, there is limited analysis on the combustion behaviours in terms of rate of heat release (RoHR) and the rate of pressure rise (RoPR) in the most of studies. In addition, none of the knocking analysis of CI engine when it fuelled with rice bran oil have been discussed in the studies (Table 2.5). Furthermore, the impact of intake air temperature in the operating parameters was not discussed among the researchers. Thus, the influence of rice bran oil and intake air temperature can potentially contribute to the analysis of combustion behaviours and knocking investigation of single cylinder four stroke direct injection CI engine using rice bran oil as a renewable fuel.

UMPSA
اونيۏرسيتي مليسيا ڤهڠ السلطان عبدالله
UNIVERSITI MALAYSIA PAHANG
AL-SULTAN ABDULLAH

Table 2.5 Engine performance characteristics, combustion behaviours and knocking of different blends (base is rice bran oil)

Engine Specifications	**Fuel and Its Blends**	**Operating Parameters**	**Engine Performance Characteristics**			**Exhaust Emissions Characteristics**				**Combustion Behaviours**			**Knocking**	**References**
			BP	**BTE**	**BSFC**	**HC**	**CO**	**NOx**	**CO_2**	**IP_{Max}**	**RoHR**	**RoPR**		
1-C, 4-S, CR-18, 3.5kw @ 1500 rpm	Rice bran oil + Hydrogen RB, RB + 7lpm, RB + 10lpm, P20, RB20 + 7lpm,RB20 + 10lpm (no additive)	@90% load for P20 + 10lpm H2		↑	↓	↓	↓	↑		↑	↑			(Hellier et al., 2019)
CR-18.5:1, 7.5 kW@1500–3500 rpm, FIP 250–500 bar	Rice bran oil B30GNP40DMC10,B30GNP80DMC10,B30GNP120DMC10 (additive:Graphene nanoparticles (GNP),Dimethyl carbonate (DMC)	@1900RPM for B30GNP40DMC10		↑	↓	↓	↓	↑						(Hirner et al., 2019)

UMPSA
UNIVERSITI MALAYSIA PAHANG
AL-SULTAN ABDULLAH

Table 2.5: Continued

Engine Specifications	Fuel and Its Blends	Operating Parameters	Engine Performance Characteristics			Exhaust Emissions Characteristics				Combustion Behaviours			Knocking	References
			BP	BTE	BSFC	HC	CO	NOx	CO_2	IP_{Max}	RoHR	RoPR		
4-C,4-S, CI engine CR-22.5:1; Rated power 89 kW at 3200 rpm	Rice bran + H2 B20, B100, B20 + A, H + B20 + A, B100, B100 + A, B100 + H + A	@2400 rpm for H + B20 + A	↑	↑	↓	↓	↓	↑						(Das et al., 2022)
1-C, CR-17.5:1, 7.5 KW at 1500 to 3000 rpm	Cottonseed + octanol + Rice bran MWCNTB20 (O5, O10, O20), B40(O5, O10, O20), B60(O5, O10, O20), B100 (O5, O10, O20)	@75% Load for B40 + O15		↓	↑	↓	↓	↑						(R. Li & Wang, 2018)

UMPSA
اونيۏرسيتي مليسيا ڤهڠ السلطان عبدالله
UNIVERSITI MALAYSIA PAHANG
AL-SULTAN ABDULLAH

Table 2.5: Continued

Engine Specifications	Fuel and Its Blends	Operating Parameters	Engine Performance Characteristics			Exhaust Emissions Characteristics				Combustion Behaviours			Knocking	References
			BP	BTE	BSFC	HC	CO	NO_x	CO_2	IP_{Max}	RoHR	RoPR		
CR-17.5:1; Rated power-5.2KW @1500	Rice bran oil + H2 + CeO2 B20H0.5C40, B20H1.0C40, B20H1.5C40, B20H0.5C80, B20H1.0C80, B20H1.5C80	B20H1.5C80		↑	↓	↓	↓	↓						(Jayaraman et al., 2022)
4-S,1-C, CR-17.5:1 Rated Power 5.2 kW @ 1500 rpm	Rice bran oil + Neem biodiesel + n-Decanol NB20;NB20DI10;NB20DI30; NB (additive:n-Decanol)			↓	↑	↓	↓	↑		↑	↑			(Sakthivadivel et al., 2022)

UMPSA
اونيۏرسيتي مليسيا ڤهڠ السلطان عبدالله
UNIVERSITI MALAYSIA PAHANG AL-SULTAN ABDULLAH

Table 2.5: Continued

Engine Specifications	Fuel and Its Blends	Operating Parameters	Engine Performance Characteristics			Exhaust Emissions Characteristics				Combustion Behaviours			Knocking	References
			BP	BTE	BSFC	HC	CO	NO_x	CO_2	IP_{Max}	RoHR	RoPR		
2-C,4-S; CR-18:1; Rated Power 3.5 kW@1500 rpm; FIT-23CA bTDC; FIP-240 bar	Karanja + Rice bran oil KB20 + H2; KB10 + H2; RB10 + H2: RB20 + H2: D:D + H2	Speed-700 to 1500 RPM for KB20		↑	↓	↓	↓	↑		↑	↑			(Krishana et al., 2022)
1-C,4-S, CI engine CR-17.5:1; Rated power 3.7 kW @ 1500 rpm	Rice bran B5D95GO30 and B15D85GO30 a((additive: Graphene oxide +Nanoparticle)	IT@23 deg for B15D85GO30		↑	↓	↓	↓	↑		↑	↑			(Hoang et al., 2021)

UMPSA
اونيۏرسيتي مليسيا ڤهڠ السلطان عبدالله
UNIVERSITI MALAYSIA PAHANG
AL-SULTAN ABDULLAH

2.13 Summary

The literature review presented in this chapter emphasises the previous studies related to the implementation and the effect of alternative fuel on engine performance characteristics, exhaust gas emission, combustion behaviours as well as knocking on CI engine. It was reported that the efficiency and the performance of the CI engine could be improved using RBO blended fuels in terms of mixture formation during the combustion process. Many studies investigated on different biodiesel and biofuel on CI engine without modification. The studies included the influence of both fuels on improved engine efficiency but not much in reducing for exhaust emissions especially in terms of HC and CO_2. The studies also presented the effect of intake air temperature using biofuel on CI engine resulted in better and uniform fuel formation and thus complete combustion by considering the ignition delay period. There is limited study on the effect of using RBO on combustion behaviours and knocking intensity. Therefore, it is necessary to conduct studies on combustion techniques which focusing on the intake air temperature parameter and alternative fuel (RBO) that can inhibit the production of emissions in during combustion process and improving combustion behaviours.

UMPSA
UNIVERSITI MALAYSIA PAHANG
AL-SULTAN ABDULLAH

CHAPTER 3

METHODOLOGY

3.1 Introduction

The experimental work was conducted using RBO blended with pure diesel to examine its physicochemical properties, engine performance characteristics, combustion behaviours and knocking intensity on single-cylinder four-stroke direct injection compression ignition engine. The experimental setup and facilities utilized for the physicochemical properties measuring, engine testing and data acquisition system have been presented. The setup of single-cylinder four-stroke direct injection compression ignition engine system consists of a diesel engine, intake manifold, exhaust manifold, fuel pump, fuel tank, gas analyser, in-cylinder pressure, crank angle sensor, dynamometer, controller and data acquisition system. Figure 3.1 illustrates a flow chart representing the research methodology.

اونيۏرسيتي مليسيا ڤهڠ السلطان عبدالله
UNIVERSITI MALAYSIA PAHANG
AL-SULTAN ABDULLAH

The study commenced by examining the physicochemical properties of RBO blended fuel encompassing parameters such as density, kinematics viscosity, calorific value (CV) and cetane number (CN). Then, the investigation proceeds to analyse the engine performance characteristics attributes by using RBO blended and intake air temperature as the input parameter on CI engine, including engine brake power (BP), brake specific fuel consumption (BSFC), brake thermal efficiency (BTE), carbon monoxide (CO), carbon dioxide (CO_2), hydrocarbon (HC) and oxide of nitrogen (NO_X). The subsequent research is then focused on analysing the combustion behaviours exhibited by CI engines when utilizing RBO blended. This encompasses the analysis of exhaust gas temperature (EGT), in-cylinder pressure (IP), rate of heat release (RoHR) and rate of pressure rise (RoPR). Finally, the present study evaluates the influence of RBO and intake air temperature on knocking intensity (KI) on a CI engine.

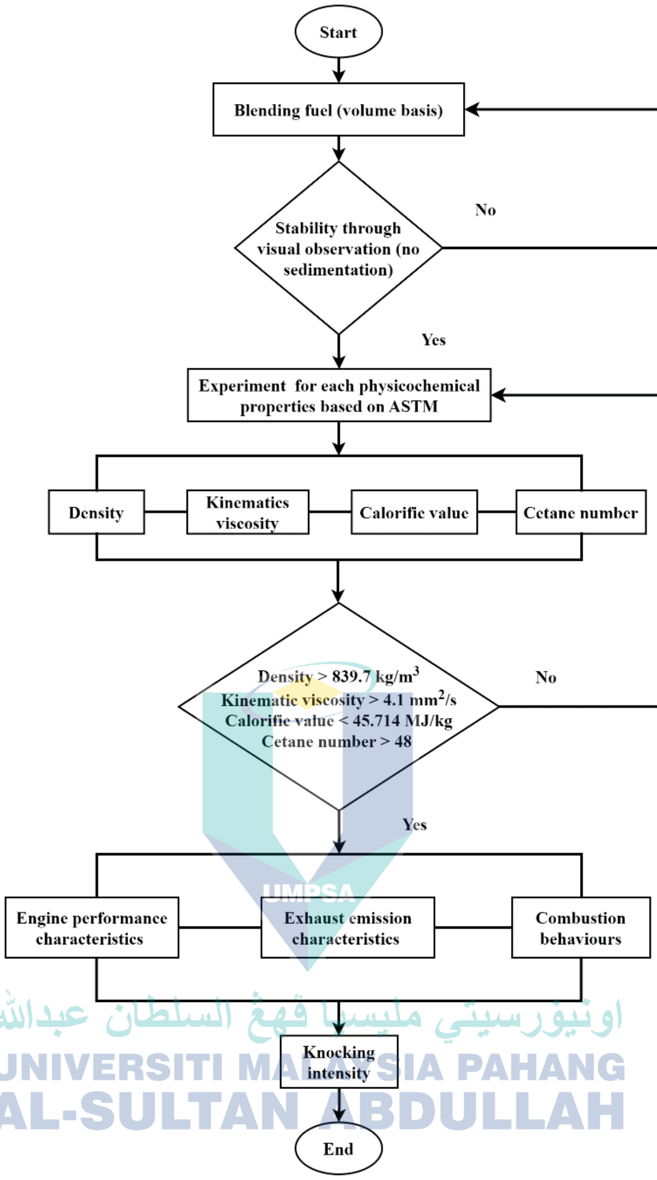

Figure 3.1 Experimental and research methodology flow chart

3.2 Experimental Setup

The experiment was performed at engine performance laboratory located at University Malaysia Pahang Al-Sultan Abdullah (UMPSA), Pekan, Pahang. The engine testing equipment used in the engine test cell is shown in Figure 3.2 and Figure 3.3 and included a DEWETRON data acquisition (DAQ) system, a 150-kW eddy current

اونيۏرسيتي مليسيا ڤهڠ السلطان عبدالله
UNIVERSITI MALAYSIA PAHANG
AL-SULTAN ABDULLAH

dynamometer equipped with a KIPOR 170 FS single-cylinder, four-stroke, air-cooled, Compression Ignition (CI) diesel engine. A sample of 10000 ml of all blends was used without treatment beforehand. The blended fuels were fed to air-cooled diesel engines for performance and emission as well as combustion tests. The engine injection pressure varies with a governor's engine rotation per minute (rpm), allowing injection pressure of 20-200 bar depending on the engine speed. For all experiments, the engine was fuelled by pure diesel first, and in each different RBO blended was also used in intervals to ensure smooth running and fuel line flushing for the different RBO blended. In each test, the engine will be warmed up for 20 minutes to ensure optimal engine temperature is reached. Measurements of the load increment range from full to no loads were tabulated. A 30-cc fuel consumption time was recorded for each experiment. Each experiment was repeated three times to ensure the repeatability and validity of the measurements. The exhaust gas temperature and emission data, the ambient temperature and the inlet air flow rate, were recorded for each test.

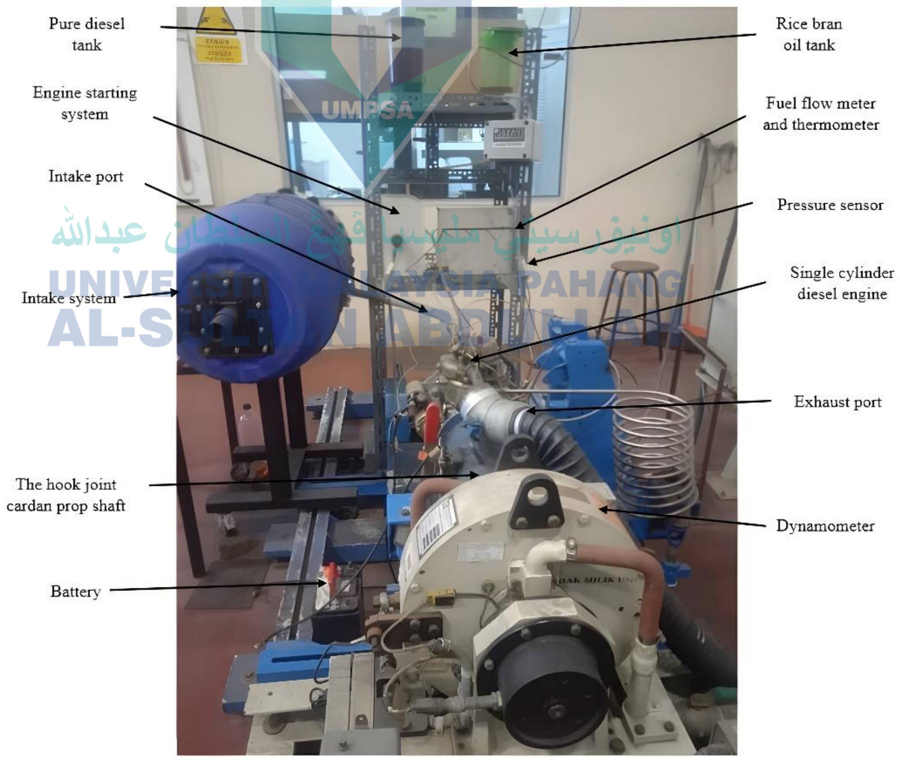

Figure 3.2 Engine test rig with dynamometer equipped with a KIPOR 170 FS single-cylinder, four-stroke, air-cooled, compression ignition engine installed with major components (front view)

Figure 3.3 Engine test rig with dynamometer equipped with a KIPOR 170 FS single-cylinder, four-stroke, air-cooled, compression ignition engine installed with major components (side view)

3.2.1 Engine Test Bed

A single-cylinder, four-stroke, air-cooled compression ignition engine connected to a hydraulic dynamometer on a fixed test bed is used for conducting the study. The engine tank has a fuel capacity of 2.5 litres, and the engine uses an electrical starter. The diesel engine has a power capacity that reaches a peak power of 3.5 kW at a speed of 3600 rpm. Table 3.1 shows the engine model and engine specification. The detailed data of the engine are presented in Appendix C and D.

UMPSA
اونيۏرسيتي مليسيا ڤهڠ السلطان عبدالله
UNIVERSITI MALAYSIA PAHANG
AL-SULTAN ABDULLAH

Table 3.1 Engine specifications for KIPOR 170 FS

Description	Specification
Type	4-stroke, Vertical Cylinder, Air-Cooled Diesel Engine
Number of Cylinders	1
Combustion System	Direct Injection
Bore x Stroke	(70 x 55 mm)
Compression Ratio	20.1 ± 0.5
Maximum Engine Power	3.5 kW
Maximum Torque	9.28 Nm

Source: Stone (1999)

Experimental facility arrangements for the study are represented in Figure 3.4. A single-cylinder compression ignition diesel engine was used in the experimental setup. It was coupled to an eddy current (EC) dynamometer from Dynalec. Engine speed, torque and load were controlled by Dynalec controllers (Figure 3.5). The DAQ controller and the dynamometer system connected the pressure encoder sensors to the PC, respectively.

UMPSA
UNIVERSITI MALAYSIA PAHANG
AL-SULTAN ABDULLAH

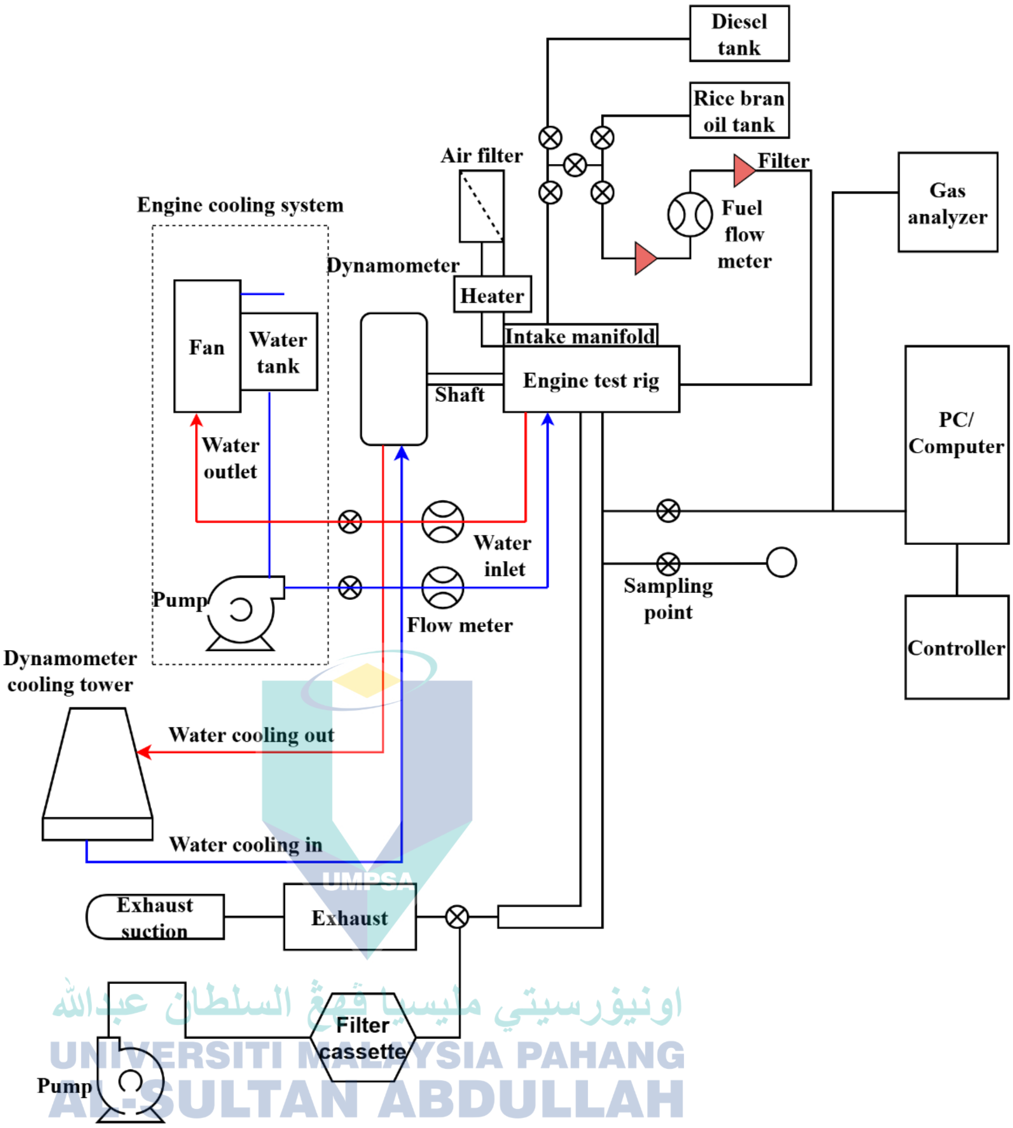

UMPSA
اونيورسيتي مليسيا قهڠ السلطان عبدالله
UNIVERSITI MALAYSIA PAHANG
AL-SULTAN ABDULLAH

Figure 3.4 Experimental facility arrangement with installed dynamometer, engine cooling system, fuel tank, gas analyzer, controller, exhaust gas system

Figure 3.5 Engine test bed KIPOR 170FS with ECB-15 kW dynalec controller

UMPSA
اونيۏرسيتي مليسيا ڤهڠ السلطان عبدالله
UNIVERSITI MALAYSIA PAHANG
AL-SULTAN ABDULLAH

3.2.2 Fuel Measurement

In general, the properties of biofuel from different sources are slightly different depending on the biodiesel feedstock according to the ASTM fuel standard. The blending of biofuel with mineral diesel is one of the common methods to introduce biofuel as a fuel for direct usage in diesel engine under the ASTM blended fuel standard (Sun et al., 2019). Selection of the maximum percentage of biofuel for blending with diesel according to the blended fuel standard depends on the biofuel feedstock property. Therefore, evaluating the blended fuel properties is the most important criteria to choose the suitable blend ratio (Gülüm, 2022). RBO was purchased from a local bio-oil-producing company in Selangor, Malaysia. Pure diesel fuel was provided by a commercial company known as Rahar Jati Sdn. Bhd. It is a local industrial enterprise located in Pekan, Pahang, Malaysia, provided Diesel Euro 2, a type of diesel fuel known as pure diesel. The RBO blended with pure diesel blended into RBO00 fuel

(100% vol. pure diesel + 0% vol. rice bran oil), RBO25 fuel (75% vol. pure diesel + 25% vol. rice bran oil), RBO50 fuel (50% vol. pure diesel + 50% vol. rice bran oil), RBO75 fuel (25% vol. pure diesel + 75% vol. rice bran oil) and RBO100 fuel (0% vol. pure diesel + 100% vol. rice bran oil) tabulated in Table 3.2.

Table 3.2 Types of fuel and blended fuel percentage

Types of Fuel	**Blended Fuel Percentage**
RBO00	0 % vol. RBO + 100 % vol. Pure Diesel
RBO25	25 % vol. RBO + 75 % vol. Pure Diesel
RBO50	50 % vol. RBO + 50 % vol. Pure Diesel
RBO75	75 % vol. RBO + 25 % vol. Pure Diesel
RBO100	100 % vol. RBO + 0 % vol. Pure Diesel

A UP400St-Hielscher ultrasonic processor (Figure 3.6) was used to blend samples of blended rice bran oil with pure diesel. The technical specifications of ultrasonic processors are shown in Table 3.3 below. Before being tested, these blend fuels were swirled and stirred constantly for an hour to establish good blending and then allowed for an hour to reach stability (Aghbashlo et al., 2021). Different blending of the different fuels using rice bran oil could induce limitations like higher cetane number, lower volatility, shorter ignition delay, ignitability reduction, and higher lubricity (Sharma & Murugan, 2017). The density of tested fuels was determined at a temperature of 15 °C using the device of Specific Gravity Meter (model DA-130N). The testing of the viscosity of the sample fuels was conducted using a device of K23376-KV1000 model; digital constant temperature kinematic viscosity bath, which maintained a consistent temperature of 40 °C ±0.01. Additional fuel qualities that have an impact on engine characteristics on diesel-biodiesel blends encompass energy content. As a result, there has been a scarcity of study undertaken on the assessments of

UMPSA
اونيۏرسيتي مليسيا قهڠ السلطان عبدالله
UNIVERSITI MALAYSIA PAHANG
AL-SULTAN ABDULLAH

energy content, providing little information regarding the instruments, equipment, and thorough techniques applied for analysis (Mahmudul et al., 2017).

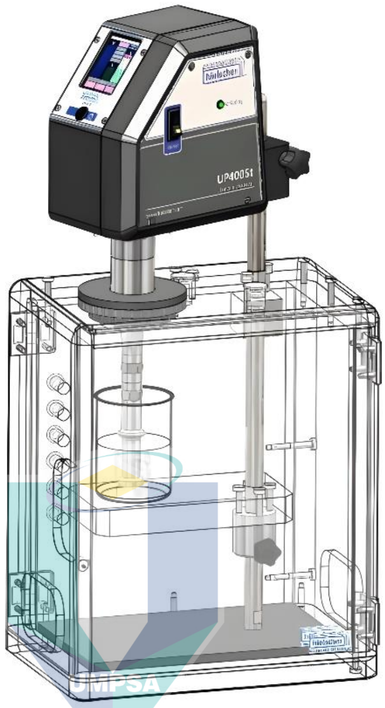

Figure 3.6 UP400St-Hielscher ultrasonic processors (cross section)

UNIVERSITI MALAYSIA PAHANG AL-SULTAN ABDULLAH

Table 3.3 Technical specification of UP400St-Hielscher ultrasonic processors

Technical Specification of UP400St-Hielscher Ultrasonic Processors	
Efficiency (%)	>90 %
Working frequency (kHz)	24
Control range (Hz)	± 500
Output control (%)	20 - 100
Pulse-pause mode factor (% per second)	10 – 100 (1-5-10 steps)

3.2.2.1 Density

The density of the fuel samples was determined at 15°C using the portable density/specific gravity meter, model DA-130N, as shown in Figure 3.7 according to ASTM D1298. This system has an LED display and is controlled by a microprocessor. Its precision is +/- 0.001 g/cm^3, and its range is 0.0000 to 2.0000 g/cm^3.

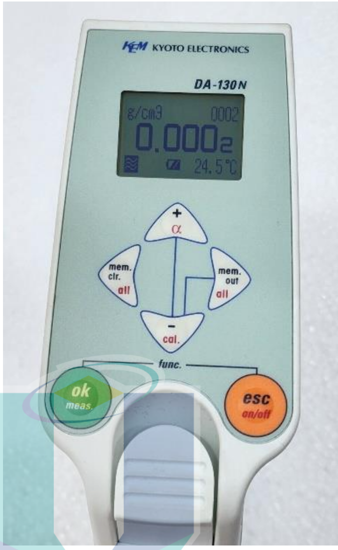

Figure 3.7 Portable density/specific gravity meter (DA-130N)

UNIVERSITI MALAYSIA PAHANG
AL-SULTAN ABDULLAH

This test method covers the laboratory determination using a glass hydrometer in conjunction with a series of calculations of the density, relative density, or American Petroleum Institute (API) gravity of crude petroleum, petroleum products, or mixtures of petroleum and nonpetroleum products normally handled as liquids and with Reid vapor pressures of 101.325 kPa or less. The values are determined at the existing temperature and corrected to 15°C using a series of calculations and international standard tables.

Cleaning the measuring cell before and after each measurement series is important to ensure reliable readings. If the measuring cell is not thoroughly cleaned, residue may build up inside it. This can be seen if there is a change in the deionized water's density values. Therefore, it's crucial to take regular deionized water check readings. A correction is necessary if the water density measurements differ by more than 0.001 g/cm^3 at the specified temperature. A readjustment is possible only when the computed difference between the measured and theoretical value is less than 0.01 g/cm^3, and the water temperature is between 15 and 25°C.

3.2.2.2 Kinematic Viscosity

The kinematic viscosity was determined using the capillary viscometer method described in ASTM 445-01 using a Cannon-Fenske routine viscometer for transparent liquids with size No. 75, which is utilized for kinematic viscosity ranges of 1.6 to 8 mm^2/s. The digital constant temperature kinematic viscosity bath illustrated in Figure 3.8 was used to measure viscosity at a temperature of 40 ± 0.1 °C. A stopwatch was used to time how long it took for the liquid level to decrease from the upper to the lower mark on the viscometer, as illustrated in Figure 3.9, to the nearest one-fifth of a second.

UMPSA
UNIVERSITI MALAYSIA PAHANG
AL-SULTAN ABDULLAH

Figure 3.8 Digital constant temperature kinematic viscosity bath (K23376 KV1000)

The result is considered accurate only when there is less than a 1% difference between two readings in a row. The flow time of the liquid under investigation was determined by taking the average of at least three observations. According to the ASTM 445-01, the purpose of this test method is to determine the kinematic viscosity of liquid petroleum products, both transparent and opaque, by measuring how long it takes for a volume of liquid to flow through a calibrated glass capillary viscometer.

This test method provides results depending on the behaviour of the sample and is intended to be applied to liquids in which shear stress and shear rate are proportional (Newtonian flow behaviour). However, if the viscosity varies significantly with the rate of shear, results may differ between viscometers with different capillary diameters. The range of kinematic viscosities covered by this test method is from 0.2 mm^2/s to 300 000 mm^2/s at temperatures 40 ± 0.1 °C.

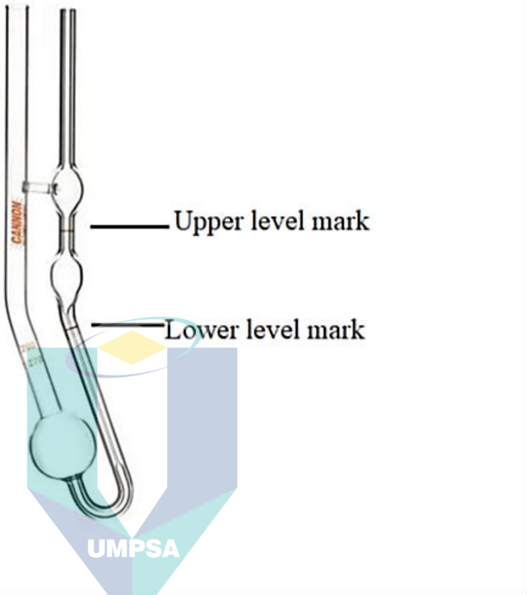

Figure 3.9 Cannon-Fenske routine viscometer for transparent liquids
Source: N. Kumar &Raheman (2022)

UMPSA
UNIVERSITI MALAYSIA PAHANG
AL-SULTAN ABDULLAH

3.2.2.3 Calorific Value

The amount of heat units released by a unit mass of a sample when burned with oxygen in a container of constant volume is referred to as the heating value (heat of combustion) of a sample. The Oxygen Bomb Calorimeter model 6772 (Parr Instrument Company, USA) was used to calculate the heating value of the fuel samples in accordance with ASTM D4809, as indicated in Figure 3.10. This test method is used to determine the heat of combustion of hydrocarbon fuels. It is designed for the analysis of aviation turbine fuels where the permissible variance between duplicate determinations is less than 0.2 %. This method can be applied to a wide range of volatile and non-volatile materials that tolerate a slight degree of precision variation. This precision can only be achieved through strict adherence to all details of the procedure, since the error generated by each individual measurement must be kept below 0.04 %, in so far as possible. The calorific value of the fuel affects the power and performance of the engine operated with the diesel-biofuel blends (Loh et al., 2017).

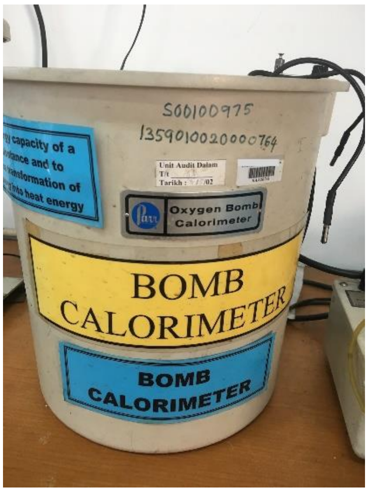

Figure 3.10 Oxygen bomb calorimeter (Parr 6772)

3.2.2.4 Cetane Number (CN)

The cetane number (CN) serves as an indicator of the ignition quality of diesel fuels. The information illustrates the ignition delay, denoting the duration required for diesel fuel to undergo spontaneous combustion after its injection into heated air via the fuel injector. The CN of diesel fuels serves as an indicator of its ignition quality, explicitly referring to the ignition delay characteristics. This parameter plays a crucial role in determining the combustion process within the engine. The CN is often regarded as the most conclusive metric for characterizing the combustion efficiency of a diesel engine. Elevated cetane levels indicate a reduced ignition delay, leading to enhanced performance of diesel engines. The fuel introduced through injection undergoes combustion in a more uniform and thorough manner, leading to enhanced air quality in the exhaust, notably regarding the reduction of soot, particulate matter, and unburned hydrocarbons. The primary determinant of diesel fuel quality is the CN measurement. This phenomenon is closely associated with a fuel's ignition delay time when injected into the combustion chamber. An increase in the cetane number leads to a decrease in the duration of the ignition delay, facilitating the cold start process and reducing the

UMPSA
UNIVERSITI MALAYSIA PAHANG
AL-SULTAN ABDULLAH

noise level during idling (Abdalla, 2018). On the contrary, the ignition occurs towards the latter stages of the expansion process, leading to incomplete combustion, decreased power output, fuel conversion inefficiency, and increased engine noise (Heywood, 1988). The cetane number is measured in accordance with ASTM D4737.

3.2.2.5 Fuel System

The fuel pipeline system involves three primary outputs: one leading to the burette, another directed towards the engine, and a third facilitating the flushing of fuel back into the fuel tank. The ball valves were employed to facilitate the manipulation of fuel flow within the fuel pipeline, allowing for the initiation or termination of fuel transmission. The measurement of the gasoline occurred during the opening of the second ball valve. In this configuration, the fuel is directed linearly towards the engine (as depicted in Figure 3.11 and Figure 3.12), and the measurement can be obtained by observing the burette rather than relying on the fuel tank.

Figure 3.11 The fuel pipeline system with installed fuel valves

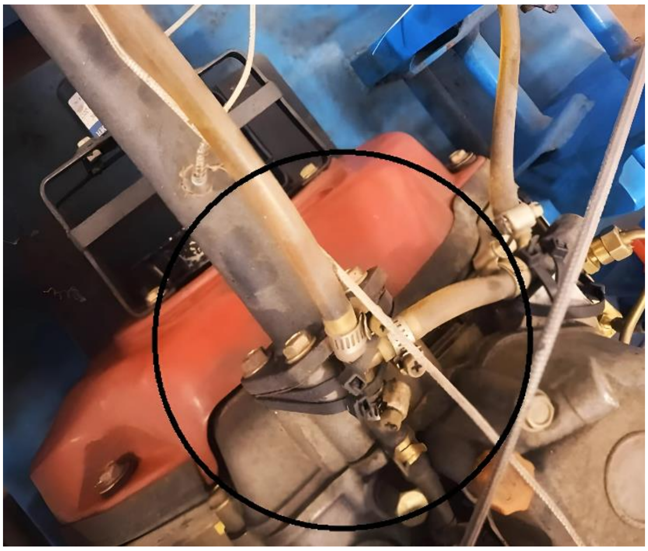

Figure 3.12 The fuel flows piping system to the engine (side view)

Figure 3.13 The fuel flows to the engine (front view)

The suitability of all blended fuel usage properties is the most critical indicator and must be compared with fuel standards (Constantino et al., 2019). Alternative fuel blends must be studied for their properties and analysed before each fuel is used on any combustion engine (Dharmaraja et al., 2019; Zaharin et al., 2018).

3.3 Experimental Instrumentation

The instruments used to measure the experimental data are thermocouples, gas analysers, lambda sensors, pressure transducers, in-cylinder pressure sensors, data acquisition system and digital anemometer. Figure 3.14 show the schematic diagram of engine test bed and instrumentation. The following section describes all the instruments used in the experiment work.

UMPSA
اونيۏرسيتي مليسيا ڤهڠ السلطان عبدالله
UNIVERSITI MALAYSIA PAHANG
AL-SULTAN ABDULLAH

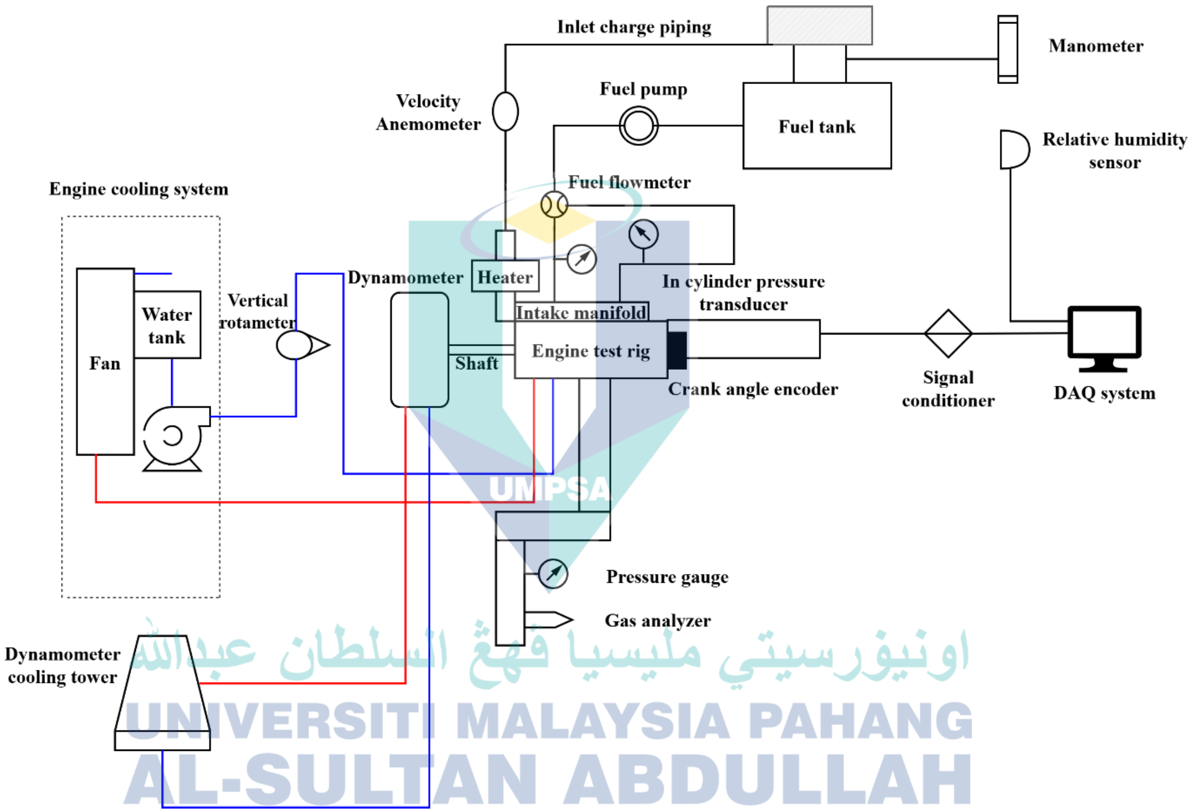

UMPSA
اونيۏرسيتي مليسيا ڤهڠ السلطان عبدالله
UNIVERSITI MALAYSIA PAHANG
AL-SULTAN ABDULLAH

Figure 3.14 Experimental facility arrangement with installed instrumentation

3.3.1 Thermocouples

There are two K-type thermocouples were used in this study. The engine room's ambient temperature was measured using a single thermocouple. The engine and exhaust temperatures were tracked using thermocouples throughout the process. The thermocouple was mounted at the engine body's rotary blade, as shown in Figure 3.15 (b). The thermocouple reading was linked to the electronic control unit, which transmitted the information to the computer. In order to provide real-time exhaust temperature readings with less heat loss to the atmosphere, a second thermocouple was added close to the exhaust port (Figure 3.15 (a)). The inlet temperature sensor, which is located near the inlet port, is shown in Figure 3.15 (c). The standalone thermocouple reader device's display screen can be used to collect temperature readings directly and effectively.

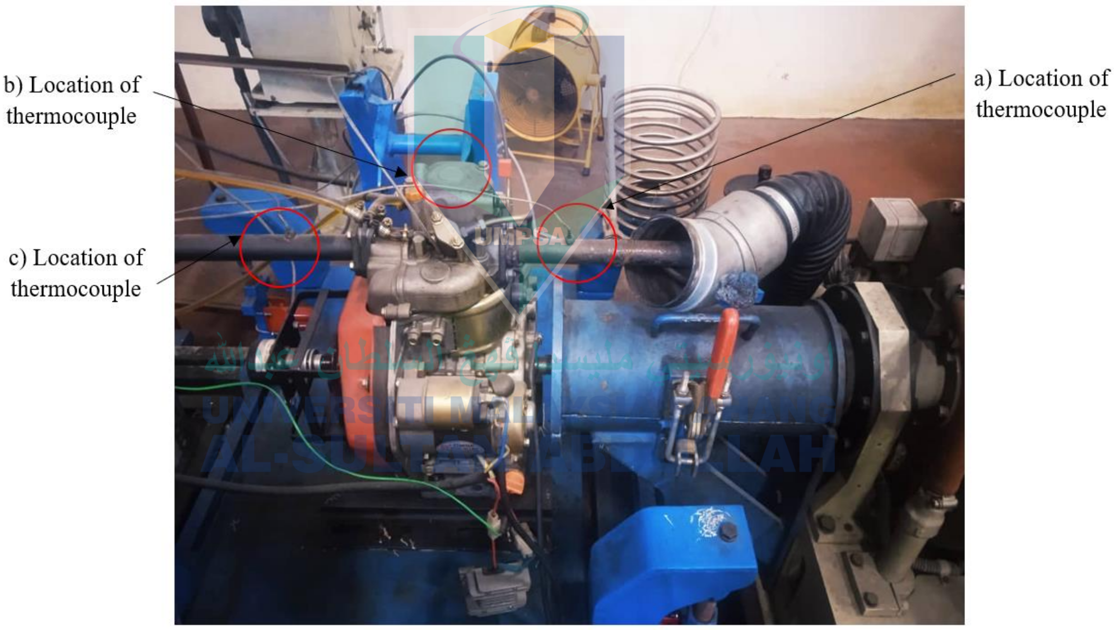

Figure 3.15 Location of thermocouples

3.3.2 Gas Analyzer

One of the most significant findings from this study relates to exhaust gas emissions. Using a gas analyzer, the exhaust gas emissions, including combustion byproducts, were monitored at the exhaust port. The exhaust gas emissions were tracked and recorded using a QROTECH QRO-401 gas analyzer. The CO, HC, and CO_2 using measuring methods use Non-Dispersive infrared (NDIR), while O_2 and NO_X using electrochemical cell method. Figure 3.16 shows the composition of the part QROTECH QRO-401 gas analyzer.

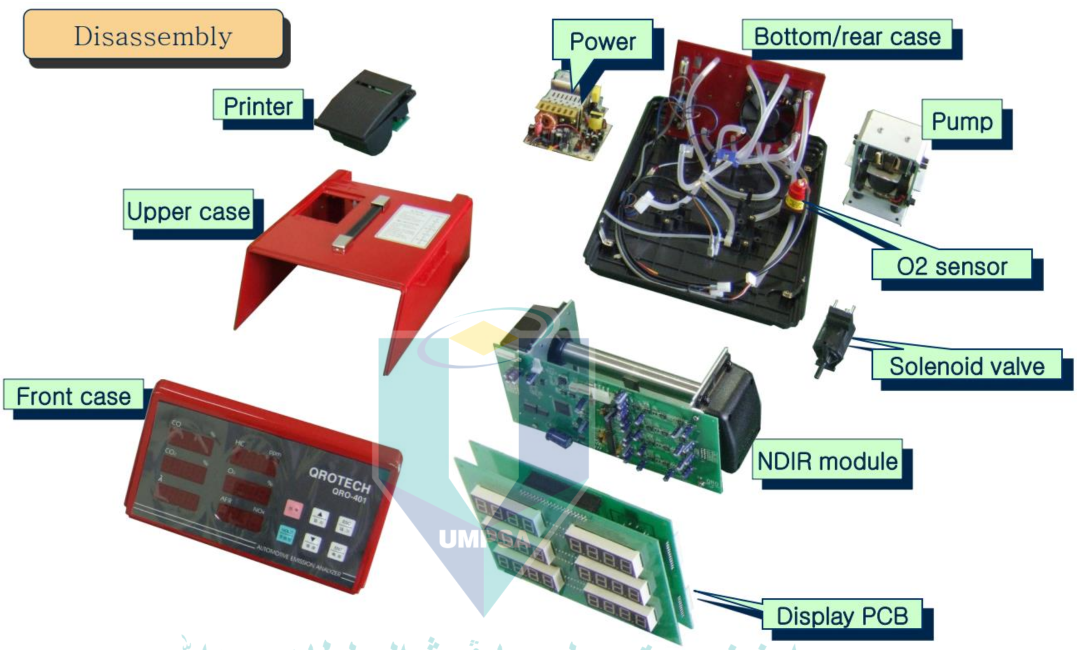

Figure 3.16 Composition of the part QROTECH QRO-401 gas analyzer

اونيۏرسيتي مليسيا ڤهڠ السلطان عبدالله
UNIVERSITI MALAYSIA PAHANG
AL-SULTAN ABDULLAH

This instrument complies with OIML, EPA, and ASM regulations and is capable of accurately measuring the gases O_2, CO_2, HC, CO, and NO_X precisely with its accuracy tabulated in Table 3.4.

A desktop computer was linked to the gas analyzer to record the data. The table below displays the operating parameters and accuracy of the gas analyzer. The manufacturer performed maintenance and calibration on the gas analyzer before the test, and daily standard calibrations were carried out.

Table 3.4 QROTECH QRO-401 gas analyser measurement accuracy

Gases	Measuring Range	Resolution	Measuring Method
CO_2	0 - 20 %	0.1 %	
HC	0 – 9999 ppm	1 ppm	NDIR Method
CO	0 – 9.99 %	0.01 %	
NO_X	0 – 5000 ppm	1 ppm	Electrochemical Cell
O_2	0 - 25 %	0.01 %	

3.3.3 Lambda Sensor

The lambda (λ) sensor is equipped with a digital display that utilizes an MTX-L digital air-fuel ratio gauge and a Bosch heated wideband oxygen sensor, as depicted in Figure 3.17 and Figure 3.18, respectively. The exhaust gas oxygen is measured using an oxygen sensor, specifically a wide band λ sensor. The lambda sensor can calibrate itself autonomously, adapting to temperature and sensor conditions variations. The oxygen sensor is located inside the exhaust gas pipe. The sensor at different engine loads continuously obtains the data on the air-fuel ratio during the engine operation. The oxygen sensor is integrated with the engine's ECU; the fuel injection is regulated to attain a stoichiometric air/fuel ratio.

UMPSA
اونيبرسيتي مليسيا ڤهڠ السلطان عبدالله
UNIVERSITI MALAYSIA PAHANG
AL-SULTAN ABDULLAH

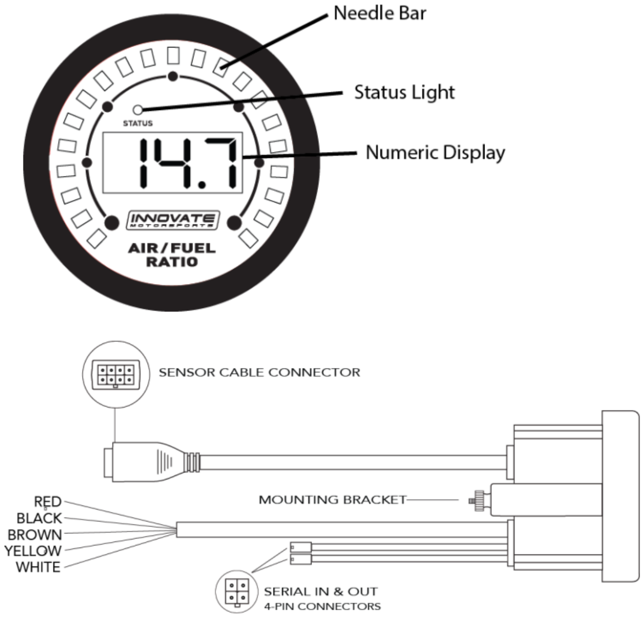

Figure 3.17 Components of innovate MTX-L digital air-fuel ratio gauge

Figure 3.18 Bosch oxygen sensor

UMPSA
اونيۏرسيتي مليسيا ڤهڠ السلطان عبدالله
UNIVERSITI MALAYSIA PAHANG
AL-SULTAN ABDULLAH

3.3.4 Pressure Transducer and In-Cylinder Pressure Sensor

The pressure transducer used for the in-cylinder pressure was an Optrand model C32294-Q. It has a sensitivity of 1.32 mV/psi at 200 °C and a pressure range of 0 to 3000 Psi. Before the signal was read by the data logger and sent to the computer, it was amplified by the transducer and linked to the pressure sensor controller box. The data logger's software was created by the vendor. Even though the pressure transducer had been factory calibrated, an essential in-house calibration was necessary for a new unit to confirm the reading from the transducer, such as the sensitivity of the pressure sensor. In-cylinder pattern, pressure rise, and indicated mean effective pressure (IMEP) readings from the software may be needed. A pressure sensor with serial number CAS-5-170001-PC was used in this experimental study (Figure 3.19).

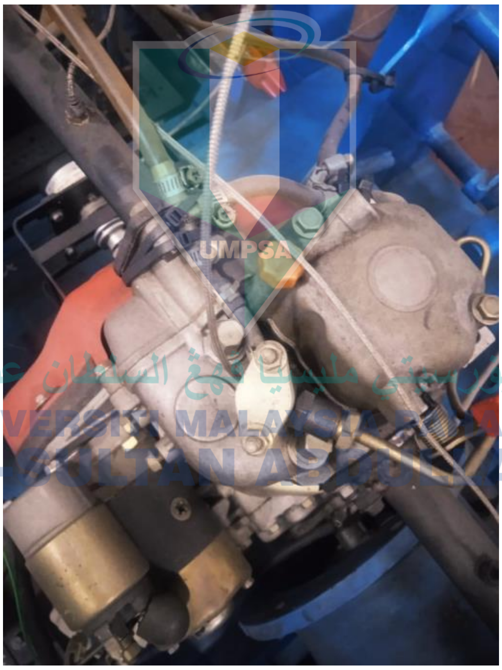

UNIVERSITI MALAYSIA PAHANG AL-SULTAN ABDULLAH

Figure 3.19 Installed in-cylinder pressure sensor with serial number CAS-5-170001-PC

3.3.5 Data Acquisition System

A single-cylinder compression ignition diesel engine was used in the experimental setup. It was coupled to an eddy current (EC) dynamometer from Dynalec. Engine speed, torque and load were controlled by Dynalec controllers. The motor was loaded using a 150-kW eddy-current type water-cooled dynamometer model ECB-15kW SR No. 615 from Dynalec Controls with a controller, as shown in Figure 3.20.

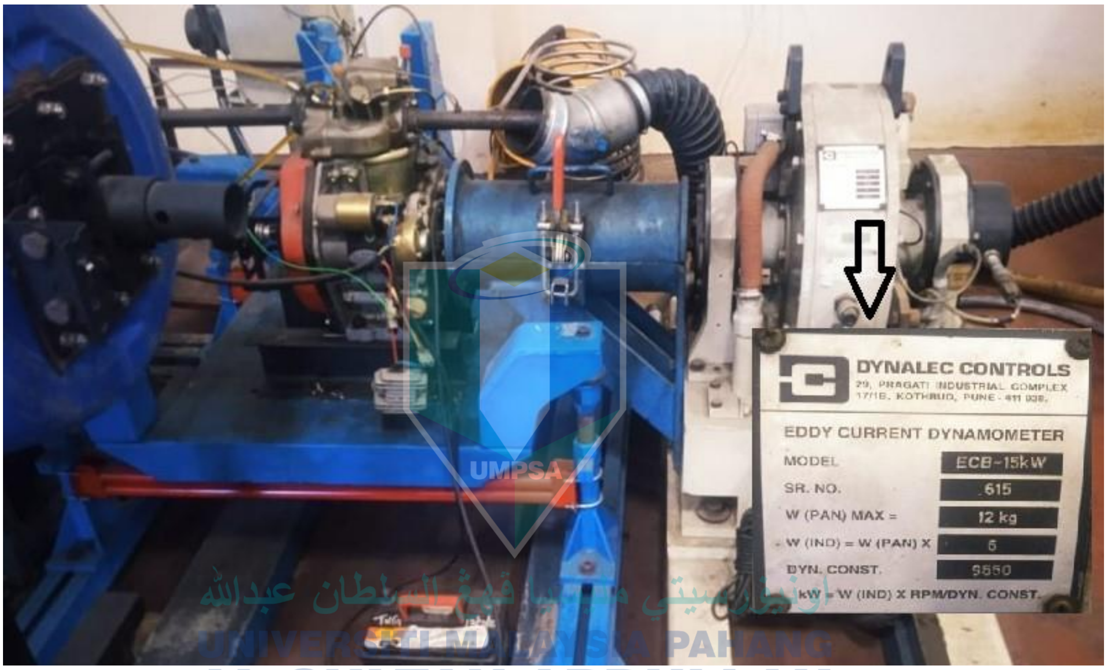

UNIVERSITI MALAYSIA PAHANG
AL-SULTAN ABDULLAH

Figure 3.20 ECB-15 kW Dynalec controller (series number: 615)

The dynamometer is governed by a serial port data logging program provided, communicated with the controller via a computer controller, and data is obtained via a computer, as shown in Figure 3.21. The dynamometer's data logger system was connected to sensors (inlet pressure, rotating speed, exhaust temperature, and airflow meter) and actuators (load and throttle controllers).

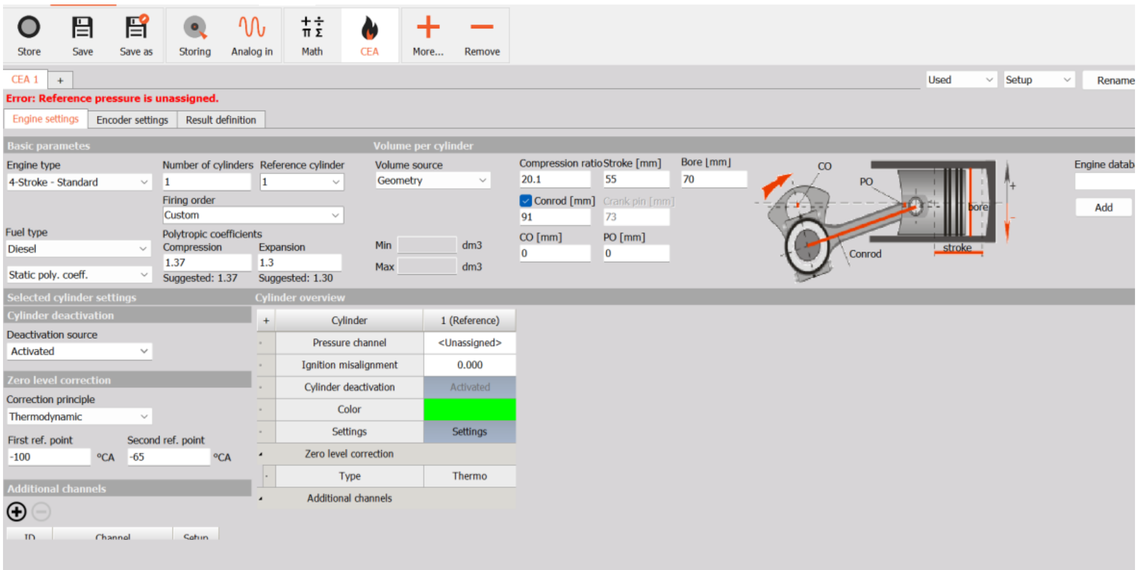

Figure 3.21 Interface of software data logger

The program displays and records dynamometer speed, torque, and dynamometer load data. Speed and torque serve as the defining characteristics of the dynamometer brake and engine working conditions. The throttle engine position handle (shown in Figure 3.22) function to controls the engine speed by increasing or decreasing it. The test rig will operate more steadily if the brake is more potent than the engine above the chosen speed. The detailed data on the throttle lever position are presented in Appendix B.

اونيۏرسيتي مليسيا ڤهڠ السلطان عبدالله
UNIVERSITI MALAYSIA PAHANG
AL-SULTAN ABDULLAH

Figure 3.22 Throttle lever position controller

3.3.6 Digital Anemometer

The exhaust flow rate was calculated using a digital anemometer. The VICTOR VC-816B Digital anemometer (as depicted in Appendix G) was used to measure the exhaust gas suction produced by the exhaust system. The specifications of the VICTOR VC-816B can be seen in Table 3.5 which provides the VICTOR VC-816B's specifications. 0.0504 m^3/s is the average exhaust suction volume flow rate. A dynamic pressure formula, which is $0.5\rho V^2$, was used to determine the pressure, where V is the exhaust gas velocity and ρ is the exhaust gas density (0.9025 kg/m^3).

UMPSA
اونيۏرسيتي مليسيا ڤهڠ السلطان عبدالله
UNIVERSITI MALAYSIA PAHANG
AL-SULTAN ABDULLAH

Table 3.5 VICTOR VC-816B digital anemometer specifications

		Air velocity		
Unit	Range	Resolution	Threshold	Accuracy
m/s	0-45	0.1	0.3	±3% ±0.1 dgts
ft/min	0-8800	19	60	±3% ±10 dgts
knots	0-88	0.2	0.6	±3% ±0.1 dgts
km/h	0-140	0.3	1	±3% ±0.1 dgts
mph	0-100	0.2	0.7	±3% ±0.1 dgts
		Temperature		
Unit	Range	Resolution	Accuracy	
°C	0±45	0.2	±2	
°F	32-113	0.36	±3.6	
Power supply		9V Battery		
Operating temperature		-10±50°C (14-122°F)		
Operating humidity		40-85%RH		
Store temperature		-20±60°C (-4-140°F)		
Store humidity		10-90%RH		

UMPSA
UNIVERSITI MALAYSIA PAHANG
AL-SULTAN ABDULLAH

3.4 Experiment Methodology

The experiment was performed at engine performance laboratory located at UMPSA, Pekan, Pahang. The engine testing equipment used in the engine test and included a DEWETRON data acquisition (DAQ) system, a 150-kW eddy current dynamometer equipped with a KIPOR 170 FS single-cylinder, four-stroke, air-cooled, compression ignition engine. SAE J1312-Procedure for Mapping Performance-Compression Ignition Engines and SAE J1349-Standard Engine Power Test Code for diesel engine was implemented to carry out standard engine testing method. According to this standard, engine power is calculated as the product of torque obtained at maximum engine load and engine dynamometer speed. The output power, torque, and the consumption of fuel data were provided by manufacturer for the engine of KIPOR 170FS. The diesel engine was fuelled using pure diesel to produce the performance curve at 50% throttle position. This performance curve was developed according to SAE J1349-Engine Power Test Code for diesel engines (SAE, 1995). The following characteristics were measured in accordance with SAE J1349: torque, engine speed, water and oil in the engine, ambient temperatures, and inlet air pressure. Based on the power curve, the data were recorded for five operating speeds, between lowest and maximum speed recommended by the manufacturer.

Five corresponding engine speeds were 1500 rpm, 2000 rpm, 2500 rpm, 3000 rpm and 3500 rpm. A sample of 10000 ml of all blends was used without treatment beforehand. The blended fuels were fed to air-cooled compression ignition engine for engine performance, emission as well as combustion tests. The engine injection pressure varies with a governor's engine rotation per minute (rpm), allowing injection pressure of 20-200 bar depending on the engine speed. For all experiments, the engine was fuelled by pure diesel first, and in each different fuel blend diesel was also used in intervals to ensure smooth running and fuel line flushing for the different fuel blends. All measurements were carried out on a 200 ml sample that had not been pre-treated using. The air-cooled CI engine employed a 200-bar injection pressure. The engine was initiated using a designated fuel mixture and let to reach operating temperature for a duration of 20 minutes. The measurements were recorded for various incremental loads, running from no load to full load.

All of the observations have been gathered. The inlet air flow rate, time for 30 cc of fuel consumption, ambient temperature, exhaust gas temperature, outlet cooling water flow rate, and ammeter and volt meter readings were recorded for each loading, and the experiments were repeated three times to ensure that the measurements were repeatable (Sun et al., 2019). In each test, the engine will be warmed up for 20 minutes to ensure optimal engine temperature is reached. Measurements of the load increment range from full to no loads were tabulated. A 30-cc fuel consumption time was recorded for each experiment. Each experiment was repeated three times to ensure the repeatability and validity of the measurements. There are three main experiments were involved in this study. The input parameters were involved in an Experiment 1 including the engine speed range from 1500 rpm to 3500 rpm; the interval is 500 rpm. Then, it involved the engine load which ranging from 0 to 100 %. The second experiment is focusing on three different types of intake air temperature: 30°C, 45°C and 65°C at 2500 rpm. Lastly, constant engine speed which is at 1500 rpm at various equivalent ratio as input parameters for Experiment 3.

Table 3.6 Operating conditions for experiment 1

	Experiment 1	
Fuel Types	**Engine Speed (rpm)**	**Engine Load (%)**
RBO00	1500	0-100
	2000	
	2500	
	3000	
	3500	
RBO25	1500	0-100
	2000	
	2500	
	3000	
	3500	
RBO50	1500	0-100
	2000	
	2500	
	3000	
	3500	
RBO75	1500	0-100
	2000	
	2500	
	3000	
	3500	
RBO100	1500	0-100
	2000	
	2500	
	3000	
	3500	

UMPSA
اونيۏرسيتي مليسيا ڤهڠ السلطان عبدالله
UNIVERSITI MALAYSIA PAHANG
AL-SULTAN ABDULLAH

Table 3.7 Operating conditions for experiment 2

Experiment 2			
Fuel Types	**Intake Air Temperature (°C)**	**Engine Speed (rpm)**	**Crank Angle (°C)**
RBO00	30	2500	0-720
	45	2500	0-720
	65	2500	0-720
RBO25	30	2500	0-720
	45	2500	0-720
	65	2500	0-720
RBO50	30	2500	0-720
	45	2500	0-720
	65	2500	0-720
RBO75	30	2500	0-720
	45	2500	0-720
	65	2500	0-720
RBO100	30	2500	0-720
	45	2500	0-720
	65	2500	0-720

UMPSA
اونيۏرسيتي مليسيا ڤهڠ السلطان عبدالله
UNIVERSITI MALAYSIA PAHANG
AL-SULTAN ABDULLAH

Table 3.8 Operating conditions for experiment 3

Experiment 3		
Fuel Types	**Engine Speed (rpm)**	**Equivalent Ratio**
RBO00	1500	0.1-0.7
RBO22	1500	0.1-0.7
RBO50	1500	0.1-0.7
RBO75	1500	0.1-0.7
RBO100	1500	0.1-0.7

3.4.1 Experimental Error

The experimental error must be reduced to the minimum possible to ensure the accuracy of the work. The total error can arise from the experimental design, measurement instruments, test conditions, calibration and data reading (Sathish Kumar et al., 2022). The experimental readings errors, the work was repeated at least three times in this work. The error of each parameter has been considered in the experimental design.

3.5 Summary

اونيۏرسيتي مليسيا ڤهڠ السلطان عبدالله
UNIVERSITI MALAYSIA PAHANG
AL-SULTAN ABDULLAH

This investigation is undertaken to achieve the objectives outlined in this thesis. The present chapter comprehensively discusses the experimental setup, experimental instrumentation, experimental procedures, and data measurement to analyse the engine performance, combustion behaviours and knocking intensity. A detailed discussion of the experimental setup layout was undertaken. This section discusses the instruments employed in the study, including the data gathering system, installed thermocouples, gas analyser, lambda sensor, pressure transducer, in-cylinder pressure sensor, data acquisition system and digital anemometer and lastly, the experimental accuracy and error also presented in this chapter.

CHAPTER 4

RESULTS AND DISCUSSION

4.1 Introduction

This chapter is details experimental research employing a KIPOR 170FS engine, a single-cylinder, four-stroke CI engine running on pure diesel fuel as a baseline and RBO blended to examine the physicochemical properties of the RBO blended, engine performance characteristics, combustion behaviours and knocking intensity. The findings of the measurements of the fuel qualities discussed in this Section 4.2.

The following sections discuss and assess the engine performance outcomes including exhaust emission in Section 4.3 and 4.4, respectively. Then, the combustion behaviours and knocking intensity were examined in the following section (Section 4.5 and Section 4.6, respectively). The summary of the possibilities of RBO fuels as substitute fuels for CI engines is included in Section 4.7.

UMPSA
اونيۏرسيتي مليسيا ڤهڠ السلطان عبدالله
UNIVERSITI MALAYSIA PAHANG
AL-SULTAN ABDULLAH

4.2 Analysis of Physicochemical Properties of Rice Bran Oil Blended

In general, the properties of biofuel from different sources are slightly different depending on the feedstock according to the ASTM fuel standard. The blending of biofuel with pure diesel is one of the common methods to introduce biofuel as a fuel for direct usage in CI engine under the ASTM blended fuel standard (Sun et al., 2019). Selection of the maximum percentage of biofuel for blending with pure diesel according to the blended fuel standard depends on the biofuel feedstock property. Therefore, evaluating the blended fuel properties is the most important criteria to choose the suitable blend ratio (Gülüm, 2022).

An overview of the physical, chemical, and fuel attributes of rice bran oil and its blend fuels can be found in Table 4.1. These characteristics will affect the blends' performance and appropriateness as CI engine fuels, as well as their quality and behaviour. The most crucial indicate is the suitability of all mixed fuel utilisation qualities in comparison with fuel standards (Fu & Turn, 2019). The investigation of fuel attributes and analysis of alternative fuel blends is necessary prior to their use in combustion engines (Dharmaraja et al., 2019; Zaharin et al., 2018).

Table 4.1 presented the results of physicochemical property for each fuel blend, conducted according to the standard test technique. In general, RBO blended showed and indicated the improved physicochemical properties in terms of density, KV and its CN when compared with the pure diesel as a baseline. On the contrary, RBO blended resulted in lower CV than pure diesel which indicated the energy content in the fuel. The details discussion on each physicochemical properties presented in Section 4.2.1 until Section 4.2.4

Table 4.1 Tested physicochemical properties results

Properties	**Testing Method**	**RBO00**	**RBO25**	**RBO50**	**RBO75**	**RBO100**
Density (kg/m^3)	ASTM D1298	839.7	849.1	862.62	874.08	897.0
Kinematic Viscosity (mm^2/s)	ASTM D445-01	4.1	4.4	4.5	4.8	5.2
Calorific Value (MJ/kg)	ASTM D4809	45.714	44.221	43.8684	42.9456	41.100
Cetane Number	ASTM D4737	48	50	52	54	55

UMPSA
اونيۏرسيتي مليسيا ڤهڠ السلطان عبدالله
UNIVERSITI MALAYSIA PAHANG
AL-SULTAN ABDULLAH

4.2.1 Density

The fuel density is determined by the composition of chemicals of the fuel. In general, RBO blended exhibits a higher density when compared to pure diesel fuels based on Table 4.1. When considering engines with identical capacity and power, it is observed that the BSFC tends to increase. The higher density of RBO fuel compared to conventional diesel fuel has an impact on the penetration of fuel sprays and the production of fuel droplets (Hoang et al., 2021). The density of RBO100 exhibits a minor increase of 6.82 % compared to pure diesel fuel. The data presented illustrates a positive correlation between the percentage of RBO blended fuel and the density of the fuel. RBO100 has a highest density (897.0 kg/m^3) than other RBO fuels. As a result, B100 delivers a slightly greater amount of fuel during injection at a given setting. Density is important for various CI engine performance aspects. This is due to the larger and more complex molecules found in RBO as compared to pure diesel fuel. RBO contains triglycerides, which are esters of fatty acids, whereas pure diesel is primarily composed of hydrocarbon molecules. As a result of the larger and more complex molecules in RBO, its density is higher. Furthermore, RBO contains oxygen atoms in its molecular structure, primarily in the form of ester groups in triglycerides. Since RBO molecules contain oxygen atoms, their overall mass is greater, resulting in a higher density than pure diesel (839.7 kg/m^3), which contains primarily carbon and hydrogen atoms. The increased density of varios RBO leads to the transportation of a somewhat larger quantity of fuels throughout the injection procedure at a specific injector configuration and has an impact on fuel droplet formation and spray penetration. This leads to an increased BSFC for an equivalent engine output (Hoang et al., 2021). The fuel energy content has a direct impact on the engine power output. As a result of the increased density, there is a possibility of increased cylinder penetration during fuel injection. It is expected that the mixing process will be enhanced because of the increased penetration, since the mixture will be spread over a wider area. Therefore, an increase in fuel density should result in an increase in premixed combustion. Therefore, this increase in density, combined with a large proportion of fuel-borne oxygen, will lead to an increase in the extent of premixed combustion (Karmakar & Halder, 2019).

4.2.2 Kinematic Viscosity (KV)

The lubricity of fuel is mostly associated with kinematic viscosity (KV). The condition mentioned above pertains to molecular mass, dimensions, hydrocarbon classification for fuel. Table 4.1 provides information on the KV of the tested fuels examined in this study. It is observed that RBO100 exhibits the highest KV among the test fuels, measuring at 5.2 mm^2/s. Pure diesel exhibits a lower KV of 4.1 mm^2/s in comparison to other RBO blends. The reduction of 26.8 % RBO100 in KV compared with pure diesel because of RBO molecules are generally larger and more irregular in shape than those in pure diesel. It is believed that larger molecules and molecules of irregular shape are more resistant to flow, resulting in higher KV. Furthermore, RBO contains a mixture of saturated and unsaturated fatty acids, while pure diesel is primarily composed of saturated hydrocarbons. RBO contains unsaturated fatty acids such as oleic and linoleic acids that are usually higher in KV than saturated hydrocarbons. In addition, RBO contains polar compounds, such as phospholipids and glycolipids, which provide to form intermolecular interactions and hydrogen bonds, thus contributing to a higher KV than pure diesel. In addition, it can cause larger droplets, poorer vaporization, narrower injection spray angle and greater in-cylinder penetration of the fuel spray (Puricelli et al., 2021). Furthermore, the use of fuel with a high KV can lead to undesired consequences, such as poor fuel atomization during spraying, engine deposits, wear on fuel pump elements and injectors and additional energy required to pump the fuel (Hoekman & Broch, 2018). Fuel injection systems measure by volume and thus, the engine output power is influenced by changes in density due to the different injected fuel masses. The utilisation of fuel with reduced KV is linked to a decline in both maximum fuel delivery and engine power output due to the occurrence of leaks in injectors and pumps. The influence of fuel KV on atomization and spray characteristics within the combustion chamber is an important consideration. The diminutive Sauter mean droplet diameters are subject to the influence of reduced fuel KV, which consequently leads to an augmentation in the surface area of the droplets. As a result, the evaporation process is impacted in terms of its duration (Pulkrabek, 2014).

اونيۏرسيتي مليسيا ڤهڠ السلطان عبدالله
UNIVERSITI MALAYSIA PAHANG
AL-SULTAN ABDULLAH

4.2.3 Calorific Value (CV)

The term "calorific value" also known as CV, pertains to the energy content inherent in fuels. Generally, CV refers to the amount of energy that is contained within a fuel, which represents the amount of heat created by the combustion process of the fuel. There is a corresponding reduction (average 5.86 %) in the CV of the blended fuel as RBO ratios in blended fuel increase reprented in Table 4.1. The CV of RBO is reduced in comparison to pure diesel due to its higher oxygen concentration (Hoang et al., 2021). The data interpreted in Table 4.1 that 41.1 MJ/kg of RBO100 is the lowest among other fuels. This can be explained by its substantial oxygen content; it is generally accepted that RBO from all sources has about 10% lower mass energy content (MJ/kg) than pure diesel. In addition, it may be a result of the low heating value of RBO100 fuel that leads to a lower energy conversion with a higher BSFC when implementing in CI engine. Considering that the fuel injection pump operates on a volume basis, the RBO100 with the highest density (897.0 kg/m3) produces more energy than pure diesel at the same load condition if all parameters are equal. The observed phenomenon can be ascribed to the CV obtained for each fuel based on physicochemical properties. RBO molecule contains oxygen atoms, which reduces its CV when compared to a pure hydrocarbon fuel which is pure diesel indicating the highest in CV; 45.714 MJ/kg. The oxygen atoms in RBO contribute to the combustion of combustion products such as water and carbon dioxide, which decreases the amount of energy released per unit mass of fuel during combustion process (Perumalla Vijaya et al., 2022). Furthermore, RBO is composed primarily of triglycerides, which are esters of fatty acids. The molecules are composed of carbon, hydrogen, and oxygen atoms. In contrast, pure diesel is primarily composed of hydrocarbons, which contain only carbon and hydrogen atoms. When compared with compounds containing oxygen, hydrocarbons typically possess a higher energy content per unit mass. This is due to the fact that combustion of hydrocarbons results in the release of more energy per atom of carbon. The fuel energy content has a direct impact on the engine power output and this leads to lower the engine speed and power (Karmakar & Halder, 2019).

UNIVERSITI MALAYSIA PAHANG AL-SULTAN ABDULLAH

4.2.4 Cetane Number (CN)

The primary determinant of diesel fuel quality is the measurement of the CN. The high quality of diesel fuel contribute to the a shorter ignition delay, which leads to a smoother operation of the compression ignition engine and reduced exhaust gas emissions.This occurrence has a strong correlation with the ignition delay duration of a fuel upon its injection into the combustion chamber. RBO100 fuel exhibits a better CN in comparison other types of fuel according to Table 4.1. The CN values for the tested fuels, namely as RBO00 (pure diesel), RBO25, RBO50, RBO75 and RBO100 which are 48, 50, 52, 54 and 55 respectively are presented in Table 4.1. The data indicates that pure diesel has a lowest CN of 48 in comparison to the other RBO tested fuels. However, the introduction of minor quantities of RBO fuel results in an increase in the CN. The inclusion of RBO in the test fuels is observed to result in an elevation of the CN. The high elevation presented as 14.58 % of CN in RBO100 compared with pure diesel. This can be explained that the CN of RBO is controlled by the source of crude oil by the refining process. In addition, RBO contains polar compounds, such as phospholipids and glycolipids, which are capable of forming hydrogen bonds and intermolecular interactions, therefore contributing to its higher cetane rating. An increase in CN yields a shorter ignition delay duration, resulting in an easier cold start and a lower idling noise. Conversely, the ignition occurs late in the expansion process, resulting in incomplete combustion, reduced power output, inefficient fuel conversion, and increased engine noise. As compared to other fuels, RBO100 fuel has the highest CN which is 55 based on Table 4.1. A positive correlation exists between the CN and the ignition delay duration, such that the increase in the CN is associated with a decrease in the ignition delay duration. Hence facilitating the cold start process and reducing the level of noise during idling (Abdalla, 2018). On the contrary, the ignition takes place towards the latter stages of the expansion process, leading to an incomplete combustion, a reduction in output power, inefficiency in fuel conversion, and an elevation in engine noise (Heywood, 1988).

UMPSA
اونيۏرسيتي مليسيا ڤهڠ السلطان عبدالله
UNIVERSITI MALAYSIA PAHANG
AL-SULTAN ABDULLAH

4.3 Analysis of Engine Performance Characteristics on the Engine

The parameters of BSFC, BTE, EGT, output power, and volumetric efficiency, reveal how effectively CI engines employ alternative fuels. Furthermore, the compression ratio, air-fuel mixing methods, engine cooling, and operating circumstances all have significant impacts on engine performance (Altarazi et al., 2022). Some novel ideas and upgraded technologies have been created recently to increase engine output power while decreasing pollutant emissions (Dabi & Saha, 2019). Besides using unique fuel compositions, other methods have been used to enhance the process of combustion and reach maximum efficiency, such as improving engine technical qualities, injection approach, and so on (Adithyan et al., 2023).

This section provides an overview of the experimental findings pertaining to the RBO blended under investigation. The experimental analysis involved the use of a KIPOR 170FS diesel engine, which was operated using a RBO blended and pure diesel as baseline. The foremost objective of this study is to facilitate an inclusive analysis of engine performance. The experiments were conducted employing pure diesel fuel and RBO was obtained through a collaborative effort with local bio-oil producing company. The studies were conducted at five distinct of various speeds (1500 – 3500 rpm); interval of 500 rpm. In the subsequent part, a comprehensive analysis is provided on the encompassing the patterns seen in BP, BSFC and BTE characteristics. Engine performance experimentation involves the systematic evaluation and analysis of various aspects of an engine, such as the combustion process, fuel efficiency, emissions, power output, and other relevant characteristics, while subjecting the engine to diverse operating situations. The data required for the improvement of engine design, calibration, and operation to provide enhanced performance and reduced environmental impact.

4.3.1 Engine Brake Power (BP)

The concept of BP pertains to the engine's capacity to carry out productive activity, which is contingent upon the engine's size and configuration for a specific duration. The determination of an engine's power can be achieved by calculating the product of its torque and angular speed, which can be accurately measured with a dynamometer (Heywood, 1988). The current investigation involves the assessment of BP by the utilization of engine torque readings at different engine speed. The correction factor has been considered following the guidelines outlined in the SAE J1349- Engine Test Code for engines powered by diesel. There are five fuel types were utilised in this study, namely as RBO00 (pure diesel), RBO25, RBO50, RBO75, and RBO100. The engine testing was performed in the initial test-operating condition. The highest level of BP achieved was recorded when utilising pure diesel fuel at a 3500 rpm (speed of engine). The power output of pure diesel fuel exhibits an approximate increase of 6.7% compared to RB0100 fuels. The observed discrepancy can be attributed to the elevated viscosity (13.5%) and reduced energy content (11.2%) of RBO100 fuel. RBO100 exhibits the highest viscosity, measuring at 5.2 mm^2/s compared with other fuels. In contrast, it is shown in Table 4.1 that pure diesel has a reduced viscosity of 4.5 mm^2/s in comparison to alternative fuel mixtures. The higher oxygen content in RBO100 results in a decrease in the highest BP of B100 fuel (Hoang et al., 2021). The BP at various engine speeds for the pure diesel, RBO25, RBO50, RBO75, and RBO100 blend fuels is illustrated in Figure 4.1.

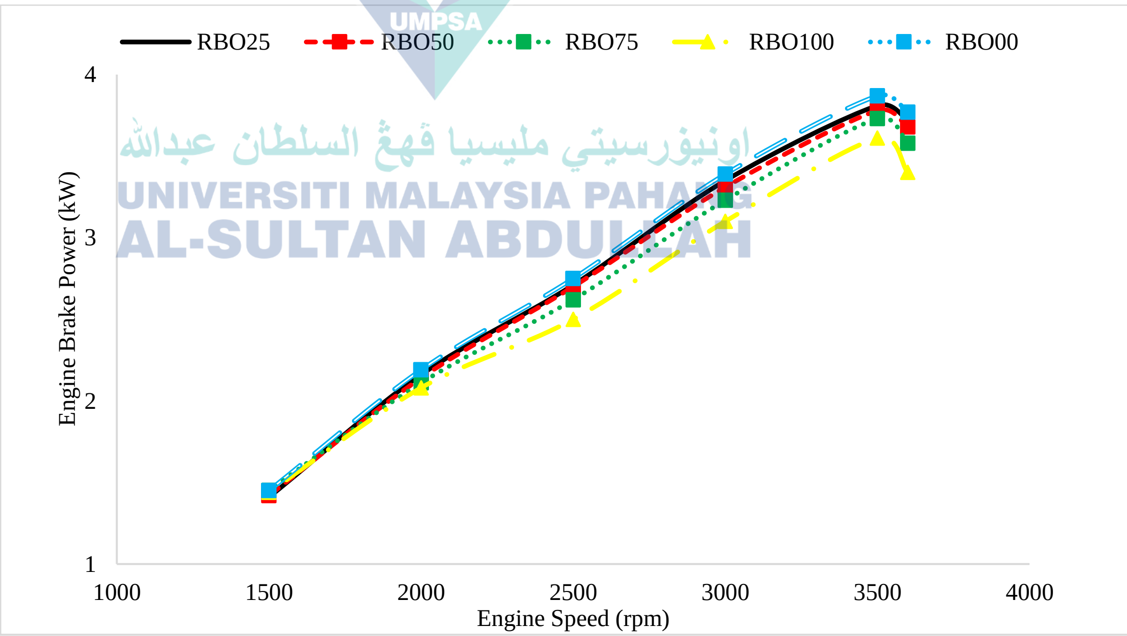

UMPSA
اونيۏرسيتي مليسيا ڤهڠ السلطان عبدالله
UNIVERSITI MALAYSIA PAHANG
AL-SULTAN ABDULLAH

Figure 4.1 Variation of engine brake power with speed for different type of fuels

In general, the findings indicate a positive correlation between engine speed and BP across all fuel types examined. Moreover, it is noteworthy that the peak BP is attained at approximately 3500 rpm. The BP that is accessible at various speeds is contingent upon the engine torque at those respective engine speeds (Cengel & Boles, 2006). Moreover, throughout the range of fuels that were assessed, it was noted that pure diesel fuel demonstrates the greatest BP throughout all engine speeds. The figure illustrates that pure diesel exhibits a greater BP in comparison to the other test fuels. Specifically, at 3500 rpm, pure diesel achieves the greatest engine brake power of 3.87 kW. This is followed by RB025, RBO50, RBO75, and RBO100, which achieve BP of 3.81 kW, 3.78 kW, 3.72 kW, and 3.61 kW, respectively. The reported effectiveness of RBO blended does not surpass the performance attained by RBO00. These RBO blends demonstrated the ability to effectively feed the engine without encountering any difficulties. The empirical data strongly supports the notion that rice bran oil, derived from organic sources, has the promising as a viable renewable fuel to conventional compression engine. The BP of a CI engine is subject to the influence of multiple factors, one of which is the intake air temperature. The subsequent analysis presents a graphical representation, as depicted in the Figure 4.2, the comparison between brake power and various types of fuels in relation to intake air temperature at three distinct levels: 30°C, 45°C, and 65°C, which corresponded to near-standard, high, and extremely high intake air temperatures, respectively. The empirical findings indicate that there is a positive correlation between the intake air temperature and BP, whereby a rise in the former leads to an increase in the latter. The influence of intake air temperature becomes evident in instances where the intake air temperature is elevated, such as at 65ºC. The pure diesel has more 7.2 % of BP compared with RBO blends when it measured at 65°C intake air temperature. The utilisation of a rising intake air temperature is employed to enhance fuel vaporisation and promote a more uniform air-fuel mixture, resulting in a modest reduction in the SOI time. The experiment demonstrates that the intake air temperature is a significant parameter in the generation of a homogenous mixture, leading to an increase in engine torque and subsequently enhancing its BP. Nevertheless, an excessively elevated intake air temperature might result in a decrease in engine performance as a consequence of diminished engine volumetric efficiency and the occurrence of misfiring charge (Jayaraman et al., 2023).

UMPSA
اونيۏرسيتي مليسيا ڤهڠ السلطان عبدالله
UNIVERSITI MALAYSIA PAHANG
AL-SULTAN ABDULLAH

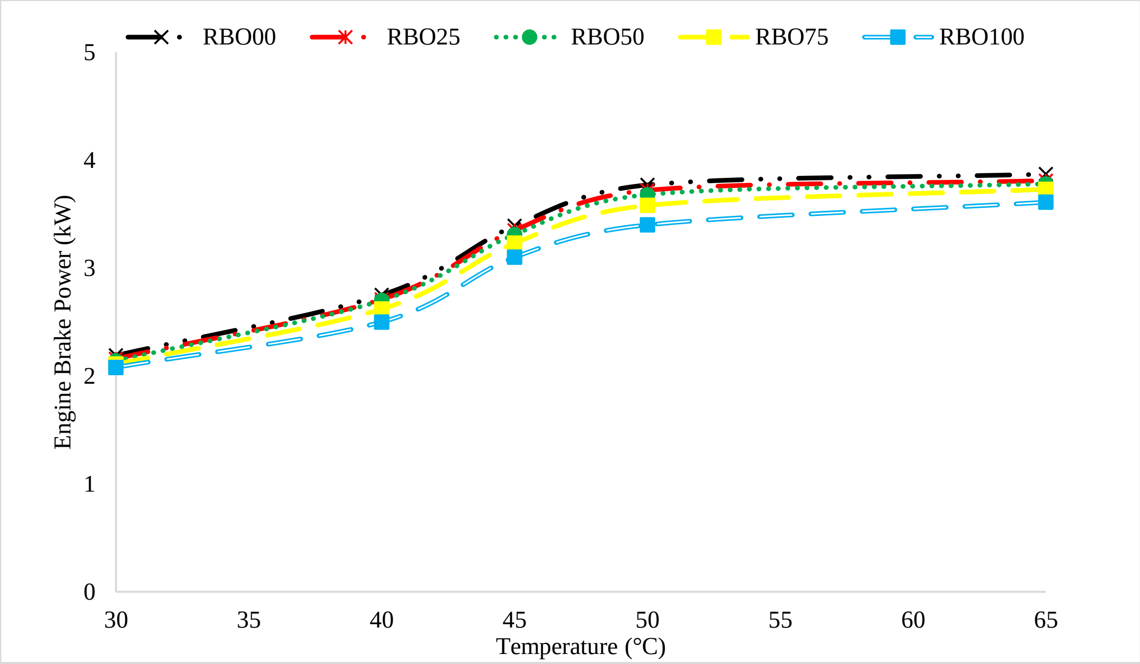

Figure 4.2 Variation of engine brake power with intake air temperature for different type of fuels

4.3.2 Brake Specific Fuel Consumption (BSFC)

The BSFC is the amount of fuel that an engine uses to produce power. The majority diesel-powered vehicles have their own "economy" speeds that give the least amount of BSFC at the least amount of use. It may additionally be employed to measure how effectively an engine works by how much fuel it uses. BSFC is also a key to figuring out how well an engine works with different types of fuel by figuring out the BP and the fuel flow rate for various engine speed. Typically, when the engine speed deviates from the most economical speed, the BSFC tends to increase. This cause of this occurrence to the requirement of additional fuel to counteract mechanical friction at the onset of engine operation. Moreover, as the speed of engine increases, the heat dissipation becomes more pronounced, causing in a heightened fuel consumption (Heywood, 1988; Pulkrabek, 2014). The various BSFC patterns observed for several fuel blends, namely RBO00 (pure diesel), RBO25, RBO50, RBO75, and RBO100 shown in Figure 4.3.

UMPSA
اونيبرسيتي مليسيا ڤهڠ السلطان عبدالله
UNIVERSITI MALAYSIA PAHANG
AL-SULTAN ABDULLAH

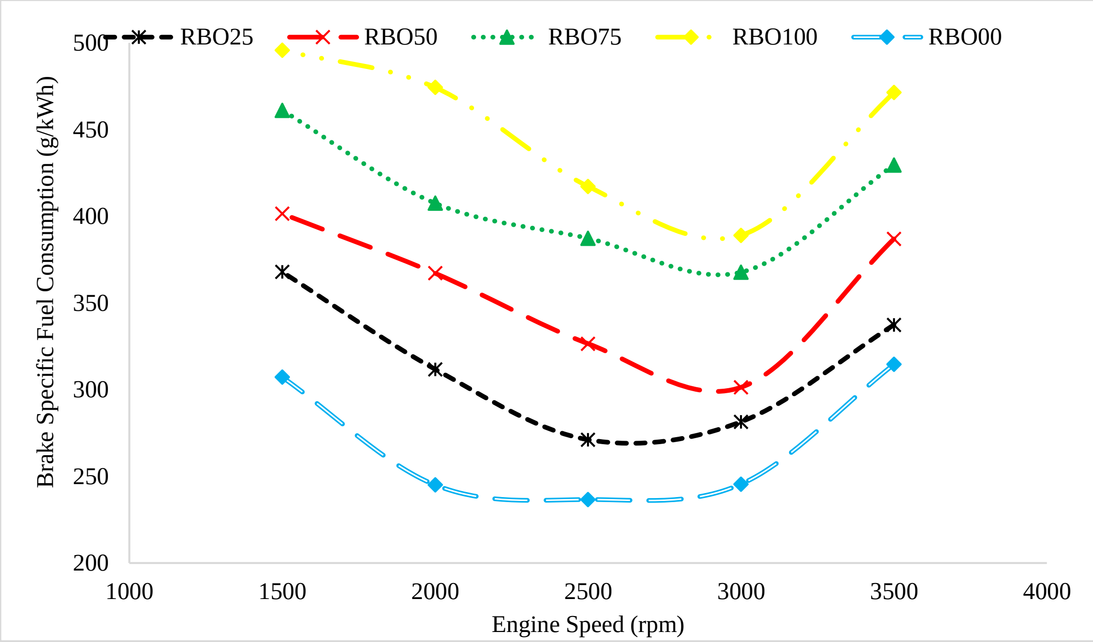

Figure 4.3 Variation of brake specific fuel consumption with speed for different type of fuels

UMPSA
اونيۏرسيتي مليسيا ڤهڠ السلطان عبدالله
UNIVERSITI MALAYSIA PAHANG
AL-SULTAN ABDULLAH

The data shown that the BSFC values for RBO25, RBO50, RBO75, and RBO100 exhibit a modest increase in comparison to those of RBO00. The decrease in CV presented by RBO100 in comparison to pure diesel contributes to the increase in BSFC. According to the data, it can be noticed that pure diesel fuel exhibited the lowest BSFC across the whole various engine speeds. Furthermore, the lowest BSFC value was recorded at 2500 rpm. At the same engine speed, it costs about 50.1% less than RB0100 fuel. The reason for this difference is that pure diesel fuel has more energy (11.2%) than RBO100. It is necessary to increase the BSFC of RBO100 to offset the reduction in fuel energy to provide consistent BP. Several investigations have indicated that the use of RBO and biodiesel with LHV in both light and heavy-duty engines resulted in notable elevations in BSFC (Hoang et al., 2021; Silitonga et al., 2018). Therefore, to get a similar power output to pure diesel when using LHV fuels such as RBO or biodiesel, a greater amount of fuel must be injected. It has been discovered that the relationship between the LHV of fuels and the speed of the engine has a significant impact on the variance of BSFC (Altarazi et al., 2022). For all operations of pure diesel and RBO blends, it was discovered experimentally that the BSFC decreases until at 3000 rpm engine speed and then starts to increase as the engine speed is raised (Surya

Kanth, 2021). This phenomenon may be attributed to the fact that the rate of increase in engine speed surpasses the rate of rise in fuel consumption. Additionally, as BP increases, cylinder wall temperature rises, reducing ignition delay. Consequently, reducing the ignition delay increases combustion while reducing fuel consumption (Chen et al., 2018). Lower engine speeds, on the other hand, had seen a faster decline in BSFC than higher engine speeds. At higher speed conditions, the increase in BSFC for RBO100 was also greater than for other blends operations. This was because RBO100 has a higher KV than other blends. The highest BSFC obtained for RBO100 is around 471.33 g/kWh at 3500 rpm followed by RBO75, RBO50, RBO25 and RBO000 with 429.6 g/kWh, 386.95 g/kWh, 337.38 g/kWh and 314.62 g/kWh respectively at same engine speed. In addition, there is a possibility that incomplete combustion of fuels is the primary cause of increased BSFC as it would require an excess amount of fuel to achieve the same power output. Increases in the proportion of RBO in fuel blends, combined with increased viscosity and hydrogen deficiency index, and reductions in LHV, lead to partial combustion and hence increases in BSFC.

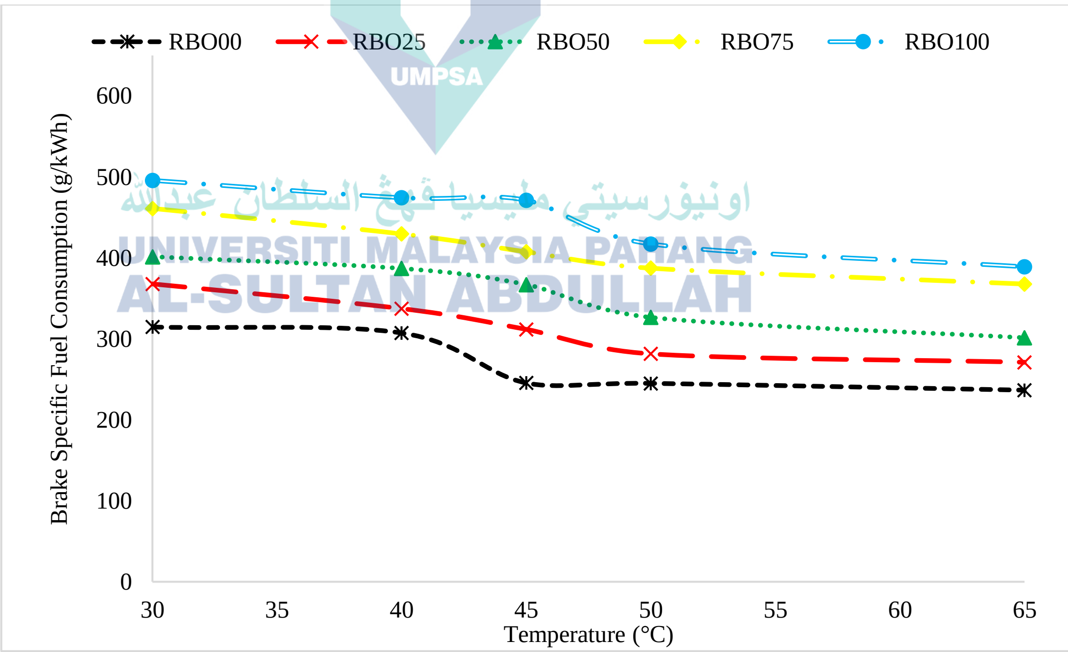

Figure 4.4 Variation of brake specific fuel consumption with intake air temperature for different type of fuels

The various BSFC patterns with intake air temperature observed for several fuel blends, namely RBO00 (pure diesel), RBO25, RBO50, RBO75, and RBO100 shown in the Figure 4.4. The intake air temperatures were manipulated to three different levels: 30°C, 45°C, and 65°C, which corresponded to near-standard, high, and extremely high temperatures, respectively. Based on the experimental results, it has been observed that elevating the temperature of the intake air results in a reduction in the BSFC of the engine.

At a moderate intake air temperature of 45°C, the expenses of RBO100, RBO75, RBO50, and RBO25 are approximately 47.9%, 39.8%, 33.2%, and 21.5% higher than that of pure diesel fuel. This can be explained with CV of RBO is lower than that of pure diesel. The rise in BSFC becomes apparent with the introduction of higher quantities of RBO blends. However, BSFC for RBO100 increases slightly at intake air temperatures of 45°C. Nevertheless, when the intake temperature is 65°C, the BSFC is reduced. The increase in load with moderate operating conditions (2500 rpm) may result in an increase in the temperature of the cylinder walls. As a consequence of the unstable operation conditions to control the combustion temperature inside the engine, the power generated during combustion is lower as a result of a comparable intake air temperature.

اونيۏرسيتي مليسيا ڤهڠ السلطان عبدالله
UNIVERSITI MALAYSIA PAHANG
AL-SULTAN ABDULLAH

An improved BSFC could be studied in the near future if the engine is able to achieve a suitable intake air temperature. It has been suggested that the BSFC for CI engines can be further improved by controlling the combustion with other parameters, such as a high compression ratio, a leaner mixture, and application of EGR. Consequently, the BSFC for RBO tends to be higher when compared to pure diesel fuel. The occurrence of uncontrolled engine combustion and reduced engine output was attributed to elevated intake air temperature, therefore necessitating the imposition of temperature limitations (Praveena et al., 2023).

4.3.3 Brake Thermal Efficiency (BTE)

The BTE serves as a measurement in evaluating the operational effectiveness of an engine with respect to the test fuels used. Therefore, the ratio of thermal power generated by the fuel to mechanical power delivered by the engine to the crankshaft will change depending on the BTE. The engine's thermal efficiency is significantly impacted by the different physicochemical properties of the tested fuels, leading to enhanced combustion process and its behaviours and lower the exhaust gas emissions. The heating value of the fuel is what ultimately influences the process of energy conversion; hence the thermal efficiency is directly related to it. The BTE calculation is arrived at by first calculating the value of BP, and then measuring the amount of energy contained in the fuel being evaluated at a predetermined speed. In a general context, it can be observed that there is a positive relationship between rotational speed of the engine and the BTE as the former gradually reaches 2500 rpm according to Figure 4.5. The experimental findings demonstrate that the BTE of RBO100 surpasses that of pure diesel by 58.57% when the engine is operating at a speed of 2500 rpm.

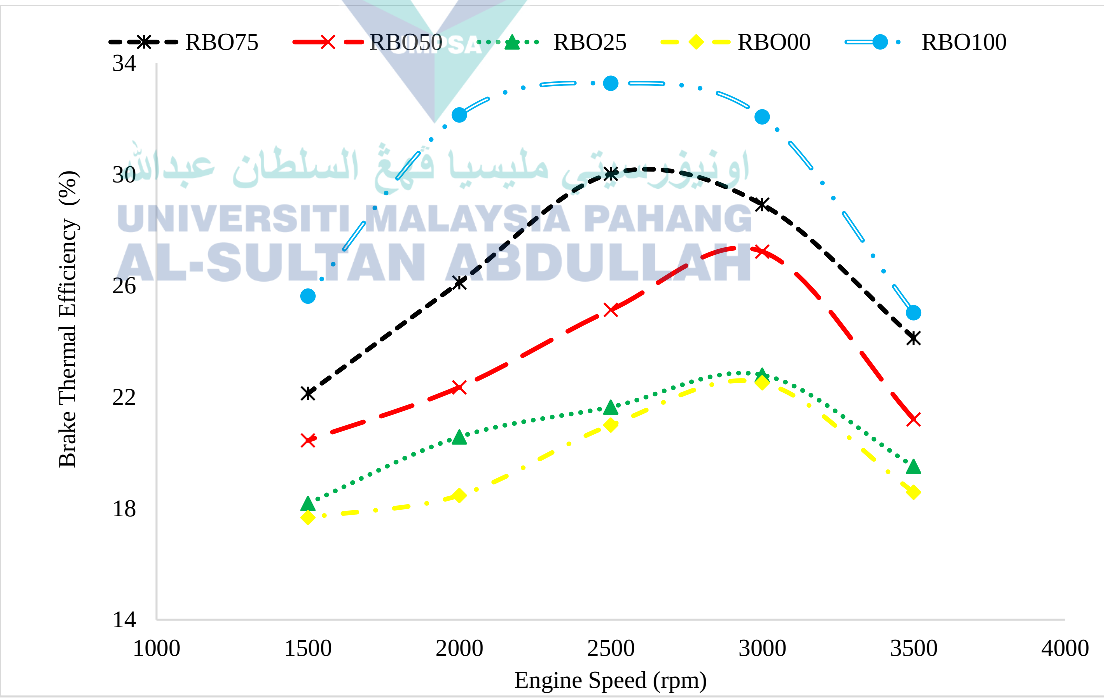

Figure 4.5 Variation of brake thermal efficiency with speed for different type of fuels

UNIVERSITI MALAYSIA PAHANG AL-SULTAN ABDULLAH

The presence of a higher oxygen percentage in RBO100, as opposed to pure diesel, is expected to improve the combustion process and its behaviours. Hence, prior research has shown evidence that the utilisation of RBO blended has resulted in enhanced BTE when operated with the CI engines (Acharya 2010,; Hoang, 2021). However, the research conducted noted a decrease in BTE across all fuel types analysed once the engine speed above 2500 rpm. The observed phenomenon of partial combustion can be ascribed to an insufficiency in the provision of sufficient air supply (Sajjad et al., 2023). The varied BTE patterns that were observed in relation to the intake air temperature for a variety of fuel blends, including RBO00, RBO25, RBO50, RBO75, and RBO100, are depicted in the Figure 4.6. The temperatures of 30°C, 45°C, and 65°C were set as the intake air temperatures, respectively corresponding to near-standard, high, and extremely high levels. There are several factors that can affect the BTE of a compression ignition engine, including the temperature of the intake air. According to the findings of the experiments, raising the temperature of the intake air leads to an increase in the BTE of the engine.

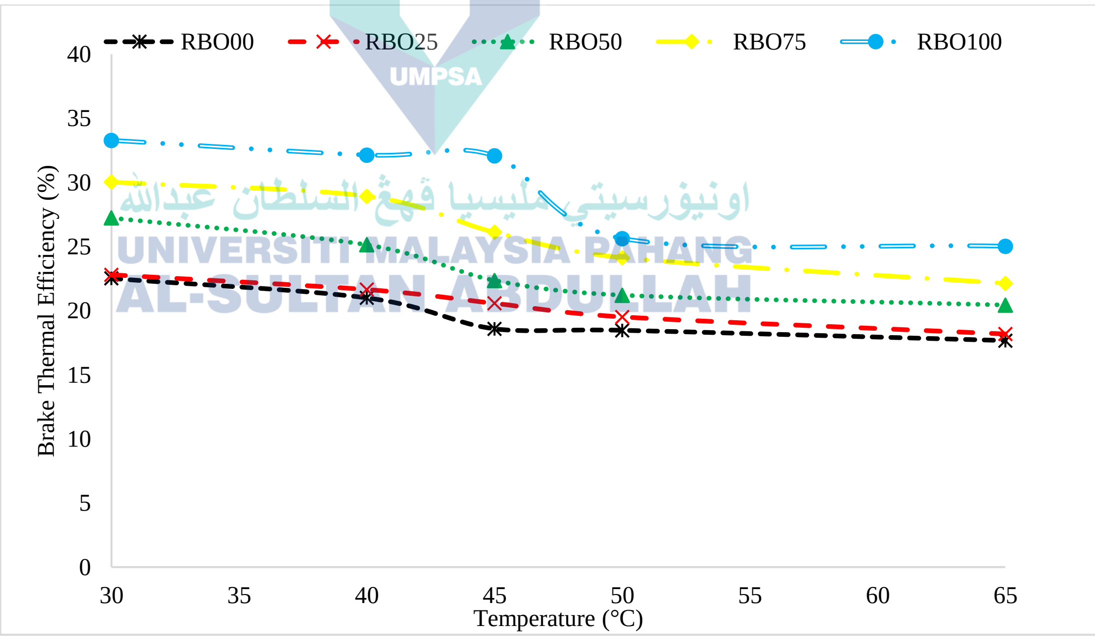

Figure 4.6 Variation of brake thermal efficiency with intake air temperature for different type of fuels

UMPSA
اونيۏرسيتي مليسيا ڤهڠ السلطان عبدالله
UNIVERSITI MALAYSIA PAHANG AL-SULTAN ABDULLAH

The BTE pattern illustrates the comparative effectiveness of RBO versus pure diesel fuel in terms of various intake air temperatures. There is no significant difference between the pattern of BTE for RBO and pure diesel fuel at low RBO content. A high RBO blend of RBO100 results in a high BTE as compared to other tested fuels based on the presented graph. However, pure diesel fuel tends to increase at high intake at both low and high lambda temperatures. This is due to the fact that pure diesel fuel triggers combustion in CI engines, which in turn increases the peak temperature due to the high CV, therefore increasing the RoHR and thus the BSFC. The BTE for RBOs are competitive with the BTE for pure diesel fuel at all engine loads. The reason for this is due to its improved physicochemical properties as RBO has higher density and KV characteristics than pure diesel fuel. When the intake air temperature is high which is 45°C, the impact of the intake air may be clearly seen. The graph interpreted that the RBO blends have a higher BTE of 42.06% in comparison to pure diesel fuel. The researchers have utilised an increasing intake air temperature as a means to improve fuel vaporisation and provide a more homogeneous air-fuel combination, hence leading to a little decrease in the SOI time (Sajjad et al., 2023). The experiment provides evidence that the intake air temperature is a crucial factor in the production of a uniform mixture, resulting in enhanced engine torque and brake power, hence improving brake thermal efficiency. Overall, the blending strategy seems to be effective for short-term application in the existing CI engines, although the use of RBO in CI engines is limited because of its high KV and low CV. This can be supported by the study conducted by Pham (Pham et al., 2018). The CV value of other types of vegetable oils has also been reported to be lower than that of pure diesel, and these differences have been shown to have a significant impact on engine performance and emission parameters. Pham examined the effects of unheated and preheated Jatropha oil on engine performance and emissions. The BTE of an engine powered by unpreheated and preheated (to 90 °C) Jatropha oil was respectively 29.76% and 32.83% when compared with pure diesel (i.e., 36.19%). The long-term use of vegetable oil or fuels derived from vegetable oils in diesel engines may lead to lubricating oil degradation or the formation of large deposits in/on the injector holes and on the piston crowns. In spite of this, it is believed that further research is necessary for RBO blends and pure diesel can be used in CI engines for a long period of time.

UMPSA
اونيۏرسيتي مليسيا ڤهڠ السلطان عبدالله
UNIVERSITI MALAYSIA PAHANG
AL-SULTAN ABDULLAH

4.4 Analysis of Exhaust Emission Characteristics on the Engine

This section provides an overview of experimental investigations conducted to examine the impact of pure diesel as a baseline and RBO blended fuels on exhaust gas emission characteristics. The experiments were carried out using a KIPOR 170FS CI engine, which features a single-cylinder and operates on a four-stroke cycle. The studies were conducted at five distinct engine speeds, spanning from 1500 rpm to 3500 rpm, with an interval of 500 rpm. An investigation of exhaust emissions in CI engines is crucial for both human health and the environment, as well as for the automobile industry. It is crucial to possess a thorough comprehension of the emissions linked to pure diesel as well as alternating fuels, such as RBO. Exhaust emissions contain harmful particles that can lead to detrimental impacts such as acid rain, ozone depletion, and respiratory disorders. Through the analysis of exhaust emissions, researchers can get insights into the processes that impact the creation of these pollutants and device control mechanisms to mitigate their presence. The exhaust emissions from a diesel engine are significantly affected by the diverse psychochemical qualities and various types of RBO blends. An essential part of assessing the viability of using RBO as a substitute for diesel fuel is comprehending the attributes of exhaust emissions from the diesel engine. The impact of RBO on exhaust emissions, namely the number of polluting gases, is influenced by various factors such as operating conditions, types of diesel engines, and the quality and source of the RBO. Gaining insight into the strong correlation between exhaust emission characteristics and RBO mix will aid engine manufacturers in enhancing their engines to be compatible with increasing proportions of RBO blends. In this study, several different characteristics of exhaust emissions, including CO, CO_2, HC, and NO_X, were measured and analysed

4.4.1 Carbon Monoxide (CO) Emissions

The emission of CO in internal combustion engines is primarily determined by the air-fuel ratio and the fuel's capacity to achieve complete combustion during engine operation. Nevertheless, the diverse range of fuel qualities can offer varying insights into the impact of gasoline on CO emissions in diesel engines. Carbon monoxide (CO) is the crucial exhaust emission that necessitates minimization. Figure 4.7 illustrates the relationship between CO levels and engine speed (rpm). The amounts of oxygen content and CN that are present in the fuel are directly correlated to the amount of CO that is emitted. RBO blended have a higher percentage of oxygen in their composition when compared with pure diesel. Consequently, the blends with higher oxygen content are associated with an incomplete combustion process. When the engine was fed only pure diesel, measurements showed that it produced the maximum levels of CO emissions at a speed of 3500 rpm. It is clear that fuel blend RBO100 exhibits the lowest CO emissions compared to other fuels across all speed circumstances.

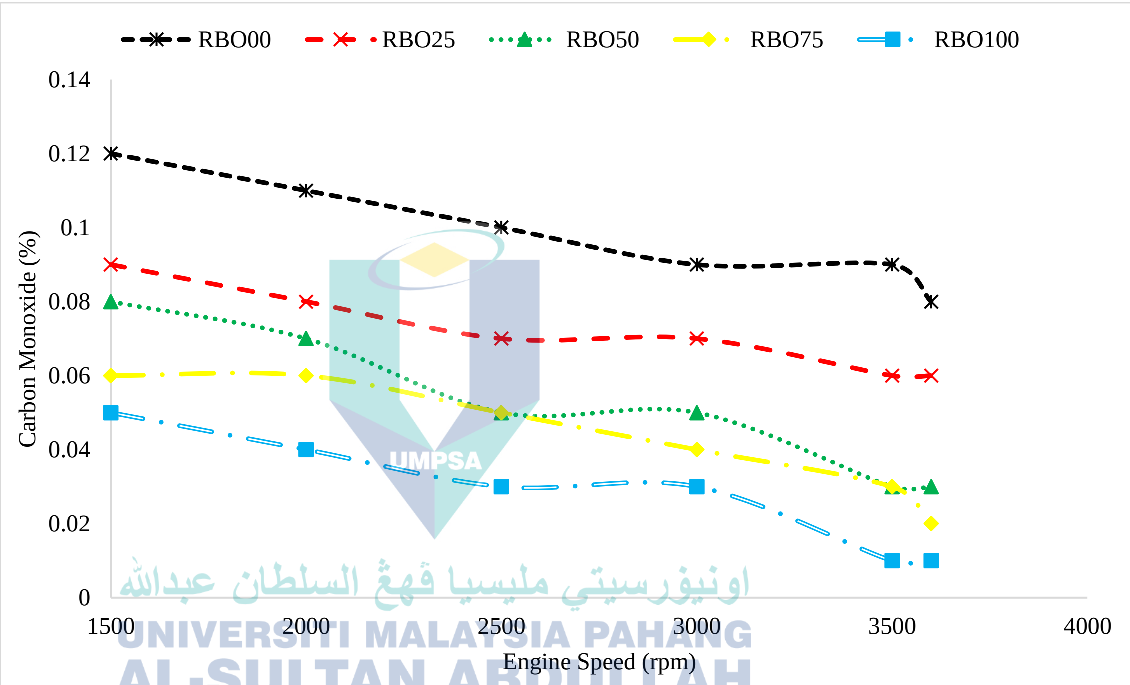

UMPSA
UNIVERSITI MALAYSIA PAHANG
AL-SULTAN ABDULLAH

Figure 4.7 Variation of carbon monoxide with engine speed for different types of fuel

An increase in the amount of the blend results in a reduction in the emissions of CO, with RBO100 demonstrating the minimal CO emissions of all the blend's components. This phenomenon can be explained by the existence of extra oxygen within the RBO, which makes for a more complete and efficient process of combustion. Figure 4.7 depicts the relationship between engine speed and the exhaust emission of carbon monoxide. It is evident that the RBO100 exhibits the lowest carbon monoxide emissions across all engine speeds (rpm). At a speed of 3500 rpm, the released amount of CO reaches its lowest point, regardless of the fuel mixture being used. This observation indicates that an increase in velocity necessitates a greater supply of oxygen for the combustion process within the engine, a requirement that is not adequately met by the augmented fuel injection (Chen et al., 2018). This phenomenon tends to result in an increase in the release of CO. This outcome is consistent with previous research indicating that the utilisation of RBO leads to a decrease in unburned hydrocarbon and carbon monoxide emissions. Under low-speed conditions, the temperature of the cylinder was seen to be insufficiently low. However, as the loading increased, the temperature subsequently rise due to the injection of a greater amount of fuel into the cylinder. The various fuels to CI engine had minimal impact on the decrease of CO emissions at low speeds (Dharmaraja et al., 2019). The study additionally indicated that under increased temperature conditions, the engine's performance exhibited enhancement due to more efficient combustion of the fuel. Therefore, this has a significant impact on the reduction in CO emissions. The analysis and investigation continue with the impact of high engine speed at 3500 rpm to the CO emissions. The lowest recorded level of CO was around 0.01%, detected for RBO100. This was followed by RBO75 with a level of 0.03%, RBO50 also at 0.03%, RBO25 at 0.06%, and the highest level of approximately 0.09% for RBO00. The elevated levels of CO predicted in RBO00 can perhaps be attributed to the prolonged ignition delays (ID) resulting from the fuel composition. The study demonstrates that an increase in BSFC and longer ID leads to a reduction in the air-to-fuel ratio within the combustion chamber. Consequently, this decrease in ratio results in a reduced air volume available for achieving complete combustion (Hoang et al., 2021). Consequently, this has a significant impact on the increase in CO emissions. The varied of CO patterns that were observed in relation to the intake air temperature for a variety of RBO blended, including RBO00, RBO25, RBO50, RBO75, and RBO100, are depicted in the Figure 4.8. Temperatures of 30°C, 45°C, and 65°C were set as the intake air temperatures, respectively corresponding to near-standard, high, and extremely high levels of temperature. There are a number of factors that can have an impact on the CO produced by a CI engine, including the temperature of the intake air. According to the findings of the experiments, it is observed that the CO levels tend to decrease as the intake air

UMPSA
اونيۏرسيتي مليسيا ڤهڠ السلطان عبدالله
UNIVERSITI MALAYSIA PAHANG
AL-SULTAN ABDULLAH

temperatures increase for all fuels that were tested. When the intake air temperature is high, such as 45°C, the impact of the CO may be clearly seen.

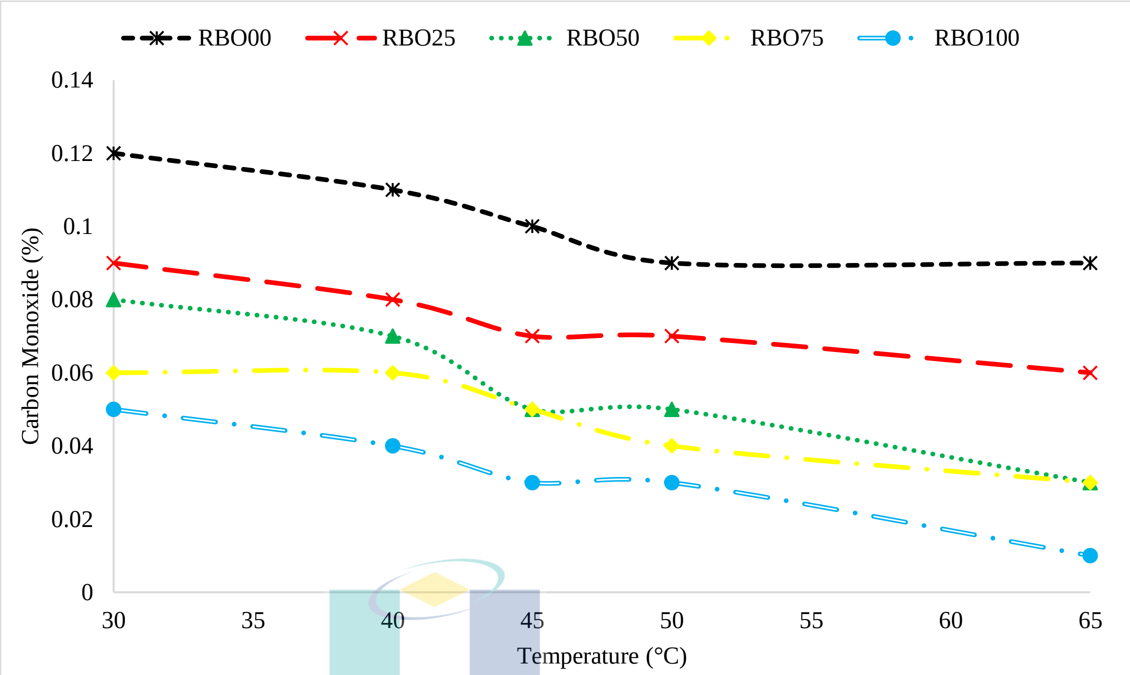

Figure 4.8 Variation of carbon monoxide with intake air temperature for different types of fuel

An intake air temperature of 45°C results in RBO100, RBO75, RBO50, and RBO25 having approximately 0.03%, 0.05%, 0.06%, and 0.07% lower than pure diesel fuel (0.09%). The production of CO emissions is influenced by the intake air temperature, which results in an elevated combustion temperature and increased duration for CO oxidation during the expansion stroke. This observation aligns with the findings previously reported by Praveena. The CO emission level and the performance of RBO were shown to be considerably influenced by the intake air temperature. The inclusion of oxygen in RBO exerts a beneficial influence on the regulation of soot production. Praveena once again reached a consensus that the findings indicate a drop in CO emission levels as the intake air temperature increases, resulting in advanced injection timing (Praveena et al., 2023). The elevating the intake air temperature resulted in an increase in the level of cylinder gas temperature. This, in turn, led to a notable acceleration in the oxidation of CO.

UMPSA
UNIVERSITI MALAYSIA PAHANG AL-SULTAN ABDULLAH

4.4.2 Carbon Dioxide (CO_2) Emissions

CO_2 is produced through the burning of fuel containing carbon chains. The replacement of diesel fuel with RBO has not been met with general agreement on how to reduce CO_2 emissions (Milano et al., 2018). Several studies have indicated that the utilisation of RBO as a fuel source in CI engines resulted in higher CO_2 emissions when compared to the combustion of pure diesel fuel.

The discharge of carbon dioxide to the surroundings is the result of the full burning of the fuel. The higher oxygen concentration of all mixes compared to diesel utilized alone allows for more complete combustion. The emission of carbon dioxide is also increased as a result of the complete burning of fuel mixes (Praveena et al., 2023). The data presented in Figure 4.9 indicates that the CO_2 emissions resulting from the use of pure diesel is comparatively lower due to incomplete combustion, in comparison to the emissions produced by RBO blends.

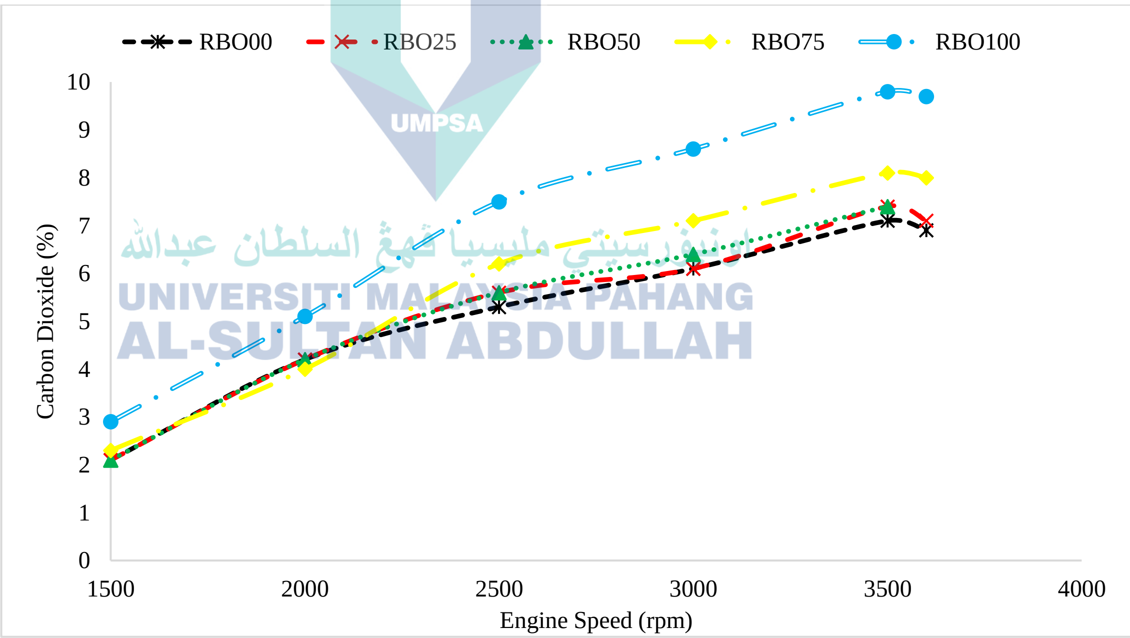

Figure 4.9 Variation of carbon dioxide with engine speed for different types of fuel

It was observed that RBO100 and RBO75 demonstrated the most elevated levels of CO2 emissions across all engine speed settings. This may be supported by the fact that they are capable of undergoing total combustion. Consequently, these fuel blends

UMPSA
UNIVERSITI MALAYSIA PAHANG
AL-SULTAN ABDULLAH

can be considered the most optimal in terms of CO2 exhaust emission performance. The relationship between the increase in CO_2 and the increase in CN of RBO blends is directly proportional. The greater oxygen concentration that is characteristic of RBO blended may be responsible for this association. CO_2 significantly impacts greenhouse gases by creating a greenhouse effect in the atmosphere, hence contributing to global warming. With an increase in engine speed, CO_2 typically rises. The CO_2 emissions of pure diesel are found to be at their minimum level while the engine running at 1500 rpm. The CO_2 emissions exhibit a similar level across all the RBO blends except RBO100 at a rotational speed of 2000 rpm. The RBO blended exhibited a greater level of CO_2 emission. The amount of CO_2 emitted by RBO100 is 38.02 % higher than the amount emitted by pure diesel fuel when the engine speed is at maximum; 3500 rpm. The measurement of CO_2 emission serves as an indicator of the combustion efficiency within the combustion chamber. The Figure 4.10 illustrates the diverse CO_2 emission patterns observed in response to the intake air temperature for several fuel mixes, namely RBO00, RBO25, RBO50, RBO75, and RBO100.

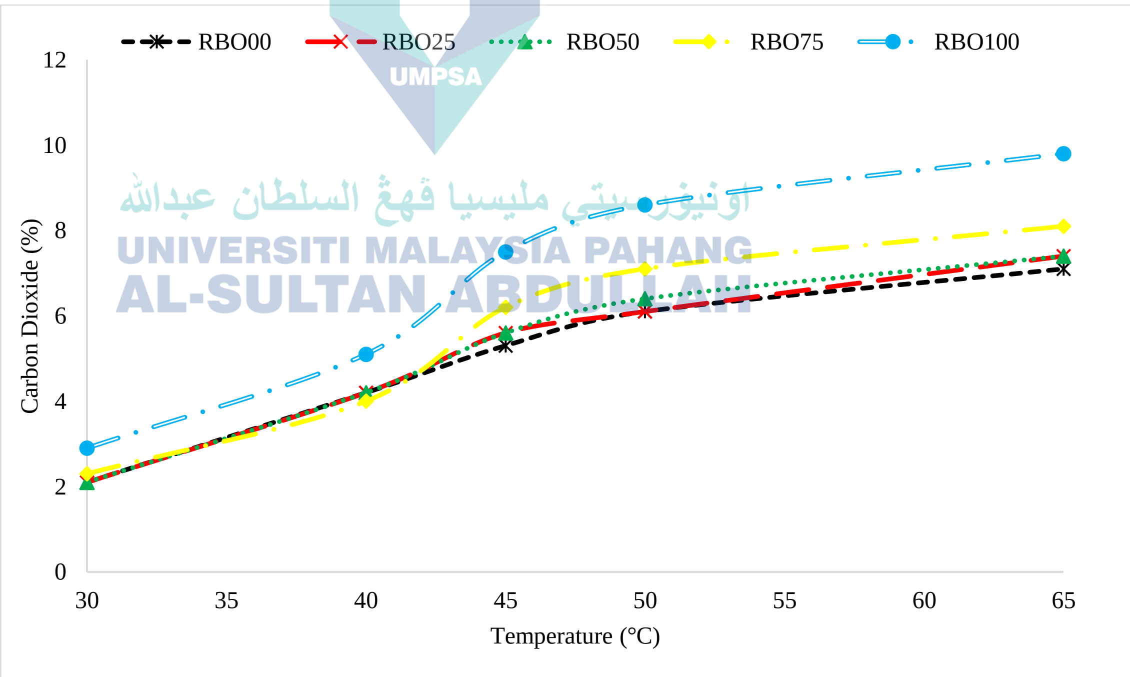

Figure 4.10 Variation of carbon dioxide with intake air temperature for different types of fuel

UMPSA
UNIVERSITI MALAYSIA PAHANG AL-SULTAN ABDULLAH

The intake air temperatures were set at 30°C, 45°C, and 65°C, representing near-standard, high, and extremely high levels of temperature, respectively. The temperature of the intake air is a significant factor that can impact the CO_2 emissions of a CI engine, along with other variables that may also exert an influence. Based on the experimental results, it is evident that there is a positive correlation between intake air temperatures and CO_2 emission levels across all tested fuels. In addition, the observable effects of CO_2 become more pronounced in instances of elevated intake air temperature, such as 65°C. An intake air temperature of 65°C results associated with RBO100, RBO75, RBO50, and RBO25 exhibit an approximate increase of 9.8%, 8.1%, 7.4%, and 7.4% respectively, compared to the cost of pure diesel fuel which stands at 7.1%. The relationship between the CO–CO_2 reaction and temperature has been investigated by Singh and Agarwal. There was an observed increase in the in-cylinder gas temperature, leading to enhanced chemical reactions at high intake air temperature. Therefore, CO underwent oxidation, resulting in the formation of CO_2. Consequently, with the culmination of full combustion, a substantial quantity of CO_2 is produced as a result of the process (Singh & Agarwal, 2016). Overall, the effect of RBO on CO_2 emissions in terms of mixture formation primarily hinges on its ability to atomize, vaporize, and combust efficiently. Proper mixing with air, achieving the correct air-fuel ratio, and ensuring complete combustion are crucial factors that determine the amount of CO_2 produced per unit of energy obtained from burning rice bran oil. Efficient combustion systems and emission control technologies play a significant role in mitigating CO_2 emissions from the combustion when it fuelled with vegetable oils such as RBO.

UMPSA
اونيۏرسيتي مليسيا ڤهڠ السلطان عبدالله
UNIVERSITI MALAYSIA PAHANG
AL-SULTAN ABDULLAH

4.4.3 Hydrocarbon (HC) Emissions

Hydrocarbons, commonly referred to as HC, represent uncombusted fuel substances and are quantified in units of parts per million (ppm). In order for an engine to function well, it is imperative that the combustion process effectively oxidises the majority of the fuels, resulting in minimal presence of unburned fuel in the exhaust. The permissible concentration of HC is 50 ppm or lower (Pulkrabek, 2014). Elevated concentrations of HC may potentially arise from heightened oil consumption resulting from compromised piston rings or deteriorated valve guides. A prevalent factor contributing to elevated levels of HC emissions is a malfunction within the ignition system. The HC emissions produced by the mixes are of a lesser magnitude when compared to those produced by diesel in its purest form because of complete combustion takes place. There is a comparable decrease in the concentration of hydrocarbons that takes place as the proportion of volume of RBO that is present in the blend increases. According to Figure 4.11, it is evident that the pure diesel blend RBO100 exhibited the lowest levels of hydrocarbon emissions in comparison to the other blends. The HC of pure diesel fuel exhibits a reduction as the speed increases, and this trend is similarly observed with other fuel blends.

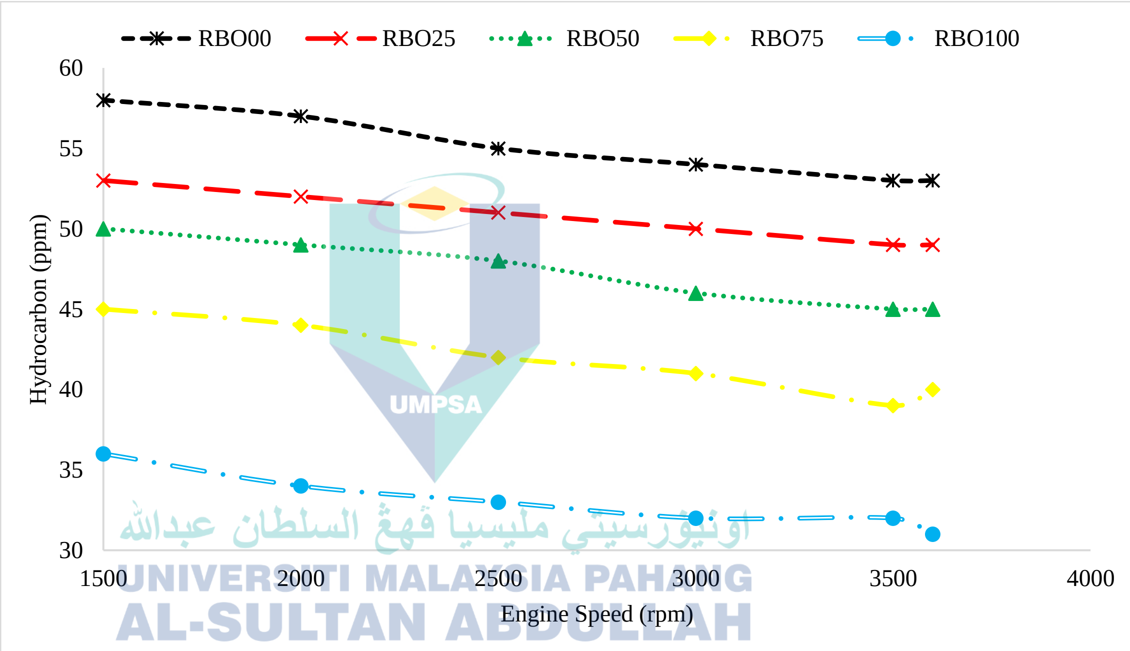

UMPSA
اونيۏرسيتي مليسيا ڤهڠ السلطان عبدالله
UNIVERSITI MALAYSIA PAHANG
AL-SULTAN ABDULLAH

Figure 4.11 Variation of hydrocarbon with engine speed for different types of fuel

In general, an inverse relationship was seen between the HC and engine speeds, resulting in a reduction in HC as the speed increased. The findings further highlighted the observation that the RBO100 exhibits a significant reduction of 37.93 % in HC emissions compared to RBO00 (pure diesel) at low speeds, with both fuels demonstrating a further decrease at 3500 rpm. The data shown provide evidence of decreased emissions of CO and HC when utilising blends of RBO. The causes can be ascribed to the oxygen content present in the fuels. According to research, it has been observed that unburned hydrocarbons tend to originate from specific areas within a cylinder where the fuel/air combination is inadequate (Ali et al., 2022). This deficiency is significant enough to exceed the combustion limit. The RBO100, RBO75, RBO50, and RBO25 fuels exhibited consistently lower levels of HC emissions in comparison to pure diesel at all tested speeds.

Combustion byproducts elevated temperatures in RBO fuel contribute to the mitigation of increased hydrocarbon condensation, hence resulting in a reduction of HC emissions (Xiao et al., 2019). An elevation in the CN of RBO results in a decline in HC products owing to a reduction in the time interval between fuel injection and ignition (Uyumaz, 2020). The Figure 4.12 illustrates the diverse HC emission patterns detected in correlation to the intake air temperature for all RBO blended which are RBO00 (pure diesel), RBO25, RBO50, RBO75, and RBO100. The intake air temperatures were set at 30°C, 45°C, and 65°C, representing low, high, and extremely high levels of temperature, respectively.

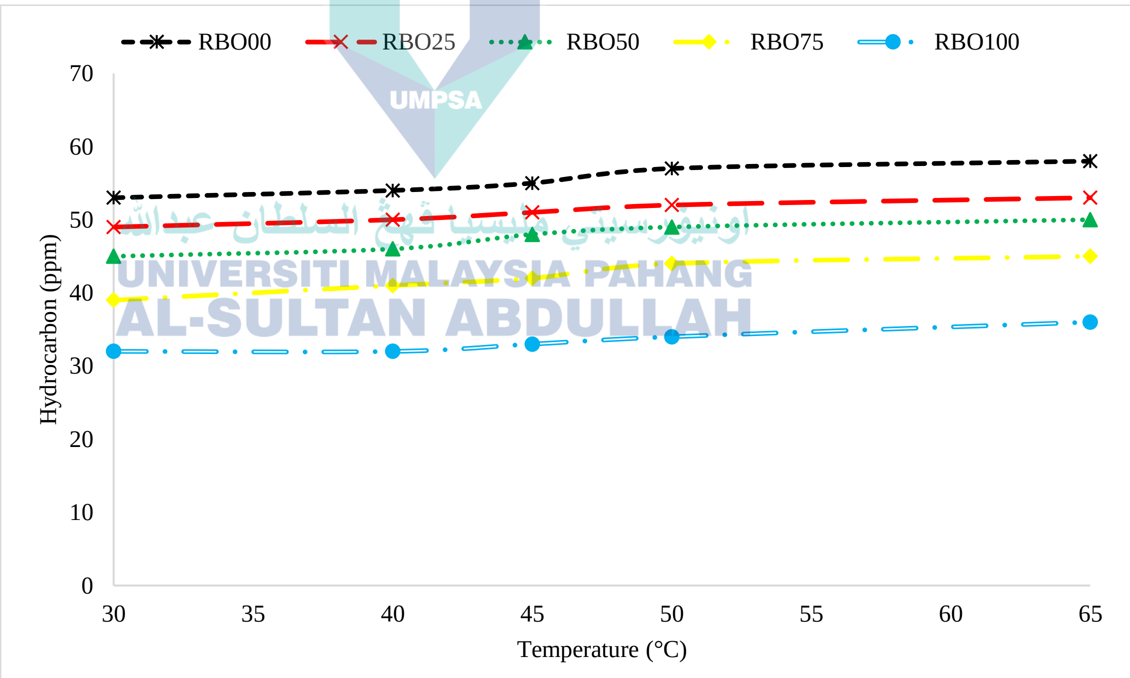

UMPSA
UNIVERSITI MALAYSIA PAHANG
AL-SULTAN ABDULLAH

Figure 4.12 Variation of hydrocarbon with intake air temperature for different types of fuel

HC emissions from a CI engine can be influenced by the intake air temperature, as well as other factors. It can be shown that there is a positive correlation between air intake temperatures and hydrocarbon levels across all evaluated fuels based on the experimental results. The observation of HC influence becomes more pronounced when the intake air temperature reaches at 65°C. An intake air temperature of 65°C resulted in the HC emission levels for RBO100, RBO75, RBO50, and RBO25 exhibit a reduction of approximately 389 ppm, 378 ppm, 370 ppm, and 360 ppm, respectively, in comparison to the HC levels observed in pure diesel fuel (350 ppm).

In addition, it observed an increase in HC levels when the intake air temperature was increased. Increasing intake air temperature results in an increase in HC emissions for all fuels. This can be supported by other researchers had similar experimental results (Uyumaz et al., 2020). They conducted an experiment to determine the effect of intake air temperature on the alternative fuel methanol and found that three factors influenced this parameter. The first effect of longer ignition delay is that it increased the mass of mixture that was leaner than the lean combustion limit. Also, higher evaporation heat of fuel resulted in a higher quenching temperature. Lastly, a lower level of cylinder gas temperature resulted in a greater amount of incomplete combustion fuel being produced.

UMPSA
اونيۏرسيتي مليسيا ڤهڠ السلطان عبدالله
UNIVERSITI MALAYSIA PAHANG
AL-SULTAN ABDULLAH

Furthermore, the observed rise in HC emissions can be attributed to the elevated air intake temperature, which is typically a result of inadequate oxidation processes. This phenomenon results in the occurrence of HC emissions within the cylinder temperature boundary layer, as well as an increase in the gap between the piston rings. The underlying cause of this phenomenon is attributed to reduced volumetric efficiency resulting from decreased airflow to the engine under conditions of elevated air intake temperatures. The emissions of HC are influenced by both the formation of the fuel-air combination and the intake air temperature. Therefore, 45 °C (moderate) is considered to be an optimum operating temperature for the uniform formation of a mixture.

4.4.4 Oxide of Nitrogen (NO_X) Emissions

NO_X is an achromatic, insipid, and odorless gaseous compound upon its emission from the engine. On the other hand, when the gases interact with more oxygen in the atmosphere, the formation of nitrogen dioxide (NO_2) occurs. NO_2 exhibits a reddish-brown hue and emits an acidic and unpleasant odor. NO and NO_2 are commonly grouped together and collectively referred to as NO_X, where the variable x indicates any number of oxygen atoms.

NO_X, which is the designated symbol for all nitrogen oxides, is the fifth gas that is routinely examined via a gas analyzer. The EGR system serves as the primary control mechanism for mitigating the production of NO_X (Kannan & Vijayakumar, 2022). The exhaust product which is NOx are contingent upon the levels of oxygen concentration and the duration of burning. Under all operating conditions, the NO_X emissions of the fuel blends consistently exceed those of pure diesel fuel. This can be led to the higher oxygen concentration and amended combustion timing present in the blends. The potential cause of increased NO_X emissions could be attributed to the reduced ignition delay. Both RBO blends and pure diesel exhibit identical trends based on the Figure 4.13.

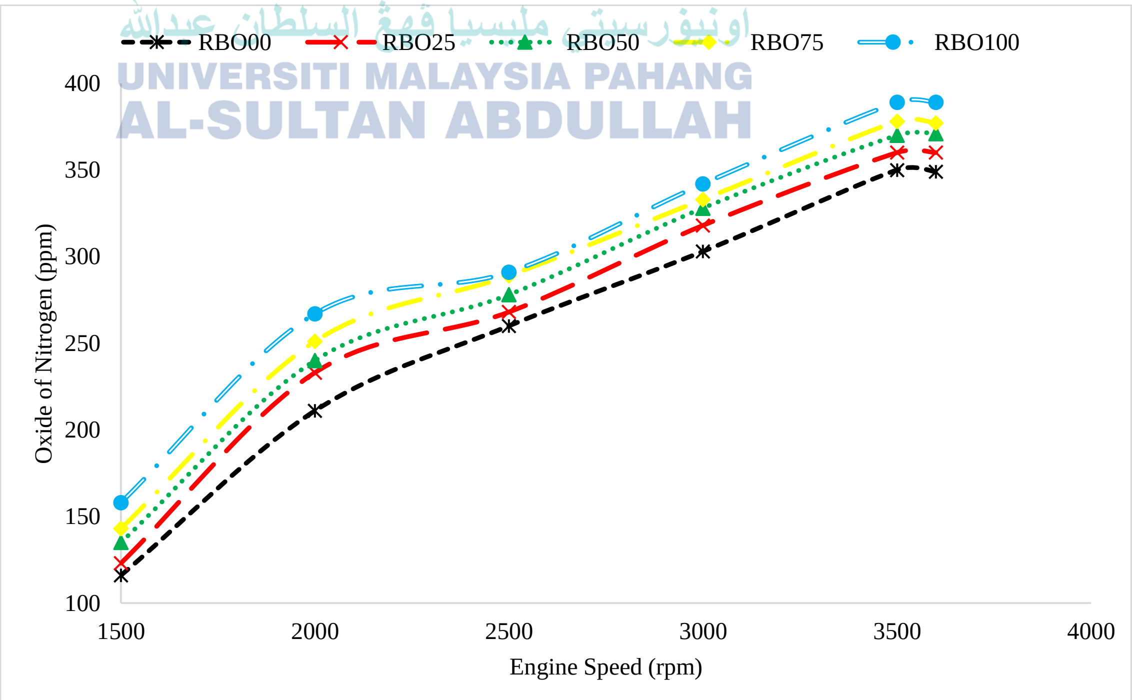

UMPSA
اونيۏرسيتي مليسيا ڤهڠ السلطان عبدالله
UNIVERSITI MALAYSIA PAHANG
AL-SULTAN ABDULLAH

Figure 4.13 Variation of oxide of nitrogen with engine speed for different types of fuel

At high speeds (over 2000 rpm), all fuel blends exhibit NO_X values exceeding 233 ppm, however the NO_X value of pure diesel fuel remains below this threshold at equivalent speeds. The fuel type known as RBO100 exhibits the highest level of NOx emissions, measuring at 389 ppm at 3500 rpm. In comparison, among all the fuel types examined, RBO00 demonstrates the lowest NOx emission level, measuring at 350 ppm. When the speed of the engine is increased, there is an associated increase in the amount of NOx that are emitted by the engine for all fuel mixes. On the other hand, it was discovered that running the engine speed at 1500 rpm while fuelled RBO00 resulted in the lowest amounts of NOx emissions. This was the case even when both fuel types were used. At lower engine speed, the temperature of the engine block and cylinders remained relatively low, resulting in a minimal generation of NOx (Mirhashemi & Sadrnia, 2020). However, empirical research has consistently demonstrated a decrease in NOx emissions during various testing procedures (Perumalla Vijaya et al., 2022). According to their statement, the emission of NOx is influenced by factors such as oxygen content, peak pressure, combustion temperature, and duration. Based on the analysis, it can be inferred that alterations in both combustion temperature and stoichiometry will have an impact on the generation of NOx. In conclusion, the data shown in the Figure 4.13 illustrates a progressive rise in NOx emissions across all fuel types when the speed is elevated. Figure 4.14 illustrates the diverse NO_X emission patterns observed in correlation with the intake air temperature for different fuel, namely RBO00 (pure diesel), RBO25, RBO50, RBO75, and RBO100.

UMPSA
اونيۏرسيتي مليسيا ڤهڠ السلطان عبدالله
UNIVERSITI MALAYSIA PAHANG
AL-SULTAN ABDULLAH

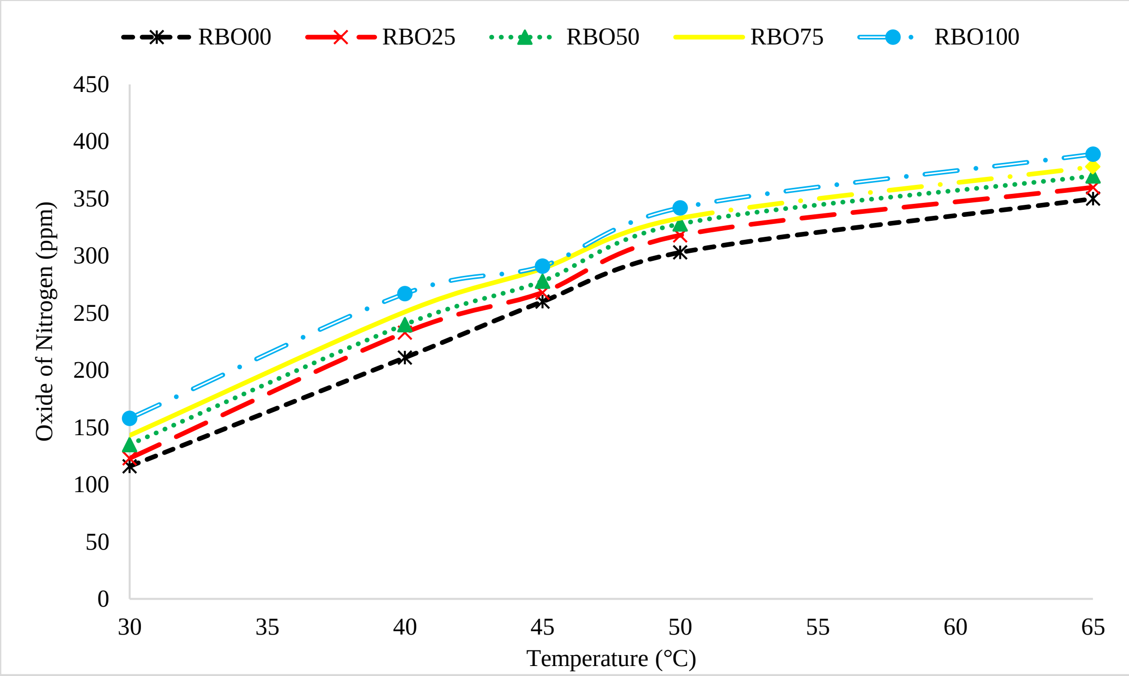

Figure 4.14 Variation of oxide of nitrogen with intake air temperature for different types of fuel

The intake air temperatures were measured as 30°C, 45°C, and 65°C, representing near-standard, high, and extremely high levels of temperature, respectively. Temperature of the intake air can influence the NO_X emissions of a CI engine, along with other factors that may also play a role. It is evident that the levels of NO_X exhibit an upward trend with increasing air intake temperatures across all evaluated fuels based on the experimental results. The observable effects of NO_X become more pronounced when the intake air temperature is elevated, reaching a value of 45°C. At an increased ambient temperature of 45°C, the concentrations of NO_X emissions for RBO100, RBO75, RBO50, and RBO25 are estimated to be roughly 291 ppm, 289 ppm, 278 ppm, and 268 ppm respectively, surpassing the concentration of NO_X emissions from pure diesel fuel, which is measured at 260 ppm. A drop in the NO_X emission was interpreted when the intake air temperature was increased. This decrease resulted in an increase in the equivalence ratio, bringing it closer to stoichiometric conditions. Therefore, the decrease in λ (indicating a richer mixture) was a contributing factor to the increase in NOx emissions (Sakthivadivel et al., 2022).

UMPSA
اونيۏرسيتي مليسيا ڤهڠ السلطان عبدالله
UNIVERSITI MALAYSIA PAHANG
AL-SULTAN ABDULLAH

4.5 Analysis of Combustion Behaviours on the Engine

This section will provide a description of the impact that various RBO blended on the combustion behaviours of a KIPOR 170FS single-cylinder engine. The pressure in the cylinder of the tested fuels is monitored and recorded in order to compute and calculate, including the RoHR and RoPR. The EGT is also presented in this study. This study investigates the combustion behaviours by analysing the in-cylinder pressure data and CAD measurements. Combustion behaviours analysis involves examining the processes and variables that impact the fuel efficiency, engine performance, and exhaust emissions of a CI engine. This study involves performing experimental measurements for analysing the process of spray production, ignition, combustion, and pollutant formation between pure diesel fuel and RBO blended. It can enhance the efficiency and functionality of CI engines, resulting in improved performance and reduced environmental impact. A comprehensive investigation of the combustion behaviours of the various fuels is elaborated upon extensively in specific subsections.

4.5.1 Exhaust Gas Temperature (EGT)

EGT is the term used to describe the average temperature of the exhaust gas stream. Figure 4.15 displays the EGT for various RBO blended and pure diesel under different engine loads. RBO00 (pure diesel), which functioned as the baseline, as well as blends like RBO25, RBO50, RBO75, and RBO100, were tested. As the engine load was expanded the EGT for the experimental fuel exhibited a rise due to the utilization of a greater quantity of fuel to generate the requisite torque for surpassing the engine load (Sajjad et al., 2023). The limited dynamometer restriction caused the fuel to burn in the exhaust manifold area rather than in the combustion chamber. The thermocouple measurement obtained directly at the exhaust port was subject to external factors, resulting in elevated EGT readings while the engine was not under any load. Thus, due to that reason, the test started up with 20% engine load in this research.

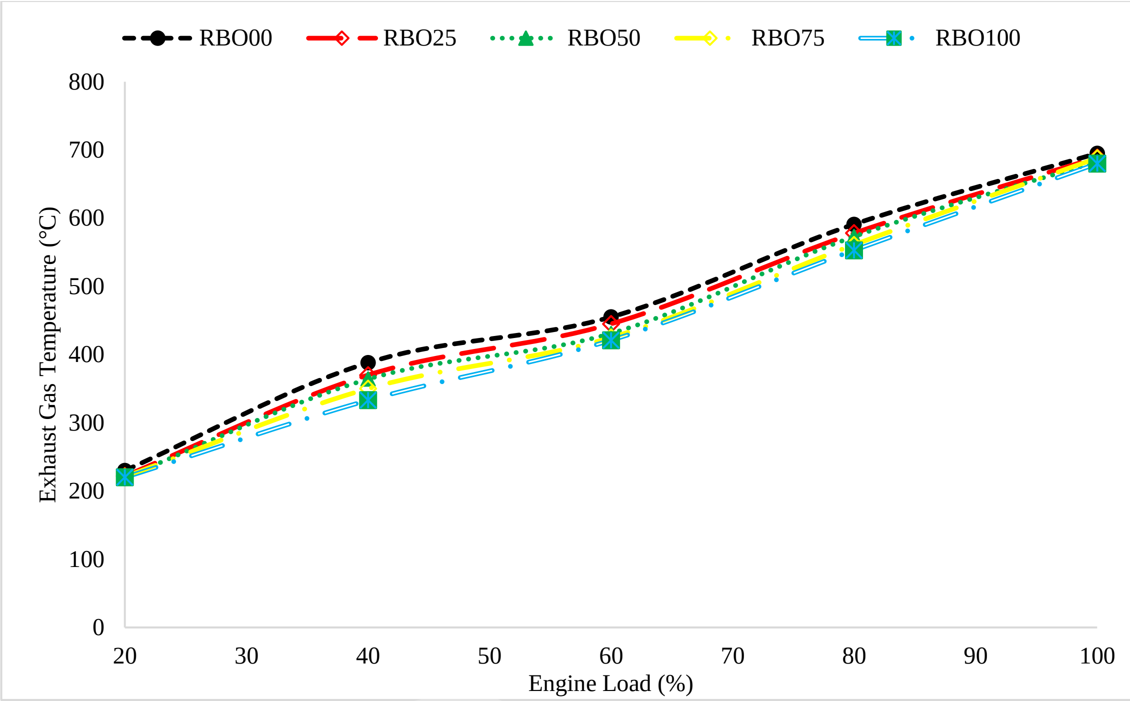

Figure 4.15 Exhaust gas temperature for rice bran oil blends versus engine load

The major increment in Figure 4.15 is for RBO00, which are subsequently followed by RBO25, RBO50, and RBO100. The RBO00 blend had a highest CV compared to the RBO25, RBO50, RBO75, and RBO100 blends. Consequently, the RBO00 blend generated more heat per unit mass. This observation was further supported by the high EGT measurement obtained for the pure diesel. Oxygen percentage in fuel has been identified as the primary factor determining EGT during combustion. This can be attributed to the higher EGT observed with pure diesel as compared with RBO blended diesel. In addition, RBO ignition delay is deemed to decrease with decrease in percentage volume concentration. It has been suggested that RBO should be blended with pure diesel at concentrations lower than 20% to minimize the increase in EGT. However, some published studies have reported a decreasing trend or fluctuations in the EGT for blended RBO. A major reason for the decrease in EGT observed could be the higher latent heat of vaporization of RBO blended fuel in comparison with pure diesel fuel during combustion. A poor or heterogeneous mixture could be formed due to the higher CV, low CN, and higher volatility of pure diesel compared to RBO, resulting in incomplete combustion and less-dominant premixed combustion (Hellier et al., 2019).

Another significant element was the prolonged ignition delay of pure diesel, which lengthened the fuel-burning process and raised temperature of the combustion gas leaving the combustion chamber. This is because of pure diesel consists mainly of hydrocarbons which contain only carbon and hydrogen atoms. Hydrocarbons are generally having higher energy content per unit mass compared to compounds containing oxygen, as the combustion of hydrocarbons results in the release of more energy per carbon atom. On the other hand, RBOs contains polar compounds such as phospholipids and glycolipids which can contribute to higher KV due to their ability to form intermolecular interactions and hydrogen bonds. This also clarifies that RBO100 blend with a short ignition delay have the lowest EGT, as combustion proceeds more quickly and the EGT exhibits a slight decrease prior to exiting the combustion chamber (Rajan et al., 2020). RBOs result in low exhaust as temperature typically help in preventing pre-ignition and knocking and more controlled combustion environment. Meanwhile, the excessive high exhaust gas temperature, can create hot spots and increase the risk of pre-ignition and knocking. The influence of RBOs in EGT reduces the likelihood of uncontrolled combustion events occurring before the spark plug ignites the air-fuel mixture. It also contributes to maintaining optimal combustion timing, consistent flame propagation and heat release rate. This results in smoother engine operation, reduced engine vibrations and improved the overall drivability.

4.5.2 In-Cylinder Pressure (IP)

The acquisition of data related to monitoring and evaluating in-cylinder pressure is expected to be highly valuable in the context of the development and measurement processes for CI engine. The graphs of the pressure inside the cylinder can be utilized to obtain useful information, such as the peak pressure, the indicated mean effective pressure, the optimum pressure for fuel delivery, the combustion time, and the ignition delay. By utilizing the equations derived from the first law of thermodynamics for ideal gases, it becomes possible to assess and predict several supplementary factors such as air mass flow, combustion analysis, and oxide of nitrogen emissions (Rajasekar &

Selvi, 2014). It has been found that the maximum in-cylinder pressure in CI engines is greatly influenced by the proportion of fuel used during the premixed combustion phase, sometimes referred to as the first combustion stage. Two possible patterns for changes in engine cylinder pressure during blended RBO combustion are as follows: i) The elevated CN and oxygen content exhibited by RBO and its mixes, when contrasted with conventional petroleum diesel fuel, resulted in a notable augmentation in peak pressure, ii) Conversely, the comparatively lower LHV and iii) higher viscosity of RBO, when compared to petroleum diesel fuel, resulted in a reduction in peak pressure. Figure 4.16 and Figure 4.17 indicate cylinder pressure for RBO blends versus crank angle, specifically illustrating the effects of 50% as well as full load circumstances, respectively.

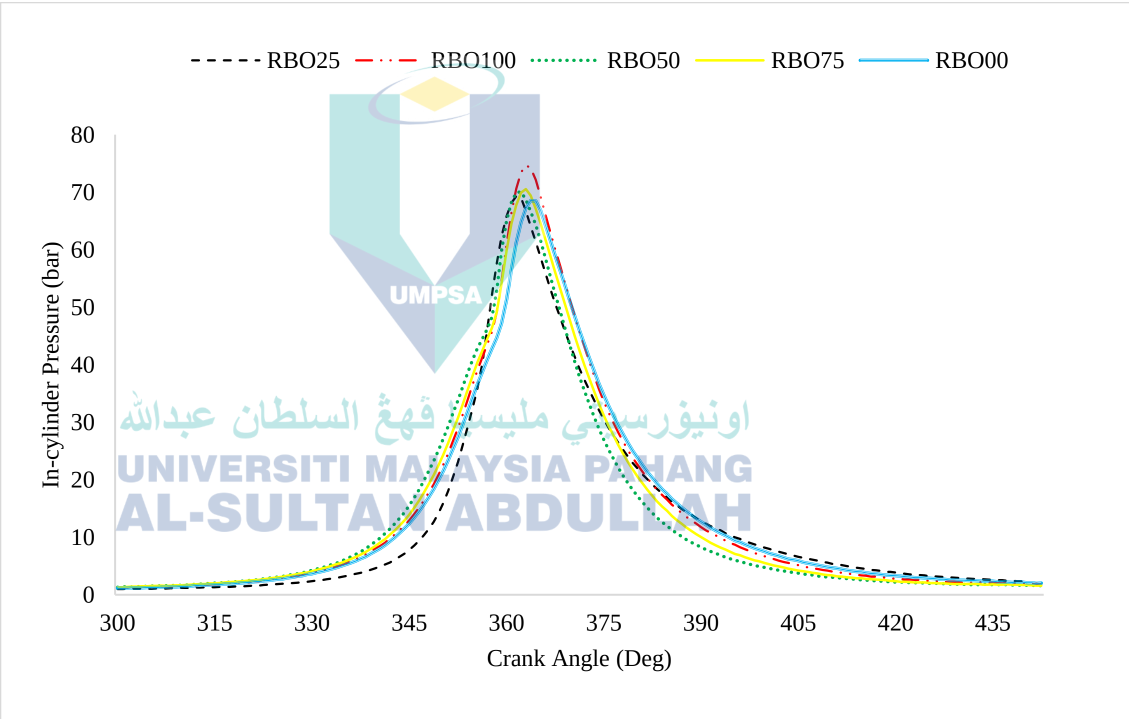

Figure 4.16 Cylinder pressure for rice bran oil blends versus crank angle at 50 % engine load

RBO100 achieved the highest cylinder pressure in both 50% and 100% engine load settings. The cylinder pressure for RBO00 (pure diesel) was seen to be the lowest under both 50% and 100% engine load circumstances. When the engine is functioning at maximum efficiency, the pressure within the cylinder experiences an increase while the ignition delay is reduced. Cylinder pressure determines whether mixed fuel may ignite when it combines with air. The RBO's higher oxygen concentrations are what cause their high pressures for both half and full load conditions. Under half load condition, the RBO100 blend had the highest peak pressure, which was followed by the RBO75, RBO50, RBO25 and RBO00 blends, with values of 74.67, 70.53, 69.9, and 68.48 bar, respectively. The trend is the same for under full load condition. The RBO100 blend had the maximum peak pressure, which was followed by the RBO75, RBO50, RBO25 and RBO00 blends, with values of 92.65, 91.06, 90.18, 79.58 and 64 bar, respectively. In conjunction of this, the CN is an essential aspect in determining cylinder pressure. The fuel with the highest cetane number and the most oxygen is RBO. The RBOs blend with a higher cetane number also often has a rapid premixing process and a reduce igniting delay for absolute combustion. In addition, RBOs exhibit distinctive combustion behaviours with different fuel types and engine loads based on both 50 % and 100 % engine load. It has been observed that pure diesel undergoes a gradual transition from concentration dominated to diffusion dominated combustion, as indicated by a shift from an advanced CA50 to a retarded CA50 with SOI gradually postponed from – 40 to – 10 CA ATDC. However, the RBOs blend shows a significantly different trend from pure diesel. When the fuel blend concentration of RBOs is increased, CA50 for RBOs is advanced as SOI is retarded; however, the diffusion-dominated combustion stage of delayed CA50 with further retarded SOI is not observed. There can be two main reasons for the discrepancies between pure diesel and RBO blends in terms of combustion process. Firstly, RBOs have a higher volatility than pure diesel, so they require less mixing with fresh air before ignition. In addition, the differences are also related to the consumption of premixed background fuels. RBOs demonstrate a higher combustion rate than pure diesel, resulting in a higher combustion temperature in the cylinder and facilitating the evaporation and mixing of the remaining unburned fuel. Consequently, RBOs do not exhibit a diffusion-dominated combustion stage. Further, it is important to note that RBOs have a later CA50 than pure diesel at the same SOI, despite the higher fuel reactivity of RBOs. It is primarily due to the higher latent heat and lower heating value of RBOs, which increase the fuel mass needed to maintain the same energy provided and reduce the local temperature in the cylinder (Jayaraman et al., 2023).

UMPSA
اونيۏرسيتي مليسيا ڤهڠ السلطان عبدالله
UNIVERSITI MALAYSIA PAHANG
AL-SULTAN ABDULLAH

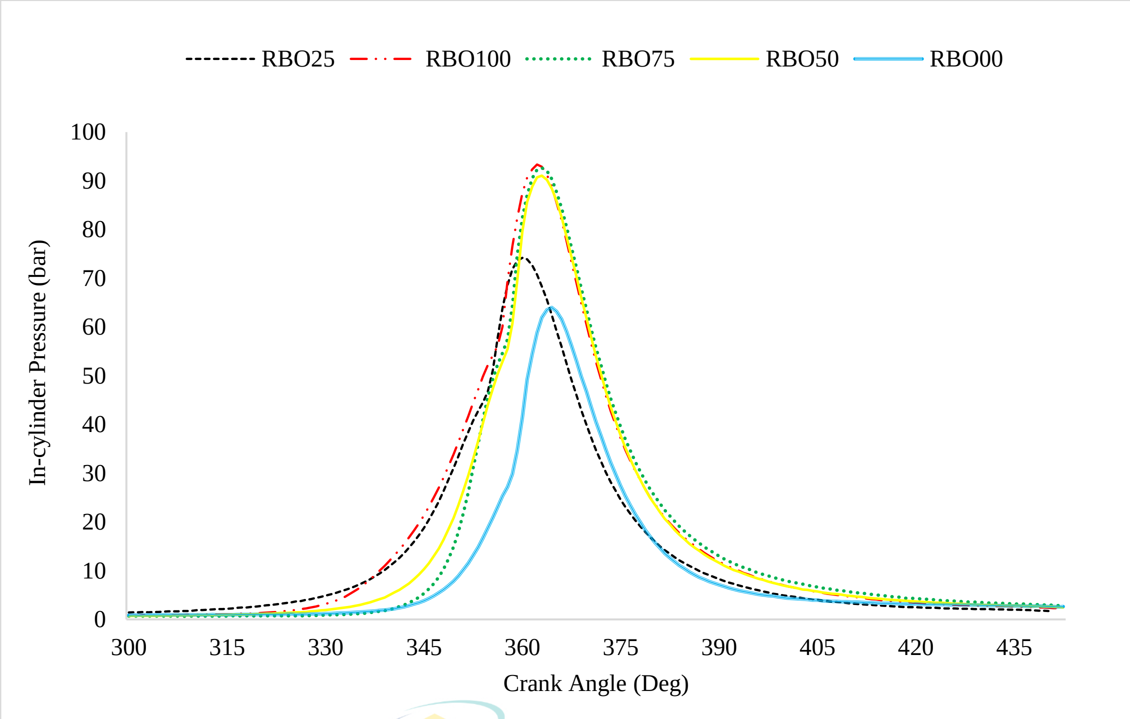

Figure 4.17 Cylinder pressure for rice bran oil blends versus crank angle at 100 % engine load

Figure 4.18 until Figure 4.20 illustrates the diverse cylinder pressure patterns detected in connection to the intake air temperature for several fuel mixes, namely RBO00, RBO25, RBO50, RBO75, and RBO100. The intake air temperatures were set at 30°C, 45°C, and 65°C, representing near-standard, high, and extremely high levels of temperature, respectively. The cylinder pressure of a compression ignition engine can be influenced by the intake air temperature, along with other factors that may exert an impact. It can be shown that there is a positive correlation between air intake temperatures and cylinder pressure levels across all evaluated fuels based on the experimental results. The observation of cylinder pressure influence becomes more pronounced when the intake air temperature reaches elevated levels, such as 30°C and 65°C. At an increased ambient temperature of 30°C and 65°C, the cylinder pressure for RBO100, RBO75, RBO50, and RBO25 exhibit increased in comparison to the in-cylinder pressure observed in pure diesel fuel.

UMPSA
اونيۏرسيتي مليسيا ڤهڠ السلطان عبدالله
UNIVERSITI MALAYSIA PAHANG
AL-SULTAN ABDULLAH

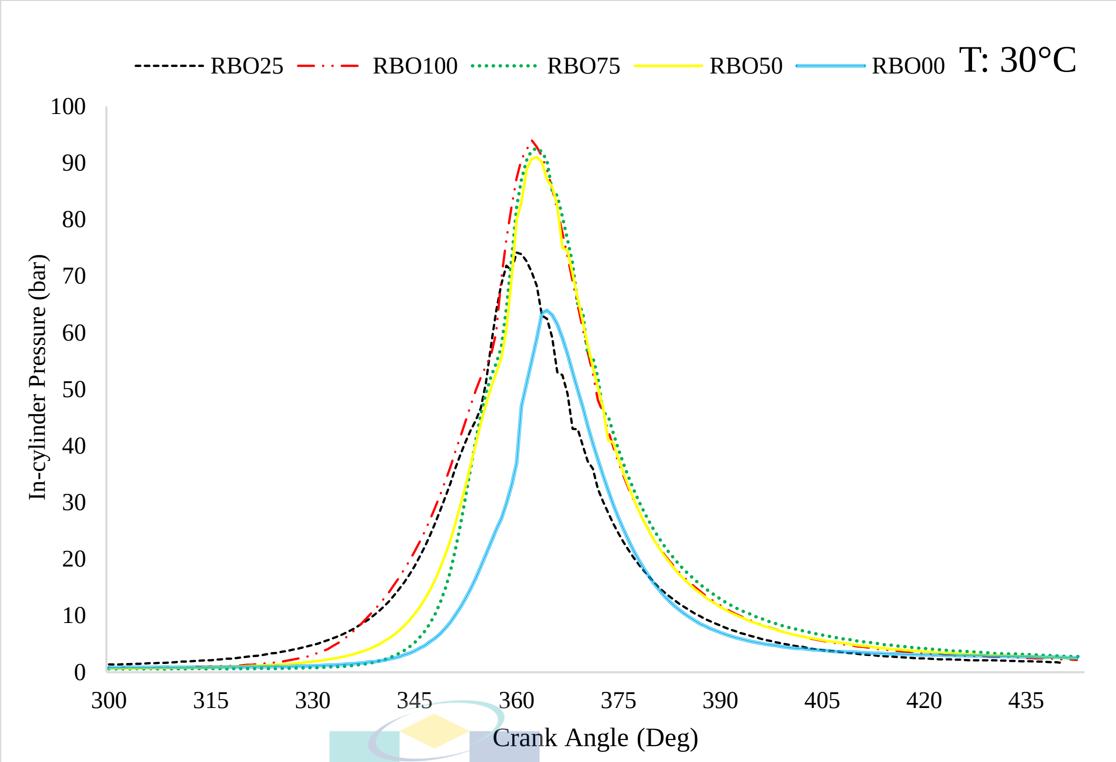

Figure 4.18 Cylinder pressure for rice bran oil blends versus crank angle at 30 °C intake air temperature

UMPSA
اونيۏرسيتي مليسيا ڤهڠ السلطان عبدالله
UNIVERSITI MALAYSIA PAHANG
AL-SULTAN ABDULLAH

The manipulation of intake air temperature led to a corresponding augmentation in the peak cylinder pressure. In the initial experimental setup utilizing solely diesel fuel, it was observed that the maximum pressure rise from 63.93 bar to 65 bar and 68 bar as the inlet temperature was raised from 30°C to 45°C and 65°C, correspondingly. The inclusion of gaseous fuels in the mixes significantly augmented the in-cylinder pressure. The primary factor contributing to this increase is the greater calorific values observed in fuels that possess higher energy content, such as RBO25 (44.221 MJ/kg) and RBO50 (43.8684 MJ/kg). The rise in peak pressure was linearly proportional to the intake temperature and the RBO mixes in the fuel mix. The observed rise in peak pressure ranged from 45% to 48%. This was demonstrated in the scenario where the intake air temperature was set at 45°C (Figure 4.19), resulting in an increase in pressure from 65 bar to 96 bar. Similarly, when intake air temperature was set at 30°C, the pressure increased from 63.93 bar to 92.22 bar.

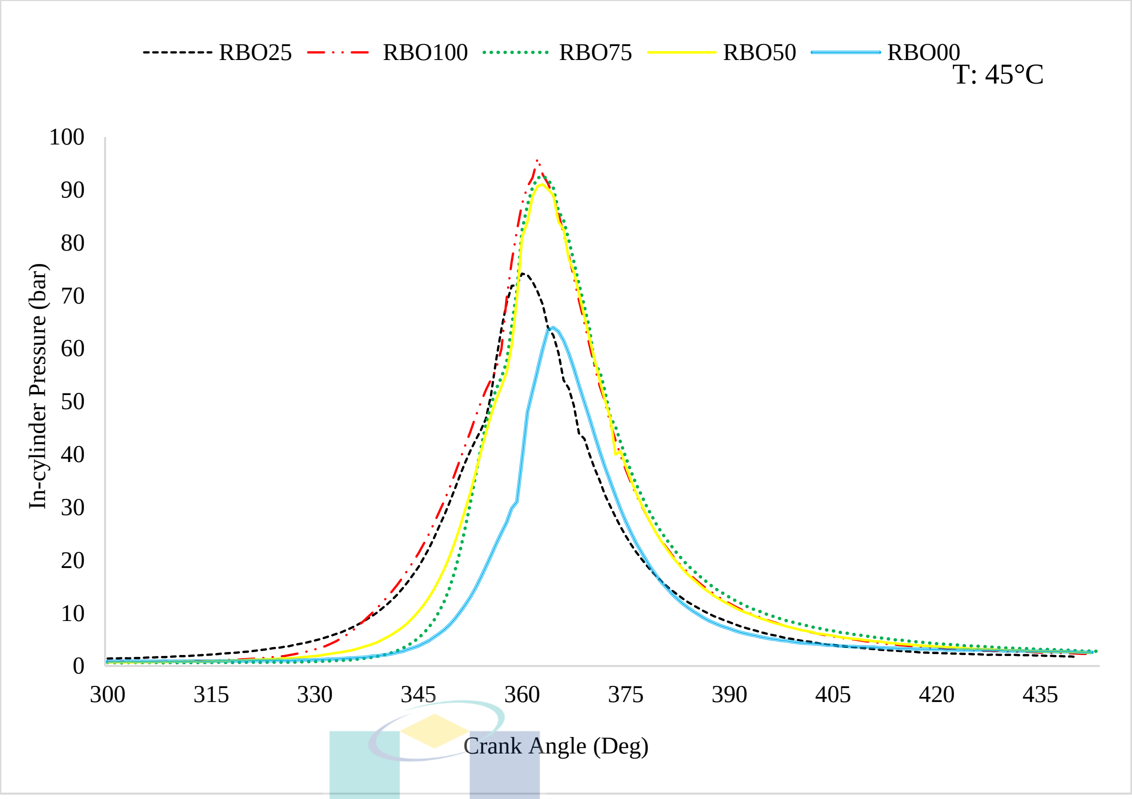

Figure 4.19 Cylinder pressure for rice bran oil blends versus crank angle at 45 °C intake air temperature

It is anticipated that an increase in intake air temperature will result in accelerated combustion. The period of combustion was extended due to the presence of extra air which resulted in the dilution of the charge mixture. A higher intake air temperature facilitates the establishment of auto-ignition conditions within the combustion chamber, hence expediting chemical reactions. The rapid chemical reactions result in an escalation of the pace at which heat is released. As a result, the swift release of heat results in an elevated rate of pressure rise. An increase in intake air temperature leads to a decrease in combustion duration

UMPSA
اونيۏرسيتي مليسيا ڤهڠ السلطان عبدالله
UNIVERSITI MALAYSIA PAHANG
AL-SULTAN ABDULLAH

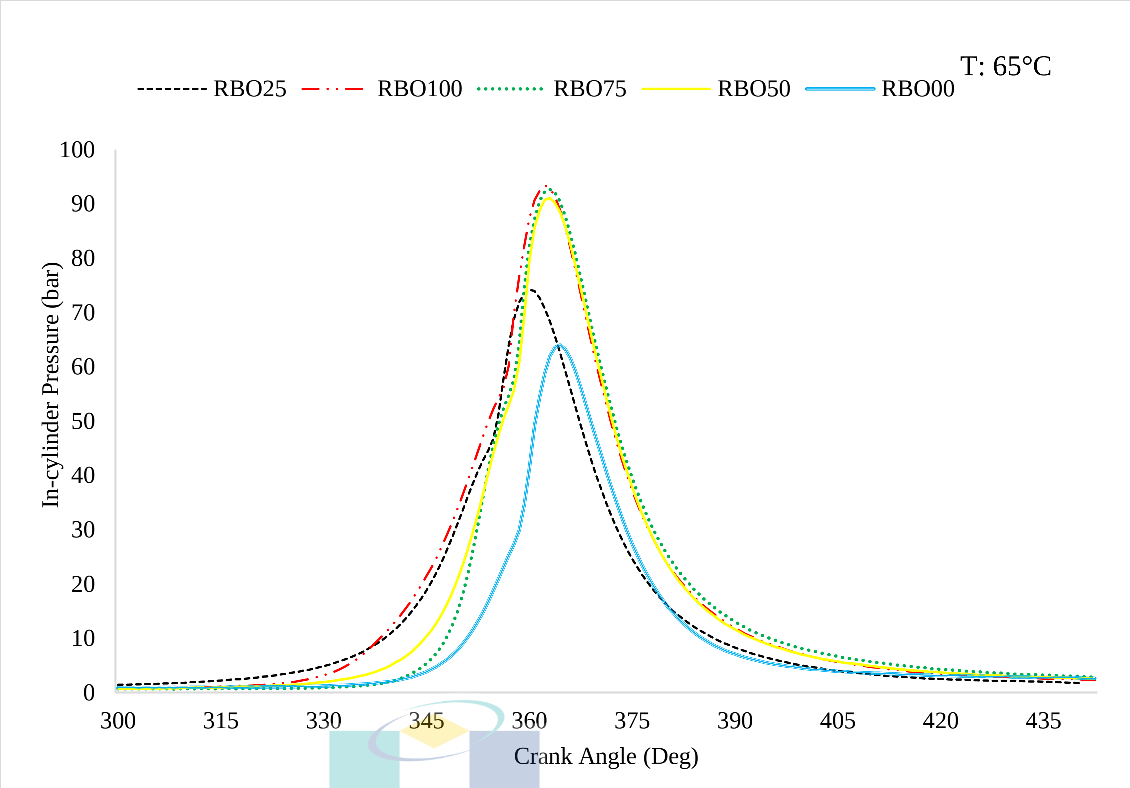

Figure 4.20 Cylinder pressure for rice bran oil blends versus crank angle at 65 °C intake air temperature

The decrease in combustion duration can be attributed to the accelerated chemical reactions occurring within the combustion chamber. Chemical reactions occurring between oxygen and hydrocarbon molecules exhibit a tendency to occur more rapidly when the intake air temperature rises. Consequently, the process of combustion commenced at an earlier point in time (Stone, 1999).

UMPSA
اونيۏرسيتي مليسيا قهڠ السلطان عبدالله
UNIVERSITI MALAYSIA PAHANG
AL-SULTAN ABDULLAH

4.5.3 Rate of Heat Release (RoHR)

The principles of the First Law of Thermodynamics of closed volume in CI cycles implemented to calculate the net rate of heat release values by analysis of the recorded in-cylinder pressure. The phrase "heat release" pertains to the quantity of thermal energy that must be supplied to the cylinder in order to attain the intended the change in pressure. The measurement of heat release is a crucial factor in the examination of the combustion properties of CI engines and provides a dependable measure of fuel consumption. The term "sensible enthalpy" refers to the rate at which thermal energy is generated during the process of combustion, resulting from the conversion of chemical energy derived from a fuel source. The term "start of combustion" (SOC) refers to the initiation of heat release, while the "end of combustion" (EOC) is defined as the point in the crank angle where the rate of heat release exceeds 95% of the total heat release (Heywood, 1988). The duration of combustion refers to the temporal span between the SOC and EOC as a function of crank angle degrees. The fundamental principles of heat release analysis were established by Krieger and Borman (Borman & Nishiwaki, 1987; Krieger, 1994) with the objective of determining the rate at which fuel mass is burned. Numerous academics have conducted extensive investigations pertaining to the determination of heat release rate in a work-related context. The process of fuel vaporisation initiates during the ignition delay period, resulting in an initial negative heat release. Subsequently, after the initiation of the combustion process, there occurs a transition in the rate of heat release, resulting in a change towards a positive value. The word "ignition time" refers to the moment when the release of heat begins in the process of combustion. The entirety of the combustion duration encompasses the temporal interval that encompasses both the commencement and completion of the release of heat (Heywood, 1988).

Figure 4.21 displays the RoHR as a function of the CAD for the experimental fuels at a moderate engine load of 50% at 2500 rpm. The figure presented illustrates a notable escalation in the rate of heat release observed in the experimental fuels as the RBO blended gradually augment. The RBO100 fuel has a higher maximum RoHR in comparison to other tested fuels and pure diesel when subjected to identical operating conditions. Specifically, this maximum rate is measured at 65 J/deg.CA at 354 CAD. Nonetheless, it is worth noting that RBO100 exhibits a notable delay in ignition and a shorter period of combustion in comparison with pure diesel fuel. This is due to the RBO100, characterised by its increased density and viscosity, exhibits a slower rate of vaporisation in comparison to pure diesel. Consequently, a reduced quantity of air-fuel combination is available for combustion.

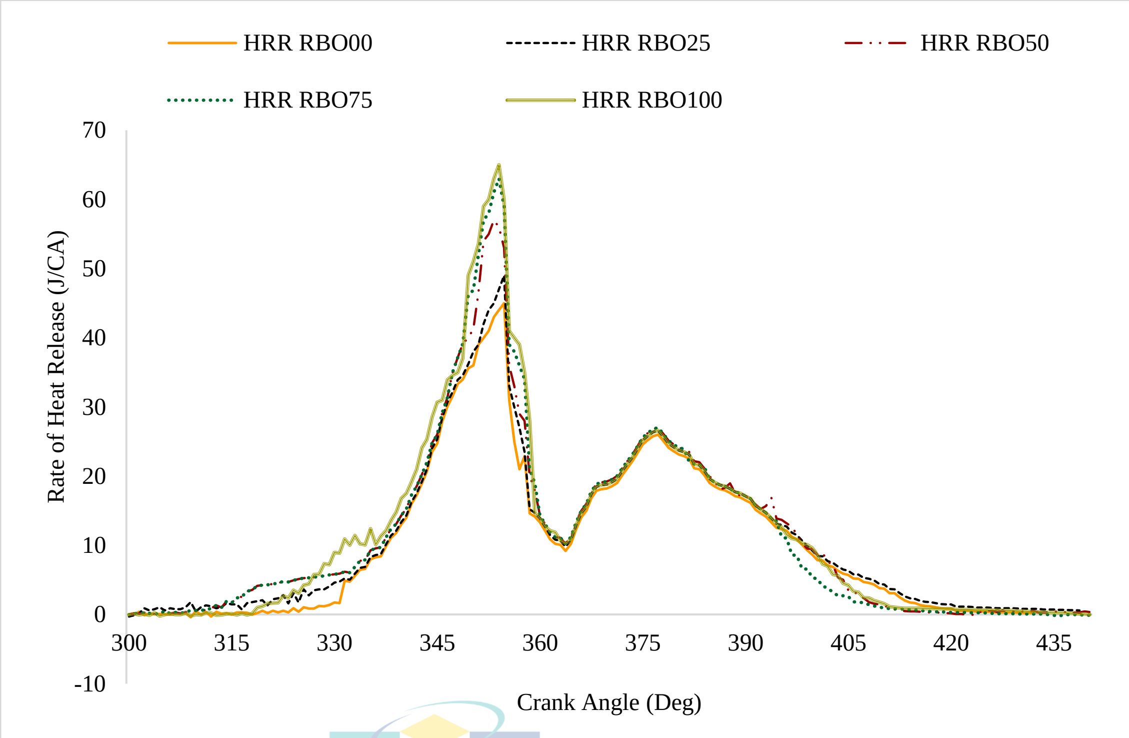

Figure 4.21 Variation of rate of heat release with crank angle at 50 % engine load

Figure 4.22 depicts the RoHR versus CAD for various fuel mixes including RBO00 (pure diesel), RBO25, RBO50, RBO75, and RBO100. The measurements were conducted during periods of high engine load (100 %), with a consistent engine speed of 2500 rpm. The empirical evidence suggests that there is a direct correlation between engine loads and the rate of heat emission for the test fuels. A comparative analysis reveals that the highest RoHR for RBO25, RBO50, and RBO75 exhibits a fair increase of 2.89%, 6.19%, and 7.29% respectively, as compared to the use of RBO00 at high load conditions. The occurrence of this phenomena can be attributed to the escalation in engine loads, resulting in a subsequent elevation in cylinder pressure. Based on the result, it is observed that RBO100 has a higher maximum RoHR compared to pure diesel, especially under high engine load conditions. This can be credited to the notable increases in both pressure and temperature within the reaction zone.

UNIVERSITI MALAYSIA PAHANG AL-SULTAN ABDULLAH

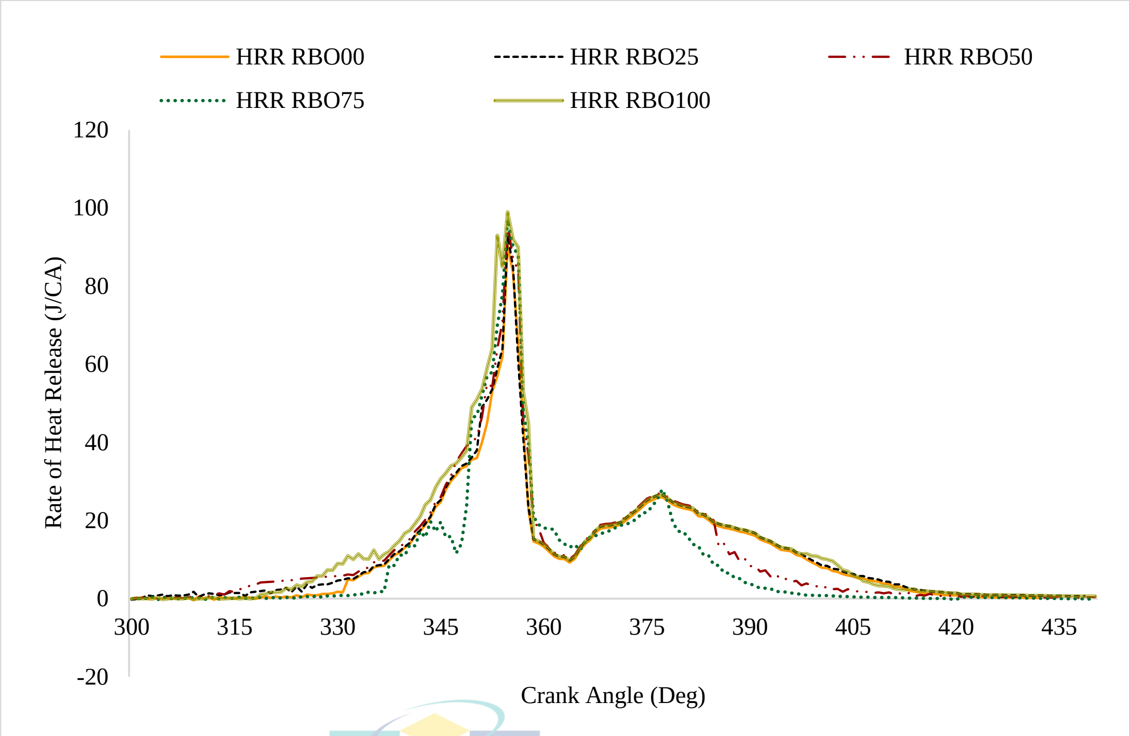

Figure 4.22 Variation of rate of heat release with crank angle at 100 % engine load

The effects of RBOs influence by several factor. Firstly, RBOs were atomized into small droplets with different spray characteristics when compared to pure diesel. These characteristics include the size distribution of droplets, the penetration of the spray, and the spray angle. The viscosity and surface tension of RBOs play an important role in the atomization process. In addition, the volatility of RBOs influences their ability to mix with air in the combustion chamber. It has been observed that RBOs with a higher volatility tend to vaporize more readily, which may result in better mixing with air and more uniform combustion. Then, the presence of an oxygenated component in RBO100 leads to a quicker initiation of combustion and a reduced length of combustion when compared to pure diesel fuel (Jayaraman et al., 2023). Consequently, the initiation of combustion is postponed, leading to increased fuel combustion and subsequently yielding a heightened maximum cylinder temperature. In summary, the RoHR comparison indicates that the peak RoHR of RBOs is greater than that of pure diesel fuel. Thus, the fuel concentration in RBOs is closely related to the volatility of pure diesel, and this has a significant impact on the combustion of premixed fuels. The most significant effect of pure diesel implementation on compression ignition engines is on the SOI. There is a significant multistage combustion profile as the SOI decreases with the mixing premixed pure diesel. This multi-stage heat release phenomenon has not been observed in RBOs in the present study. In addition, the higher reactivity of RBOs causes a faster ignition as a result of their good volatility, which enhances mixing. The decrease in ignition delay and the consequent increase in fuel consumption during combustion after ignition can be attributed to the higher CN of RBO (Hoang et al., 2021).

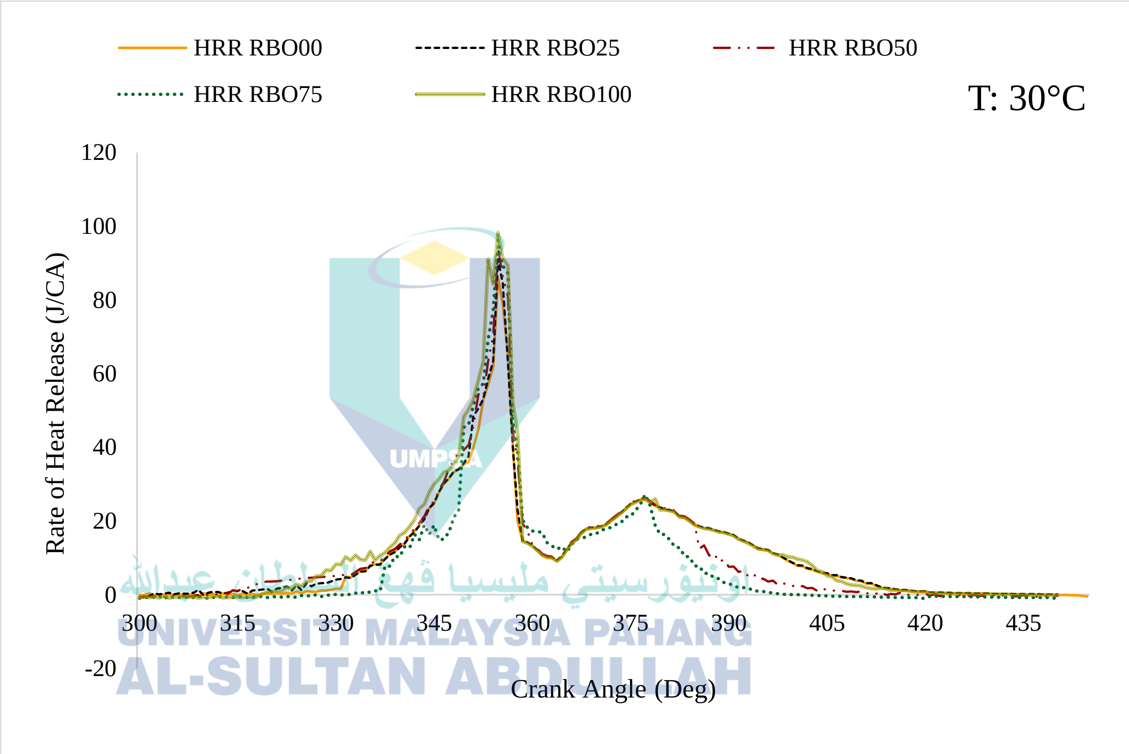

Figure 4.23 Variation of rate of heat release with crank angle at 30°C intake air temperature

The Figure 4.23 - Figure 4.25 illustrate the diverse rate of heat release patterns detected in connection to the intake air temperature for several fuel mixes, namely RBO00, RBO25, RBO50, RBO75, and RBO100. The intake air temperatures were set at 30°C, 45°C, and 65°C, representing near-standard, high, and extremely high levels of ambient air temperature, respectively. The rate of heat release of a compression ignition engine can be influenced by the temperature of the intake air, along with other factors that may exert an impact. Based on the experimental results, it can be shown that there is a positive correlation between air intake temperatures and rate of heat release across all evaluated fuels. The observation of rate of heat release influence becomes more pronounced when the intake air temperature reaches elevated levels, such as 65°C.

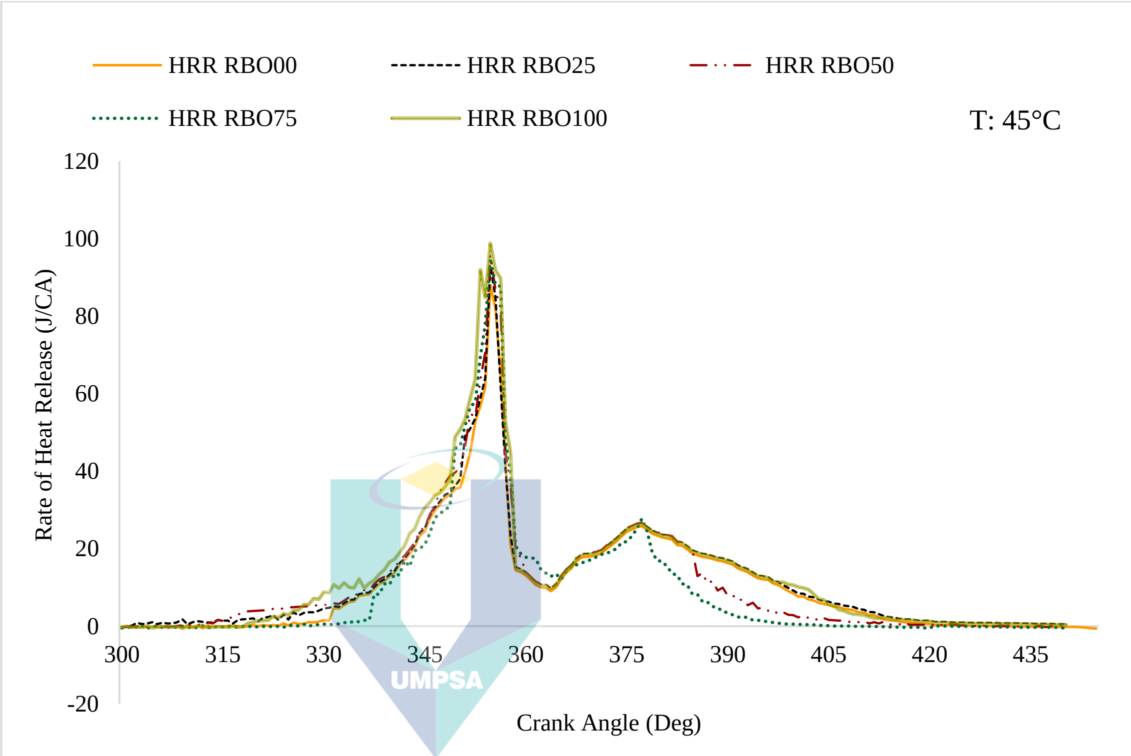

Figure 4.24 Variation of rate of heat release with crank angle at 45°C intake air temperature

UNIVERSITI MALAYSIA PAHANG
AL-SULTAN ABDULLAH

The relationship between the maximum RoHR and intake air temperature, as well as the amount of RBO blended, becomes more intricate with increasing intake air temperature. In general, there was an observed increase in the peak rate of heat release values as the intake temperature was raised. At an intake air temperature of 30°C, the peak rate of heat release values observed were 86 J/CA, 91 J/CA, 94 J/CA, 96.2 J/CA, and 98.3 J/CA, respectively, as the blend transitioned from RBO00 to RBO25, RBO50, RBO75, and ultimately RBO100. Furthermore, it was observed that the peak rate of heat release values exhibited an upward trend as the intake air temperature reached 45°C. The RBO100 exhibits the highest rate of heat emission, measuring at 98.8 J/CA.

Subsequently, the RB075, RBO50, RBO25, and RBO00 models exhibit peak rates of heat release measuring 95.7 J/CA, 95 J/CA, 92.98 J/CA, and 88 J/CA, correspondingly.

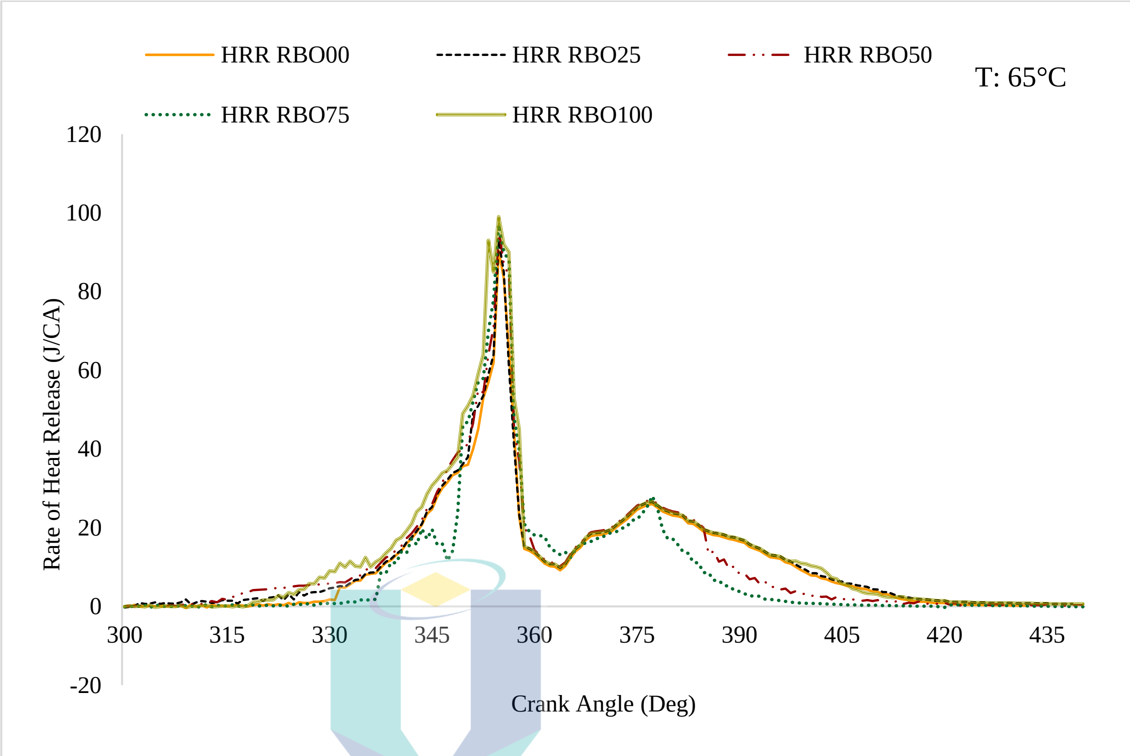

Figure 4.25 Variation of rate of heat release with crank angle at 65°C intake air temperature

UMPSA
اونيۏرسيتي مليسيا ڤهڠ السلطان عبدالله
UNIVERSITI MALAYSIA PAHANG
AL-SULTAN ABDULLAH

At an intake air temperature of 65°C, one can detect a greater degree of variation in both the peak rate of heat release values and the positions of the CAD where these peaks occur. The maximum RoHR started at a pressure of 90.4 bar while using pure diesel fuel and reached its top at 99 bar when utilising RBO100 fuel, representing a 6%–7% augmentation compared to the RoHR achieved at an intake air temperature of 30°C. The maximum RoHR at the CAD location initially occurred at 367 °CA, subsequently decreased, and then increased again at 364°CA and 362°CA. The influence of intake air temperature on compression ignition engine when using RBOs as fuel is significantly affected the fuel air mixture inside the engine cylinder. Higher intake air temperature led to more complete combustion of the fuel. This can be described as RBOs has a higher KV when compared to pure diesel, improved its atomization and one of the combustion properties which RoHR. Additionally, the high intake air temperature also results in rapid evaporation of the injected fuel, which is caused by the heat energy entrained in the spray. In the presence of intake air temperatures of 30 °C, 45 °C, and 65 °C, the ignition timing is rapidly advanced, but the effect is not significant at 65 °C. The reason is that, when fresh air with a temperature of 65 °C is inhaled, the change in intake air temperature does not significantly affect the combustion chamber temperature. Meanwhile, the peak of RoHR was reduced as the intake air temperature increased, and the combustion period was prolonged as the intake air temperature increased. It is believed that increasing the intake air temperature will improve the evaporation rate of the fuel, but it will also reduce the ignition delay, hence reducing the formation of the premixed combustion mixture. As a result, less heat was released at the peak of the combustion process and the combustion reaction was more evenly distributed throughout the entire combustion chamber area.

4.5.4 Rate of Pressure Rise (RoPR)

RoPR is a pivotal parameter that is intricately related to engine performance. The highest RoPR is stated when the engine load is augmented, followed by a significant decrease mostly owing to the impact of the premixed phase at lower loads. The shorter ignition delay of RBO blended results in a greater maximum RoPR when compared to pure diesel (Hoang et al., 2021). The analysis of Figure 4.26 indicates that the RoPR is significantly greater for RBO100, RBO75, RBO50, and RBO25 compared with RBO00 (pure diesel). This disparity can be ascribed to the shorter ignition delay exhibited by these RBO blends. Nevertheless, fluctuations in the RoPR for the fuels under examination are observed to transpire within the range of 364 CAD to 405 CAD during periods of moderate engine load. It is comprehensible that following the initiation of combustion, the tested fuels commence the process of burning and continue until the end of combustion. RBO100, RBO75, RBO50, and RBO25 are higher oxygenated fuels than pure diesel and have a greater RoPR increase than pure diesel.

UMPSA
اونيۏرسيتي مليسيا ڤهڠ السلطان عبدالله
UNIVERSITI MALAYSIA PAHANG
AL-SULTAN ABDULLAH

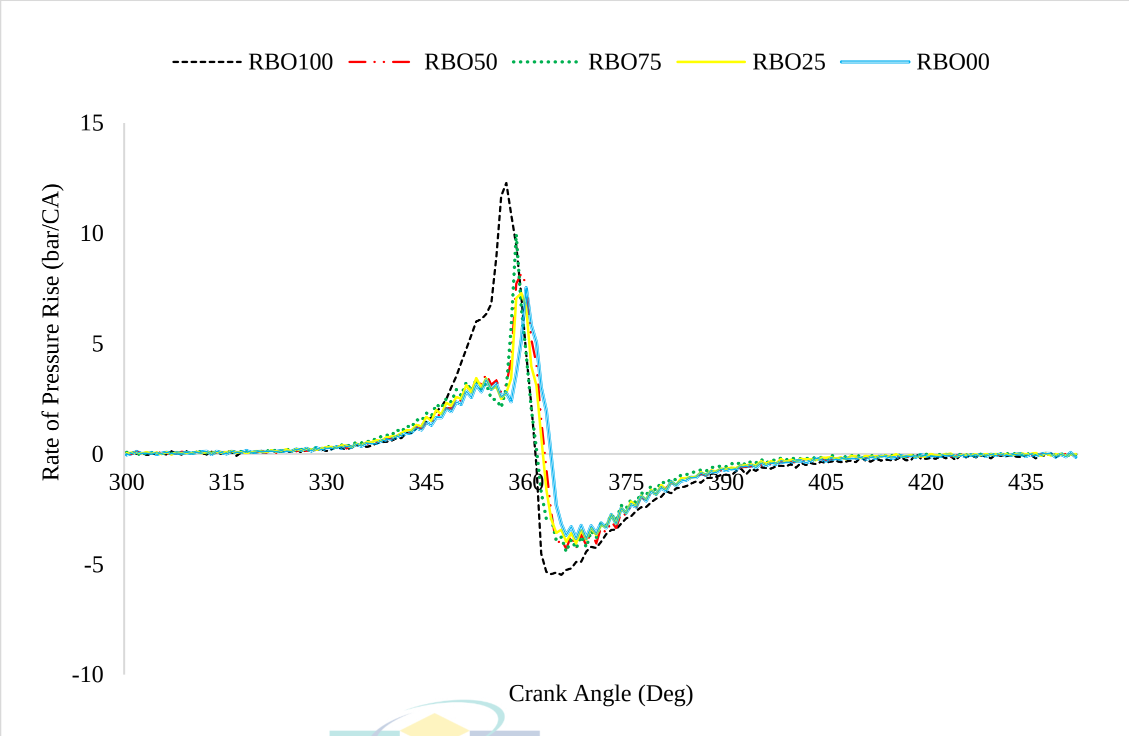

Figure 4.26 Variation of rate of pressure rise with crank angle at 50 % engine load

An elevation in engine loads leads to a significant amplification of engine in-cylinder pressure measurements. The pressure increase rate for the test fuels under a 100% engine load, while keeping a constant engine speed of 2500 rpm, is illustrated in Figure 4.27. The data clearly demonstrates that within the range of 345 CAD to 360 CAD, the RoPR patterns observed for the test fuels were similar to those of pure diesel under identical operating conditions. The study reveals that the rise in cylinder pressure for the different fuels has a direct impact on the rate of pressure increase (Ming et al., 2018; Ramachandran et al., 2023). The graph depicted in Figure 4.27 demonstrates the variations in the rate of pressure increase for the tested fuels as subjected to high engine load circumstances, while keeping the engine speed constant at 2500 rpm.

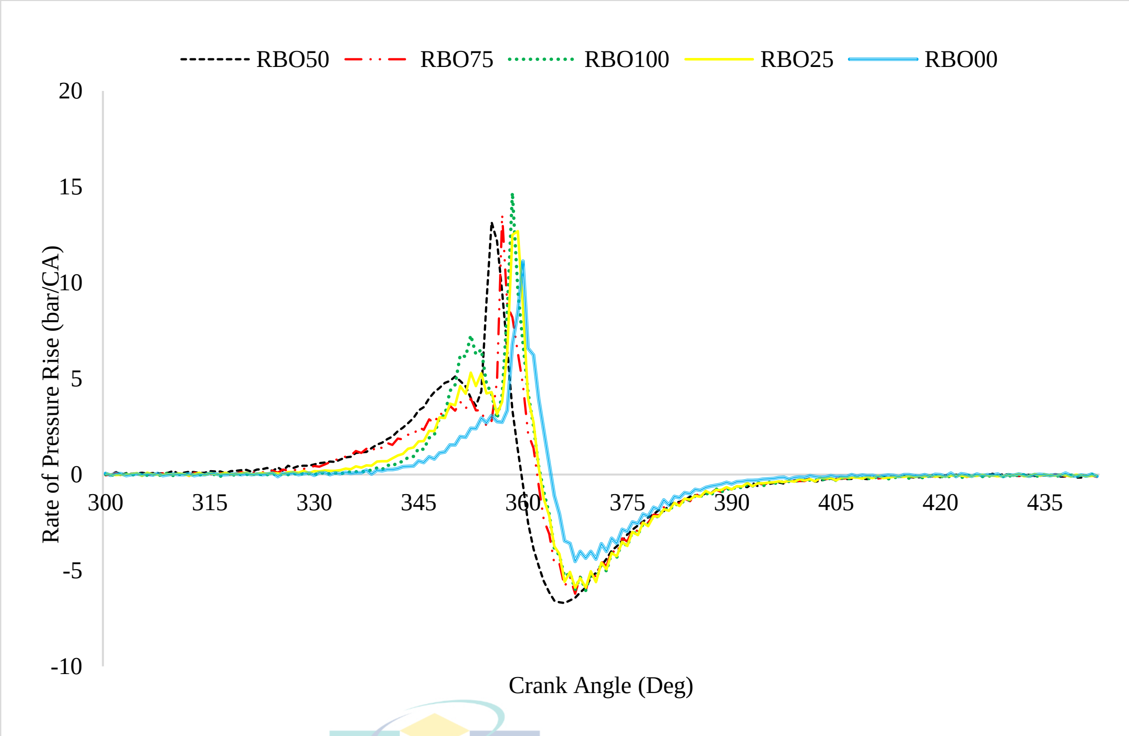

Figure 4.27 Variation of rate of pressure rise with crank angle at 100 % engine load

A significant discrepancy in the rate of pressure escalation is found among the tested fuels when the engine load shifts from medium to extremely high levels. This phenomenon is mostly associated with the rise in cylinder pressure, as depicted in Figure 4.16 and Figure 4.17, which leads to an elevated rate of pressure growth. The data demonstrates that pure diesel fuel demonstrates a comparatively minimum RoPR in comparison with other RBO blended fuels. This trend is observed from 357 CAD to 405 CAD, with the lowest rate of pressure rise (RoPR) recorded at 1.70 bar/deg.CA occurring at 14 CAD. Nevertheless, the RBO50 exhibits the most elevated Rate of Pressure Rise (RoPR) at 358.5 CAD when subjected to a pressure of 14.7 bar/deg.CA.

In addition to this, it can be observed that RBO25, RBO50, RBO75, and RBO100 exhibit a significantly greater RoPR compared to RBO00. The study shows that the incorporation of higher amounts of RBO blends leads to corresponding increases in cylinder pressure, which vary depending on the engine loads and exert an influence on the RoPR. The correlation between the RoPR and cylinder pressure is comprehensible, as both of them are predominantly influenced by the combustion process of the fuel. In pure diesel, it can be observed that peak RoPR shows a significant decrease with retarded SOI, although a significant increase in CA50 occurs as the SOI is postponed from - 40 to - 30 °CA ATDC. The reason for this is that the pure diesel with the retarded SOI is less sufficient, resulting in a decrease in the ignition reactivity of the premixed RBOs mixture, resulting in a lower RoHR.

Additionally, the primary factor affecting the RoPR increase is the cylinder pressure of the test fuels. Then, it followed by the mixture formation of RBOs. The atomization RBOs into small droplets exhibit the different spray characteristics compared to pure diesel. It includes droplet size distribution, spray penetration and spray angle. Then, the flame propagation factor also influences the rate and completeness of RBOs combustion which are fuel-air ratio, temperature and turbulence affect speed and shape. One of the RBOs fuel properties is its high oxygen content. The introduction of fuel mixes with higher oxygen content has ultimately resulted in enhancements to both cylinder pressure and the rate at which pressure increases, thus, result to the uniform combustion process and led to the better engine performance and thermal efficiency (Asadi et al., 2019).

UMPSA

4.6 Analysis of Knocking Intensity on Engine

اونيۏرسيتي مليسيا ڤهڠ السلطان عبدالله
UNIVERSITI MALAYSIA PAHANG
AL-SULTAN ABDULLAH

The purpose of the current section is to offer a comprehensive review of the knocking study that is included in this thesis. The purpose of this study is to gather data and enhance understanding of the relationship between the physicochemical properties of fuel, engine performance, combustion behaviours, exhaust emissions characteristics, and knocking intensity on the KIPOR 170FS CI engine. This engine is a single-cylinder, four-stroke diesel engine that operates on both pure diesel fuel as baseline RBO blended. The method of in-cylinder pressure analysis (direct measurement) was used in this study. Figure 4.28 and Figure 4.29 depict the evaluation of KI, a crucial parameter for determining the effect of RBO00 (pure diesel) and RBO blended (RBO25, RBO50, RBO75, RBO100) combustion, across various equivalency ratios at an engine speed of 1500 rpm. The value 5 MW/m^2 is suggested for use as the limiting value of KI (Dernotte J, 2014).

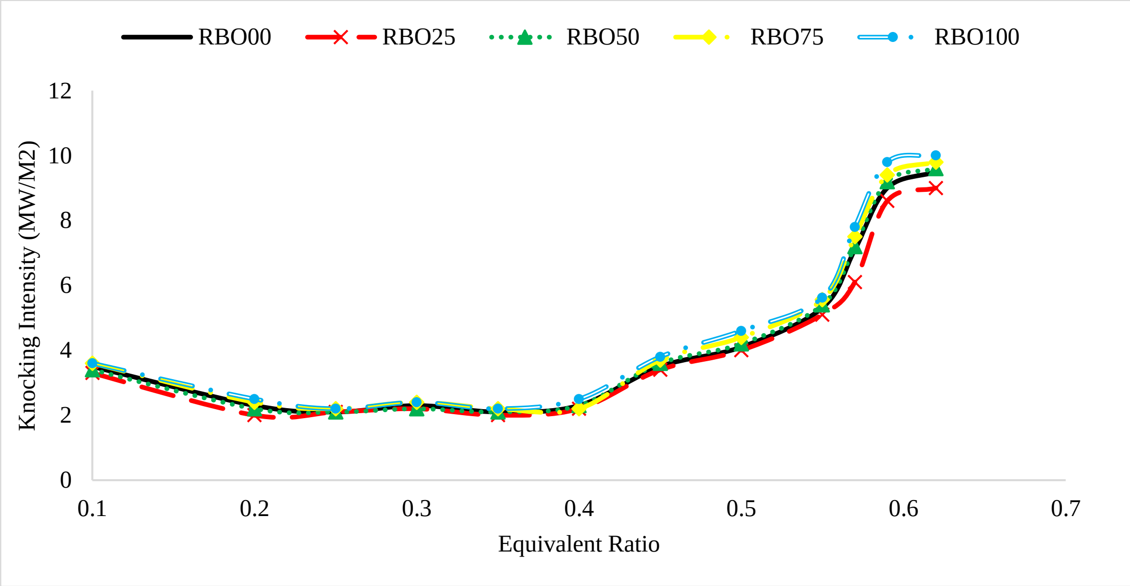

Figure 4.28 Influence of equivalent ratio on knocking intensity at 1500 rpm

Increasing combustion temperatures has resulted in a significant increase in the equivalency ratio, which has led to an increase in KI. This temperature increase took place from 999 K at ϕ = 0.1 to 2000 K at ϕ = 0.55 observed in the direct injection CI engine across all fuel types (RBO00, RBO25, RBO50, RBO75, and RBO100). The observed KI was determined to be below the established threshold when the equivalency ratio was systematically varied within the range of 0.1 to 0.55. This observation indicates the presence of a stable combustion mode characterized by controlled auto-ignition phenomenon. Once the equivalency ratio surpassed 0.55, the KI value increased took place from 5.62 MW/m^2 at ϕ = 0.56 to 9.8 MW/m^2 at ϕ = 0.62, beyond the established threshold. This observation implies that the combustion mode becomes unstable and experiences uncontrolled auto-ignition, resulting in extreme knocking combustion (Nema et al., 2022). It also disrupts the normal air-fuel mixing process in the combustion chamber. This can lead to non-uniform fuel distribution, uneven air-fuel ratio and thus poor mixture homogeneity can exacerbate knocking tendencies and affect combustion stability. Then, it also impacts fuel atomization during fuel injection. Increased turbulence and pressure fluctuations in the combustion chamber can disturb the breakup of fuel droplets, leading to larger droplet sizes and uneven fuel distribution. High knocking intensity may necessitate retarding ignition timing to reduce the risk of knock. Retarding the ignition timing delays the start of combustion relative to the piston position, allowing more time for the air-fuel mixture to compress before ignition. However, delayed ignition timing can also lead to decreased engine efficiency and power output.

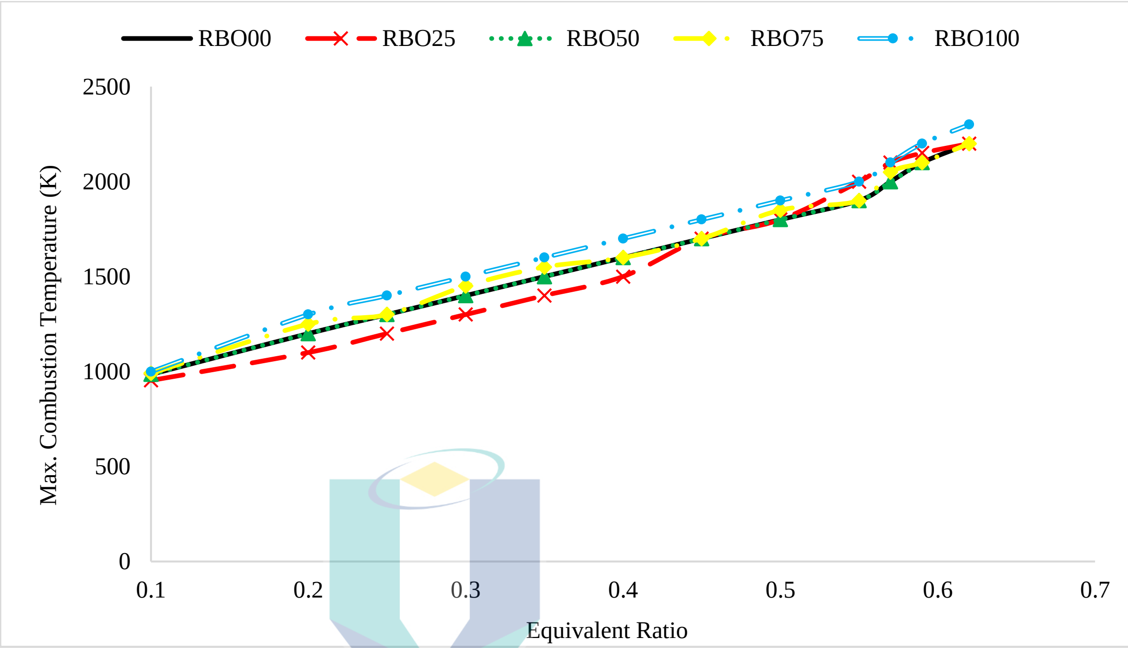

Figure 4.29 Influence of equivalent ration on maximum combustion temperature at 1500 rpm

UMPSA
اونيۏرسيتي مليسيا ڤهڠ السلطان عبدالله
UNIVERSITI MALAYSIA PAHANG
AL-SULTAN ABDULLAH

The increase in KI can be attributed to a substantial rise in the equivalency ratio, leading to an elevated combustion temperature. RBO25 demonstrated the lowest KI which is 5.1 MW/m^2 at equivalent ratio is 0.54 compared with other fuels. It led to the stable and complete combustion. This result suggested the existence of a stable combustion mode that is distinguished by a regulated auto-ignition occurrence. Overall, high knocking intensity can negatively impact mixture formation, ignition process, and combustion process in an internal combustion engine. It can lead to inefficient combustion, increased emissions, decreased engine efficiency, and potential engine damage if not addressed promptly. Engine designers typically employ strategies such as optimizing fuel injection timing, adjusting spark timing, and implementing knock detection and control systems to mitigate the effects of knocking and ensure reliable engine operation.

4.7 Summary

This research has established new green fuel and enhanced a body of knowledge which advances the understanding of the effect of RBO blends enriched with pure diesel fuel on light-duty (single-cylinder), four-stroke compression ignition engines on chemical properties of fuel, performance of the engine, combustion qualities, exhaust emissions characteristics, and knocking. The results of the study are summarized starting with engine performance characteristics. RBO25, RBO50, RBO75, and RBO100 are suitable for direct utilization in diesel engines without requiring any engine modifications. The BP of pure diesel fuel demonstrates a relative rise of approximately 6.7% compared to RB0100. The observed disparity can be ascribed to the increased viscosity (13.5%) and decreased energy content (11.2%) of B100 compared to pure diesel fuel. Throughout the entire range of engine speeds, pure diesel fuel exhibited the lowest BSFC and was observed at 2500 rpm. At the same engine speed, it costs about 50.1% less than RB0100 fuel. This difference is because pure diesel fuel has more energy (11.2%) than RBO100. The BTE of RBO100 fuel is 58.57 % more than that of pure diesel when operating at an engine speed of 2500 rpm. The presence of a higher oxygen percentage in RBO100, as opposed to pure diesel, is expected to improve the combustion process. Hence, prior research has shown evidence that the utilization of rice bran oil blends has resulted in enhanced BTE in diesel engines.

اونيۏرسيتي مليسيا ڤهڠ السلطان عبدالله
UNIVERSITI MALAYSIA PAHANG
AL-SULTAN ABDULLAH

Exhaust emission findings indicate that the engine speed of 3500 rpm yielded the lowest carbon monoxide (CO) emissions. Specifically, the RBO100 fuel blend demonstrated the lowest CO emissions at around 0.01%. This was followed by RBO75 (0.03%), RBO50 (0.03%), RBO25 (0.06%), and the highest CO emissions of approximately 0.09% were seen for RBO00. In the case of RBO00, the elevated levels of carbon monoxide (CO) can be attributed to the extended ignition delays (ID) resulting from the fuel composition. At the maximum rotational speed of 3500 rpm, the emission of CO_2 for RBO100 is 38.02 % greater in comparison to that of pure diesel. The measurement of CO_2 emission serves as an indicator of the combustion efficiency within the combustion chamber. The findings highlighted the observation that the RBO100 exhibits a significant reduction of 37.93 % in HC emissions compared to pure diesel at low speeds, with both fuels demonstrating a further decrease at 3500 rpm. The RBO blends presented consistently lower levels of HC emissions in comparison to pure diesel at all tested speeds. Combustion byproducts that increase the temperature in RBO fuel have the effect of inhibiting the condensation of higher hydrocarbons (HC), hence resulting in a reduction of HC emissions. A greater cetane number of RBO leads to a reduction in HC emissions due to a shorter ignition delay. RBO100 shows the highest level of NOx emissions, measuring 389 ppm when the engine was operated at 3500 rpm engine speed. Among all the fuel types examined, RBO00 demonstrates the lowest NOx emission level, measuring 350 ppm. As the engine speed is augmented, there is a corresponding increase in the emission of NOx across all fuel mixtures.

Then, the result focuses on the combustion behaviours. The significant increments are for RBO00, which RBO25, RBO50, and RBO100 subsequently follow. In addition to the high calorific value of the fuel blends, which produced more heat per unit mass than RBO25, RBO50, RBO75, and RBO100 blends had a high EGT measurement. Under half load condition, the RBO100 blend had the highest peak pressure, which was followed by the RBO75, RBO50, RBO25 and RBO00 blends, with values of 74.67, 70.53, 69.9, and 68.48 bar, respectively. The trend is the same for under full load conditions. The RBO's higher oxygen concentrations cause high pressures for 50% and 100% engine loads. RBO100 attained the maximum cylinder pressure in both half- and full-load conditions. Under both half and full-load conditions, the cylinder pressure for RBO00 (pure diesel) was the lowest. When the engine is operating at full capacity, the pressure inside the cylinder increases as the ignition delay shortens. Cylinder pressure determines whether mixed fuel may ignite when it combines with air. The RBO's higher oxygen concentrations cause their high pressures for both 50% and 100% engine loads. The RBO100 fuel has a higher maximum RoHR compared with tested fuels under 50% engine load and pure diesel when subjected to identical operating conditions. Precisely, this maximum rate is measured at 65 J/deg.CA at 354 CAD. Nonetheless, it is worth noting that RBO100 exhibits a notable delay in ignition and a shorter combustion period when compared to RBO00 fuel. This is because RBO100, characterized by its increased density and viscosity, exhibits a slower rate of vaporization in comparison to pure diesel. Consequently, a reduced quantity of

اونيۏرسيتي مليسيا ڤهڠ السلطان عبدالله
UNIVERSITI MALAYSIA PAHANG
AL-SULTAN ABDULLAH

air-fuel combinations is available for combustion. A comparative analysis reveals that the highest RoHR for RBO25, RBO50, and RBO75 exhibits a fair increase of 2.89%, 6.19%, and 7.29%, respectively, as compared to the utilization of RBO00 fuel at 100% engine load conditions. This occurrence is due to the rise in engine loads, consequently leading to an increase in cylinder pressure. Based on the obtained data, it can be inferred that the maximum RoHR for the tested fuels exhibits an upward trend as the engine loads (50% and 100%) increase. Furthermore, when comparing RBO00 with RBO25, RBO50, RBO75, and RBO100, it can be shown that the diffusion combustion phase is longer for RBO00. The decrease in ignition delay and higher fuel usage during combustion after ignition can be ascribed to the high CN of RBO. The analysis of RoPR indicates the increase is significantly greater for RBO100, RBO75, RBO50, and RBO25 in comparison with pure diesel. This disparity can be attributed to the shorter ignition delay exhibited by these RBO blends.

Lastly, the study continues with KI. An increase in the combustion temperature, the equivalency ratio has significantly increased, leading to an increase in the knocking intensity. This temperature increase occurred from 999 K at $\phi = 0.1$ to 2000 K at $\phi = 0.55$, observed in the direct injection CI engine across all fuel types (RBO00, RBO25, RBO50, RBO75, and RBO100). The observed KI was determined to be below the established threshold when the equivalency ratio was systematically varied within the range of 0.1 to 0.55. This observation indicates the presence of a stable combustion mode characterized by a controlled auto-ignition phenomenon. Once the equivalency ratio surpassed 0.55, the KI value increased took place from 5.62 MW/m2 at $\phi = 0.56$ to 9.8 MW/m2 at $\phi = 0.62$, beyond the established threshold. This observation implies that the combustion mode becomes unstable and experiences uncontrolled auto-ignition, resulting in extreme knocking. RBO25 demonstrated the lowest KI which is 5.1 MW/m^2 at equivalent ratio is 0.54 compared with other fuels. It led to the stable and complete combustion. This result suggested the existence of a stable combustion mode that is distinguished by a regulated auto-ignition occurrence.

UNIVERSITI MALAYSIA PAHANG AL-SULTAN ABDULLAH

CHAPTER 5

CONCLUSION

5.1 Introduction

This section aims to present a synopsis of the results reported in this thesis, and its focus will be on those outcomes. These observations are being made to expand new knowledge about the correlation between the physicochemical composition of the fuel, performance of the engine, combustion qualities, exhaust emissions characteristics, and knocking intensity on a KIPOR 170FS engine, which is a single-cylinder, four-stroke compression ignition engine that runs on pure diesel fuel and RBO blends. There are five fuel types involved in this study which are RBO00 (pure diesel), RBO25, RBO50, RBO75, RBO100 with different operating conditions (engine speed, engine load, intake air temperature). As a result, this chapter provides a concise summary of the findings obtained from the studies and some recommendations for future research in the applicable fields.

UMPSA
اونيۏرسيتي مليسيا ڤهڠ السلطان عبدالله
UNIVERSITI MALAYSIA PAHANG
AL-SULTAN ABDULLAH

5.2 Summary of Findings

The experimental findings align with the literature. The findings of the measurements of the physicochemical properties give a significant value for RBO blended in terms of density, KV, CV and CN. In general, RBO blended showed and indicated the improved physicochemical properties in terms of density, KV and its CN when compared with the pure diesel as a baseline. On the contrary, RBO blended resulted in lower CV than pure diesel which indicated the energy content in the fuel.

The experimental results on the engine performance of direct injection CI engine presented as improved when the engine fuelled with RBO blended. The BP of pure diesel fuel exhibits a comparatively higher increase in comparison to RBO blended. The experimental results demonstrated that in general, the engine operating with RBO and 45 °C intake air temperature produces higher BTE and higher BSFC (but still in optimal range 200 – 400 gkW/h) due to low energy content of RBO as compared to pure diesel. The NO_X emissions is slightly higher, but lower CO and HC are produced.

Then, the study on influence of RBO and intake air temperature on combustion behaviours of the direct injection CI engine can be summarized in this section. RBO blended achieved the high cylinder pressure in both half-load and full-load settings. When the engine is functioning at maximum efficiency, the cylinder pressure experiences an increase while the ignition delay is reduced. In addition, RBO blended resulted to greater maximum RoHR in comparison to pure diesel due to its high CN and oxygen content then led to rapid premixing process and a reduce ignition delay for absolute combustion.

Lastly, the observed KI was determined to be below the established threshold when the equivalency ratio was systematically varied within the range of 0.1 to 0.55. The RBO25 demonstrated the lowest KI of 5.1 MW/m^2, which is equivalent to 0.54 as compared to other fuels. As a result, the combustion was stable and complete. The results of this study suggest the existence of a stable combustion mode distinguished by regulated autoignitions.

In a nutshell, the experimental findings align with the literature. RBO has been identified as a promising option as an alternative fuel due to its extensive resource availability and high-performance standards.

UMPSA
اونيۏرسيتي مليسيا ڤهڠ السلطان عبدالله
UNIVERSITI MALAYSIA PAHANG
AL-SULTAN ABDULLAH

5.3 Recommendation for Future Work

From the results obtained on relative engine performance, combustion behaviour and emission investigations in this research, it was proven Rice Bran Oil (RBO) has been identified as promising candidates as alternative fuels due to their extensive resource availability and good performance qualities. However, more research into the dynamics of combustion using RBO as a fuel is required for optimal optimization:

- A viable approach for producing a mixture of RBO entails the inclusion of certain contaminants to maximise the efficiency of burning and fuel consumption.

- The utilisation of the Homogeneous Charge Compression Ignition (HCCI) engine in conjunction with Rice Bran Oil and other alternative fuels is proposed.

- Homogeneous Charge Compression Ignition (HCCI) engines are recommended in various engine modes.

- The introduction and utilisation of additives in RBO, when implemented in a CI engine and Homogeneous Charge Compression Ignition (HCCI) engine, is proposed.

- The integrating of Exhaust Gas Recirculation (EGR) in combination with alternative fuels in a Homogeneous Charge Compression Ignition (HCCI) engine to reduce exhaust emissions.

- The implementing of Catalytic Converter is a very effective technique for mitigating emissions without necessitating costly engine modification.

- The RBO has garnered significant interest due to its potential to lower the cost of biodiesel manufacturing. The estimated size of the RBO Market in 2024 is 532.67 million litres, with a projected increase to 714.18 million litres by 2029. This growth is anticipated to occur at a compound annual growth rate (CAGR) of 6.04% over the forecast period of 2024-2029. This demand emphasises the capacity of RBO as a substitute fuel in the transportation industry.

UMPSA
UNIVERSITI MALAYSIA PAHANG
AL-SULTAN ABDULLAH

UNIVERSITI MALAYSIA PAHANG AL-SULTAN ABDULLAH

REFERENCES

Abdalla, I. E. (2018). Experimental studies for the thermo-physiochemical properties of Biodiesel and its blends and the performance of such fuels in a Compression Ignition Engine. *Fuel, 212*, 638-655. doi:https://doi.org/10.1016/j.fuel.2017.10.064

Abdullah, B., Syed Muhammad, S. A. F. a., Shokravi, Z., Ismail, S., Kassim, K. A., Mahmood, A. N., & Aziz, M. M. A. (2019). Fourth generation biofuel: A review on risks and mitigation strategies. *Renewable and Sustainable Energy Reviews, 107*, 37-50. doi:https://doi.org/10.1016/j.rser.2019.02.018

Acharya , S., Mohanty (2010,). The use of rice bran oil as a fuel for a small horse-power diesel engine. . *Energy Sources,, Part A Recover Util Environ Eff 2010;* (33:80–8.). doi:https://doi.org/10.1080/15567030902967827

Adithyan, K. S., Edla, S., Thampi, A. D., Akhil Kumar, S., Sasidharan, B., Muhammed Arif, M., & Rani, S. (2023). Experimental investigation on the effects of clove oil as an anti-oxidant additive on the lubricant properties of transesterified rice bran oil. *Materials Today: Proceedings, 72*, 2892-2896. doi:https://doi.org/10.1016/j.matpr.2022.07.412

Aghbashlo, M., Peng, W., Tabatabaei, M., Kalogirou, S. A., Soltanian, S., Hosseinzadeh-Bandbafha, H., Lam, S. S. (2021). Machine learning technology in biodiesel research: A review. *Progress in Energy and Combustion Science, 85*, 100904. doi:https://doi.org/10.1016/j.pecs.2021.100904

Ali , S., De Poures, M. V., Damodharan, D., Gopal, K., Augustin, V. C., & Swaminathan, M. R. (2022). Prediction of emissions and performance of a diesel engine fueled with waste cooking oil and C8 oxygenate blends using response surface methodology. *Journal of Cleaner Production, 371*, 133323. doi:https://doi.org/10.1016/j.jclepro.2022.133323

Ali, S., Fazal, T., Javed, F., Hafeez, A., Akhtar, M., Haider, B., Rehman, F. (2020). Investigating biodiesel production strategies as a sustainable energy resource for Pakistan. *Journal of Cleaner Production, 259*, 120729. doi:https://doi.org/10.1016/j.jclepro.2020.120729

Altarazi, Y. S. M., Abu Talib, A. R., Yu, J., Gires, E., Abdul Ghafir, M. F., Lucas, J., & Yusaf, T. (2022). Effects of biofuel on engines performance and emission characteristics: A review. *Energy, 238*, 121910. doi:https://doi.org/10.1016/j.energy.2021.121910

Anilkumar Shere, K. A. S. (2022). Experimental investigation on effects of equivalence ratio on combustion with knock, performance, and emission characteristics of dimethyl ether fueled CRDI compression ignition engine under homogeneous

UNIVERSITI MALAYSIA PAHANG AL-SULTAN ABDULLAH

charge compression ignition mode. *Fuel 322 (2022) 124048*. doi:https://doi.org/10.1016/j.fuel.2022.124048

Asadi, A., Zhang, Y., Mohammadi, H., Khorand, H., Rui, Z., Doranehgard, M. H., & Bozorg, M. V. (2019). Combustion and emission characteristics of biomass derived biofuel, premixed in a diesel engine: A CFD study. *Renewable Energy, 138*, 79-89. doi:https://doi.org/10.1016/j.renene.2019.01.069

Ashok, B., Nanthagopal, K., Saravanan, B., Azad, K., Patel, D., Sudarshan, B., & Aaditya Ramasamy, R. (2019). Study on isobutanol and Calophyllum inophyllum biodiesel as a partial replacement in CI engine applications. *Fuel, 235*, 984-994. doi:https://doi.org/10.1016/j.fuel.2018.08.087

Asokan, M. A., Senthur Prabu, S. B., Pushpa, K. K., Nekkanti, Venkata Mukesh, & Gutta, S. S. G. (2019). Performance, combustion and emission characteristics of juliflora biodiesel fuelled DI diesel engine. *Energy, 173*, 883-892. doi:https://doi.org/10.1016/j.energy.2019.02.075

Atabani, A. E., Mofijur, M., Masjuki, H. H., Badruddin, I. A., Kalam, M. A., & Chong, W. T. (2014). Effect of Croton megalocarpus, Calophyllum inophyllum, Moringa oleifera, palm and coconut biodiesel–diesel blending on their physico-chemical properties. *Industrial Crops and Products, 60*, 130-137. doi:https://doi.org/10.1016/j.indcrop.2014.06.011

Atabani, A. E., Silitonga, A. S., Badruddin, I. A., Mahlia, T. M. I., Masjuki, H. H., & Mekhilef, S. (2012). A comprehensive review on biodiesel as an alternative energy resource and its characteristics. *Renewable and Sustainable Energy Reviews, 16*(4), 2070-2093. doi:https://doi.org/10.1016/j.rser.2012.01.003

Awad, O. I., Mamat, R., Ibrahim, T. K., Hagos, F. Y., Noor, M. M., Yusri, I. M., & Leman, A. M. (2017). Calorific value enhancement of fusel oil by moisture removal and its effect on the performance and combustion of a spark ignition engine. *Energy Conversion and Management, 137*, 86-96. doi:10.1016/j.enconman.2017.01.009

Bhattacharyya, P., Bisen, J., Bhaduri, D., Priyadarsini, S., Munda, S., Chakraborti, M., Nimbrayan, P. (2021). Turn the wheel from waste to wealth: Economic and environmental gain of sustainable rice straw management practices over field burning in reference to India. *Science of The Total Environment, 775*, 145896. doi:https://doi.org/10.1016/j.scitotenv.2021.145896

Birol, F. (2023). World Energy Outlook 2023 : Net Zero Roadmap. *International Energy Agency*.

Borman, G., & Nishiwaki, K. (1987). Internal combustion engine heat transfer. *Prog. Energy Combust. Sci., 133*, 1-46.

اونيۏرسيتي مليسيا ڤهڠ السلطان عبدالله
UNIVERSITI MALAYSIA PAHANG
AL-SULTAN ABDULLAH

Brahma, S., Basumatary, B., Basumatary, S. F., Das, B., Brahma, S., Rokhum, S. L., & Basumatary, S. (2023). Biodiesel production from quinary oil mixture using highly efficient Musa chinensis based heterogeneous catalyst. *Fuel, 336*, 127150. doi:https://doi.org/10.1016/j.fuel.2022.127150

Çalık, A. (2018). Determination of vibration characteristics of a compression ignition engine operated by hydrogen enriched diesel and biodiesel fuels. *Fuel, 230*, 355-358. doi:https://doi.org/10.1016/j.fuel.2018.05.053

Cao DN, H. A., Luu HQ, Bui VG, Tran TTH. . (2020). Effects of injection pressure on the NOx and PM emission control of diesel engine: a review under the aspect of PCCI combustion condition. *Energy Sources, Part A Recover Util Environ Eff 2020. https://doi.org/10.1080/15567036.2020.1754531*.

Cengel, Y., & Boles, M. (2006). Thermodynamics: an engineering approach, edition 5: Tata McGraw-Hill Publishing Company Limited, New Delhi.

Chakraborty, R., & Mukhopadhyay, P. (2019). Green Fuel Blending: A Pollution Reduction Approach *Reference Module in Materials Science and Materials Engineering*: Elsevier.

Charoonratana, T. (2020). Chapter 36 - Cold pressed rice (Oryza sativa) bran oil. In M. F. Ramadan (Ed.), *Cold Pressed Oils* (pp. 391-403): Academic Press.

Chatur, M. G., Maheshwari, A., & Jee Kanu, N. (2023). Comprehensive analysis of the behavior of waste cooking oil biodiesel in C.I. Engines modified using CuO nanoparticles with varying fuel injection pressure. *Materials Today: Proceedings*. doi:https://doi.org/10.1016/j.matpr.2023.03.620

اونيۏرسيتي مليسيا قهڠ السلطان عبدالله
UNIVERSITI MALAYSIA PAHANG
AL-SULTAN ABDULLAH

Chen, A. F., Akmal Adzmi, M., Adam, A., Othman, M. F., Kamaruzzaman, M. K., & Mrwan, A. G. (2018). Combustion characteristics, engine performances and emissions of a diesel engine using nanoparticle-diesel fuel blends with aluminium oxide, carbon nanotubes and silicon oxide. *Energy Conversion and Management, 171*, 461-477. doi:https://doi.org/10.1016/j.enconman.2018.06.004

Chong, C. T., Loe, T. Y., Wong, K. Y., Ashokkumar, V., Lam, S. S., Chong, W. T., Ng, J.-H. (2021). Biodiesel sustainability: The global impact of potential biodiesel production on the energy–water–food (EWF) nexus. *Environmental Technology & Innovation, 22*, 101408. doi:https://doi.org/10.1016/j.eti.2021.101408

Constantino, A. F., Cubides-Román, D. C., dos Santos, R. B., Queiroz, L. H. K., Colnago, L. A., Neto, Á. C., Lacerda, V. (2019). Determination of physicochemical properties of biodiesel and blends using low-field NMR and multivariate calibration. *Fuel, 237*, 745-752. doi:https://doi.org/10.1016/j.fuel.2018.10.045

Dabi, M., & Saha, U. K. (2019). Application potential of vegetable oils as alternative to diesel fuels in compression ignition engines: A review. *Journal of the Energy Institute, 92*(6), 1710-1726. doi:https://doi.org/10.1016/j.joei.2019.01.003

Dabi, M., & Saha, U. K. (2022). Performance, combustion and emissions analyses of a single-cylinder stationary compression ignition engine powered by Mesua Ferrea Linn oil-ethanol-diesel blend. *Cleaner Engineering and Technology, 8*, 100458. doi:https://doi.org/10.1016/j.clet.2022.100458

Das, K. C., Mohanty, S., Sahoo, P. K., Sahoo, S., Prakash, B., & Swain, P. (2022). Inclusion of different levels of solid-state fermented mahua oil cake on growth, digestibility and immunological parameters of rohu (Labeo rohita). *Aquaculture, 553*, 738049. doi:https://doi.org/10.1016/j.aquaculture.2022.738049

Dernotte J, D. J., Ji C. . (2014). Investigation of the Sources of Combustion Noise in HCCI Engines. *SAE Int J Eng . 7:730–61*. doi:https://doi.org/10.4271/2014-01-1272.

Devarajan, Y., Munuswamy, D. B., Subbiah, G., Vellaiyan, S., Nagappan, B., Varuvel, E. G., & Thangaraja, J. (2022). Inedible oil feedstocks for biodiesel production: A review of production technologies and physicochemical properties. *Sustainable Chemistry and Pharmacy, 30*, 100840. doi:https://doi.org/10.1016/j.scp.2022.100840

Dharma, S., Hassan, M. H., Ong, H. C., Sebayang, A. H., Silitonga, A. S., Kusumo, F., & Milano, J. (2017). Experimental study and prediction of the performance and exhaust emissions of mixed Jatropha curcas-Ceiba pentandra biodiesel blends in diesel engine using artificial neural networks. *Journal of Cleaner Production, 164*, 618-633. doi:https://doi.org/10.1016/j.jclepro.2017.06.065

Dharmaraja, J., Nguyen, D. D., Shobana, S., Saratale, G. D., Arvindnarayan, S., Atabani, A. E., Kumar, G. (2019). Engine performance, emission and bio characteristics of rice bran oil derived biodiesel blends. *Fuel, 239*, 153-161. doi:https://doi.org/10.1016/j.fuel.2018.10.123

El-Seesy, A. I., & Hassan, H. (2019). Investigation of the effect of adding graphene oxide, graphene nanoplatelet, and multiwalled carbon nanotube additives with n-butanol-Jatropha methyl ester on a diesel engine performance. *Renewable Energy, 132*, 558-574. doi:https://doi.org/10.1016/j.renene.2018.08.026

Fan, Y., Yang, L., Yin, C., Song, S., Wang, D., Zhang, Y., & Liu, X. (2022). Tribological properties and damage behavior of brown rice based on milling process. *Tribology International, 167*, 107353. doi:https://doi.org/10.1016/j.triboint.2021.107353

Fu, J., & Turn, S. Q. (2019). Characteristics and stability of biofuels used as drop-in replacement for NATO marine diesel. *Fuel, 236*, 516-524. doi:https://doi.org/10.1016/j.fuel.2018.09.042

UMPSA
UNIVERSITI MALAYSIA PAHANG
AL-SULTAN ABDULLAH

Gülüm, M. (2022). Effects of compression ratio, blending ratio and engine speed on fuel cost, performance and exhaust emissions of a diesel engine fueled with bio-derived alternative fuels. *Sustainable Energy Technologies and Assessments, 53*, 102464. doi:https://doi.org/10.1016/j.seta.2022.102464

Guo, M., & Song, W. (2019). The growing U.S. bioeconomy: Drivers, development and constraints. *New Biotechnology*, *49*, 48-57. doi:https://doi.org/10.1016/j.nbt.2018.08.005

Hasan, W., Kafy (2014). Prospect of rice bran for biodiesel production in Bangladesh. *Procedia Eng, 90:746–52*. doi:https://doi.org/10.1016/j.proeng.2014.11.808

He, D., & Liu, L. (2019). Chapter 7 - Analytical Aspects of Rice Bran Oil. In L.-Z. Cheong & X. Xu (Eds.), *Rice Bran and Rice Bran Oil* (pp. 169-181): AOCS Press.

Hellier, P., Jamil, F., Zaglis-Tyraskis, E., Al-Muhtaseb, A. a. H., Al Haj, L., & Ladommatos, N. (2019). Combustion and emissions characteristics of date pit methyl ester in a single cylinder direct injection diesel engine. *Fuel*, *243*, 162-171. doi:https://doi.org/10.1016/j.fuel.2019.01.022

Heywood. (1988). *Internal Combustion Engine* (Vol. 21). New York: McGraw-Hill, Inc.

Hirner, F. S., Hwang, J., Bae, C., Patel, C., Gupta, T., & Agarwal, A. K. (2019). Nanostructure characterization of soot particles from biodiesel and diesel spray flame in a constant volume combustion chamber. *Fuel, 235*, 130-149. doi:https://doi.org/10.1016/j.fuel.2018.07.092

Hoang, A. T. (2021). Combustion behavior, performance and emission characteristics of diesel engine fuelled with biodiesel containing cerium oxide nanoparticles: A review. *Fuel Processing Technology, 218*, 106840. doi:https://doi.org/10.1016/j.fuproc.2021.106840

Hoang AT, L. A., Pham VV. (2019). A core correlation of spray characteristics, deposit formation, and combustion of a high-speed diesel engine fueled with Jatropha oil and diesel fuel. *Fuel 2019;244:159–75.*

Hoang, A. T., Tabatabaei, M., Aghbashlo, M., Carlucci, A. P., Ölçer, A. I., Le, A. T., & Ghassemi, A. (2021). Rice bran oil-based biodiesel as a promising renewable fuel alternative to petrodiesel: A review. *Renewable and Sustainable Energy Reviews*, *135*, 110204. doi:https://doi.org/10.1016/j.rser.2020.110204

Hoekman, S. K., & Broch, A. (2018). Environmental implications of higher ethanol production and use in the U.S.: A literature review. Part II – Biodiversity, land use change, GHG emissions, and sustainability. *Renewable and Sustainable Energy Reviews, 81*, 3159-3177. doi:https://doi.org/10.1016/j.rser.2017.05.052

اونيۏرسيتي مليسيا ڤهڠ السلطان عبدالله
UNIVERSITI MALAYSIA PAHANG
AL-SULTAN ABDULLAH

Ijaz, U., Nadeem, H. U., Shafique, A., Rasheed, A., Batool, R., & Azeem, F. (2021). Chapter 1 - Rice bran composition and its emerging potential applications. In Inamuddin, R. Boddula, & A. M. Asiri (Eds.), *Green Sustainable Process for Chemical and Environmental Engineering and Science* (pp. 1-16): Elsevier.

Jayaraman, J., Arunkumar, T., Senthil Kumar, P., Mariadhas, A., Appavu, P., & Rangasamy, G. (2023). Performance analysis on a compression ignition engine fueled with algae, rice bran methyl esters, and their diesel blends at optimized blend proportion, injection timing and load. *Fuel, 344*, 128024. doi:https://doi.org/10.1016/j.fuel.2023.128024

Jayaraman, J., Dawn, S. S., Appavu, P., Mariadhas, A., Joy, N., Alshgari, R. A., Kumar, J. A. (2022). Production of biodiesel from waste cooking oil utilizing zinc oxide nanoparticles combined with tungsto phosphoric acid as a catalyst and its performance on a CI engine. *Fuel, 329*, 125411. doi:https://doi.org/10.1016/j.fuel.2022.125411

Jeyaseelan, T., Chacko, N., N, P., O, S. M. K., Alexander, J., & Porpatham, E. (2021). Partial hydrogenation and hydrogen induction: A comparative study with B20 operation in a turbocharged CRDI diesel engine. *International Journal of Hydrogen Energy, 46*(43), 22659-22669. doi:https://doi.org/10.1016/j.ijhydene.2021.04.068

Kale, B. N., & Patle, S. D. (2022). State of art review of algal biodiesel and its blends influence on performance and emission characteristics of compression ignition engine. *Cleaner Engineering and Technology, 7*, 100431. doi:https://doi.org/10.1016/j.clet.2022.100431

Kannan, C., & Vijayakumar, T. (2022). Chapter 7 - Application of exhaust gas recirculation for NOx reduction in CI engines. In B. Ashok (Ed.), *NOx Emission Control Technologies in Stationary and Automotive Internal Combustion Engines* (pp. 189-222): Elsevier.

Karmakar, B., & Halder, G. (2019). Progress and future of biodiesel synthesis: Advancements in oil extraction and conversion technologies. *Energy Conversion and Management, 182*, 307-339. doi:https://doi.org/10.1016/j.enconman.2018.12.066

Kothiyal, N. C., Kumar, V., Kumar, N., Saruchi, Pandey, S., & Ansar, S. (2022). Reduction of carcinogenic PAHs from petrodiesel engine exhaust by blending of green diesel (A new development in renewable fuels) with different biodiesel fuels. *Environmental Technology & Innovation, 25*, 102089. doi:https://doi.org/10.1016/j.eti.2021.102089

Krieger, F. J. (1994). Chemical Kinetics and Rocket Nozzle Design. *Journal of the American Rocket Society, 21*(6), 179-185. doi:10.2514/8.4394

UMPSA
UNIVERSITI MALAYSIA PAHANG
AL-SULTAN ABDULLAH

Krishana, K., Shashi Kanth, M., Maneiah, D., Prem Kumar, B. S., Kumar Reddy, K. V., & Raji Reddy, A. (2022). CFD analysis of karanja oil methyl ester (KOME) blend B20 and hydrogen using ANSYS-Fluent. *Materials Today: Proceedings*. doi:https://doi.org/10.1016/j.matpr.2022.11.156

Kumar Karedla, A., Surya Raj, R., Krishnamoorthy, S. V., Suganthi, A., Bhuvaneswari, K., Karthikeyan, S.,Jeyarajan Nelson, S. (2024). Validation, dissipation kinetics and monitoring of flonicamid and dinotefuran residues in paddy grain, straw, its processed produces and bran oil using LC-MS/MS. *Food Chemistry, 435*, 137589. doi:https://doi.org/10.1016/j.foodchem.2023.137589

Kumar, S., & Goga, G. (2023). Review analysis on the performance & emission characteristics of a diesel engine fuelled with various gaseous & bio fuels. *Materials Today: Proceedings, 80*, 285-292. doi:https://doi.org/10.1016/j.matpr.2023.01.189

Lee, S., Lee, C. S., Park, S., Gupta, J. G., Maurya, R. K., & Agarwal, A. K. (2017). Spray characteristics, engine performance and emissions analysis for Karanja biodiesel and its blends. *Energy, 119*, 138-151. doi:https://doi.org/10.1016/j.energy.2016.12.043

Li, H., Xu, M., Yao, X., Wen, Y., Lu, S., Wang, J., & Sun, B. (2022). The promoted hydrolysis effect of cellulase with ultrasound treatment is reflected on the sonicated rather than native brown rice. *Ultrasonics Sonochemistry, 83*, 105920. doi:https://doi.org/10.1016/j.ultsonch.2022.105920

Li, R., & Wang, Z. (2018). Study on status characteristics and oxidation reactivity of biodiesel particulate matter. *Fuel, 218*, 218-226. doi:https://doi.org/10.1016/j.fuel.2018.01.041

Lilly, L. C. R. (1984). *Diesel Engine Reference Book*. London: Butterworths.

Loh, S. K., Nasrin, A. B., Mohamad Azri, S., Nurul Adela, B., Muzzammil, N., Daryl Jay, T., Kaltschmitt, M. (2017). First Report on Malaysia's experiences and development in biogas capture and utilization from palm oil mill effluent under the Economic Transformation Programme: Current and future perspectives. *Renewable and Sustainable Energy Reviews, 74*, 1257-1274. doi:https://doi.org/10.1016/j.rser.2017.02.066

M.D. Checkel, J. D. D. (1986). Computerized knock detection from engine pressure records, . *SAE Technical Papers, https://doi.org/10.4271/860028.*

Mahmudul, H. M., Hagos, F. Y., Mamat, R., Adam, A. A., Ishak, W. F. W., & Alenezi, R. (2017). Production, characterization and performance of biodiesel as an alternative fuel in diesel engines – A review. *Renewable and Sustainable Energy Reviews, 72*, 497-509. doi:https://doi.org/10.1016/j.rser.2017.01.001

UMPSA
اونيۈرسيتي مليسيا ڤهڠ السلطان عبدالله
UNIVERSITI MALAYSIA PAHANG
AL-SULTAN ABDULLAH

Mathew, G. M., Raina, D., Narisetty, V., Kumar, V., Saran, S., Pugazhendi, A., Binod, P. (2021). Recent advances in biodiesel production: Challenges and solutions. *Science of The Total Environment, 794*, 148751. doi:https://doi.org/10.1016/j.scitotenv.2021.148751

Mathias, M. G., Okajima, I., Aoki, Y., Kong, C. Y., Itika, A., Elisante, E., & Sako, T. (2024). Extraction of high-quality rice bran oil with CO2-expanded acetone for biofuel production. *Fuel, 356*, 129491. doi:https://doi.org/10.1016/j.fuel.2023.129491

Mazaheri, H., Ong, H. C., Masjuki, H. H., Amini, Z., Harrison, M. D., Wang, C.-T., Alwi, A. (2018). Rice bran oil based biodiesel production using calcium oxide catalyst derived from Chicoreus brunneus shell. *Energy, 144*, 10-19. doi:https://doi.org/10.1016/j.energy.2017.11.073

Milano, J., Ong, H. C., Masjuki, H. H., Silitonga, A. S., Kusumo, F., Dharma, S., Wang, C.-T. (2018). Physicochemical property enhancement of biodiesel synthesis from hybrid feedstocks of waste cooking vegetable oil and Beauty leaf oil through optimized alkaline-catalysed transesterification. *Waste Management, 80*, 435-449. doi:https://doi.org/10.1016/j.wasman.2018.09.005

Ming, C., Rizwanul Fattah, I. M., Chan, Q. N., Pham, P. X., Medwell, P. R., Kook, S., Masri, A. R. (2018). Combustion characterization of waste cooking oil and canola oil based biodiesels under simulated engine conditions. *Fuel, 224*, 167-177. doi:https://doi.org/10.1016/j.fuel.2018.03.053

Mirhashemi, F. S., & Sadrnia, H. (2020). NOX emissions of compression ignition engines fueled with various biodiesel blends: A review. *Journal of the Energy Institute, 93*(1), 129-151. doi:https://doi.org/10.1016/j.joei.2019.04.003

Mobarak, H. M., Niza, E. M., H.H.Masjuki, M.A.Kalam, Muhmud, K. A. H. A., M.Habibullah, & Ashraful, A. M. (2014). The prospects of biolubricants as alternatives in automotive applications. *Renewable and Sustainable Energy Reviews, 33*, 34-43.

Moreira, B. P., Draszewski, C. P., Rosa, N. C., Tres, M. V., Zabot, G. L., Pereira, F. C., Castilhos, F. (2023). Integrated rice bran processing by supercritical CO2 extraction and subcritical water hydrolysis to obtain oil, fermentable sugars, and platform chemicals. *The Journal of Supercritical Fluids, 192*, 105786. doi:https://doi.org/10.1016/j.supflu.2022.105786

Muhammed Niyas, M., & Shaija, A. (2022). Performance evaluation of diesel engine using biodiesels from waste coconut, sunflower, and palm cooking oils, and their hybrids. *Sustainable Energy Technologies and Assessments, 53*, 102681. doi:https://doi.org/10.1016/j.seta.2022.102681

Nanthagopal, K., Ashok, B., Saravanan, B., Ramesh Pathy, M., Sahil, G., Ramesh, A., Golam Rasul, M. (2019). Study on decanol and Calophyllum Inophyllum

UMPSA
UNIVERSITI MALAYSIA PAHANG
AL-SULTAN ABDULLAH

biodiesel as ternary blends in CI engine. *Fuel, 239*, 862-873. doi:https://doi.org/10.1016/j.fuel.2018.11.037

Nayak, S. K., & Mishra, P. C. (2017). Application of neem biodiesel and dimethyl carbonate as alternative fuels. *Energy Sources, Part A: Recovery, Utilization and Environmental Effects, 39*(3), 284-290. doi:10.1080/15567036.2015.1062828

Nema, V. K., Singh, A., Chaurasiya, P. K., Gogoi, T. K., Verma, T. N., & Tiwari, D. (2022). Combustion, performance, and emission behavior of a CI engine fueled with different biodiesels: A modelling, forecasting and experimental study. *Fuel*, 126976. doi:https://doi.org/10.1016/j.fuel.2022.126976

Nguyen, D. D., Dharmaraja, J., Shobana, S., Sundaram, A., Chang, S. W., Kumar, G., Saratale, G. D. (2019). Transesterification and fuel characterization of rice bran oil: A biorefinery path. *Fuel, 253*, 975-987. doi:https://doi.org/10.1016/j.fuel.2019.05.063

Pal, A., & Das, C. (2022). New eco-friendly anti-corrosion inhibitor of purple rice bran extract for boiler quality steel: Experimental and theoretical investigations. *Journal of Molecular Structure, 1251*, 131988. doi:https://doi.org/10.1016/j.molstruc.2021.131988

Pal, P. (2017). Rice bran oil: a versatile source for edible and industrial applications. *J Oleo Sci 66*(551), 6.

Perumalla Vijaya, K., Ashok, B., kumar, M. S., Vignesh, R., Bhasker, J. P., & Kumar, A. N. (2022). Evaluation of performance, emissions and combustion attributes of CI engine using palmyra biodiesel blend with distinct compression ratios, EGR rates and nano-particles. *Fuel, 321*, 124092. doi:https://doi.org/10.1016/j.fuel.2022.124092

Pham, M. T., Hoang, A. T., Le, A. T., Said Al-Tawaha, A. R. M., Dong, V. H., & Le, V. V. (2018). Measurement and prediction of the density and viscosity of biodiesel blends. *International Journal of Technology, 9*(5), 1015-1026. doi:10.14716/ijtech.v9i5.1950

Pierce, D., Haynes, A., Hughes, J., Graves, R., Maziasz, P., Muralidharan, G., Daniel, C. (2019). High temperature materials for heavy duty diesel engines: Historical and future trends. *Progress in Materials Science, 103*, 109-179. doi:https://doi.org/10.1016/j.pmatsci.2018.10.004

Pradeep Kumar Vishnoi, P. S. G., V.K. Gupta. (2022). The impact on combustion knock in CI engine fueled with methanol-diesel-n-pentanol ternary blends. *Material Today (Proceeding), 52 (2022) 1062-1067.*

Praveena, V., Shobana Bai, F. J. J., Balasubramanian, D., Devarajan, Y., Aloui, F., & Varuvel, E. G. (2023). Experimental assessment on the performance, emission

UNIVERSITI MALAYSIA PAHANG AL-SULTAN ABDULLAH

and combustion characteristics of a safflower oil fueled CI engine with hydrogen gas enrichment. *Fuel, 334*, 126682. doi:https://doi.org/10.1016/j.fuel.2022.126682

Pulkrabek, W. W. (2004). *Engineering fundamentals of the internal combustion engine* (2 ed.): Pearson Prentice Hall New Jersey.

Pulkrabek, W. W. (2014). *Engineering fundamentals of the internal combustion engine*: Pearson Prentice Hall Upper Saddle River, NJ.

Puricelli, S., Cardellini, G., Casadei, S., Faedo, D., van den Oever, A. E. M., & Grosso, M. (2021). A review on biofuels for light-duty vehicles in Europe. *Renewable and Sustainable Energy Reviews, 137*, 110398. doi:https://doi.org/10.1016/j.rser.2020.110398

Rahman, S. M. A., Van, T. C., Hossain, F. M., Jafari, M., Dowell, A., Islam, M. A., Brown, R. J. (2019). Fuel properties and emission characteristics of essential oil blends in a compression ignition engine. *Fuel, 238*, 440-453. doi:https://doi.org/10.1016/j.fuel.2018.10.136

Rajak, U., & Verma, T. N. (2019). A comparative analysis of engine characteristics from various biodiesels: Numerical study. *Energy Conversion and Management, 180*, 904-923. doi:https://doi.org/10.1016/j.enconman.2018.11.044

Rajan, K., Sujith, V., Ganesan, M., Peer Haroon, M., Mathivanan, S. D., & Elumalai, R. (2020). Performance and emissions characteristics of DI diesel engine using biodiesel blend with different injection pressures. *Materials Today: Proceedings, 33*, 4699-4702. doi:https://doi.org/10.1016/j.matpr.2020.08.348

UMPSA
UNIVERSITI MALAYSIA PAHANG
AL-SULTAN ABDULLAH

Rajasekar, E., & Selvi, S. (2014). Review of combustion characteristics of CI engines fueled with biodiesel. *Renewable and Sustainable Energy Reviews, 35*, 390-399. doi:https://doi.org/10.1016/j.rser.2014.04.006

Raju, V. D., Venu, H., Subramani, L., Kishore, P. S., Prasanna, P. L., & Kumar, D. V. (2020). An experimental assessment of prospective oxygenated additives on the diverse characteristics of diesel engine powered with waste tamarind biodiesel. *Energy, 203*, 117821. doi:https://doi.org/10.1016/j.energy.2020.117821

Ramachandran, B., Solomon, R., Sangwan, P., Edwin Samuel, C., Fernandez-Gamiz, U., Santra, S. S., Govindan, V. (2023). An experimental analysis on performance of tobacco seed oil as an alternative fuel for diesel engine. *Alexandria Engineering Journal, 80*, 408-416. doi:https://doi.org/10.1016/j.aej.2023.08.070

Safarov, J., Ashurova, U., Ahmadov, B., Abdullayev, E., Shahverdiyev, A., & Hassel, E. (2018). Thermophysical properties of Diesel fuel over a wide range of temperatures and pressures. *Fuel, 216*, 870-889. doi:https://doi.org/10.1016/j.fuel.2017.11.125

Sahini, M. G., & Mutegoa, E. (2023). Extraction, phytochemistry, nutritional, and therapeutical potentials of rice bran oil: A review. *Phytomedicine Plus, 3*(2), 100453. doi:https://doi.org/10.1016/j.phyplu.2023.100453

Saikia, S., & Dutta, H. (2022). Chapter 13 - Gamma oryzanol. In J. Kour & G. A. Nayik (Eds.), *Nutraceuticals and Health Care* (pp. 245-257): Academic Press.

Sajeevan, A. C., & Sajith, V. (2016). Synthesis of stable cerium zirconium oxide nanoparticle – Diesel suspension and investigation of its effects on diesel properties and smoke. *Fuel, 183*, 155-163. doi:https://doi.org/10.1016/j.fuel.2016.06.048

Sajjad, M. O. A., Sathish, T., Saravanan, R., Asif, M., Linul, E., & Ağbulut, Ü. (2023). Combustion, performance and emission discussion of soapberry seed oil methyl ester blends and exhaust gas recirculation in common rail direct fuel injection system. *Energy, 278*, 127763. doi:https://doi.org/10.1016/j.energy.2023.127763

Sakthivadivel, D., Ganesh Kumar, P., Prabakaran, R., Vigneswaran, V. S., Nithyanandhan, K., & Kim, S. C. (2022). A neem oil-based biodiesel with DEE enriched ethanol and Al2O3 nano additive: An experimental investigation on the diesel engine performance. *Case Studies in Thermal Engineering, 34*, 102021. doi:https://doi.org/10.1016/j.csite.2022.102021

Sathish Kumar, T., Vignesh, R., Ashok, B., Saiteja, P., Jacob, A., Karthick, C., Muhammad Usman, K. (2022). Application of statistical approaches in IC engine calibration to enhance the performance and emission Characteristics: A methodological review. *Fuel, 324*, 124607. doi:https://doi.org/10.1016/j.fuel.2022.124607

Sebayang, A. H., Kusumo, F., Milano, J., Shamsuddin, A. H., Silitonga, A. S., Ideris, F., Reen Chia, S. (2023). Optimization of biodiesel production from rice bran oil by ultrasound and infrared radiation using ANN-GWO. *Fuel, 346*, 128404. doi:https://doi.org/10.1016/j.fuel.2023.128404

Sharkey, J. P. (1997). *Diesel Engine Analysis Guide*. Retrieved from California:

Sharma, A., & Murugan, S. (2017). Effect of blending waste tyre derived fuel on oxidation stability of biodiesel and performance and emission studies of a diesel engine. *Applied Thermal Engineering, 118*, 365-374. doi:http://dx.doi.org/10.1016/j.applthermaleng.2017.03.008

Silitonga, A. S., Masjuki, H. H., Ong, H. C., Sebayang, A. H., Dharma, S., Kusumo, F., Sugiyanto, B. (2018). Evaluation of the engine performance and exhaust emissions of biodiesel-bioethanol-diesel blends using kernel-based extreme learning machine. *Energy, 159*, 1075-1087. doi:https://doi.org/10.1016/j.energy.2018.06.202

اونيۏرسيتي مليسيا قهڠ السلطان عبدالله
UMPSA
UNIVERSITI MALAYSIA PAHANG
AL-SULTAN ABDULLAH

Singh, A., Singhania, R. R., Soam, S., Chen, C.-W., Haldar, D., Varjani, S., Patel, A. K. (2022). Production of bioethanol from food waste: Status and perspectives. *Bioresource Technology*, *360*, 127651. doi:https://doi.org/10.1016/j.biortech.2022.127651

Singh, A. P., & Agarwal, A. K. (2016). Effect of Intake Charge Temperature and EGR on Biodiesel Fuelled HCCI Engine. *SAE Technical Papers, 2016-February*(February). doi:10.4271/2016-28-0257

Singh, R., Langyan, S., Rohtagi, B., Darjee, S., Khandelwal, A., Shrivastava, M., Singh, A. (2022). Production of biofuels options by contribution of effective and suitable enzymes: Technological developments and challenges. *Materials Science for Energy Technologies, 5*, 294-310. doi:https://doi.org/10.1016/j.mset.2022.05.001

Soares, N., Martins, A. G., Carvalho, A. L., Caldeira, C., Du, C., Castanheira, É., Garcia, R. (2018). The challenging paradigm of interrelated energy systems towards a more sustainable future. *Renewable and Sustainable Energy Reviews, 95*, 171-193. doi:https://doi.org/10.1016/j.rser.2018.07.023

Srivastava, R. K., Nedungadi, S. V., Akhtar, N., Sarangi, P. K., Subudhi, S., Shadangi, K. P., & Govarthanan, M. (2023). Effective hydrolysis for waste plant biomass impacts sustainable fuel and reduced air pollution generation: A comprehensive review. *Science of The Total Environment, 859*, 160260. doi:https://doi.org/10.1016/j.scitotenv.2022.160260

Stone, R. (1999). *Introduction to internal combustion engines* (3rd ed.). Chippenham, Wiltshire: Antony Rowe Ltd.

Sun, W., Wang, Q., Guo, L., Cheng, P., Li, D., & Yan, Y. (2019). Influence of biodiesel/diesel blends on particle size distribution of CI engine under steady/transient conditions. *Fuel, 245*, 336-344. doi:https://doi.org/10.1016/j.fuel.2019.01.101

Surya Kanth, T. A., Sumita Debbarma, Biplab Das. (2021). Effect of fuel opening injection pressure and injection timing of hydrogen enriched rice bran biodiesel fuelled in CI engine. *International Journal of Hydrogen Energy 46 (2021) 28789 - 28800.*

Takeda, K., Takashi, S., Yoshida, Y., Lin, Z., Iijima, A., & Shoji, H. (2016). A Study on the Knocking Characteristics of an SI-HCCI Engine by Using In-Cylinder Visualization. *SAE Technical Papers, 2016-November*(November). doi:10.4271/2016-32-0005

Teoh, Y. H., How, H. G., Masjuki, H. H., Nguyen, H. T., Kalam, M. A., & Alabdulkarem, A. (2019). Investigation on particulate emissions and combustion characteristics of a common-rail diesel engine fueled with Moringa

UMPSA
اونيۏرسيتي مليسيا ڤهڠ السلطان عبدالله
UNIVERSITI MALAYSIA PAHANG
AL-SULTAN ABDULLAH

oleifera biodiesel-diesel blends. *Renewable Energy, 136*, 521-534. doi:https://doi.org/10.1016/j.renene.2018.12.110

Torres-Mayanga, P. C., Lachos-Perez, D., Mudhoo, A., Kumar, S., Brown, A. B., Tyufekchiev, M., Forster-Carneiro, T. (2019). Production of biofuel precursors and value-added chemicals from hydrolysates resulting from hydrothermal processing of biomass: A review. *Biomass and Bioenergy, 130*, 105397. doi:https://doi.org/10.1016/j.biombioe.2019.105397

Trivedi, T., Jain, D., Mulla, N. S. S., Mamatha, S. S., Damare, S. R., Sreepada, R. A., Gupta, V. (2019). Improvement in biomass, lipid production and biodiesel properties of a euryhaline Chlorella vulgaris NIOCCV on mixotrophic cultivation in wastewater from a fish processing plant. *Renewable Energy, 139*, 326-335. doi:https://doi.org/10.1016/j.renene.2019.02.065

Tsiligiannis, A., & Tsiliyannis, C. (2019). Renewable energy in cement manufacturing: A quantitative assessment of energy and environmental efficiency of food residue biofuels. *Renewable and Sustainable Energy Reviews, 107*, 568-586. doi:https://doi.org/10.1016/j.rser.2019.03.009

U.S. Department of Energy. (accessed 19.04.2016). Alternative fuel vehicle in use. Retrieved from http://www.afdc.energy.gov/data/10300

Uyumaz, A. (2020). Experimental evaluation of linseed oil biodiesel/diesel fuel blends on combustion, performance and emission characteristics in a DI diesel engine. *Fuel, 267*, 117150. doi:https://doi.org/10.1016/j.fuel.2020.117150

Uyumaz, A., Aydoğan, B., Yılmaz, E., Solmaz, H., Aksoy, F., Mutlu, İ., Calam, A. (2020). Experimental investigation on the combustion, performance and exhaust emission characteristics of poppy oil biodiesel-diesel dual fuel combustion in a CI engine. *Fuel, 280*, 118588. doi:https://doi.org/10.1016/j.fuel.2020.118588

Venu, H., Raju, V. D., Subramani, L., & Appavu, P. (2020). Experimental assessment on the regulated and unregulated emissions of DI diesel engine fuelled with Chlorella emersonii methyl ester (CEME). *Renewable Energy, 151*, 88-102. doi:https://doi.org/10.1016/j.renene.2019.11.010

Verma, T. N., Shrivastava, P., Rajak, U., Dwivedi, G., Jain, S., Zare, A., Verma, P. (2021). A comprehensive review of the influence of physicochemical properties of biodiesel on combustion characteristics, engine performance and emissions. *Journal of Traffic and Transportation Engineering (English Edition), 8*(4), 510-533. doi:https://doi.org/10.1016/j.jtte.2021.04.006

Veza, I., Afzal, A., Mujtaba, M. A., Tuan Hoang, A., Balasubramanian, D., Sekar, M., Tamaldin, N. (2022). Review of artificial neural networks for gasoline, diesel and homogeneous charge compression ignition engine. *Alexandria Engineering Journal, 61*(11), 8363-8391. doi:https://doi.org/10.1016/j.aej.2022.01.072

UMPSA
UNIVERSITI MALAYSIA PAHANG
AL-SULTAN ABDULLAH

Wancura, J. H. C., Brondani, M., Vezaro, F. D., Martins-Vieira, J. C., Moreira, B. P., dos Santos, M. S. N., Mayer, F. D. (2023). Motivations to produce biofuels from rice bran: An overview involving a recent panorama. *Industrial Crops and Products, 203*, 117170. doi:https://doi.org/10.1016/j.indcrop.2023.117170

Xiao, H., Yang, X., Hou, B., Wang, R., Xue, Q., & Ju, H. (2019). Combustion performance and pollutant emissions analysis of a diesel engine fueled with biodiesel and its blend with 2-methylfuran. *Fuel, 237*, 1050-1056. doi:https://doi.org/10.1016/j.fuel.2018.09.146

Xu, D., Hao, J., Wang, Z., Liang, D., Wang, J., Ma, Y., & Zhang, M. (2021). Physicochemical properties, fatty acid compositions, bioactive compounds, antioxidant activity and thermal behavior of rice bran oil obtained with aqueous enzymatic extraction. *LWT, 149*, 111817. doi:https://doi.org/10.1016/j.lwt.2021.111817

Xu, Z., Jia, M., Li, Y., Chang, Y., Xu, G., Xu, L., & Lu, X. (2018). Computational optimization of fuel supply, syngas composition, and intake conditions for a syngas/diesel RCCI engine. *Fuel, 234*, 120-134. doi:https://doi.org/10.1016/j.fuel.2018.07.003

Yao, P., He, J., Jiang, X., Jiao, Y., Wang, J., & Chen, Y. (2019). Factors determining gasoline soot abatement over CeO2-ZrO2-MnOx catalysts under low oxygen concentration condition. *Journal of the Energy Institute*. doi:https://doi.org/10.1016/j.joei.2019.05.005

Ye, L., Xie, F., Hong, J., Yang, D., Ma, X., & Li, X. (2018). Environmental burden mitigation potential of oil field gas-assisted coal-to-olefin production. *Energy, 157*, 1015-1024. doi:https://doi.org/10.1016/j.energy.2018.05.167

Yesilyurt, M. K. (2020). A detailed investigation on the performance, combustion, and exhaust emission characteristics of a diesel engine running on the blend of diesel fuel, biodiesel and 1-heptanol (C7 alcohol) as a next-generation higher alcohol. *Fuel, 275*, 117893. doi:https://doi.org/10.1016/j.fuel.2020.117893

Yilmaz, I. T., & Gumus, M. (2018). Effects of hydrogen addition to the intake air on performance and emissions of common rail diesel engine. *Energy, 142*, 1104-1113. doi:https://doi.org/10.1016/j.energy.2017.10.018

Zaharin, M. S. M., Abdullah, N. R., Masjuki, H. H., Ali, O. M., Najafi, G., & Yusaf, T. (2018). Evaluation on physicochemical properties of iso-butanol additives in ethanol-gasoline blend on performance and emission characteristics of a spark-ignition engine. *Applied Thermal Engineering, 144*, 960-971. doi:10.1016/j.applthermaleng.2018.08.057

Zaidel, D. N. A., Muhamad, I. I., Daud, N. S. M., Muttalib, N. A. A., Khairuddin, N., & Lazim, N. A. M. (2019). 18 - Production of biodiesel from rice bran oil. In D.

UMPSA
UNIVERSITI MALAYSIA PAHANG
AL-SULTAN ABDULLAH

Verma, E. Fortunati, S. Jain, & X. Zhang (Eds.), *Biomass, Biopolymer-Based Materials, and Bioenergy* (pp. 409-447): Woodhead Publishing.

Zhou, L., Dong, K., Hua, J., Wei, H., Chen, R., & Han, Y. (2018). Effects of applying EGR with split injection strategy on combustion performance and knock resistance in a spark assisted compression ignition (SACI) engine. *Applied Thermal Engineering*. doi:https://doi.org/10.1016/j.applthermaleng.2018.09.001

Zullaikah, L. C., Vali SR, Ju YH. . (2005). A two-step acid-catalyzed process for the production of biodiesel from rice bran oil. *Bioresour Technol, 96:188996.*

UMPSA
اونيۏرسيتي مليسيا ڤهڠ السلطان عبدالله
UNIVERSITI MALAYSIA PAHANG
AL-SULTAN ABDULLAH

APPENDICES

UMPSA
اونيۏرسيتي مليسيا ڤهڠ السلطان عبدالله
UNIVERSITI MALAYSIA PAHANG
AL-SULTAN ABDULLAH

Appendix A: Digital Controller for Speed and Torque

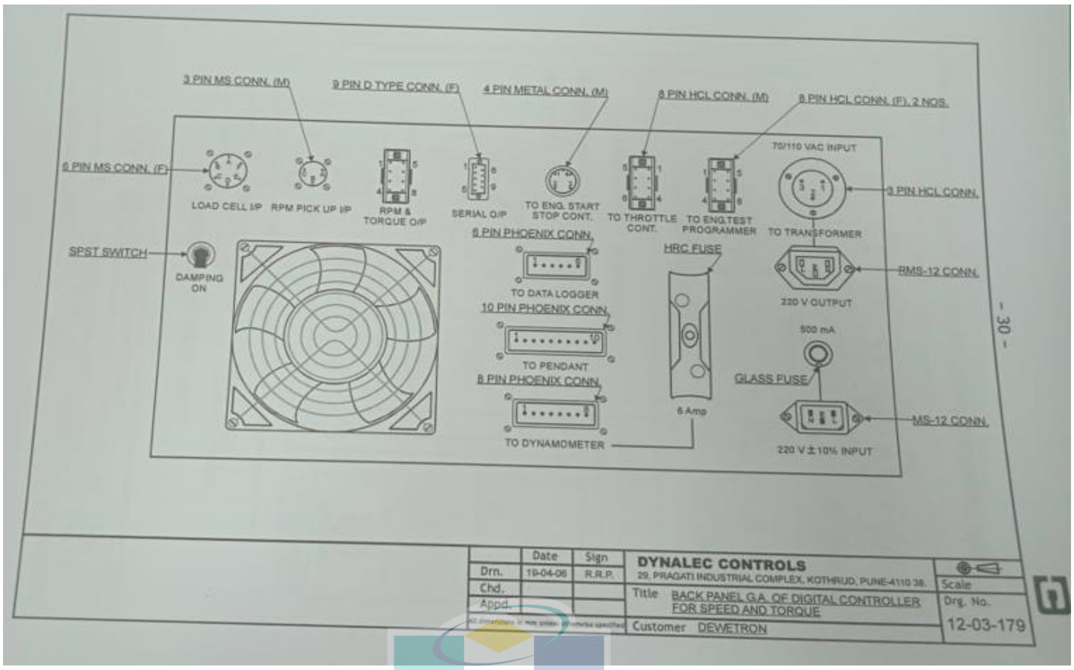

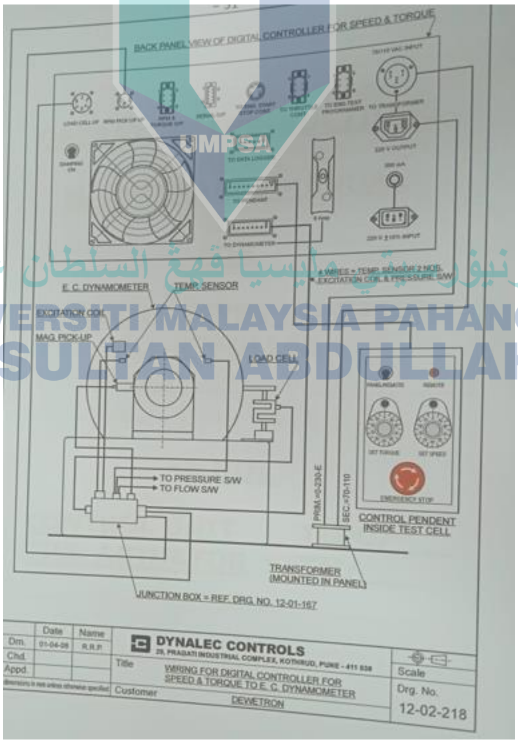

UMPSA
اونيۏرسيتي مليسيا ڤهڠ السلطان عبدالله
UNIVERSITI MALAYSIA PAHANG
AL-SULTAN ABDULLAH

Appendix B: Throttle Lever Position Controller

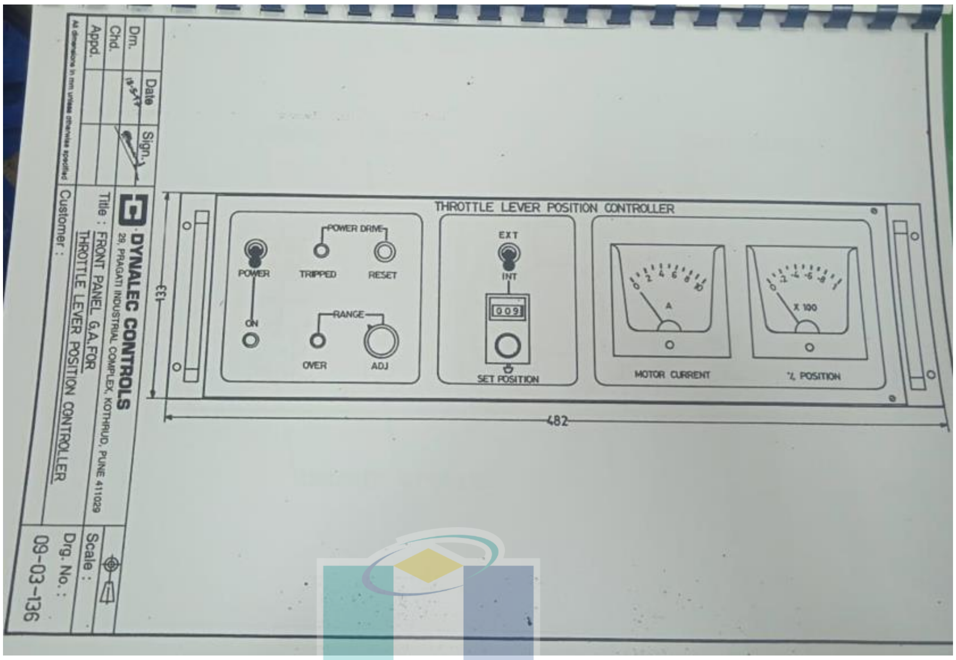

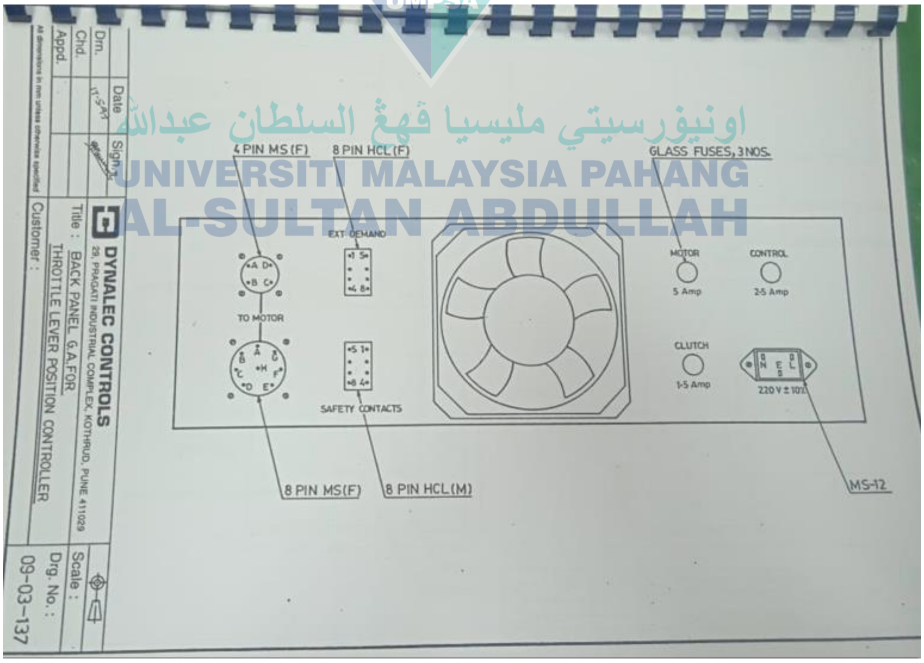

UMPSA
اونيۏرسيتي مليسيا ڤهڠ السلطان عبدالله
UNIVERSITI MALAYSIA PAHANG
AL-SULTAN ABDULLAH

3.0 SPECIFICATIONS:

3.10 THROTTLE CONTROLLER UNIT:

3.11 ELECTRICAL:

Input Supply	:	220 V ±10% A.C., 50 Hz, Single Phase
Power Output	:	Capacity to drive DC Servo Motor of 100 Watt.
Safety Input	:	Normally closed potential free contact. When contact opens out, throttle lever comes to 0% position. (i.e. engine idle)
Ext. Set Position I/P	:	0 to 10 V DC
Position Setting	:	By 10 turn potentiometer with dial having locking arrangement.
Zero Setting	:	Approx. 20 % of Max. range
Range Setting	:	Approx. 50 % of Max. range
Fuse protection	:	Motor – 5.0 Amp. Control – 2.5 Amp. Clutch – 1.5 Amp.

3.12 MECHANICAL:

Overall Dimensions	:	482 (w) x 135 (h) x 400 (d) mm
Cutout size	:	440 (w) x 134 (h) mm

3.13 ENVIRONMENTAL:

Temperature	:	0 °C to 55 °C
Humidity	:	R.H. 95% maximum

UMPSA
اونيۏرسيتي مليسيا قهڠ السلطان عبدالله
UNIVERSITI MALAYSIA PAHANG
AL-SULTAN ABDULLAH

Appendix C: Technical Specification and Data for KIPOR 170FS Engine

CHAPTER 1 MAIN TECHNICAL SPECIFICATION AND DATA

1-1 Main Technical Specification

Item	Technical specification					
Model	170F(E)	170FS(E)	178F(E)	178FS(E)	186F(E)	186FS(E)
Type	Single-cylinder, vertical, 4-stroke, air-cooled, dire t-injection					
Bore x stroke(mm)	70x55		78x62		86x70	
Displacement(L)	0.211		0.296		0.406	
Normal speed(r/min)	3000	3600	3000	3600	3000	3600
Normal Power KW(PS)	3.8	4.2	5.5	6	8.5	9
Mean effective pressure kPa (kgf/cm²)	443.2(452)	430.9(44)	540.5(552)	496.6(507)	561.6(573)	543.5(555)
Consumption rate of fuel g/KW(g/PS.h)	≤287(211)	≤299.2(220)	≤280.3(206)	≤292.5(215)	≤273.5(201)	≤285.7(210)
Consumption rate of machine oil g/KW≤4.08(3)	≤4.08(3)		≤4.08(3)		≤4.08(3)	
Fuel tank capacity (L)	2.5		3.5		5.5	
Lub.oil Full Capacity (L)	0.75		1.10		1.65	
Rotary direction of Crankshaft	Clockwise from flywheel end					
Cooling type	Forced air-cooled system					
Lub. type	Pressure, splash					
Starting type	Recoil manual start and optional electric start					
Net weight (kg)	27		33		48	

Overall Figure

اونيۏرسيتي مليسيا ڤهڠ السلطان عبدالله
UMPSA
UNIVERSITI MALAYSIA PAHANG
AL-SULTAN ABDULLAH

Engine Model		170F(S)/E	178F(S)/E	186F(S)/E	186FA/E	188FA/E	188FB/E
Bore*stroke		70*55	78*62	86*70	86*72	88*72	88*75
Type		Forced Air-cooled,4-Stroke,Direct-injection					
Displacement	cc	211	296	406	416	438	456
Max Output	HP	3.8/3000 3.8/1500 | 4.5/3600 4.5/1800	5.36/3000 5.36/1500 | 6.6/3600 6.6/1800	8.57/3000 8.57/1500 | 9.85/3600 9.85/1800	8.57/3000 | 9.85/3600	11.3/3000 | 12/3600	12.7/3000 | 13.3/3600
Fuel		0#(SUMMER) /-10#(WINTER) Diesel Light Fuel(BS-AI or Equivalent					
Fule Tank Capacity	L	2.5	3.5	5.5	5.5	5.5	5.5
Lubricating Oil Capacity	L	0.75	1.1	1.65	1.65	1.65	2.65
Lubricating System		Pressure splashed					
Starting System		Manual/electric start					
Packing size (L*W*H)	MM	415*385*470	485*475*525	500*470*555	500*470*555	500*470*555	500*470*555
Net weight	KG	26	35	48	48	49	50

اونيۏرسيتي مليسيا ڤهڠ السلطان عبدالله
UNIVERSITI MALAYSIA PAHANG
AL-SULTAN ABDULLAH

Appendix D: Part List of KIPOR 170FS Engine

No.	Code	Name of part	Unit	Qty each set
19	70/78-17180	Air cleaner Bottom Case Assem	Piece	1
	86-1718003		Piece	1
20	70/78-17178	Sealing ring I of shock proof	Piece	1
	86-1718001		Piece	1
21	70/78-17181	Shock absorbor of air filter	Piece	1
	86-1718101		Piece	1
22	70/78-1710103	Collar(GB6177-86)	Piece	1
	86-1710114	Collar(GB6177-86)	Piece	1
23	70/78-17182	Shock absorber of air filter (aquare)	Piece	1
	86-1720106		Piece	1
24	17177	Washer	Piece	1
25	70/78-1710107	Butterfly nut M6	Piece	1
	85-1710109	Butterfly nutM8	Piece	1

No.	Code	Name of part	Unit	Qty each set
17	70-1704101	Wind leading case welded	Piece	1
	78-1704102		Piece	1
	86-1704105		Piece	1
17S	78-1704106	78F wind leading case welded Assem	Piece	1
18	78-1710622	bolt M6*22(GB5787-86)	Piece	5
	70/86-1710622		Piece	4
19	78-1710207	Washer6(GB90-85)	Piece	5
	70/86-1710207		Piece	4
20	78-17145	Collar	Piece	5
	70/86-17145		Piece	4
21	78-17143	shock absorber	Piece	5
	70/86-17143		Piece	4
22	17144	pieces of shock pads	Piece	1
23	78/86-17127	shock isolation piece of wind leading plate	Piece	1
24	78/86-17129	Collar	Piece	1
25	78/86-17128	Pad	Piece	1
26	70-1700401	Wind leading plate	Piece	1
	78-1700402		Piece	1
	86-1700403		Piece	1
27	70-1710712	bolt M6*12(shaped piece)	Piece	1
	78-1710718	bolt M6*18(shaped piece)	Piece	1
	86-1710614	bolt M6 22shaped piece)	Piece	1

Note: the parts of recoil starter Assem.

UMPSA
UNIVERSITI MALAYSIA PAHANG
AL-SULTAN ABDULLAH

Fuel system

No.	Code	Name of part	Unit	Qty each set
1	1710745	Bolt M8*45(GB5787-86)	Piece	1
2	17185	Fastened bolt for upper bracket of fuel tank	Piece	1
3	1710208	Flat washer 8(GB97.1-85)	Piece	1
4	70-1705801	Upper bracket of fuel tank	Piece	1
	78-1705802		Piece	1
	86-1705803		Piece	1
5	1705301	Injector	Piece	1
6	17212	Fuel leak-off pipe connecting	Piece	2
7	17192	Fuel leak-off pipe	Piece	1
8	17184	Shock absorbing pad of fuel tank	Piece	4
9	70-1704201	Fuel tank	Piece	1
	78-1704202		Piece	1
	86-1704203		Piece	1
10	17212	Fuel pipe connecting	Piece	2
11	17147	Fuel pipe	Piece	1
12	17151	Gasket of fuel draining M6(GB6177-86)	Piece	1
13	17152	Cock offuel draining (fuel pipe)	Piece	1
14	17183	Lower bracket of fuel tank	Piece	1
15	1710714	BoltM6*14(GB5787-86)	Piece	2
16	1710106	NutM6(GB6177-86)	Piece	2
17	1710206	Flat washer6(GB97.1-85)	Piece	1
18	17150	Fuel tank cock Assem	Piece	1
19	17154	Flat washer	Piece	1
20	1719403	Clamp of fuel oil pipe	Piece	2
21	17189	Fuel oil pipe	Piece	1
22	17148	Gasket of fuel oil filter	Piece	1
23	70-1704301	Fitter element Assem	Piece	1
	78-1044302		Piece	1
	86-1704303		Piece	1
24	70-1704702	Fuel injection pump	Piece	1
	78-1704702		Piece	1
	86-1704700		Piece	1
25	70-1705601	High pressure fuel pipe	Piece	1
	78-1705602		Piece	1
	86-1705603		Piece	1

Piston connecting rod and crankshaft balancing mechanism

No.	Code	Name of part	Unit	Qty each set
1	70-1701403	Piston ring group	Piece	1
	78-1701402		Piece	1
	86-1701404		Piece	1
2	70-1701601	Retainer of piston pin ø19	Piece	2
	78-1701602	Retainer of piston pin ø21	Piece	2
	86-1701603	Retainer of piston pin ø23	Piece	2
3	70-1701200	Piston	Piece	1
	78-1701202		Piece	1
	86-1701204		Piece	1
	78FS-1701203		Piece	1
4	70-1701701	Piston pin	Piece	1
	78-1701702		Piece	1
	86-1701703		Piece	1
5	70-1701301	Connecting rod body	Piece	1
	78-1701302		Piece	1
	86-1701303		Piece	1
6	70-1701501	Connecting rod bush	Piece	1
	78-1701502		Piece	1
	86-1701503		Piece	1
7	70-1710001	Bearing 202(GB/T276-94)	Piece	2
	78-1710001		Piece	2
	86-1710000	Bearing203(GB/T276-94)	Piece	2
8	70-1706501	Balancing shaft	Piece	1
	78-1706502		Piece	1
	86-1706503		Piece	1
9	1710507	Key 5 × 7(GB1096-79)	Piece	2
10	70-1707701	Balancing shaft timing gear	Piece	1
	78-1707702		Piece	1
	86-1707703		Piece	1
11		Bolt(for F shaft accompany with the diesel engine)	Piece	1
12	70-1700801	Crankshaft timing gear	Piece	1
	78-1700802		Piece	1
	86-1700803		Piece	1
13	70/78-1710512	Key 5 × 12(GB1096-79)	Piece	2
	86-1710512	Key 5 × 12(GB1096-79)	Piece	1

UMPSA
اونيۏرسيتي مليسيا ڤهڠ السلطان عبدالله
UNIVERSITI MALAYSIA PAHANG
AL-SULTAN ABDULLAH

No.	Code	Name of part	Unit	Qty each set
13A	86-1710514	Key 5 × 14(GB1096-79)	Piece	1
14	70-1710530	Key 5 × 30(GB1096-79)	Piece	1
	78/86-1710563	Key 6 × 63(GB1096-79)	Piece	1
15	70-1700601	Crankshaft	Piece	1
	78-1700701		Piece	1
	86-1700708		Piece	1
16	1711601	Plug 6 × 8	Piece	1
17	70-1707801	Driving gear of balancing shaft	Piece	1
	78-1707802		Piece	1
	86-1707803		Piece	1
18	70-1704400	Flywheel	Piece	1
	78-1704404		Piece	1
	86-1704409		Piece	1
19	70/78-17156	Gasket for nut of flywheel	Piece	1
	86-1715601		Piece	1
20	70/78-17155	Nut of flywheel	Piece	1
	86-1715501		Piece	1
21	70-1704501	Gear ring of flywheel(for starting motor)	Piece	1
	78-1704502		Piece	1
	86-1704504		Piece	1
22	1704705	Sleeve of fuel pump tappet	Piece	1
23	70-1705101	Push rod	Piece	2
	78-1705102		Piece	2
	86-1705103		Piece	2
24	70-17157	Tappet	Piece	2
	78-17157		Piece	2
	86-1715701		Piece	2
25	70/86-1710514	Key 5 × 14(GB1096-79)	Piece	1
	78-1710504	Key 4 × 12(GB1096-79)	Piece	1
26	70-1701001	Camshaft	Piece	1
	78-1701002		Piece	1
	86-1701000		Piece	1
26S	78-1701003	FS camshaft	Piece	1
27	70-1701101	Camshaft timing gear	Piece	1
	78-1701102		Piece	1
	86-1701103		Piece	1

No.	Code	Name of part	Unit	Qty each set
19	70-1702403	Mechanical process parts of cylinder head	Piece	1
	78-1702402		Piece	1
	86-1702404		Piece	1
20	70/78-1710955	Double ends bolt AM6 × 55(GB900-88)	Piece	2
	86-1710956	Double ends bolt AM6 × 75(GB900-88)	Piece	2
21	70-1702501	Intake valve	Piece	1
	78-1702601		Piece	1
	86-1702503		Piece	1
22	70-1702502	Exhaust valve	Piece	1
	78-1702602		Piece	1
	86-1702605		Piece	1
23	1710103	Nut M6(GB6177-86)	Piece	2
24	1717302	Press plate of fuel injector	Piece	1
25	1724502	Adjusting gasket of fuel injector	Piece	1
26	70-1712201	Fastened bolt of fuel injectorAM6 × 42	Piece	2
	78-1712201	Fastened bolt of fuel injectorAM6 × 42	Piece	2
	86-17122	Fastened bolt of fuel injector(long)	Piece	2
27	17141	Breather assembly	Piece	1
28	1711312	"O" type ring 12 × 1.9	Piece	1

UMPSA
UNIVERSITI MALAYSIA PAHANG AL-SULTAN ABDULLAH

Appendix E: Summary of Classification of Internal Combustion (IC) Engine

Classification of Internal Combustion (IC) Engine	
Characteristics	**Explanation**
Types of Ignitions	1. Spark Ignition (SI) 2. Compression Ignition (CI)
Engine Cycle	1. Two Strokes Cycle 2. Four Strokes Cycle
Valve Location	1. Valves in head (overhead valve/I Head engine) 2. Valves in block (flat head/L Head engine) 3. One valve in head (F Head engine)
Basic Design	1. Reciprocating Engine 2. Rotary Engine
Position and Number of Cylinders of Reciprocating Engines	1. Single cylinder 2. In-line cylinder 3. V - engine 4. Opposed cylinder engine 5. W – engine 6. Opposed piston engine 7. Radial engine

UMPSA
اونيورسيتي مليسيا ڤهڠ السلطان عبدالله
UNIVERSITI MALAYSIA PAHANG
AL-SULTAN ABDULLAH

Appendix E: Continued

Classification of Internal Combustion (IC) Engine	
Characteristics	**Explanation**
Air Intake Process	1. Naturally Aspirated 2. Supercharged 3. Turbocharged 4. Crankcase Compressed
Fuel Used	1. Gasoline 2. Diesel Oil or Fuel Oil 3. Gas, Natural Gas, Methane 4. Liquefied Petroleum Gas (LPG) 5. Alcohol-Ethyl, Methyl 6. Dual Fuel
Application	1. Automobile, Truck, Bus 2. Locomotive 3. Stationary 4. Marine 5. Aircraft 6. Small Portable, Chain Saw, Model Airplane
Types of Cooling	1. Air Cooled 2. Liquid Cooled, Water Cooled

Source: Pulkrabek (2014)

UMPSA
اونيۏرسيتي مليسيا ڤهڠ السلطان عبدالله
UNIVERSITI MALAYSIA PAHANG
AL-SULTAN ABDULLAH

Appendix F: Emission Legislation of Compression Ignition (CI) Engine

Regulated Emissions

In the present day, Europe, the United States, and Japan, which are considered the three major regions, have implemented regulatory measures to control the levels of oxides of nitrogen (NOx). In the context of automotive emissions, NOx refers explicitly to the binary compounds nitric oxide (NO) and nitrogen dioxide (NO_2). Nitric oxide (NO) accounts for approximately 90% of the nitrogen oxide (NOx) emissions generated by an internal combustion engine, while nitrogen dioxide (NO_2) constitutes the remaining 10% of the NOx emissions.

Particulate Matter (PM) can be alternatively denoted as Diesel Particulate Matter (DPM) or Total Particulate Matter (TPM). Diesel particulate matter (PM) comprises a combination of carbonaceous soot along with various solid and liquid substances. Hydrocarbons (HC) encompass two categories: total hydrocarbons (THC) and non-methane hydrocarbons (NMHC). Additionally, Carbon Monoxide (CO) is another constituent.

UMPSA

Unregulated Emissions

اونيۏرسيتي مليسيا ڤهڠ السلطان عبدالله
UNIVERSITI MALAYSIA PAHANG
AL-SULTAN ABDULLAH

Unregulated emissions can be characterized as pollutant emissions for which there exists a justifiable rationale for potential future regulation. Numerous supplementary uncontrolled pollutants have been detected in the exhaust of compression ignition (CI) engines, with a significant portion exhibiting concentration levels considerably lower than those of regulated emissions. Indeed, certain entities constitute a fraction of the intricate particulate matter (PM) emissions, while others exist as gaseous compounds.

The subsequent substances have the potential to be subject to future regulatory measures: i) Polycyclic aromatic hydrocarbons (PAHs) are a class of atmospheric pollutants characterized by the presence of fused aromatic rings. Certain polycyclic aromatic hydrocarbon (PAH) molecules have been recognized as possessing carcinogenic properties (U.S. Department of Energy, accessed 19.04.2016). ii) Nitrous oxide, often known as N_2O, is a potential future worry due to its utilization as an oxidant in certain after-treatment systems. It is worth noting that nitrous oxide is not accounted for in NO_X measurements. N_2O, functioning as a pollutant, exhibits a significantly heightened greenhouse effect, approximately 298 times more potent than CO_2. However, the duration of its presence as N_2O is subject to debate due to its propensity to react with oxygen, resulting in the formation of NO (Venu, Raju, Subramani, & Appavu, 2020). iii) Aldehydes include a component of the gaseous discharge originating from compression-ignition (CI) engines.

Acetaldehyde and formaldehyde, both classified as potential carcinogens, have the potential to induce various health consequences (Tsiligiannis & Tsiliyannis, 2019). Aldehydes can be identified by their O=CH at the end of a group R of in determined length; formaldehyde is the simplest (CH_2O). iv) Sulphur dioxide (SO_2) is emitted as a result of the presence of sulphur in both the fuel and lubricating oil. In the past, the levels of sulphur in fuel were or still are significantly elevated, surpassing 400 parts per million (ppm). These levels may continue to persist in certain developing markets. Sulphur dioxide serves as a precursor to the formation of acid rain and atmospheric particulate matter (Teoh et al., 2019).

The issue of sulphur poisoning has garnered significant recent attention, not solely due to its direct environmental impact. Sulphur has the ability to deactivate the catalytic sites of automotive catalysts, rendering them ineffective or "poisoned" (Pulkrabek, 2014). The oil corporations and legislative authorities have responded to this by reducing or eliminating the quantities of sulphur in fuel and lubricant oil. v) The topic of discussion pertains to metal oxides and metallic particulate matter (PM). Various fuel and engine oil additives incorporate metallic elements. The combustion process yields various metal oxide and elemental emissions, encompassing metals such as iron, copper, zinc, cerium, calcium (included in the fuel to mitigate particulate matter), and phosphorus (Chatur, Maheshwari, & Jee Kanu, 2023).

Metal oxide emissions and small nano metallic particulates have the potential to exhibit toxicity and carcinogenic properties, with nano particulates being particularly noteworthy in this regard. vi) Nitrogen dioxide (NO_2) constitutes a part of the NOx

UMPSA
اونيۏرسيتي مليسيا ڤهڠ السلطان عبدالله
UNIVERSITI MALAYSIA PAHANG
AL-SULTAN ABDULLAH

emission (it is more toxic than NO, the other component of NOx). It could be anticipated that in the future NO_2 may be regulated individually. vii) Dioxins, namely polychlorinated dibenzodioxins, possess lipophilic characteristics, enabling them to dissolve in fats. These compounds are recognized as teratogens, capable of inducing birth deformities, as well as mutagens, and are also considered potential human carcinogens.

The field of environmental health offers extensive opportunities for research in a vast geographical expanse. The issue of dioxin emissions arises exclusively in situations when chlorine is present during the process of combustion (Praveena et al., 2023). As a result, there are currently stringent regulations in place to restrict the quantities of chlorine in diesel. Biodiesels have the potential to include trace amounts of chlorine if specific herbicides are utilized throughout the production process. Therefore it is imperative to prevent such contamination (Brahma et al., 2023).

UMPSA
اونيۏرسيتي مليسيا ڤهڠ السلطان عبدالله
UNIVERSITI MALAYSIA PAHANG
AL-SULTAN ABDULLAH

Appendix G: VICTOR VC-816B Digital anemometer

UMPSA
اونيۏرسيتي مليسيا ڤهڠ السلطان عبدالله
UNIVERSITI MALAYSIA PAHANG
AL-SULTAN ABDULLAH

LIST OF PUBLICATIONS AND PRESENTATIONS

Journal Articles

M.Norhafana, C.K.Ihsan, M.M.Noor, A.A.Hairuddin, K.Kadirgama, Rice Bran Oil as Emerging Green Fuels: Exploration on Combustion Behaviors of Single-cylinder Diesel Engine (Light-Duty Engine), Journal of Advanced Research in Applied Science and Engineering Technology, November 2023 (Indexed by Scopus, Under Review).

M.Norhafana, M.M.Noor, A.A.Hairuddin, S.Harikrishnan, K.Kadirgama, D.Ramasamy, The Effects of Nano-Additives on Exhaust Emissions and Toxicity on Mankind, Material Today, 22, 1181-1185, (Scopus Indexed Journal) 2019.

M.Norhafana, C.K.Ihsan, M.M.Noor, A.A.Hairuddin, K.Kadirgama, D.Ramasamy, Effect on Blending Diesel Fuel with Rice Bran Oil on the Emission Characteristics of a Compression Ignition Engine, Journal of Advanced Research in Applied Science and Engineering Technology, February 2024 (Submitted to Scopus Journal), 08 Feb 2024.

M.Norhafana, C.K.Ihsan, M.M.Noor, A.A.Hairuddin, K.Kadirgama, D.Ramasamy, Comprehensive Analysis of Combustion Behaviors and Knocking on Direct Injection Compression Ignition Engine (Light-Duty Engine) Fueled using Rice Bran Oil Blended, Journal of Advanced Research in Applied Science and Engineering Technology, February 2024 (Submitted to Scopus Journal), 08 Feb 2024.

Conference Papers

M.Norhafana, C.K.Ihsan, M.M.Noor, A.A.Hairuddin, K.Kadirgama, D.Ramasamy, Experimental Investigation on Performance Characteristics Evaluation of Compression Ignition Engine using Rice Bran Oil as Renewable Fuel, Engineering Technology International Conference (ETIC 2022).

M.Norhafana, C.K.Ihsan, M.M.Noor, A.A.Hairuddin, K.Kadirgama, D. Ramasamy, Emission Characteristics Effect on Rice Bran Oil Enriched with Diesel Fuel on Compression Ignition Engine, Lecture Notes in Mechanical Engineering - Technological Advancement in Mechanical and Automotive Engineering, 2023, pp. 75–88 (Scopus Indexed).

M.Norhafana, M.M.Noor, A.A.Hairuddin, 2020, Concentration Measurement on Preparation of Blending SiO2 Nano Biodiesel, Energy Security and Chemical Engineering Congress, IOP Conf. Series: Materials Science and Engineering, 736 (2020) 022114, (Scopus Indexed).

M.Norhafana, M.M.Noor, F.Y.Hagos, A.A.Hairuddin, 2020, Diesel and Various Blending Nanoparticles Based Diesel, Fuel Properties Study, IOP: Materials Science and Engineering, 788 (2020) 012061, (Scopus Indexed).

UMPSA
اونيۏرسيتي مليسيا ڤهڠ السلطان عبدالله
UNIVERSITI MALAYSIA PAHANG
AL-SULTAN ABDULLAH

M.Norhafana, M.M.Noor, P.M.Sharif, F.YHagos, A.A.Hairuddin, K.Kadirgama, D.Ramasamy, M.M.Rahman, R.Alenezi, A.T.Hoang, 2019, A Review of the Performance and Emissions of Nano Additives in Diesel Fuelled Compression Ignition-Engines, IOP: Materials Science and Engineering 469 (2019), 012035, (Scopus Indexed).

M.Norhafana, M.M.Noor, A.A.Hairuddin, F.Y.Hagos, S.I.Ayob, K.Kadirgama, D.Ramasamy, 2019, An Experimental Study of the Performance and Emission Characteristics of a Compression Ignition Engine Fueled with Palm Oil Based Biodiesel, AIP Conference Proceedings 2059, 020036 (2019); (Scopus Indexed).

M.Norhafana, C.K.Ihsan, M.M.Noor, A.A.Hairuddin, K.Kadirgama, D.Ramasamy, A.M.hussein, Enhancement of Efficiency And Mitigation Of Pollution Emissions In A Compression Ignition Engine By The Utilization Of Rice Bran Oil As Green Fuel.

UMPSA
اونيۏرسيتي مليسيا ڤهڠ السلطان عبدالله
UNIVERSITI MALAYSIA PAHANG
AL-SULTAN ABDULLAH